Author:
Cruise, Thomas

Title:
Effect of Metabotropic Glutamate Receptor 5 Modulation on Blood Pressure and the Adaptive Immune System in Hypertension

Effect of Metabotropic Glutamate Receptor 5 Modulation on Blood Pressure and the Adaptive Immune System in Hypertension

Thomas Cruise

A dissertation submitted to the University of Bristol in accordance with the requirements for award of the degree of Doctor of Philosophy in the Faculty of Biomedical Sciences, School of Physiology, Pharmacology and Neuroscience.

December 2017

42484 Words

Acknowledgements:

I would like to express my gratitude to my supervisor, Prof. Julian Paton, as well as to Dr. Paul Marvar for their essential support throughout the duration of my project. In addition, I would like to thank everyone in the lab who assisted me with valuable advice, especially Dr. Wioletta Pijacka and Dr. Dawid Walas, who were always there to help.

Thanks also are due to Dr. Mark Tricklebank, Dr. Lisa Broad and everyone else at Eli Lilly and Company who assisted me in my studies.

Author's declaration

I declare that the work in this dissertation was carried out in accordance with the requirements of the University's *Regulations and Code of Practice for Research Degree Programmes* and that it has not been submitted for any other academic award. Except where indicated by specific reference in the text, the work is the candidate's own work. Work done in collaboration with, or with the assistance of, others, is indicated as such. Any views expressed in the dissertation are those of the author.

SIGNED:
..... DATE:.....

Contents

Abstract:

Hypertension is a worldwide epidemic responsible for 12.8% of all deaths. Approximately 10% of hypertensive patients do not respond to current treatments and diagnoses are becoming more frequent, necessitating a deeper understanding of the disease as well as the development of novel antihypertensive therapies. More than half the cases of hypertension are believed to be of neurogenic origin, meaning that sympathetic outflow is elevated. In this context, I investigated the feasibility of the central nervous system as a novel pharmacological target for the treatment of hypertension. Glutamate is the major excitatory neurotransmitter in the brain and I sought to test the effects of compounds that modulate metabotropic glutamate receptor 5 on blood pressure and to determine whether their antagonism could reduce blood pressure in a well-established rodent model of hypertension. In addition, I investigated the involvement of the adaptive immune system in the pathology of human hypertension, since sympathetic outflow is known to drive inflammation and inflammation itself is pro-hypertensive. Using immunohistochemistry in autonomic regions of the brain, I found no obvious difference in the expression of metabotropic glutamate receptor 5 between normotensive and neurogenically hypertensive rat strains. However, using radio-telemetry, I observed a short-term increase in blood pressure of normotensive wild-type rats, produced by potentiation of the response of metabotropic glutamate receptor 5 to endogenous glutamate and a short-term decrease in the blood pressure of hypertensive rats with an antagonist of the same receptor. I also demonstrated a difference between the immunophenotypes of hypertensive and normotensive human males, consistent with increased activity of the adaptive immune system in hypertension. Further studies are needed to explore the potential of mGluR5

receptors as a central nervous system target for lowering arterial pressure in neurogenic hypertension. My data fully support a specific inflammatory process associated with hypertension and future studies will need to disentangle the cause-effect relationship between autonomic and adaptive inflammatory mechanisms. Nevertheless, combination therapy targeting specific metabotropic glutamatergic receptors and inflammatory mechanisms may offer a novel approach for ameliorating high blood pressure.

List of Publications Arising From This Work:

Marvar P, Cruise T, Hart E, Burchell A, Ratcliffe L, Nightingale A & Paton J (2014). Increased memory and decreased naïve T cells in human hypertension (1074.9). *FASEB J* **28,** 1074.9.

Marvar PJ, Hendy EB, Cruise TD, Walas D, DeCicco D, Vadigepalli R, Schwaber JS, Waki H, Murphy D & Paton JFR (2016). Systemic leukotriene B4 receptor antagonism lowers arterial blood pressure and improves autonomic function in the spontaneously hypertensive rat. *J Physiol* **594,** 5975–5989.

Glossary of Terms:

A5	A5 area of the ventrolateral Pons
Ab	Antibody
ACE:	Angiotensin-converting enzyme
Ach	Acetylcholine
ADH	Antidiuretic hormone
AF488	Alexa Fluor 488
AF647	Alexa Fluor 647
AF700	Alexa Fluor 700
AMPA	α-amino-3-hydroxy-5-methyl-4-isoxazolepropionic acid
ANG I:	Angiotensin I
ANG II:	Angiotensin II
AP5	(2*R*)-amino-5-phosphonovaleric acid
APC	Allophycocyanin
AT1R	Angiotensin Receptor Type 1
BBB	Blood-brain-barrier
BP	Blood pressure
BV650	Brilliant violet 650
CCL21	Chemokine (C-C motif) ligand 21
CD	Cluster of differentiation
CNI1493	Semapimod
CNQX	6-cyano-7-nitroquinoxaline-2,3-dione
CNS:	Central nervous system
CO	Cardiac output
CRIC	Clinical Research and Imaging Centre
CVLM	Caudal ventrolateral medulla
CVO	Circumventricular organ
Cy5.5	Cy5 dye
Cy7	Cyanine dye
DAB	Diaminobenzidine
DAG	Diacylglycerol
dH_2O	Distilled water
DHPG	(S)-3,5-Dihydroxyphenylglycine
dlPAG	Dorsolateral periaqueductal grey area
dmPAG	Dorsomedial periaqueductal grey area
DOCA	Deoxycorticosterone acetate
EDTA	Ethylenediaminetetraacetic acid
EF660	eBioscience fixable viability dye 660
eNOS	Endothelial nitric oxide synthase
FACS	Fluorescence-activated cell sorting
FITC	Fluorescein isothiocyanate
FMO	Fluorescence minus one
FSC	Forward scatter
GABA	Gamma-Aminobutyric acid
GlyCAM-1	Glycosylation-dependent cell adhesion molecule-1

gp39	Glycoprotein precursor 39
GPCR	G-protein-coupled receptor
GRK	G-protein-coupled receptor kinase
H_2O_2	Hydrogen peroxide
HBSS	Hank's Balanced Salt Solution
HEPES	4-(2-hydroxyethyl)-1-piperazineethanesulfonic acid
HPA	Hypothalamic–pituitary–adrenal axis
HR	Heart rate
HT	Hypertension
HTN	Hypertensive
ICAM-1	Intercellular adhesion molecule 1
ICV	Intracerebroventricular
IFN-γ	Interferon gamma
IgE	Immunoglobulin E
IgG	Immunoglobulin G
IHC	Immunohistochemistry
IL-10	Interleukin 10
IL-17	Interleukin 17
IL-1β	Interleukin 1 beta
IL-2	Interleukin 2
IL-21	Interleukin 21
IL-22	Interleukin 22
IL-23	Interleukin 23
IL-4	Interleukin 4
IL-6	Interleukin 6
IML	Intermediolateral nucleus
IMS	Industrial methylated spirit
IP	Intraperitoneal
IP3	Inositol 1,4,5-trisphosphate
IV	Intravenous
JAM-1	Junctional adhesion molecule-1
Lck	Lymphocyte-specific protein tyrosine kinase
LFA-1	Lymphocyte function-associated antigen 1
lPAG	Lateral periaqueductal grey area
LPS	Lipopolysaccharide
LSNA	Lumbar sympathetic nerve activity
mABP	Mean arterial blood pressure
MAP	Mean arterial pressure
mGluR4	Metabotropic glutamate receptor 4
mGluR5	Metabotropic glutamate receptor 5
MHC I	Major histocompatibility complex I
MHC II	Major histocompatibility complex II
MIP-3	Macrophage inflammatory protein-3
MK-801	Dizocilpine
MPEP	2-Methyl-6-(phenylethynyl)pyridine
MRP	Multidrug resistance proteins

MTEP	3-((2-Methyl-4-thiazolyl)ethynyl)pyridine
NA	Noradrenaline
nAChR	Nicotinic acetylcholine receptor
NADPH	Nicotinamide adenine dinucleotide phosphate
NF-κB	Nuclear factor kappa-light-chain-enhancer of activated B cells
NK cell	Natural killer cell
NMDA	N-Methyl-D-aspartate
NO	Nitric oxide
NTN	Normotensive
NTS	Nucleus of the solitary tract
PacBlue	Pacific Blue
PAG	Periaqueductal Grey Area
PAM	Positive allosteric modulator
PBS	Phosphate buffered saline
PBS-T	PBS with 0.05% Tween-20
PE	Phycoerythrin
PerCP	Peridinin chlorophyll protein
PFA	Paraformaldehyde
PIP2	Phosphatidylinositol 4,5-bisphosphate
PKC	Protein kinase C
PVN	Paraventricular nucleus of the hypothalamus
qPCR	Quantitative polymerase chain reaction
RAG	Recombination-activating gene
RAS:	Renin-angiotensin system
RGS	Regulators of G-protein signalling
ROS	Reactive oxygen species
RVLM	Rostral ventrolateral medulla
SFO	Subfornical organ
SHANK3	SH3 and multiple ankyrin repeat domains
SHR	Spontaneously hypertensive rat
SNA	Sympathetic nerve activity
SNAP-25	Synaptosomal-associated protein of 25 kDa
SSC	Side scatter
TGF-β	Transforming growth factor beta
TH1	Type 1 helper T cell
TH17	Type 17 helper T cell
TH2	Type 2 helper T cell
TNFα	Tumour necrosis factor alpha
TPR	Total peripheral resistance
Treg	Regulatory T cell
V450	BD Horizon V450
vlPAG	Ventrolateral periaqueductal grey area
WKY	Wistar-kyoto
WT	Wild type

Chapter 1: General Introduction

Hypertension:

Hypertension is a worldwide epidemic. It is estimated to cause 12.8% of all deaths globally (World Health Organistation, 2017). The condition affects 1 in 3 people in the United States (Merai *et al.*, 2016) and the UK (Health Survey for England, 2015). It is the primary risk factor for stroke and is a risk factor for heart attack, heart failure and kidney disease as well as other debilitating and deadly conditions such as vascular dementia (Forette *et al.*, 1998). It is usually asymptomatic, which can result in at-risk hypertensives failing to seek treatment until a severe consequence has been realised.

95% of hypertensives are diagnosed with "primary" (or "essential") hypertension, meaning that the condition is not secondary to a known pre-existing condition (Carretero & Oparil, 2000). Despite a great deal of research, a clear understanding of the aetiology of hypertension has not yet been attained. Several behavioural factors and lifestyle choices are believed to be contributing factors, such as high salt intake, lack of physical activity, obesity and stress (Carretero and Oparil, 2000). Genetic factors are also believed to play a role. Most research has focussed on the culpability of the renal system and because of this, most therapeutic interventions target components of it, such as the enzymes of the renin-angiotensin system (RAS), for example angiotensin-converting enzyme inhibitors (ACE inhibitors) and diuretics, used to simply reduce blood volume and thereby blood pressure. These treatments are effective in some patients, but some remain hypertensive despite receiving a number of pharmacological interventions. A patient that remains hypertensive despite receiving three antihypertensive drugs of different classes (one of which must be

a diuretic) is classified as having resistant hypertension. These patients account for approximately 10% of hypertensives (Persell, 2011).

The fact that we are unable to control the blood pressure of many hypertensive patients along with the fact that the number of sufferers is expected to increase means that the global burden of hypertension is bound to worsen. This necessitates the development of novel therapeutic interventions.

Over 50% of cases of hypertension are estimated to be neurogenic (Esler *et al.*, 2010) which refers to hypertension in which sympathetic outflow and consequently angiotensin II (ANG II) are elevated. Like drugs targeting the RAS, other drugs targeting the downstream mediators of sympathetic activity such as β adrenergic receptor blockers (β blockers) have had some success in treating the condition. It was my intention to target the sympathetic nervous system upstream of this, in the CNS itself, in an attempt to investigate the feasibility of the CNS as a novel pharmacological target for the treatment of hypertension.

Basics of Blood Pressure Control:

Blood pressure (BP) is controlled by the autonomic nervous system. This complex neuronal network integrates afferent information from chemical and mechanical sensors in the periphery and adjusts the efferent sympathetic and parasympathetic tone that flows out to organs with the capability to effect changes in BP such as the heart, blood vessels and kidneys. An increase in sympathetic activity results in contraction of vascular smooth muscle, causing vasoconstriction, which results in an increase in total peripheral resistance (TPR) which reduces blood flow and increases arterial pressure. Sympathetic activation causes heart rate and contractility to increase. It also causes the

kidneys to retain more salt and release renin, which elevates circulating angiotensin II, and aldosterone which results in increased blood volume. These effects synergise to produce an increase in the cardiac output (CO). Thus, mean arterial pressure (MAP) can be defined as follows:

MAP = CO x TPR

Blood pressure is normally around 120/80mmHg where 120 mmHg is the systolic pressure and 80 mmHg is the diastolic pressure (Blood Pressure UK, 2017). Systolic pressure is the pressure exerted on the blood vessels during the heart beat and the diastolic reading is the pressure when the heart is resting between beats. Hypertension (high blood pressure) is defined as BP that is measured consistently at or above 140/90mmHg (Blood Pressure UK, 2017). Figure 1 is a chart displaying how different blood pressure readings are medically categorised for adults:

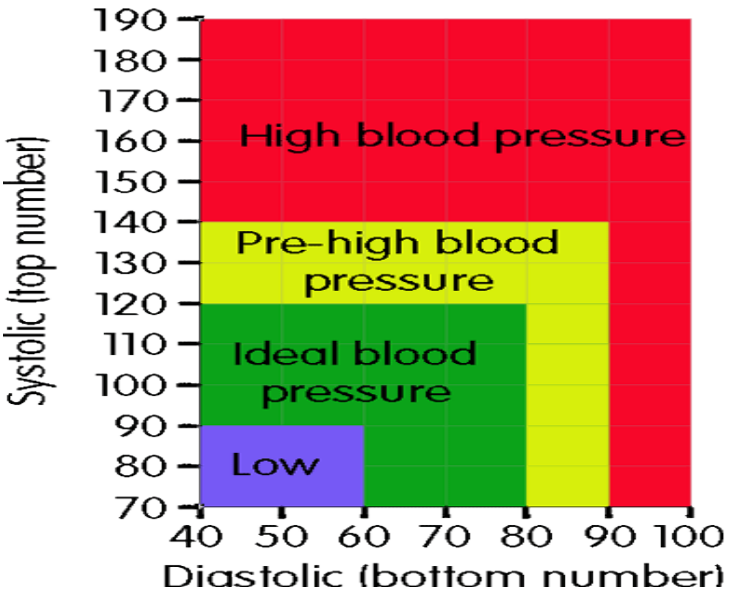

Figure 1: Blood pressure categories as defined by Blood Pressure UK

Blood pressure fluctuates throughout the day and has a diurnal rhythm. It also has a minute-to minute variability reflecting body posture, mental state and the level of physical activity, for example. Despite these fluctuations, the average

BP over the course of a day is tightly controlled. The mechanism by which the set point (120/80 mmHg) is established and how this may change in the case of hypertension is not fully understood. However, a great deal of information concerning the operation of blood pressure control neural circuitry has been obtained and will be discussed later on.

The Autonomic Nervous System and Angiotensin II:

As alluded to earlier, blood pressure is controlled by the autonomic nervous system. The efferent fibres of the autonomic nervous system constitute the sympathetic and parasympathetic systems; parallel neuronal networks. The sympathetic pre-ganglionic neurones located in the intermediolateral cell column of the spinal cord project to and innervate the post-ganglionic sympathetic motor neurons in the paravertebral chain. The latter cells project to and control vascular smooth muscle and visceral organs such as the kidney. These post-ganglionic motor neurones are mostly noradrenergic, whereas the preganglionic neurons are cholinergic. The visceral afferents providing sensory information to the CNS are primarily glutamatergic.

Stimulation of post-ganglionic sympathetic motor neurones causes contraction of vascular smooth muscle (increased vasomotor tone), increased heart rate / contractility and increased renin release in the kidneys. Renin is a component of the renin-angiotensin system (RAS), which acts to increase blood pressure by raising peripheral vascular resistance and increasing blood volume. Renin is an enzyme which converts circulating angiotensionogen into angiotensin I (ANG I). ANG I is then converted into angiotensin II (ANG II), mostly in the lungs by angiotensin converting enzyme (ACE). ANG II is pharmacologically active and acts via receptors on vascular smooth muscle cells to cause vasoconstriction. It

also stimulates thirst and causes the release of vasopressin from the pituitary gland, which is an endogenous antidiuretic.

The circumventricular organs (CVOs) are structures in the CNS that are incompletely protected by the blood brain barrier (BBB)- a selectively-permeable membrane that separates circulating blood from the cerebrospinal fluid in order to protect the brain parenchyma from chemicals that would otherwise damage it. This incomplete barrier of CVOs allows certain pharmacologically active agents in the circulating blood to act on targets in the CNS and ANG II is one such agent. It acts at the subfornical organ (SFO), another CVO which contains AT_1 receptors. Activation of these receptors stimulates neurones in the SFO which project to and excite neurones in the paraventricular nucleus of the hypothalamus (PVN), which itself projects to the medulla oblongata of the brainstem (simply termed the medulla from here on), a region containing the most essential nuclei concerned with blood pressure control, which will be discussed later, and the spinal cord. These PVN projections are sympathoexcitatory in function and when activated, raise arterial blood pressure.

Sympathetic preganglionic neurones also innervate the adrenal glands, from which adrenaline, noradrenaline (NA) and aldosterone are released. All of these hormones raise blood pressure; adrenaline and NA act via α and β adrenoreceptors to increase peripheral vascular resistance (via contraction of vascular smooth muscle) and increasing heart rate/contractility, respectively. Aldosterone, like vasopressin, causes the renal system to retain more sodium, resulting in water retention. This increases blood volume and thereby blood pressure.

The parasympathetic efferents concerned with blood pressure control project from the CNS to ganglia within or adjacent to their target organs; the heart and some blood vessels. Their activity has opposite effects to the sympathetic nervous system, reducing heart rate and contractility and thereby blood pressure. Most blood vessels do not have parasympathetic innervation although some do, such as those in the genital erectile tissue as well as gastrointestinal and salivary glands. Parasympathetic activity causes vasodilation in these vessels, facilitating specialist functions where increased blood flow is required locally. (Purves *et al.*, 2001; Sato & Ishii, 2017)

Since neurogenic hypertension is characterised by over-activity of the sympathetic nervous system, sympathetic outflow will be the focus of this thesis.

CNS Regions Involved in the Control of Blood Pressure:

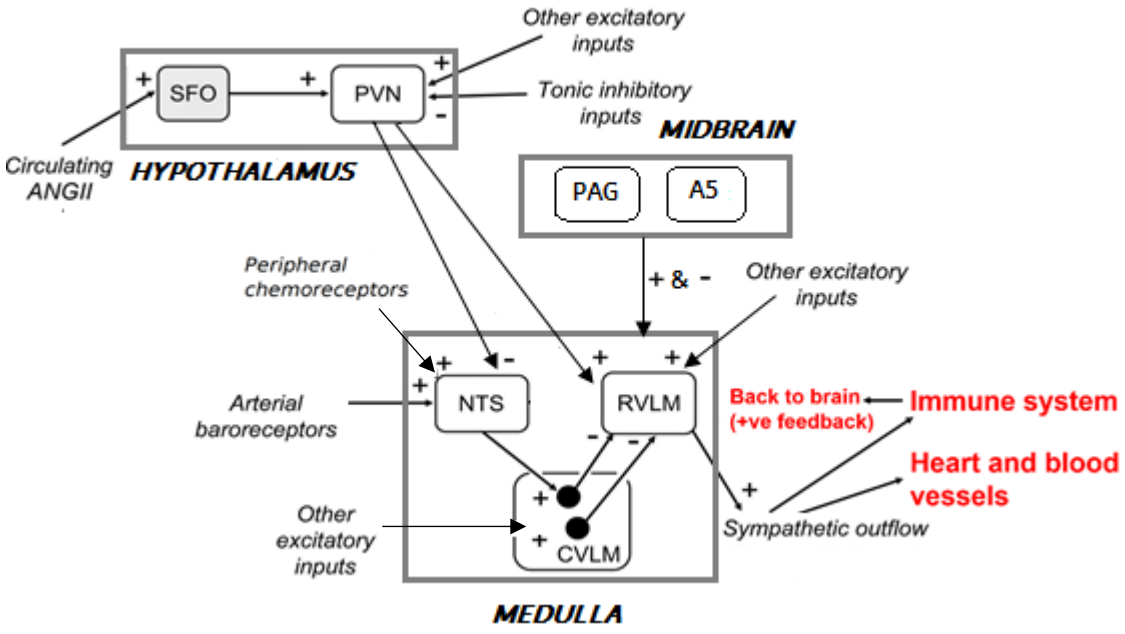

Figure 2: Schematic outlining key nuclei involved in blood pressure control. **SFO**: Subfornical organ; **PVN**: Paraventricular nucleus of the hypothalamus; **PAG**: Periaqueductal grey area; **A5**: A5 area of the ventrolateral pons; **NTS**: Nucleus tractus solitarii; **RVLM**: Rostral ventrolateral medulla; **CVLM**: Caudal ventrolateral medulla. Plus signs indicate excitatory inputs, minus signs indicate inhibitory inputs.

Situated in the brainstem, the rostral ventrolateral medulla (RVLM) contains important sympathetic vasomotor premotor neurons that are responsible for the

tonic excitatory drive that maintains vasomotor tone as well as heart rate and cardiac contractility (Dampney, 1994; Blessing, 1997; Guyenet, 2006). These neurons, along with others that innervate the kidneys and are able to control sodium retention and renin release, project to the intermediolateral nucleus (IML) in the spinal cord from where they stimulate the preganglionic sympathetic neurons (Ross *et al.*, 1984; Brown & Guyenet, 1985; Morrison *et al.*, 1988; Milner *et al.*, 1988; Lipski *et al.*, 1995; Schreihofer & Guyenet, 1997).

Stimulation of the RVLM greatly increases sympathetic nerve activity (SNA) and BP (Willette *et al.*, 1983; Ross *et al.*, 1984; Guyenet & Brown, 1986; Morrison *et al.*, 1988; Schreihofer *et al.*, 2000). Inhibition of the region has the opposite effect (Schreihofer *et al.*, 2000). More recently, Bukre *et al.*, used an optogenetic approach to selectively stimulate the C1 catecholaminergic neurones of the RVLM and observed cardiorespiratory hypertension (Burke *et al.*, 2014). Abbott *et al.* used a different optogenetic approach and observed "*sizeable sympathoactivation and a rise in blood pressure in response to selective stimulation of the C1 neurones of the RVLM*" (Abbott *et al.*, 2009). The essential role played by the RVLM in BP control is extremely well established (Figure 2).

The C1 neurones are a group of adrenergic neurons situated in the RVLM. Many of the caudal C1 neurones project to higher centres such as the hypothalamus. The rostral C1 neurones are considered sympathetic premotor neurones since they project to the spinal cord and carry efferent sympathetic activity.

The caudal ventrolateral medulla (CVLM) moderates the sympathetic outflow from the RVLM via tonic GABAergic inhibition. Injecting bicuculline into the RVLM in order to inhibit $GABA_A$ receptors markedly increases SNA and BP

(Willette *et al.*, 1984; Kubo & Kihara, 1987; Masuda *et al.*, 1992; Natarajan & Morrison, 1999) and preventing GABA synthesis via injection of 3-mercaptopropionic acid produces the same effect (Kubo & Kihara, 1987). The CVLM is known to contain GABA-containing neurones that project to the RVLM (Minson *et al.*, 1997; Chan & Sawchenko, 1998). Excitation of neurons in the CVLM via injection of glutamate reduces SNA and BP (Willette *et al.*, 1983; Minson *et al.*, 1997). Inhibiting these cells produces the reverse effect (Willette *et al.*, 1983; Natarajan & Morrison, 1999). Conclusively, inhibition of GABA receptors in the RVLM abolishes the effects observed with stimulation or inhibition of upstream neurons in the CVLM (Willette *et al.*, 1984; Blessing, 1988). Goodchild and Moon reviewed evidence demonstrating the involvement of the CVLM in cardiovascular regulation in 2009 (Goodchild & Moon, 2009).

The CVLM receives projections from the Nucleus of the Solitary tract (NTS), located in the dorsal medulla (Aicher *et al.*, 1995). The NTS is a critical component of the autonomic nervous system and is involved in the operation of both sympathetic and parasympathetic regulation of blood pressure. Lesioning of the NTS causes fatal hypertension (Doba & Reis, 1973). This hypertension was characterised by extreme vasoconstriction and was not prevented by prior removal of adrenal glands and kidneys, nor was it due to changes in blood gas concentrations, as these were measured (Doba & Reis, 1973). It was however, blocked by phentolamine, an α-adrenergic receptor antagonist, which suggests that the hypertension was neurogenic (Doba & Reis, 1973). The effect of NTS lesioning was prevented by mid-collicular decerebration, implicating more rostral structures in the hypertensive response, such as the paraventricular nucleus of the hypothalamus (discussed later). The normal reflex bradycardia evoked by intravenous infusion of norepinephrine or angiotensin II was

abolished by NTS lesioning (Doba & Reis, 1973) and sometimes tachycardia was observed. This means that not only was tonic control of baseline BP lost as a result of the lesions, but reflex control in response to acute challenge was lost as well.

The NTS is the site of visceral afferent termination (Andresen & Kunze, 1994) and serves as the point of integration of afferent signals from mechanosensitive baroreceptors located in the carotid sinus and the aortic arch, as well as chemoreceptors, which detect the concentration of oxygen and carbon dioxide along with pH. These are also located at the bifurcation of the common carotid artery and in the aortic arch but exist as 'bodies', separate to the baroreceptors (Pijacka *et al.*, 2018).

The findings from Doba and Reis' paper can partially be explained by the loss of the baroreflex. The baroreflex is an essential negative feedback mechanism for the control of blood pressure. The mechanosensitive baroreceptors are specialised afferents innervating the arterial wall (Blessing, 1997). These afferents project to the NTS and fire action potentials continuously (tonic activity). When the arterial wall is distended due to systole, the rate at which these action potentials are fired increases proportional to the magnitude of the distension. With every beat of the heart, impulses are relayed to the NTS. In the case of the carotid sinus baroreceptors, the signal is sent via the carotid sinus nerve, which is a branch of the glossopharyngeal nerve (IXth cranial nerve). The aortic baroreceptor afferents project to the NTS via the aortic nerve, a branch of the vagus nerve (Xth cranial nerve). Afferents from the carotid and aortic bodies (chemoreceptors) arrive at the NTS together with the baroreceptor afferents via glossopharyngeal and vagal projections, respectively.

There are 2 subdivisions of baroreceptor afferents. Type 1 afferents have myelinated axons, giving them fast conduction velocities. They have pulse modulated discharge patterns and are believed to be involved in the response to sudden changes in BP (Seagard *et al.*, 1990). Blocking these fibres attenuates the baroreflex but overall MAP remains unchanged (Dean & Seagard, 1997).

Type 2 baroreceptor afferents are smaller and have little or no myelination. As a result, they have slow transmission velocities and they discharge with minimal pulse modulation but increase firing as arterial pressure is raised. These afferents are believed to be involved in long-term baseline control of BP around a set point but this remains controversial (Seagard *et al.*, 1990).

When baroreceptors are activated, action potentials are sent to the NTS via the glossopharyngeal and vagal nerves that excite neurons in the NTS which project to and excite (via glutamate) neurons in the CVLM. This results in release of GABA and the resulting inhibition of presympathetic neurons in the RVLM as discussed earlier. There may be an additional sympathoinhibitory pathway from the NTS directly to the IML (Coote & Macleod, 1974; Lewis & Coote, 1995). Baroreceptor inputs to the NTS also activate neurons that project to the nucleus ambiguus and dorsal motor nucleus of the vagus (McAllen & Spyer, 1978; Standish *et al.*, 1995; Jones *et al.*, 1998; Jones, 2001; Llewellyn-Smith & Anthony Verberne, 2011). These nuclei send pre-ganglionic parasympathetic efferents to the heart, reducing heart rate via post-ganglionic neurones located within ganglia on the heart itself (Dampney, 1994).

Neurons projecting from the NTS to the CVLM and operating as part of the baroreflex arc are not the only source of excitatory drive stimulating the CVLM to engage in GABAergic inhibition of the RVLM. Iontophoretic application of

bicuculline to the RVLM causes activation of presympathetic neurons even under conditions in which BP has been lowered to below the threshold for baroreflex activation (Sun & Guyenet, 1985). Further, at low BP, neurons in the RVLM still receive inhibitory post-synaptic potentials despite the lack of baroreflex activation. Microinjection of bicuculline into the RVLM of animals that have had their baroreflex abolished via sinoaortic denervation sill results in an increase in SNA and BP (Kubo & Kihara, 1987; Dampney *et al.*, 1988). From these studies we can conclude that the RVLM receives chronic GABAergic inhibition that is independent of the baroreflex. The fact that inhibition of the CVLM exacerbates the increased SNA and BP caused by sinoaortic denervation or lesioning of the NTS provides evidence that the source of this baroreflex-independent inhibition of the RVLM is the CVLM (Cravo & Morrison, 1993).

Structures in the midbrain are involved in blood pressure control. The neurons of the A5 area of the ventrolateral pons (A5 area) have spinal projections targeting mostly the intermediolateral cell column (Loewy *et al.*, 1979*b*; Byrum & Guyenet, 1987). These neurons are thought to regulate sympathetic outflow, especially in relation to respiration (Koshiya & Guyenet, 1994; Hilaire *et al.*, 2004; Zanella *et al.*, 2006).

The A5 area connects to the NTS, CVLM, RVLM, caudal pressor area and the retrotrapezoid nucleus (which detects CO_2 and pH in order to regulate breathing) in the medulla oblongata, with the medial, Kölliker–Fuse and lateral parabrachial nuclei (which regulate normal respiratory rate) in the pons, and, the PVN and the amygdala in the hypothalamus (Byrum & Guyenet, 1987; Tavares *et al.*, 1997; Sun & Panneton, 2005; Rosin *et al.*, 2006; Abbott *et al.*, 2012).

The fact that the A5 area is associated with these other nuclei suggests a possible role for it in the control of cardiorespiratory activity (Spyer, 1994; Dampney *et al.*, 2003; Taxini *et al.*, 2011). Guyenet *et al.* showed that neurons in the A5 area are excited in response to peripheral chemoreceptor activation due to hypoxia (Guyenet *et al.*, 1993). Increasing blood pressure causes spontaneous activity of A5 neurons to decrease and vice versa (Andrade & Aghajanian, 1982). This suggests that A5 neurones are modulated by visceral afferents controlling cardiorespiratory function.

Various groups have attempted to delineate the specific role A5 neurons play in autonomic regulation. Using methods including microinjection of glutamate agonists and electrical stimulation, several groups observed slight changes in blood pressure (Loewy *et al.*, 1979*a*; Neil & Loewy, 1982; Stanek *et al.*, 1984; Maiorov *et al.*, 1999, 2000). The precise role of the neurons was not clearly established, as it is very difficult to stimulate these neurons selectively, given their small number and sparse distribution within the dorsolateral pons as well as the fact that they are located close to the superior olivary complex, the reticular formation and the trigeminal nerve, neurons from each of which were almost certainly stimulated along with the A5 neurons.

An optogenetic approach has been taken in order to stimulate the A5 neurons specifically (Kanbar *et al.*, 2011). This produced a large but short-lasting increase in renal sympathetic outflow, followed by a short period of inhibition. A similar but considerably smaller effect was observed in the lumbar sympathetic outflow. It is not known whether the A5 area contains mGluR5 but if it does it may be the case that modulation of mGluR5 in this region could

reduce sympathetic outflow from the RVLM and contribute to reducing BP in hypertension.

Another midbrain structure involved in the control of blood pressure is the periaqueductal grey (PAG). The PAG is divided into four regions based upon function. These regions consist of columns that run longitudinally and are defined by their location relative to the fourth ventricle (Figure 3): The dorsomedial PAG (dmPAG), dorsolateral PAG (dlPAG), lateral PAG (lPAG) and ventrolateral PAG (vlPAG).

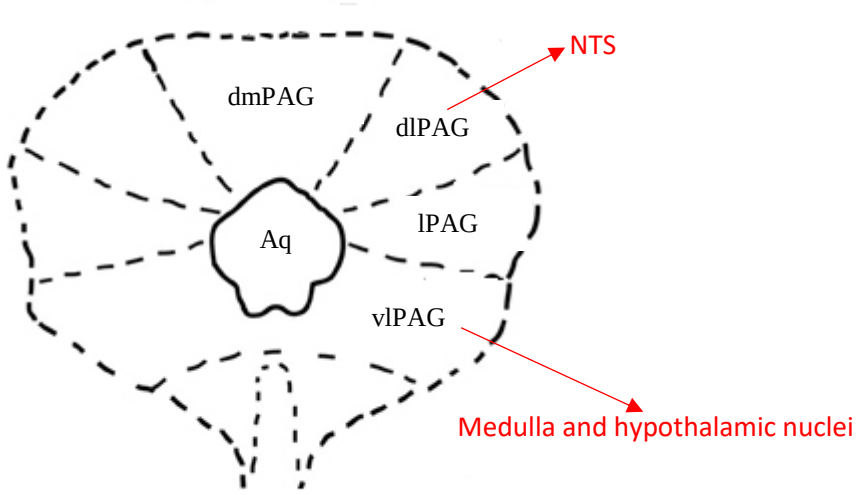

Figure 3: Schematic of a coronal section of the periaqueductal gray area (PAG) of the rat brain showing the various subregions and the cardiovascular control regions their neurones project to. **dmPAG:** Dorsomedial PAG; **dlPAG:** dorsolateral PAG; **lPAG:** Lateral PAG; **vlPAG:** Ventrolateral PAG; **Aq:** Cerebral aqueduct; **NTS:** Nucleus of the solitary tract

The vlPAG contains many neurones that project to key areas involved in the control of blood pressure such as the medulla (Carrive *et al.*, 1988) and hypothalamic nuclei (ter Horst *et al.*, 1984; Uschakov *et al.*, 2009). Stimulation of the vlPAG reduces BP and HR in anaesthetised animals via inhibition of sympathetic premotor neurones in the RVLM (Lovick, 1992; Farkas *et al.*, 1998) and there is some evidence that dorsal PAG is overactive in SHR (Schenberg *et al.*, 1995). Stimulation of the PAG either by chemical or electrical means

facilitates the arterial baroreflex in anaesthetised wild type rats (Inui *et al.*, 1994).

The dorsolateral PAG is known to play a vital role in the "fight or flight" response that is initiated in response to a perceived threat such as a predator. This response is characterised by several immediate changes to cardiovascular and respiratory activity including tachycardia, hyperventilation, increased blood pressure, baroreceptor reflex inhibition and an increase in blood flow to the skeletal muscles (Carrive, 1993; Hayward, 2007; Netzer *et al.*, 2011). Interestingly, due to distinct but parallel circuitry within the PAG, the opposite pattern of cardiovascular and respiratory effects is elicited from the ventrolateral area and under conditions in which a threat is inescapable (Bandler *et al.*, 2000). This generates a "play dead" response and whether it is this response or the "fight or flight" response that is elicited by a threat depends upon activity higher in the cerebrum. Chemical ablation of the dlPAG results in an increase in baroreflex tachycardia but has no effect on reflex bradycardia (Pelosi *et al.*, 2007) suggesting the dlPAG tonically inhibits the baroreflex. The dlPAG is known to contain afferents that project to the NTS (Boscan & Paton, 2005). Taken together, the above evidence demonstrates a role for the PAG, in particular the dlPAG and vlPAG in cardiovascular control.

Sympathetic Nervous System Activity is Elevated in Hypertension:

Increased sympathetic nerve activity has been implicated in the pathogenesis of hypertension. The spontaneously hypertensive rat (SHR) is an animal model of essential hypertension in which sympathetic nerve activity has been shown to be elevated (Judy *et al.*, 1976; Li & Pan, 2007). The same has been observed in hypertensive humans (Anderson *et al.*, 1989; Grassi, 1998; Mancia *et al.*, 1999)

The paraventricular nucleus of the hypothalamus (PVN) is a key region involved in neuroendocrine and cardiovascular homeostasis. (Martin & Haywood, 1992; Coote *et al.*, 1998; Dampney *et al.*, 2005). Lesioning of the PVN in spontaneously hypertensive rats (SHRs) reduces blood pressure (Ciriello *et al.*, 1984; Takeda *et al.*, 1991) and inhibition of the PVN with muscimol, a $GABA_A$ receptor agonist, reduces BP and SNA in these animals (Akine *et al.*, 2003). Interestingly, antagonism of glutamate receptors in the PVN in normotensive rats has little effect on blood pressure or sympathetic activity (Chen *et al.*, 2003; Zahner & Pan, 2005). These findings suggest that glutamatergic signalling in the PVN does not have a large role to play in the tonic regulation of sympathetic vasomotor tone in normotensive animals but may be contributing to the pathological increase in SNA observed in hypertension.

Li and Pan (2007) bilaterally injected AP5, an NMDA antagonist, or CNQX, an AMPA/kainite receptor antagonist, into the PVN and with both drugs, observed a dose-dependent reduction in lumbar SNA, mABP and HR in SHRs but not in Wistar-Kyoto (WKY) normotensive rats. Separately, they also injected gabazine, a $GABA_A$ receptor antagonist into the PVN and found that this increased lumbar SNA, mABP and HR in both SHRs and normotensive WKY rats. Interestingly, this effect was much larger in the normotensive animals than it was in the hypertensives and it was blocked by kynurenic acid, a glutamate antagonist. This work provided further evidence that the elevated sympathetic vasomotor tone observed in hypertension is maintained, at least in part, by tonic glutamatergic signalling in the PVN.

Metabotropic Glutamate Receptor 5 (mGluR5):

Glutamate is the principle excitatory neurotransmitter in the CNS. It acts via both ionotropic receptors, which are ligand gated ion channels which are directly involved in very fast responses such as neurotransmission, as well as metabotropic receptors that act more slowly through a second messenger (Hermans & Challiss, 2001). mGluR5 is a class C metabotropic G-protein-coupled receptor (GPCR) for glutamate. The class C GPCRs have a large extracellular N-terminal sequence containing a hydrophilic ligand-binding region, seven transmembrane domains and a cytoplasmic C-terminal domain with which a G-protein is associated (Bräuner-Osborne *et al.*, 2007) . The G-proteins transduce the signal from the ligand via an intracellular signalling cascade with various end products and effects depending on the protein. mGluRs are divided into 3 groups based on their pharmacology, sequence homology and transduction mechanisms (Niswender & Conn, 2010; Yin & Niswender, 2014). mGluR5, of which there are two isoforms: mGluR5a and mGluR5b, along with mGluR1 are classed as a group 1 mGluRs. mGluR5a dominates in the early post-natal developmental period while mGluR5b is most prevalent in the adult (Minakami *et al.*, 1993; Romano *et al.*, 1996). These receptors are expressed on post-synaptic neuronal membranes and are coupled to $G_{q/11}$, a heterotrimeric G protein subunit that is composed of Gα, Gβ and Gγ (Syrovatkina *et al.*, 2016). When activated via a ligand-induced conformational change in the associated metabotropic receptor, phospholipase C is activated (Harden *et al.*, 2011). This enzyme hydrolyses membrane phosphatidylinositol 4,5-bisphosphate (PIP2), resulting in the formation of inositol 1,4,5-trisphosphate (IP3) and diacylglycerol (DAG) (Essen *et al.*, 1997). IP3 diffuses through the cytosol to IP3 receptors on the endoplasmic reticulum. These

receptors are ligand-gated ion channels for Ca^{2+} and their activation allows calcium to flow from the endoplasmic reticulum into the cytosol (Berridge, 2009). Ca^{2+} activates protein kinase C (PKC), an enzyme family that phosphorylates hydroxyl groups on amino acid residues of other proteins. DAG activates the same enzyme (Matosin *et al.*, 2012). Increased intracellular calcium and the activity of PKC increase the excitability of the cell, making action potentials more likely (Li and Pan, 2014). An overview of mGluR5 signalling is shown in Figure 4:

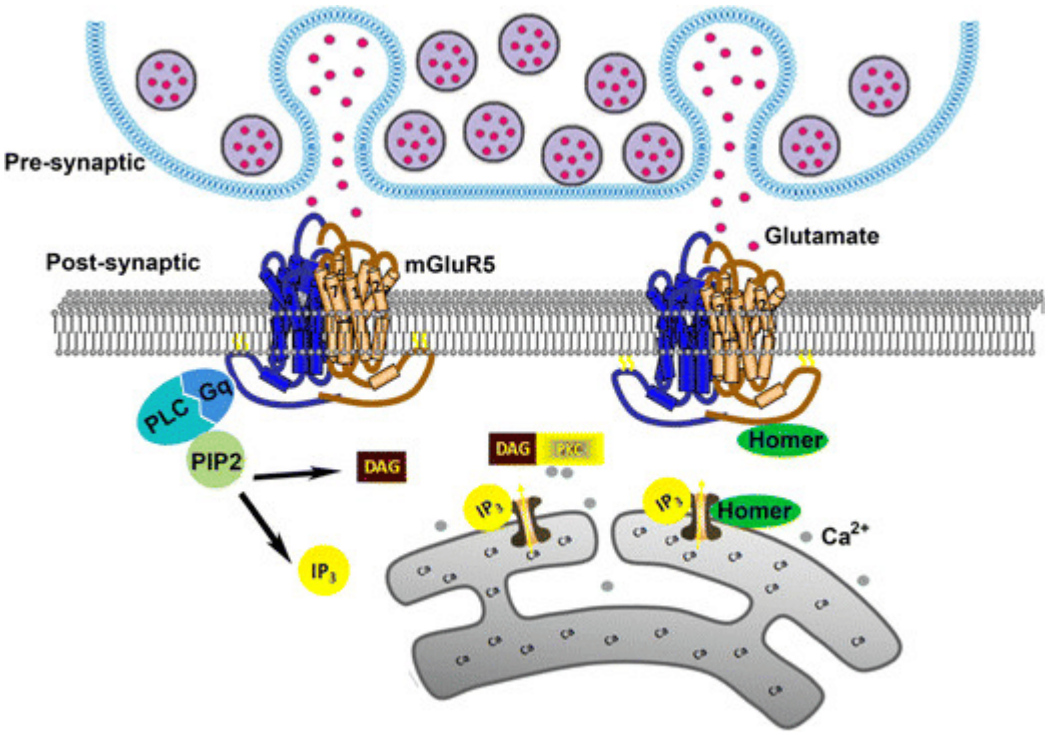

Figure 4: Schematic outlining mGluR5 signalling pathway from Yang *et al.* (2004). mGluR5 = metabotropic glutamate receptor 5, DAG = diacylglycerol, IP3 = Inositol trisphosphate, PKC = Protein kinase C.

The cytosolic C-terminal domain of mGluR5 is bound to Homer proteins. Homer proteins are scaffolding proteins present primarily at the post-synaptic density in neurones throughout the CNS. They can be divided into two

categories; the short form (1a) and the long forms (1b, 1c 2 and 3). The long form Homers are expressed constitutively (Xiao *et al.*, 1998; Soloviev *et al.*, 2000) and multimerize via their c-terminal coiled-coil domains, which in combination with interaction with other scaffolding proteins such as SH3 and multiple ankyrin repeat domains protein (SHANK3), promotes localisation of mGluR5 to the post-synaptic density of the synapse and couples the receptor to its downstream mediators, thereby facilitating synaptic transmission (Kato *et al.*, 1998; Tu *et al.*, 1998; Xiao *et al.*, 1998). The short form 1a variant is expressed in response to synaptic activity (Brakeman *et al.*, 1997; Vazdarjanova *et al.*, 2002). Homer 1a lacks the coiled-coil domain used by the long forms to multimerize and as such is unable to do so. This means that Homer 1a disrupts long form Homer chains and inhibits mGlur5 function (Xiao *et al.*, 2000; Kammermeier & Worley, 2007). Thus, Homer 1a is induced after synaptic activity and acts as a homeostatic mechanism to uncouple mGluR5 and reduce intracellular Ca^{2+} release, thereby preventing excessive neuronal activity and excitotoxicity.

Evidence for involvement of mGluR5 in arterial pressure control specifically in the PVN was demonstrated by Li and Pan (Li & Pan, 2010), when they bilaterally injected specific antagonists for both group 1 mGluRs into the PVN and observed dose-dependent decreases in mABP, lumbar SNA and HR in SHRs but not in WKY rats. The effects were greater with antagonism of mGluR5 compared to mGluR1 suggesting a key role for mGluR5 in particular. Further, injection of the non-specific group 1 mGluR agonist (S)-3,5-Dihydroxyphenylglycine (DHPG) into the PVN caused an increase in mABP, LSNA and HR in both strains of animal. This effect was attenuated with blockade of either mGluR1 or mGLuR5. Also, blocking NMDA receptors in the

PVN via microinjection of AP5, markedly reduced the sympathoexcitatory response evoked by agonism of group 1 mGluRs, suggesting that NMDA receptors mediate this response (Li and Pan, 2010). Figure 5 summarises these findings.

Li *et al.* went on to study NMDA receptor involvement in more detail in cultured neurons harvested from the PVN of WKY rats and SHRs where they blocked post-synaptic NMDA receptors via intracellular dialysis of MK-801, an open-channel blocker of the receptor, and found that this abolished the increase in neuronal firing caused by application of DHPG, supporting post-synaptic NMDA receptors in the sympathoexcitatory effect of mGluR5 stimulation in the PVN. The fact that excitatory post-synaptic current was not affected by application of DHPG further supports this, as it shows that mGluR5 does not mediate glutamate release from presynaptic neurons. Importantly, they also showed that mGluR5 blockade had the same effect in animals that had their blood pressure lowered by celiac ganglionectomy as in animals that underwent sham surgery, suggesting that mGluR5 over activity in SHRs is contributing to hypertension, rather than manifesting as a response to it. They found further evidence for this using western blotting and qPCR on tissue homogenates to show that mGluR5 was upregulated in the PVN and RVLM of SHRs compared to WKY rats.

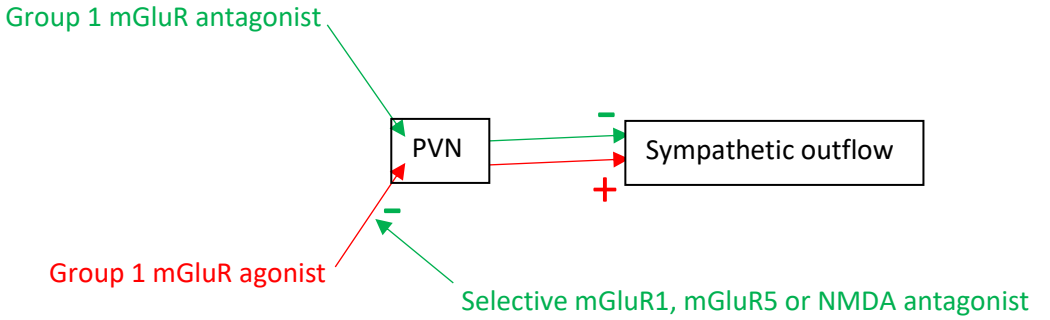

Figure 5: Schematic outlining the evidence obtained by Li and Pan's microinjection experiments (Li and Pan, 2010), which suggests mGluR5 is present in the PVN and plays a role in the control of sympathetic outflow. mGluR: Metabotropic glutamate receptor, PVN: Paraventricular nucleus of the hypothalamus, NMDA: N-methyl-D-aspartate receptor.

The Autonomic Nervous System Modulates the Immune System:

The lymphoid organs are heavily innervated by the autonomic nervous system. In the 1960s, it was observed that vagus nerve stimulation increased Ach release from the spleen (Brandon & Rand, 1961; Leaders & Dayrit, 1965). Watkins *et al.* (1995) later discovered that IL-1β administered intra-abdominally would only cause fever if the vagus nerve was intact, meaning that sensory afferents transmit information regarding the presence of inflammatory molecules to the CNS. Niijima *et al.* (Niijima *et al.*, 1991; Niijima, 1995, 1996) recorded action potentials travelling from the liver to the brainstem via the vagus nerve and discovered that this afferent signal to the brainstem triggered efferent neurotransmission descending to the spleen and thymus. They showed that intra[hepatic]portal injection of IL-1β dose-dependently increased afferent activity in the hepatic branch of the vagus nerve and caused reflex efferent activity in the splenic (sympathetic) and vagal thymic nerves. This activity was eliminated in hepatic vagotomised rats nor was it observed if the cytokine was administered into the systemic venous circulation. From this Niijima *et al.* concluded that there were sensors for IL-1β in the hepatic portal blood and these relayed information regarding IL-1β to the CNS where descending activity was activated (Niijima *et al.*, 1996).

In the early 2000s, it was observed that CNI1493, a cytokine blocker, was only able to block cytokine release if the vagus nerve was intact (Borovikova *et al.*, 2000*a*) and that in animals with induced endotoxaemia, directly stimulating the vagus nerve reduced TNFα synthesis (Borovikova *et al.*, 2000*b*).

This evidence from Watkins *et al.*, Niijima *et al.*, Borovikova *et al.* and other groups was taken together and reviewed by Tracey in Nature in (2002), when the elucidation of neuronal immunological reflexes maintaining homeostasis was considered revolutionary. Tracey wrote that this reflex was mediated by the parasympathetic system (Tracey 2002) but this has since been disproven. The afferent arm of the reflex is humoral and the efferent is sympathetic as outlined below.

Overview of the Inhibitory Inflammatory Reflex:

Inflammation is a critical response to injury or infection. The mobilisation of innate immune cells along with their molecular mediators and their subsequent localisation to the damaged site is the initial phase of healing and pathogen neutralisation. However, if inflammation is excessive or if it is not contained within the locus of the noxious stimuli that initiated it, severe, possibly fatal, tissue damage can occur. The autonomic nervous system provides rapid regulation of the inflammatory response (Waldburger & Firestein, 2010). Its action is complimentary to the slower paracrine signalling by regulatory T cells (T_{reg}), immunosuppressive T cells which downregulate proliferation of effector T cells and the production of pro-inflammatory cytokines in order to curtail the immune response.

The first way in which the autonomic nervous system can regulate inflammation is via the hypothalamic–pituitary–adrenal axis (HPA), through which a signalling cascade results in the release of glucocorticoids from the adrenal cortex, which suppress production of pro-inflammatory cytokines (Besedovsky *et al.*, 1986). This action is global as the glucocorticoids are released into the general circulation.

Activation of the HPA axis occurs as a result of humoral messengers such as inflammatory cytokines and prostaglandins acting in the brain (Besedovsky *et al.*, 1986; Turrin & Rivest, 2004; Saper *et al.*, 2012). The preoptic area, a region of the hypothalamus, is of particular significance for this action.

The other way in which the sympathetic nervous system can control inflammation is via its innervation of the spleen. The spleen is the main source of TNFα (Huston *et al.*, 2006) resulting from injection of lipopolysaccharide (LPS), an endotoxin produced by bacteria and commonly used by researchers to provoke an inflammatory response. The efferent arm of the cholinergic anti-inflammatory pathway innervates this organ (Figure 6).

In response to detection of LPS, neurones in the greater splanchnic nerve are stimulated. This efferent activity stimulates adrenergic splenic neurons situated in the celiac ganglion, which project to the spleen and terminate in structures analogous to synapses in the white pulp (Rosas-Ballina *et al.*, 2011). NA released from the splenic efferents binds to β2 receptors on certain T cells expressing choline acetyltransferase, a crucial enzyme involved in Ach synthesis (Rosas-Ballina *et al.*, 2011).

Ach produced by splenic T cells binds to α7 nAChR on macrophages in the non-lymphoid red pulp and in the marginal zone of the spleen (Rosas-Ballina *et al.*, 2011). Activation of this receptor suppresses NF-κB (Wang *et al.*, 2003), resulting in a down-regulation of cytokine synthesis, thereby reducing inflammation. Mice lacking α7 nAChR are extremely susceptible to generating an inflammatory response as a result of endotoxaemia or adjuvant arthritis (Wang *et al.*, 2003; van Maanen *et al.*, 2010), demonstrating the critical role for this receptor in the control of inflammation.

MacNeil *et al*., (1997) showed that ICV injection of indomethacin, an inhibitor of prostaglandin synthesis, blocked the increase in activity of the splenic nerve that normally occurs as a result of intravenous injections of LPS. This demonstrated that prostaglandin acting in the CNS mediated the reflex activation of the splenic nerve. Partly due to this work, it is thought that along with the HPA, the afferent arm of the cholinergic immune reflex is also humoral, but it has not yet been elucidated. Figure 6 provides an overview of the cholinergic immune reflex:

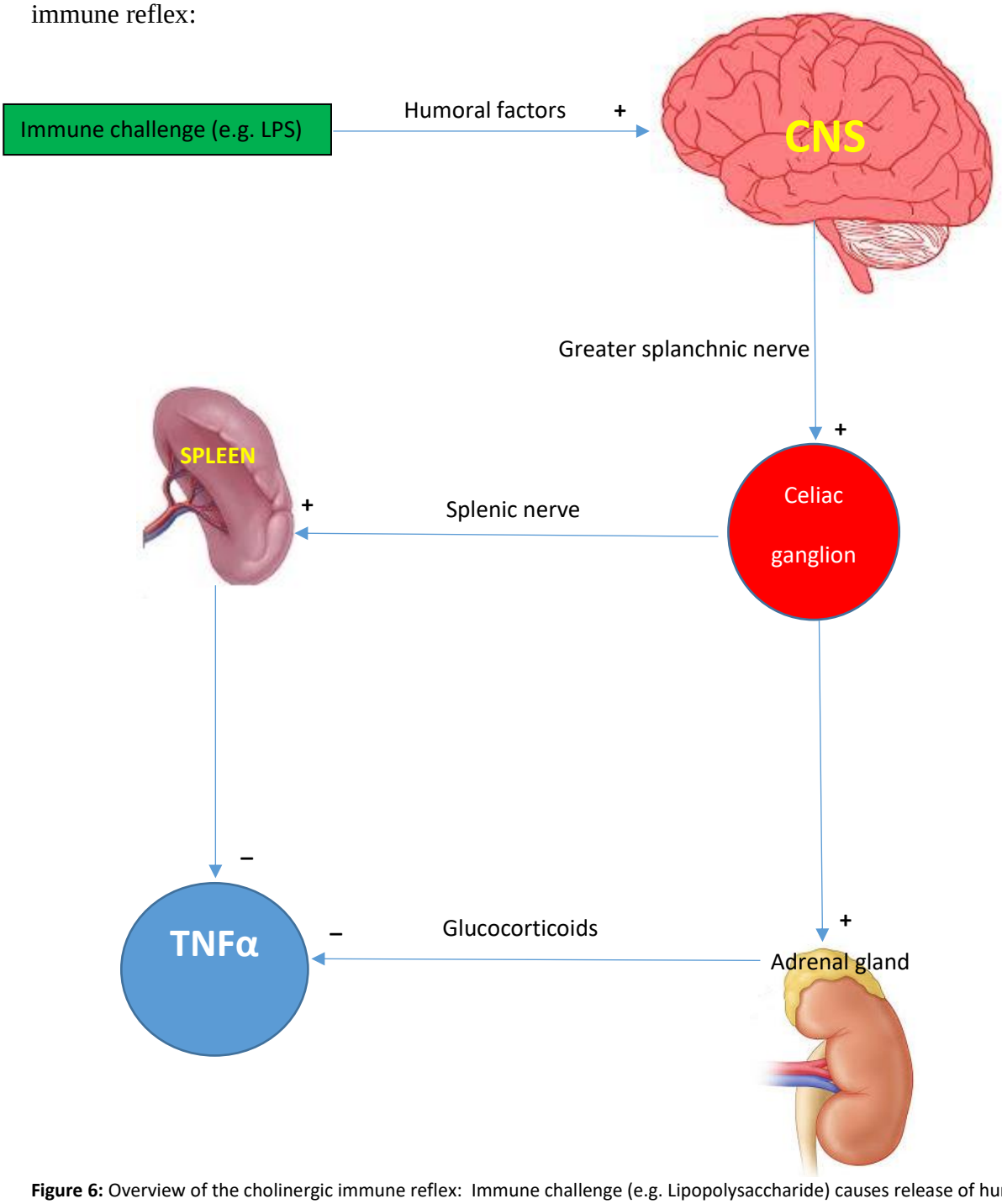

Figure 6: Overview of the cholinergic immune reflex: Immune challenge (e.g. Lipopolysaccharide) causes release of humoral factors which stimulate neurones within the central nervous system, causing the firing of action potentials that are sent via the neurones of the greater splanchnic nerve, exciting (via the celiac ganglion) neurones innervating the spleen and adrenal gland. This downregulates synthesis of TNFα via release of glucocorticoids from the adrenal gland and cholinergic inhibition of $NF_{\kappa}B$ in the spleen. **LPS:** Lipopolysaccharide, **CNS:** Central Nervous system, **TNFα:** Tumor necrosis factor alpha

The Adaptive Immune Response:

In a normal adaptive immune response, antigen-presenting cells collect non-self proteins (e.g. those of viruses) and process them into peptides such that the immunogenic region of these proteins can be externalised and presented to T-cells for potential recognition by unique receptors.

Helper T cells are mostly activated by antigen presentation from dendritic cells. These antigen-presenting cells process antigens in phagosomes (specialised vesicles containing hydrolytic enzymes) and present the antigenic peptide within major histocompatibility complex II (MHC II). The cells then migrate to secondary lymph organs (e.g. lymph nodes and the spleen) where they await an interaction with a T cell that has a receptor that is complementary to the peptide in question. This interaction, along with other interactions between co-stimulatory molecules expressed on the antigen-presenting cell and the T cell, begin an immunological signalling cascade resulting in effector T cell proliferation and differentiation, cytokine production, evacuation from secondary lymph organs, mobilisation into the blood stream and homing to sites of inflammation in the periphery via chemotaxis. Dendritic cells are not the only antigen-presenting cells. Other cells with this ability include macrophages, B-cells and activated endothelial cells (Pober *et al.*, 2001; Gelin *et al.*, 2009).

Helper T cells interact with B cells and promote the production of antibodies (Jr *et al.*, 2001). Cytotoxic T cells do not interact with B cells and are not involved in promoting antibody synthesis but are able to produce molecules such as granzymes and perforin both of which destroy other cells directly. They also secrete cytokines that orchestrate the immune response.

Helper T Cell Activation, Differentiation and the Resulting Cytokine Profile:

Helper T cells activation results in their differentiation into TH_1, TH_2 and the more recently discovered TH_{17} subtypes, each with the capability to secrete different combinations of cytokines. Depending on the invading pathogen, helper T cells will differentiate into the relevant subtype in order to facilitate the production of appropriate cytokines required for an effective response.

TH_1 cell differentiation is triggered by IL-2 and the cells produce IFN-γ, IL-2 and TNF-α. These cells are involved in inflammation resulting from invasion of pathogens such as viruses, intracellular bacteria and protozoa. They are also involved in auto-immune pathology (Notley *et al.*, 2008; Fletcher *et al.*, 2010). Their cytokines target macrophages, CD8+ cytotoxic T cells, IgG B cells and dendritic cells. IFN-γ is able to inhibit viral replication directly, activates the phagocytic functions of macrophages and causes nitric oxide synthase to produce cytotoxic ROS. It also increases expression of MHC class II in dendritic cells in order to facilitate antigen presentation.

The TH_1 subset is thought to be involved in hypertension as it is involved in other inflammatory conditions. The T cells in atherosclerotic plaques are TH_1-polarised (Gisterå & Hansson, 2017). Enteracept, which inhibits the TNF-α secreted by TH_1 cells, blocks vascular dysfunction and hypertension caused by ANG II infusion (Guzik *et al.*, 2007). Chronic enteracept treatment prevents the development of hypertension in fructose-fed rats (Tran *et al.*, 2009). Infusion of ANG II increases differentiation of helper T cells to the TH_1 subtype (Shao *et al.*, 2003). This is known as TH_1 polarisation. Human patients with essential hypertension have elevated levels of circulating interferon-gamma-inducible

protein 10 (Stumpf *et al.*, 2011), which is indicative of TH_1 polarisation of helper T cells, since this, as its name suggests, is induced by IFN-γ, which is a hallmark secretion of TH_1 cells.

TH_2 cells specialise in combating extracellular parasites such as helminths and are involved in allergic reactions (Lloyd & Hessel, 2010). Differentiation of CD4+ T cells into this subtype is triggered by IL-4 and this cytokine is produced by TH_2 cells in a positive feedback loop in order to amplify differentiation. The TH_2 subtype also secretes interleukins 5, 9, 10 and 13. Their effector cells are B cells (production of IgE antibodies), as well as mast cells, basophils and oesinophils.

TH_{17} cells produce IL-17, IL-21 and IL-22. IL-17 is also produced by NK cells, mast cells and neutrophils (Witowski *et al.*, 2004). Chronic infusion of ANG II markedly increases the percentage of helper T cells of the TH_{17} subtype and increased vascular levels of IL-17 (Madhur *et al.*, 2010). Genetically modified mice lacking IL-17 exhibit reduced vascular dysfunction and a lesser hypertensive response when infused with ANG II (Madhur *et al.*, 2010). Also, the vascular accumulation of leukocytes normally seen as a result of ANG II infusion was all but eliminated in these animals. This evidence strongly implicates IL-17 and thereby TH_{17} cells in hypertension. Daily intraperitoneal injection of IL-17 promotes endothelial dysfunction and hypertension in mice (Nguyen *et al.*, 2013). IL-17 is a major contributor to the pro-inflammatory cytokine milieu that promotes vascular dysfunction and thereby hypertension.

Activated helper T cells produce pro-inflammatory cytokines and contribute to hypertension. Regulatory T cells, which act to suppress the immune response by

dampening induction of effector (activated) T cells and T cell proliferation, protect against hypertension in rats (Viel *et al.*, 2010).

The Sympathetic Nervous System Modulates Helper T Cell Differentiation and Promotes a Pro-Inflammatory, Pro-Hypertensive Cytokine Profile in Hypertension:

Both primary (thymus and bone marrow) and secondary (spleen and lymph nodes) lymphoid organs receive sympathetic innervation and almost all cells of both the innate and adaptive immune systems express receptors for neurotransmitters and neurohormones (Nance & Sanders, 2007). Immune cells express adrenergic β receptors. T lymphocytes preferentially express the β2 subtype but β1 are also expressed (Sanders & Straub, 2002). Through these receptors, the sympathetic nervous system is able to modulate the immune response by affecting clonal expansion, cell migration and cell trafficking (Sanders & Straub, 2002; Steinman, 2004; Bellinger *et al.*, 2008).

NA can modulate polarisation of naïve helper T cells to the TH_1 subtype, resulting in either an increase or decrease in polarisation depending on the presence of other cytokines (Swanson *et al.*, 2001). These effects are prevented by blockade of β2 adrenorecptors (Swanson *et al*., 2001).

Mice that are deficient in dopamine β hydroxylase, an enzyme that catalyses the conversion of dopamine into NA, exhibit impaired TH_1 polarisation when infected with *listeria monocytogenes*, an intracellular bacterial pathogen to which TH_1 polarisation is the appropriate response. (Alaniz *et al.*, 1999).

Chronic systemic infusion of catecholamines causes atrophy of the spleen and reduces the number of T cells it contains. It also decreases the percentage of

cells of the cytotoxic and regulatory subsets (Harris *et al.*, 1995). These effects were blocked by propranolol, a β adrenoreceptor antagonist.

Helper T cells were activated and T cell infiltration into the aorta was increased by chronic infusion of NA (Marvar *et al.*, 2010).

Patients with chronic heart failure who were treated with beta-blockers (β adrenoreceptor antagonists) or ACE (angiotensin converting enzyme) inhibitors had a decreased ratio of TH_1/TH_2 cytokines (Gage *et al.*, 2004). This means that modulating the effects of sympathetic outflow can affect the cytokine milieu and thereby regulate inflammation. It is possible that the therapeutic effects of these drugs manifest partly as a result of immunomodulation in addition to their known effects on heart rate, blood volume, peripheral resistance etc.

Reactive Oxygen Species in Hypertension:

Previously thought to be exclusive to phagocytic cells of the innate immune system, T cells also produce reactive oxygen species (ROS), which eliminate pathogens (Rashida Gnanaprakasam *et al.*, 2018). ROS are metabolites of oxygen that are able to either steal electrons away from other molecules (oxidise them) or donate electrons to them (reduce them). One important ROS in cardiovascular physiology is superoxide. This is formed by the one-electron reduction of molecular oxygen (Buettner, 2011). This ROS has an unpaired electron in its outer orbit and as such it is deemed a radical. Superoxide is important because of its versatility as it is able to both oxidise and reduce other physiological molecules (Buettner, 2011). It is also a progenitor for other reactive oxygen species including the hydroxyl radical ($HO^{\cdot}$) (Buettner, 2011).

Physiological levels of ROS in the vasculature are essential for endothelial homeostasis and smooth muscle cell contraction (Touyz *et al.*, 2018). However,

overproduction of ROS or failure of normal elimination mechanisms (such as reduced superoxide dismutase, an enzyme that degrades superoxide) causes vascular dysfunction and disease via vascular remodelling. This occurs as a result of direct damage to cells, lipid peroxidation, recruitment of immune cells, activation of metalloproteinases and deposition of extracellular matrix (Vara & Pula, 2014; Raaz *et al.*, 2014; Konior *et al.*, 2014).

ROS are produced by: NADPH oxidase, uncoupled NO synthases, xanthine oxidases, cyclooxygenases and components of the mitochondrial electron transport chain (Granger & Kvietys, 2015). The most important source of ROS relating to cardiovascular physiology is NADPH oxidase, which is largely found in phagocytic cells of the immune system but is also present in T cells (Jackson *et al.*, 2004) and vascular endothelial cells, where it plays a functional role in normal cell signalling as well as pathophysiological activity (Burtenshaw *et al.*, 2017).

ANG II, aldosterone and various cytokines all cause the production of ROS via activation of NADPH oxidase, which contributes to the generation of hypertension. T cells possess AT1 receptors and ANG II stimulates T cell proliferation via these receptors (Nataraj *et al.*, 1999). The NADPH oxidase present in T cells becomes functional when T cells are activated (Jackson *et al.*, 2004), resulting in rapid ROS generation.

ROS that are produced by NADPH oxidase have been shown to play a crucial role in hypertension. Mice lacking $p47^{phox}$, a critical component of NADPH oxidase, exhibit a severely blunted hypertensive response to infusion of ANG II. In this study, superoxide production in vascular smooth muscle cells and the

endothelium was markedly increased following ANG II infusion in WT mice, but not in the p47$^{phox\ -/-}$ *animals* (Landmesser *et al.*, 2002).

Similarly, Matsuno *et al.* demonstrated that unlike WT controls, mice lacking Nox1, another component of NADPH oxidase, did not exhibit the increased vascular superoxide production or increase in blood pressure expected as a result of ANG II infusion (Matsuno *et al.*, 2005). In contrast, mice overexpressing Nox1 were sensitised to ANG II-induced hypertension (Dikalova *et al.*, 2005).

Nitric oxide (NO) is produced by a nitric oxide synthase enzyme located in the vascular endothelium (i.e. eNOS) and acts as a potent vasodilator via a signalling cascade within vascular smooth muscle cells. Superoxide reacts with endogenous NO, producing inactive nitrite and nitrate, depriving the vasculature of a crucial anti-hypertensive mechanism (Gryglewski *et al.*, 1986). This is one of a variety of ways in which ROS are known to promote hypertension.

Production of superoxide results in the formation of highly reactive γ-ketoaldehydes from the H2-isoprostane pathway (Davies *et al.*, 2004). γ-ketoaldehydes affect protein function by adducting to lysine residues (oxidative modification) and causing excessive crosslinking. Formation of such adducts has been observed at an increased rate in conditions with which oxidative stress is associated (Salomon *et al.*, 2000; Roychowdhury *et al.*, 2009; Davies *et al.*, 2011). As a result of hypertensive challenges, these adducts accumulate in dendritic cells and cause increased production of pro-inflammatory cytokines such as IL-6, IL-1β, and IL-23 (Kirabo *et al.*, 2014), as well as increased expression of co-stimulatory proteins that are involved in activation of T-cells. These changes in dendritic cells result in the proliferation of T cells (especially cytotoxic T cells), their production of IFN-γ , IL-17 and TNFα and as a result,

hypertension (Kirabo *et al.*, 2014). These pathophysiological consequences of hypertensive challenges are alleviated by compounds that scavenge γ-ketoaldehydes (Kirabo *et al.*, 2014).

In addition to this known pro-inflammatory, pro-hypertensive activity of ROS, it has been hypothesised (Harrison *et al.*, 2011) that oxidative stress could result in the modification of endogenous proteins such that they are no longer recognised as self (i.e. 'neoantigen' formation) and that this could lead to a chronic pathological auto-immune response which contributes to the generation of hypertension or the exacerbation of existing hypertension (Figure 7).

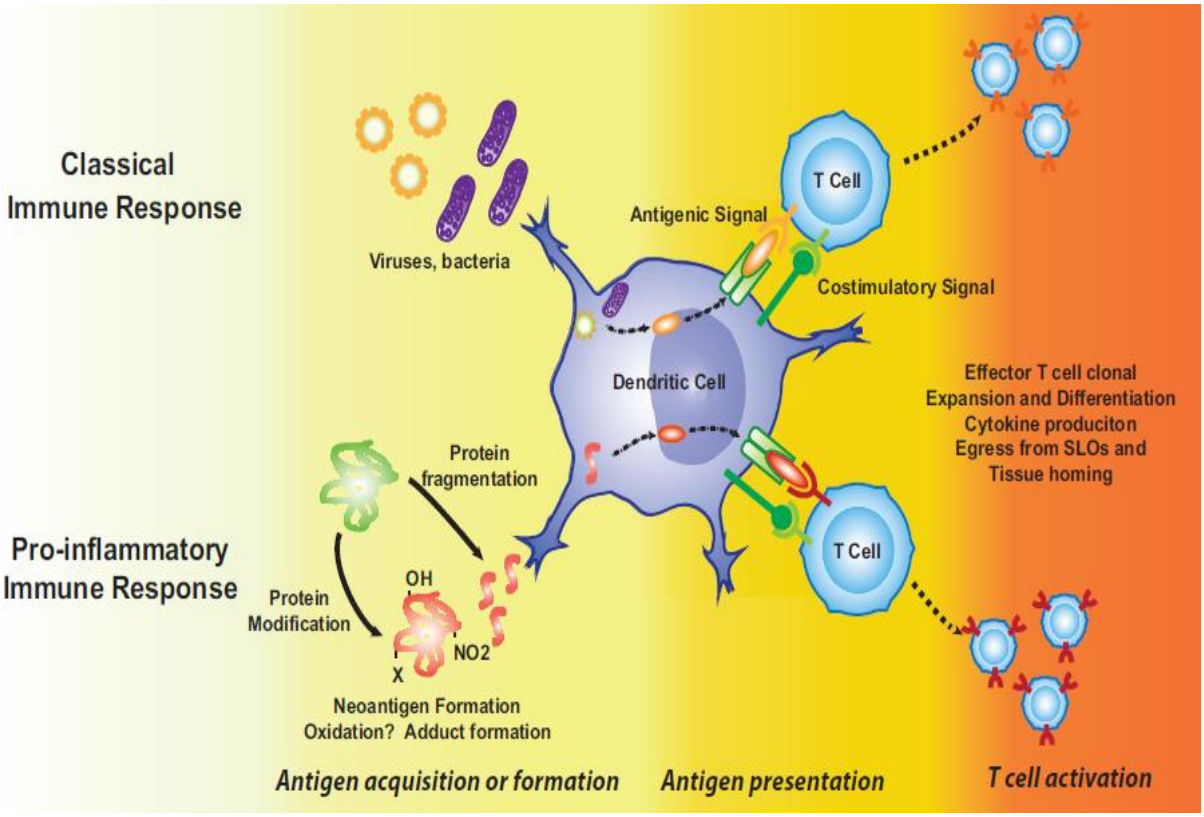

Figure 7: Schematic outlining the neoantigen hypothesis of hypertension (Harrison *et al.*, 2011). In a classical immune response, antigen-presenting cells such as dendritic cells recognise the non-self proteins (antigens) expressed by pathogens and activate T cells, resulting in appropriate and useful inflammation. Harrison *et al.* hypothesise that interactions between endogenous proteins and reactive oxygen species result in the modification of said proteins such that they are no longer recognised as self and thereby cause pathological inflammation via inappropriately triggering the classical inflammatory pathway. These modified endogenous proteins are deemed 'neoantigens'.

This hypothesis is important to this thesis and will be discussed more later.

T Cells Play a Critical Role in Hypertension:

Many studies have demonstrated a role for the adaptive immune system and specifically T cells in hypertension:

- Svendsen demonstrated, using a DOCA-salt model of hypertension, that although the initial phase of hypertension was unchanged, the chronic phase was blunted in animals that had their thymus removed (Svendsen, 1976).
- Systemic administration of activated T cells to patients with metastatic melanoma of the lung increased blood pressure (Balsari *et al.*, 1986). Preeclampsia (pregnancy-induced hypertension) is associated with immune system activation (Minagawa *et al.*, 1999).
- Suppression of the adaptive immune system lowers blood pressure in animal models of hypertension and in humans. Blood pressure can be reduced in SHRs by reducing immune cell infiltration into the kidneys (Rodríguez-Iturbe *et al.*, 2002) and the use of corticosteroids to suppress the immune system protects against ANG II-induced renal damage in rats (Muller *et al.*, 2002).
- AIDS patients, who have reduced helper T cells have a significantly lower incidence of hypertension as a population than population-matched controls whereas anti-retroviral therapy increases the rate of those with hypertension to that of the control population (Seaberg *et al.*, 2005).
- Mycophenolate mofetil (an immunosuppressant normally used for preventing transplant rejection) prevented renal damage and lowered BP in a rat model of salt-sensitive hypertension (Tian *et al.*, 2007).

> Hypertensive patients who were prescribed the same drug for the purpose of treating severe auto-immune skin conditions, saw their blood pressure lowered as a side effect (Herrera *et al.*, 2006).

In 2007, Guzik *et al.* clearly demonstrated an essential role for T cells, in the genesis of hypertension (Guzik *et al.*, 2007). They showed that the expected hypertension caused by chronic low-dose ANG II infusion is markedly reduced in mice in which the recombinase-activating gene 1 has been genetically deleted (RAG-$1^{-/-}$ mice). As a result, these animals lack both T and B cells, but expression of vascular AT1 receptors was shown to be normal, as was the vasoconstrictor response to acute high dose ANG II administration (Guzik *et al.*, 2007). This suggests that the reduced hypertensive response to ANG II challenge in the RAG-$1^{-/-}$ mice was not due to signalling problems or limited receptor availability but loss of the AT1R response mediated by T cells. Guzik also found reduced vascular superoxide production in RAG-$1^{-/-}$ mice even during ANG II infusion. Further, ANG II infusion had a minimal effect on endothelium-dependent vasodilation in RAG-$1^{-/-}$ mice and the vascular hypertrophy commonly associated with hypertension was significantly reduced in these animals compared to in the WT (Guzik *et al.*, 2007). Vascular hypertrophy can be secondary to or exacerbated by hypertension, but ANG II can directly cause vascular smooth muscle cell hypertrophy independently of hypertension/haemodynamics (Morishita *et al.*, 1994; Cai *et al.*, 2003) and it is the attenuation of this direct effect in RAG-$1^{-/-}$ mice that is evident in the Guzik study. These findings demonstrate that several major consequences of ANG II-induced hypertension are mediated via lymphocytes. Marvar *et al.* showed that

RAG-1$^{-/-}$ mice are also protected from stress-induced hypertension and the T cell activation and vascular inflammation that accompany it (Marvar *et al.*, 2012).

Crucially, Guzik *et al.* found that adoptive transfer of T but not B lymphocytes into RAG-1$^{-/-}$ mice restored hypertension and vascular superoxide production caused by ANG II infusion to the same levels observed in WT controls (Guzik *et al.*, 2007) and Marvar *et al.* found that T cell restoration restored the hypertensive response to stress (Marvar *et al*., 2012). Also, Ach-mediated vasodilation was impaired in RAG-1$^{-/-}$ mice after T cells were restored (Guzik *et al.*, 2007). These findings clearly implicate T cells specifically in the genesis of hypertension and the associated vascular dysfunction and superoxide overproduction.

The hypertension caused by ANG II infusion can be blocked by antagonism of AT1 receptors. Guzik *et al.* (2007) demonstrated that the AT1 receptors present on T cells are partially responsible for the generation of hypertension resulting from chronic ANG II infusion, since adoptive transfer of T cells from AT1$^{-/-}$ mice into RAG-1$^{-/-}$ mice did not fully restore hypertension in the RAG-1$^{-/-}$ mice to levels observed in WT controls. The same effect was observed when T cells from mice lacking the p47^{phox} subunit of NADPH oxidase were transferred into RAG-1$^{-/-}$ mice (Guzik *et al.*, 2007). This provides further evidence that ANG II is able to activate NADPH oxidase via AT1 receptors and that superoxide production by T cells is pro-hypertensive.

Not only do T cells promote hypertension as a result of systemically produced ANG II (via ACE in the lungs) but they also have their own internal renin-angiotensin system (Jankowski *et al.*, 2005). Thus, T cells produce their own ANG II. The majority of AT1 receptors expressed by T cells are cytosolic (Hoch

et al., 2009) and ANG II produced by the cells is involved in intracrine as well as autocrine signalling that modulates cell function as outlined in Figure 8:

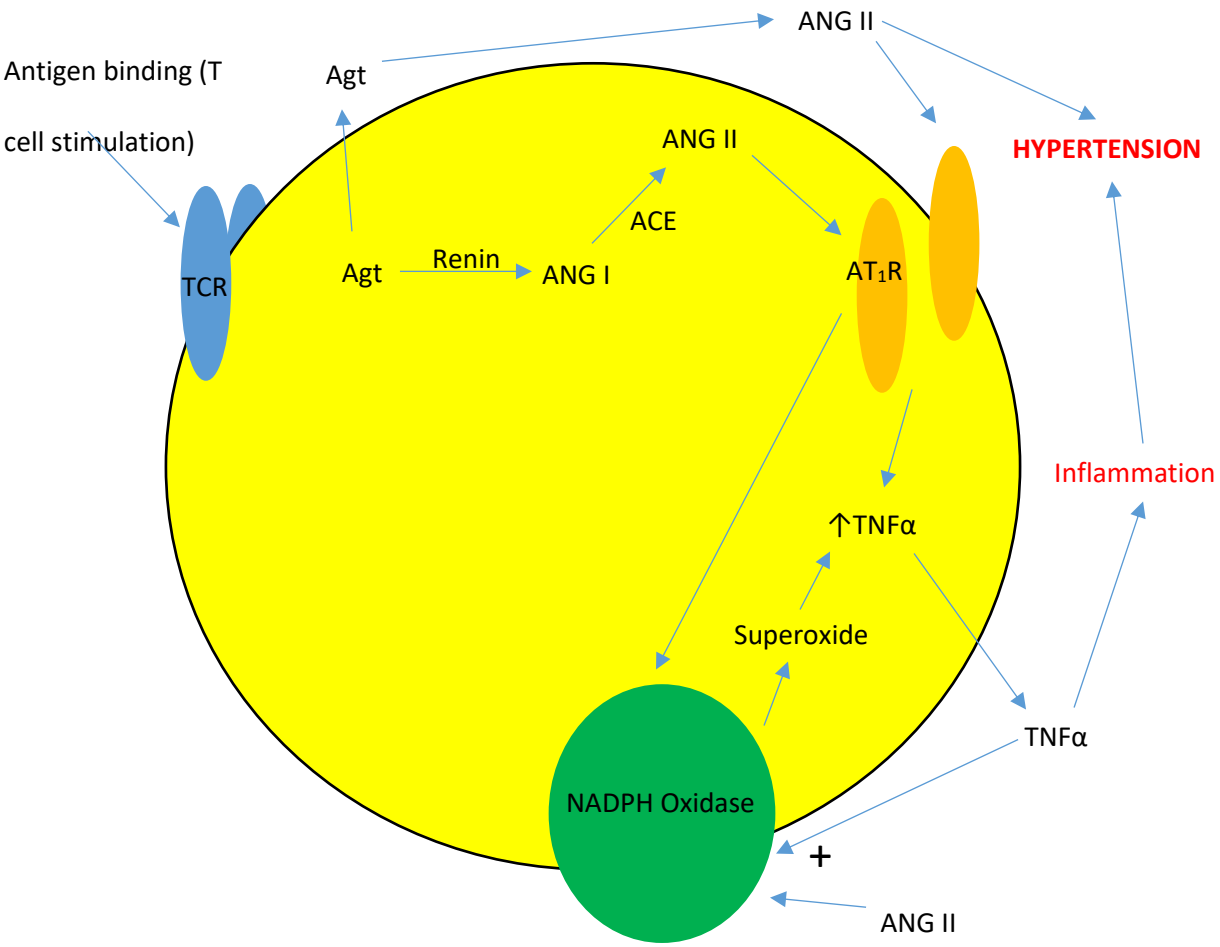

Figure 8: Schematic showing the angiotensin system within T cells and outlining the relationship between ANG II, NADPH oxidase, TNFα, ROS and hypertension. Agt = Angiotensinogen, ANG I = Angiotensin I, ANG II = Angiotensin II, ACE = Angiotensin converting enzyme, AT_1R = Angiotensin II receptor type 1, TCR= T cell receptor, TNFα = Tumor necrosis factor alpha.

T cell production of TNFα and IFNγ is increased following 2 weeks of ANG II infusion in WT but not in $p47^{phox-/-}$ mice (Guzik *et al.*, 2007), showing that both cytokines are produced as a result of NADPH oxidase activity stimulated by ANG II. Etantercept (an inhibitor of TNFα) prevented the hypertensive response to ANG II infusion in WT mice and vastly reduced the increase in vascular superoxide production (Guzik *et al.*, 2007). A neutralising anti-IFNγ antibody

did not have a significant effect on either (Guzik *et al* 2007), suggesting a critical pro-hypertensive role for TNFα in particular.

It is important to note that the pathway outlined above is not the only source of TNFα or superoxide produced by T cells. ACE inhibitors, angiotensin receptor antagonism and scavenging of superoxide only reduced TNFα production by between 30-60% (Hoch *et al.*, 2009), meaning that the cells have alternative means of production that are independent of ANG II and account for a substantial proportion of their output of these products.

Systemic administration or injection of TNF-α into various key nuclei involved in blood pressure control such as the RVLM and the PVN increases sympathetic nerve activity and blood pressure in rats (Zhang *et al.*, 2003). The fact that either central or peripheral administration elicits these effects shows that cytokines can act upon central signalling pathways either via the CVOs or perhaps via soluble mediators such as prostaglandins (Zhang *et al*., 2003). It may also be the case that cytokines that cannot normally cross the BBB are able to do so in hypertension due to the disruption of the barrier (Shi *et al.*, 2014).

Other cytokines have been shown to affect sympathetic output as well. IL-6 microinjected into the NTS attenuates baroreceptor function in rats (Takagishi *et al.*, 2010) and intracerebroventricular administration of the same cytokine increases splenic nerve activity (Helwig *et al.*, 2008). Monocyte chemoattractant protein-1 is upregulated in the NTS of SHR (Waki *et al.*, 2008). IL-1β administered centrally increases splenic, adrenal and renal sympathetic outflow (Niijima *et al*., 1991).

TNF-α, IL-6 and IL-1β are all elevated in the SHR, along with vascular inflammation. Candesartan, an AT_1 receptor blocker, lowers levels of all three

cytokines as well as vascular inflammation and BP (Ando *et al.*, 2004; Sanz-Rosa *et al.*, 2005).

TNF-α and IL1-β cause perivascular macrophages at the BBB to release prostaglandin E2, which is soluble and enters the brain parenchyma, stimulating neurons in the PVN and increasing sympathetic drive (Felder, 2010). Both cytokines increase the rate of neuronal firing by activating NF-κB (Kang *et al.*, 2009). Intracerebroventricular infusion of pyrrolidine dithiocarbamate (an NF-κB inhibitor) reduces ANG-II induced hypertension and pro-inflammatory cytokines in the PVN (Kang *et al*., 2009).

TNF-α, C-reactive protein, monocyte-chemoattractant protein 1, IL-6 and various adhesion molecules such as P-selectin and ICAM-1 have been shown to be elevated in hypertensive patients (Koh *et al.*, 2003; Fliser *et al.*, 2004) and drugs that inhibit the RAS system reduce these as well as BP (Fliser *et al*., 2004; Koh *et al.*, 2003). Receptors for cytokines are located in many cell types in the brain including neurones, astrocytes and microglia (Utsuyama & Hirokawa, 2002). Also, cytokines are able to activate inducible nitric oxide synthase and the NO produced can diffuse to adjacent tissues and affect ion-channel function, resulting in modulation of neuronal activity (Li *et al.*, 2004)

These studies provide evidence that cytokines produced by T cells, or the phagocytic cells attracted by them can promote hypertension directly, as well as by promoting pro-hypertensive behaviour of leukocytes such as endothelial binding/extravasation and ROS production.

It has been noted that in hypertension, T cells accumulate in the kidneys (Harrisson *et al.*, 2011). These increase sodium retention and are responsible for causing vascular dysfunction through the release of pro-inflammatory cytokines

(Trott & Harrison, 2014). Wilcox proposes that ROS produce a NO deficiency in the kidney, leading to increased sodium retention and thereby hypertension via increased total blood volume (Wilcox, 2005)

Activation of T Cells is Driven by Sympathetic Outflow Resulting From ANG-II Induced Oxidative Stress in the CVOs:

Owing to the incomplete formation of the BBB at the CVOs, they are exposed to circulating ANG II and this results in increased production of ROS, especially in the subfornical organ (Zimmerman *et al.*, 2004). Zimmerman *et al.* report that adenoviral-mediated delivery of cytoplasmically targeted superoxide dismutase selectively to this site, eliminates the hypertension invoked as a result of infusion of ANG II into the CNS as well as the increased production of superoxide in the subfornical organ that was associate with it.

(Lob *et al.*, 2010) produced a genetically modified mouse in which they were able to acutely delete superoxide dismutase in the CVOs. Deletion of the enzyme raised BP by 20mmHg and markedly sensitised the animals to hypertension caused by low-dose ANG II infusion. The vascular inflammation associated with ANG II infusion was significantly increased in these animals, as was the percentage of T cells of an activated phenotype. These effects were associated with an increase in sympathetic outflow (Lob *et al.*, 2010). The same group also acutely deleted $P22^{phox}$ (an essential subunit of NADPH oxidase) in the same region and the same effects were observed in response to ANG II infusion as with superoxide dismutase deletion (Lob *et al.*, 2013), confirming that increased ROS signalling in the subfornical organ mediates increased sympathetic nerve activity and lymphocyte activation evoked in response to ANG II in the CNS. These findings fit with the evidence presented by Ganta *et*

al., who found that intracerebroventricular administration of ANG II increases splenic expression of pro-inflammatory cytokines responsible for T cell activation and that this effect was blocked by lesioning of the splenic nerve (Ganta *et al.*, 2005). In keeping with this is the fact that intracerebroventricular injection of a superoxide scavenger reduces blood pressure and sympathetic drive in a rat model of salt-induced hypertension (Fujita *et al.*, 2012). Further, lesioning of the anteroventral third cerebral ventricle, a region that includes the subfornical organ, blocks ANG II induced hypertension together with the associated peripheral T cell activation and vascular inflammation (Marvar *et al.*, 2010).

There is evidence that inflammation caused by ANG II also occurs downstream of the CVOs, in the PVN. Kang *et al.* showed that pro-inflammatory cytokines, ROS and NF-κB activation are increased in the PVN in response to intravenous ANG II infusion (Kang *et al.*, 2009). These effects were blocked by central (3rd ventricle) co-administration of compounds that blockade AT_1 receptors, NF-κB and superoxide. These interventions also restored BP and sympathetic activity to normal in ANG II infused rats (Kang *et al.*, 2009), demonstrating the importance of this signalling in ANG II-induced hypertension. Further, intracerebroventricular administration of minocycline (an anti-inflammatory antibiotic) significantly reduced BP, cardiac hypertrophy and plasma NA in response to ANG II infusion in rats (Shi *et al*., 2010). This was associated with reduced microglia activity and mRNAs for a variety of pro-inflammatory cytokines in the PVN. Overexpression of the anti-inflammatory IL-10 had the same effect and administration of the pro-inflammatory IL-1β, the opposite (Shi *et al.*, 2010). This demonstrates a role for microglia and pro-inflammatory cytokines in ANG II-induced hypertension.

Leukocyte-Endothelial Interactions and Pathological Leukocyte Extravasation in the Brain:

Evidence has accumulated supporting the notion that inflammation in the microvasculature of the brain contributes to hypertension.

Ando *et al.* showed that AT_1 receptor expression was increased in endothelial cells of the brain microvasculature of SHRs (Ando *et al.*, 2004). The pathological vascular hypertrophy associated with hypertension was reversed by chronic administration of candesartan, an AT_1 receptor antagonist. Further, following the candesartan treatment, ICAM-1 (adhesion protein involved in immune cell recruitment) expression was decreased and as a result of this, macrophage infiltration into brain vessels of the SHRs was reduced (Ando *et al.*, 2004). This study provides evidence that inflammation in the brain microvasculature results from the activity of the sympathetic nervous system and that blockade of this activity can mitigate hypertension.

ANG II promotes leukocyte-endothelial interaction, which promotes inflammation (Zhang *et al.*, 2010). Junctional adhesion molecule-1 (JAM-1) forms the tight junctions between adjacent endothelial cells and is considered to be a constituent component of the BBB (Huber *et al.*, 2001). It is involved in the facilitation of leukocyte transmigration (Del Maschio *et al.*, 1999) and is associated within endothelial cells of the brainstem microvasculature. JAM-1 (Waki *et al.*, 2007), and glycoprotein precursor 39 (gp39) (Waki *et al.*, 2008) expression is increased in the NTS of SHR compared to normotensive controls, both in juveniles prior to the development of HT and in adults when it is fully established. This indicates a causative role for these proteins. Over-expression of JAM-1 in the NTS of normotensive WKY rats causes hypertension, localised

inflammation and an increase in sympathetic outflow to the peripheral vasculature (Waki *et al.*, 2008), further evidencing the pro-hypertensive role for JAM-1.

Adhesion of leukocytes to vascular endothelial cells is increased in the brainstem microvasculature of SHRs compared to normotensive WKY rats (Waki *et al.*, 2007) and the same phenomenon was demonstrated previously in the peripheral vasculature (Fukuda *et al.*, 2004). The induced HT and sympathetic activity increase resulting from JAM-1 overexpression occurred alongside leukocyte adhesion to the vascular endothelium which was not occurring prior to the intervention (Waki *et al.*, 2007). It is likely that leukocyte invasion into these vessels causes the observed HT. ROS and some of the cytokines that are produced by leukocytes are able to cross the BBB (Banks, 2005).

Monocyte chemoattractant protein 1 (a pro-inflammatory chemoattractant) expression is increased in adult SHRs compared to normotensive controls. This is not observed in normotensive, juvenile SHRs (Waki *et al.*, 2008). This may occur as a result of pathological signalling resulting from invasion of the vessels by leukocytes due to the genetically pre-determined increased expression of JAM-1 in these animals. Leukocyte adhesion to endothelial cells in the brain microvasculature has been shown to cause the production of ROS and cytokines that pass into nearby neurones. Based on this, it may be the case that increased JAM-1 expression in SHRs causes disputation to the normal function of the cardiovascular neuronal networks in the NTS and other brainstem nuclei via pathological signalling resulting from the invasion of leukocytes that is facilitated by JAM-1. ANG II, circulating at higher levels in hypertensives, could exacerbate this. Zhang *et al.* reported in 2010 that ANG II chronically

increases the permeability of the BBB via oxidative stress and increases inflammation in the brain microvasculature (Zhang *et al*., 2010). Microglial cells, a type of CNS-specific macrophage, are activated in hypertension. When activated, microglia produce cytokines and ROS, which damage the BBB (Yenari *et al.*, 2006). This can be inhibited by minocycline, which lowers BP (Shi *et al.*, 2010). The integrity of the BBB is compromised in hypertension and this probably works to maintain the condition by facilitating inflammation of the brain parenchyma.

Poor perfusion of the brainstem specifically may be a cause of hypertension. Naragchi *et al.* showed that patients with essential hypertension had neurovascular compression at the left ventrolateral medulla (Naraghi *et al.*, 1992). The RVLM contains neurons that are sensitive to hypoxia (Wang *et al.*, 2001) and as such, poor perfusion of these neurons could result in an increase in sympathetic activity in order to raise blood pressure globally and restore adequate perfusion of the brain. This has been referred to as the 'selfish brain hypothesis' of hypertension and is based on the early work of Harvey Cushing, who, in 1901, demonstrated an increase in arterial pressure caused by increased intracranial pressure (and thereby reduced brain perfusion) in dogs (Cushing, 1901). This was deemed the Cushing response. More recently Braga *et al.* showed that the spinal cord of spinalised rats is able to produce sympathoexcitation in response to ischemia, demonstrating that the Cushing response is not limited to the pontomedullary structures of the brain (Braga *et al.*, 2007).

Juvenile (normotensive) SHRs have narrower vertebral and basilar arteries than WT animals (Paton *et al.*, 2007). Dickinson and Thompson found narrowed

vertebral arteries in cadavers of patients that had essential hypertension and were unable to determine whether this was a cause or result of hypertension (Dickinson & Thomson, 1960). The findings of Paton *et al.* would suggest that congenital malformations of arteries supplying blood to the brain may predispose individuals to the development of hypertension via a Cushing response i.e. BP is increased in order to overcome hypoperfusion of the brain parenchyma. This is backed up by evidence that cerebral vascular resistance is increased in SHRs vs normotensive controls (Oseka & Koźniewska, 1997) yet brainstem blood flow is the same (Granstam *et al.*, 1998): It is likely that ischemia in the brain, exacerbated by leukocytes, evokes a Cushing response, causing or contributing to systemic hypertension. The increased sympathetic activity resulting from this contributes to further pro-hypertensive activity of leukocytes as explained previously.

Leukocytes Promote Hypertension by Increasing Haemodynamic Resistance in the Microvasculature:

Circulating monocytes and neutrophils that bind to the vascular endothelium are prothrombogenic (Gorbet & Sefton, 2004). It is possible that this could result in local hypoxia as a result of reduced vessel patency or complete occlusion of capillaries. It is also the case that owing to their relatively large size and structural rigidity compared to erythrocytes, leukocytes increase haemodynamic resistance in capillaries with single file cells (Helmke *et al.*, 1997, 1998) as they move through more slowly. This effect does not depend on biochemical interactions with the endothelium and is entirely due to the physical mechanics of the cells. It can be simulated with similarly proportioned biospheres (Helmke

et al., 1997) which do not interact biochemically with the endothelium or other cells, thereby demonstrating the effect is due only to fluid dynamics.

Leukocytes project few pseudopodia (cytoplasmic projections of the cell membrane) under conditions of shear stress (Fukuda & Schmid-Schönbein, 2002; Fukuda *et al.*, 2004) This allows the cells to remain more compact/spherical and flow more easily. The presence of glucocorticoids inhibits the suppression of pseudopodia projection (Fukuda *et al.*, 2004) and since SHRs express glucocorticoid receptors that are more sensitive and in greater numbers than in normotensive animals (Suzuki *et al.*, 1995, 1996), circulating leukocytes of SHR project significantly more pseudopodia and this impairs their flow (Fukuda *et al.*, 2004). Transfusing blood from SHR into WKY rats causes an increase in blood pressure due to impaired blood flow through the microvasculature as a result of impaired passage of leukocytes (Fukuda *et al.*, 2004). Injecting WKY rats with SHR blood did not increase BP when leukocytes were removed from the blood (Fukuda *et al.*, 2004). The increased binding of leukocytes to the endothelium in the brainstem microvasculature observed by Waki *et al.* (2007) may not only contribute to hypertension as a consequences of leukocyte invasion into the vessels and brain parenchyma, but also by inhibiting blood flow through the lumen by increasing haemodynamic resistance.

Summary of Neurogenic Hypertension Hypothesis:

Increased circulating ANG II acts via AT_1 receptors in the circumventricular organs to increase ROS production via stimulation of NADPH oxidase. The resulting ROS activate microglia which causes production of more ROS as well as pro-inflammatory cytokines. This stimulates neuronal activity and causes

stimulation of downstream nuclei such as the NTS and the RVLM in the brainstem, driving sympathetic outflow up and thereby raising BP. The increase in sympathetic activity also causes the release of catecholamines, which act via β adrenoreceptors to activate T cells, resulting in the release of further pro-inflammatory cytokines and ROS, which promote vascular dysfunction in a variety of ways; blocking endothelium-dependent vasodilation through disabling NO, direct damage to endothelial cells caused by ROS, promoting leukocyte-endothelial binding and invasion of the vessel wall and vascular remodelling (smooth muscle cell proliferation, deposition of extracellular matrix, vessel stiffening). The resultant stiff vasculature raises the total peripheral resistance and vasodilation resulting from the baroreflex is less effective, which drives up BP further, resulting in more ANG II release (due to inflammation), more catecholamine release and release of other hormones that contribute to raising blood pressure such as ADH, aldosterone and adrenocorticotropic hormone, all of which modulate renal function, resulting in increased blood volume and thereby BP. The vascular dysfunction also leads to organ hypoperfusion, which drives sympathetic outflow up further via afferents projecting to the CNS from hypoxic organs (Koeners *et al.*, 2016).

In the brain, the cytokine release, ROS and resulting pathological behaviour of leukocytes, facilitated by JAM-1, damages the integrity of the BBB, allowing activated leukocytes into the brain parenchyma and in key nuclei responsible for blood pressure control, such as the PVN, inflammation stimulates neurones that project down into the brainstem (NTS, RVLM) and ultimately stimulates further pathological sympathetic activity.

Thus, a vicious cycle forms in which ANG II, inflammation, vascular dysfunction and organ hypoperfusion are all driving up sympathetic nervous system activity and all acting reciprocally to exacerbate the pathological outflow (Figure 9).

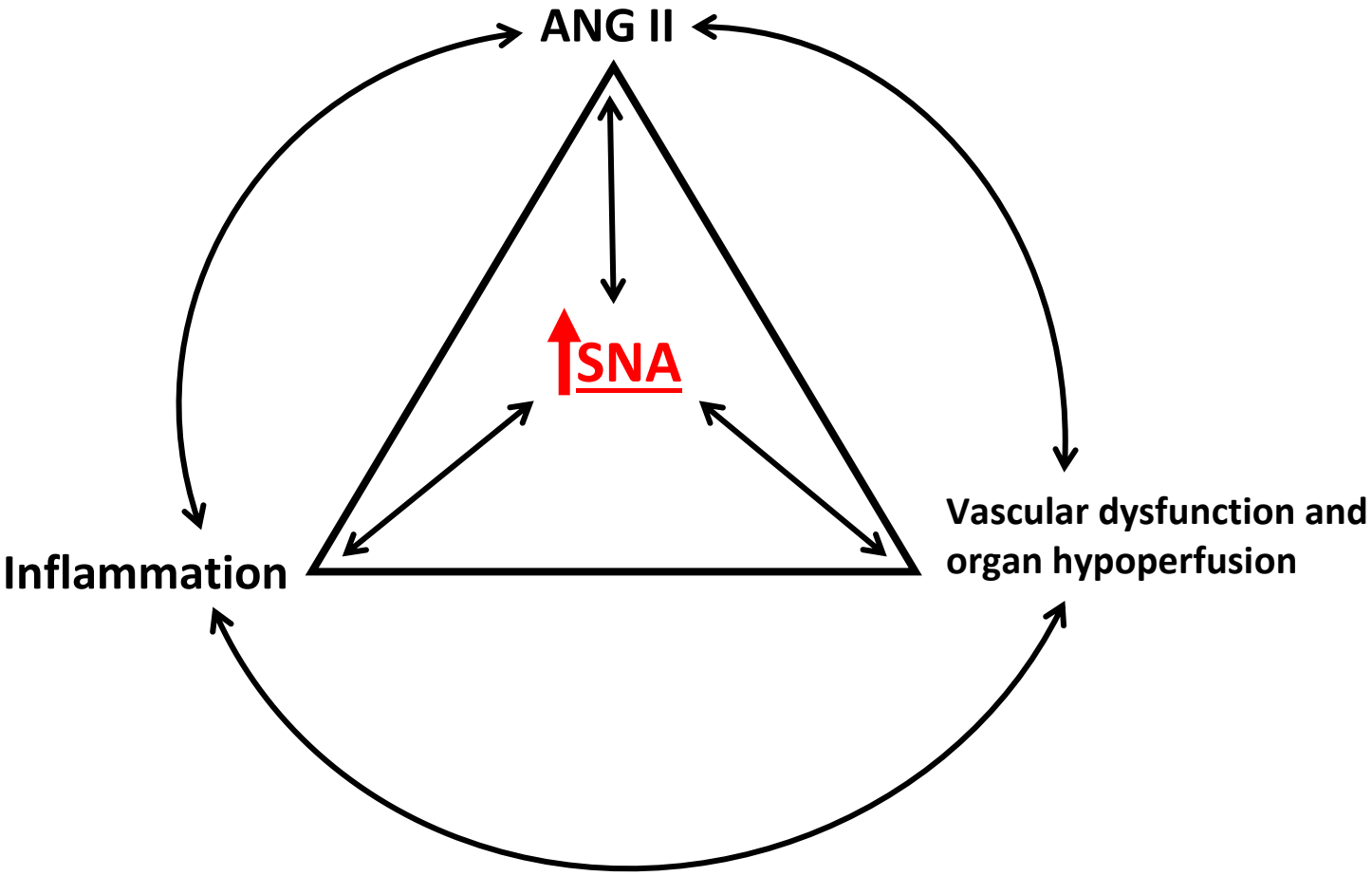

Figure 9: Triangulation of neurogenic hypertension. Positive feedback loops form between ANG II, inflammation and vascular dysfunction/organ hypoperfusion, creating an unresolving vicious cycle driving up sympathetic nerve activity.

The above scheme outlines how hypertension is maintained but not begun. The initial trigger to begin this cycle is not known but yet-to-be-discovered genetic factors are a near certainty. In addition, environmental and behavioural factors such as obesity, high salt intake, low levels of physical activity, insulin resistance and stress are known to be contributing factors and may be causal. More environmental causes may also be identified in future.

Reducing the sympathetic nerve activity at the centre of this scheme may constitute a novel anti-hypertensive strategy. Patients afflicted with essential hypertension could benefit immensely from targeting the central driver of the condition rather than the secondary consequences of it, as current pharmacological interventions do.

Objectives:

The purpose of my project was to investigate the following hypotheses:

- The use of compounds modulating the glutamatergic signalling of sympathetic nervous system activity could potentially constitute a novel antihypertensive strategy.
- Hypertensives exhibit a pro-inflammatory immunophenotype compared to normotensives.
- Modulation of glutamatergic signalling in rats will produce observable differences in immunophenotype and these will correlate with changes in blood pressure.

Chapter 2: Using Immunohistochemistry to Localise mGluR5 in Nuclei Involved in Regulation of Blood Pressure

Introduction:

Compounds modulating mGluR5 have caused changes in blood pressure when administered systemically (Figure 10).

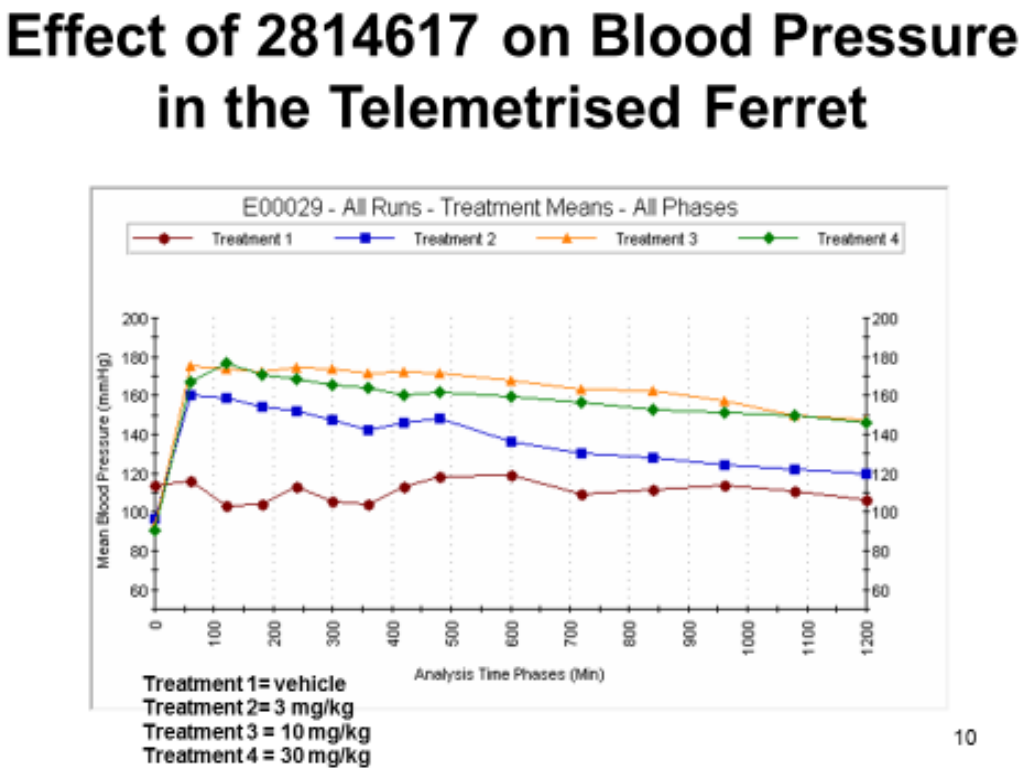

Figure 10: Effect of a single oral dose of mGluR5 positive allosteric modulator LSN2814617 on the blood pressure in ferrets. n=4 unpublished data provided by Eli Lilly and company, 2009.

Figure 10 shows pilot data from Eli Lilly and Company, demonstrating an increase in blood pressure caused by a single oral dose of LSN2814617, a positive allosteric modulator (PAM) of mGluR5. This means the compound potentiates the response of the receptor to its endogenous ligand (glutamate) but is not an agonist. Researchers at Lilly observed similar, though less pronounced effects with other mGluR5 PAMs, also administered systemically.

The extent to which mGluR5 is present in key brain nuclei responsible for blood pressure control and the exact location within these nuclei is not fully understood.

Li and Pan inferred the presence of mGluR5 in the PVN specifically in 2010 (see Chapter 1). In 2014, Li *et al.* used Western blots and qPCR to determine the presence of mGluR5 protein and mRNA in tissue homogenates from the PVN and RVLM in SHR and found mGluR5 was expressed in both nuclei and that expression was greater in SHR than it was in WKY (Li *et al.*, 2014). They found the protein and mRNA levels were much higher in the PVN and slightly higher in the RVLM of SHR compared to WKY rats.

The hypothalamic paraventricular nucleus (PVN) is heavily involved in elevated sympathetic outflow and the development of hypertension. Selectively blocking mGluR5 significantly reduces the basal firing activity of spinally projecting PVN neurons in spontaneously hypertensive rats (SHRs), but not in normotensive Wistar-Kyoto (WKY) rats (Li *et al*., 2014). Antagonism of mGluR1 had no effect on the activity of PVN neurons in either strain in this study. The group I mGluR selective agonist (S)-3,5-dihydroxyphenylglycine (DHPG) had the opposite effect, increasing the firing activity of PVN neurons in both groups (Li *et al*., 2014).

Hay *et al.* (1999) found mild mGluR5 expression in the NTS of Sprague-Dawley rats using immunohistochemistry (IHC). They did not find any expression in the CVLM or the RVLM.

The receptor has also been visualized using IHC in the dorsolateral PAG of Sprague-Dawley rats (Azkuea *et al.*,1997). In this chapter it was my intention to build on the work done by Li *et al.*, Hay *et al.* and Azkuea *et al.*

Given the fact that sympathetic nervous system activity is elevated in SHR and that much of the signaling within the sympathetic neuronal networks of the brainstem that regulate blood pressure is glutamatergic (see Chapter 1), I also sought to compare expression of mGluR5 in the hypertensive SHR vs normotensive Wistar rats. Li *et al.* already studied expression of the receptor in the PVN and NTS but I am also interested in additional regions. I will not exclude the PVN and NTS from my own study, given the fact that Li *et al.* used a different rat strain for their controls and only had an n of 4.

Using IHC in both normotensive Wistar rats and SHRs, I intended to localize mGluR5 in the RVLM, CVLM, NTS, PVN, PAG and the A5 area of the ventrolateral pons (See Chapter 1).

I divided the RVLM and CVLM each into rostral and caudal regions, creating four areas of interest in the ventrolateral medulla. I also examined rostral and caudal sections of the NTS. The specific areas of the PAG that are involved in control of blood pressure are the ventrolateral and dorsolateral regions, so I examined both of those separately. My overall aim in this chapter was to map and crudely quantify expression of mGluR5 in key CNS nuclei involved in the control of blood pressure.

Methods:

Tissue Preparation:

All animal experiments were performed in accordance with institutional guidelines and the UK Home Office (Scientific Procedures) Act (1986) with project approval from the University of Bristol, University ethics of research committee, under Home Office personal license number ICCF4B573 and project license number 70/7868. Six male Wistar and seven male Spontaneously

Hypertensive Rats (SHRs), all approximately 300g, were sourced from Harlan, UK. Wistar rats were used throughout this project instead of the more commonly used Wistar-Kyoto (WKY) rat since WKY rats were difficult to obtain at the time the research was done and as a result were out of budget. The Wistar rat is closely related to the WKY and therefore the SHR, since SHR were obtained by selectively breeding hypertensive WKY rats. Wistars have been used as controls in many published studies including those conducted by our group (Roloff *et al.*, 2018)

The animals were overdosed using sodium pentobarbital (150mg/Kg.). The animals were then transcardially perfused using a peristaltic pump, first with ~200ml phosphate buffered saline - PBS (Dulbecco tablets) and then with ~200ml 10% buffered formalin (Sakura cat#: 8726). The animals were decapitated via guillotine, the brains were carefully harvested, rinsed and washed with PBS and placed into tubes containing 10% formalin for temporary storage at 4°C until processing.

The brains were cut using a razor blade into smaller sections suitable for embedding in paraffin wax (Figure 11).

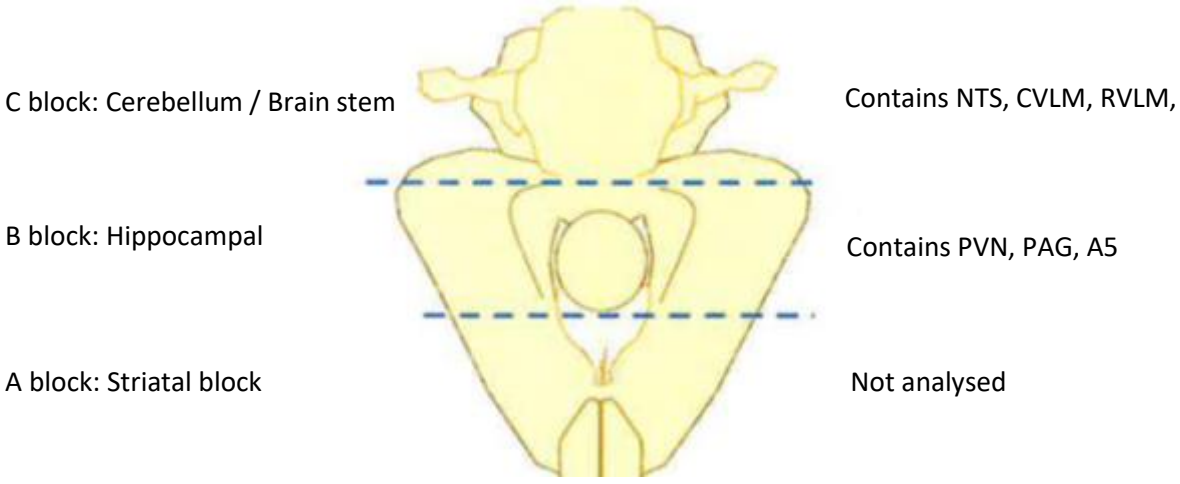

Figure 11: Schematic showing how brains were cut to fit into blocks to be sectioned on the microtome (ventral view with brainstem at top and frontal lobe at bottom).

The tissue blocks were infiltrated with paraffin wax (Sakura cat# 4502) using a Tissue-Tek VIP 6 Vacuum Infiltration Processor (Sakura) according to the program shown in Table 1.

Multiple changes of the same reagent were used to ensure reagents were clean and to reduce contamination from the previous type of reagent.

Solution	**Concentration (%)**	**Time (mins)**	**Temp (°C)**
Formalin	10	5	Room
IMS	60	75	Room
IMS	80	75	Room
IMS	90	75	Room
IMS	100	75	Room
IMS	100	75	Room
IMS	100	75	Room
Xylene	100	75	Room
Xylene	100	75	Room
Xylene	100	75	Room
Paraffin wax	100	50	60
Paraffin wax	100	50	60
Paraffin wax	100	50	60
Paraffin wax	100	Until collected	60

Table 1: Table showing the protocol used to embed tissues in paraffin wax. IMS=industrial methylated spirits

The tissue was then carefully oriented for sectioning and embedded in wax contained within Tissue-Tek III uni casettes (Sakura).

Once set and cooled to room temperature the tissue blocks were trimmed using a sharp knife and cut into 6 μm sections using a manually-operated rotary

microtome (Thermo). The sections were floated on water in a bath at ~43°C and mounted serially onto glass slides (Thermo cat# 640-ADH-006). The slides were labelled and left to dry on a heated drying rack overnight in the order in which the sections were cut.

Slide Selection:

A series of slides, evenly spaced throughout the series that was cut, was selected for solochroming in order to assist with choosing appropriate slides to stain for mGluR5. The solochroming process stains myelin deep blue. This facilitated anatomical orientation in conjunction with a brain Atlas (Paxinos & Watson, 2007). Solochromed slides that contained cardiovascular control nuclei were identified using light microscopy (Leica inverted microscope) and adjacent slides from the sequence were selected for mGluR5 staining. Four slides per region per animal were chosen.

Solochrome staining was performed manually as follows. Slides were placed by hand into racks submerged in reagents at room temperature for specified amounts of time and were agitated by hand according to Table 2.

Multiple changes of the same reagent were used to ensure reagents are clean and to reduce contamination from the previous type of reagent. (i.e. when racks are moved from xylene into IMS, they take some xylene with them and contaminate the IMS, so moving them through 3 batches of IMS for 2 mins each ensures that overall the slides spend 6 mins in purer IMS than they would if they were left for 6 mins in one batch. If 3 batches of IMS are used, the amount of xylene coming through into the third batch is negligible)

Reagent	Time (mins)	Agitation
Xylene	2	Initial
Xylene	2	Frequent
Xylene	2	Initial
IMS	2	Initial
IMS	2	Frequent
IMS	2	Initial
70% IMS	2	Frequent
Running Tap water	5	Frequent
Solochrome	12	Frequent
Running Tap water	5	Frequent
Iron Alum	0.5	Frequent
Iron Alum	1	Frequent
Iron Alum	1	Frequent
Running Tap water	5	Frequent
Cresyl Violet	3	Frequent
Running Tap water	1	Frequent
IMS 70%	1	Continuous
IMS	1	Continuous
IMS	1	Frequent
IMS	2	Frequent
Xylene	1	Frequent
Xylene	1.5	Frequent
Xylene	2	Initial
Xylene	2	Initial
Xylene	2	Initial

Table 2: Table showing the protocol used for solochroming. IMS=Industrial methylated spirits. Cresyl violet from Sigma (Cat. No. C5042) made into solution according to package instructions. Solochrome and iron alum made up according to formulations in Appendix C.

Xylene and IMS were obtained from Fisher Scientific (cat# X/0250/17 and M/4450/17 respectively).

Once solochroming was complete the slides were cover slipped using an automated coverslipping machine (Thermo). Shandon ClearVue Mountant XYL (Thermo cat# 4212) was used as the adhesive to secure the coverslips to the slides.

Staining for mGluR5:

Selected slides were run through a solvent gradient in order to remove the paraffin wax and create an aqueous tissue environment to facilitate immunocytochemical staining. This was done at room temperature in accordance with Table 3.

Multiple changes of the same reagent were used to ensure reagents were clean and to reduce contamination from the previous type of reagent.

Reagent	**Time (mins)**
Xylene	5
Xylene	5
Xylene	5
IMS	5
IMS	5
70% IMS	5
Distilled Water	5

Table 3: Table showing protocol for rehydrating tissue on slides before staining. IMS=Industrial methylated spirits

Slides were slotted into racks and placed in a pre-treatment module (Thermo) containing 1% citrate buffer (Thermo cat# TA-250-PM1X) at 65°C. The bath was then heated to 100°C over a 20-minute period for antigen retrieval,

maintained for 20 mins at 100°C before being left to cool to 75°C, which took approximately 20 mins. Antigen retrieval is a process in which methylene bridges that are formed between proteins during formalin fixation are broken in order to expose antigenic sites that are otherwise blocked by the fixation process. The complete cycle took ~1 hr.

The slides were then removed and placed into distilled water. A border was drawn around the edge of each slide using a PAP pen (thermo), which contains a hydrophobic solution in order to prevent solutions running off the slide later on. Care was taken to minimise the amount of time the slides were out of the water in order to prevent the tissue from drying out. Slides were then transferred into manual staining humidity trays / autostainer machines (Thermo).

The slides were incubated at room temperature (solutions put onto slides with a pipette) in PBS-T (PBS with 0.05% Tween-20 from Thermo) for 5 minutes. Tween-20 is a non-ionic surfactant, which helps the solution to spread more easily across the slides.

Next, the solution was tipped/blown (with compressed air) off the slides and endogenous peroxidases were blocked via incubation with 0.3% H_2O_2 (Sigma cat# H1009) in PBS-T for 10 mins. This was followed by a 5-minute rinsing step with PBS-T.

Non-specific binding of the antibody to tissue sites other than the intended ligand was blocked via incubation with 5% Normal Goat Serum (Vector Labs cat# S-1000) in PBS-T for 30 mins. This was then tipped/blown off the slide and without rinsing, the tissue was incubated with primary antibody (Rabbit anti-rat mGluR5, Merck Millipore cat# AB5675) at a dilution of 1:5000 in PBS-T for 60 mins. This concentration was selected after a series of pilots were performed

with a wide range of concentrations (1 in 50 to 1 in 500000) as part of antibody characterisation/optimisation process using otherwise the same protocol outlined here. After incubation was complete, the slides were rinsed with PBS-T for 5 mins before a 30 min incubation with the secondary antibody (Biotinylated goat anti-rabbit IgG, Vector labs, cat# BA-9200) at a dilution of 1:200 in PBS-T. A secondary Ab is used for the purpose of signal amplification (Figure 12).

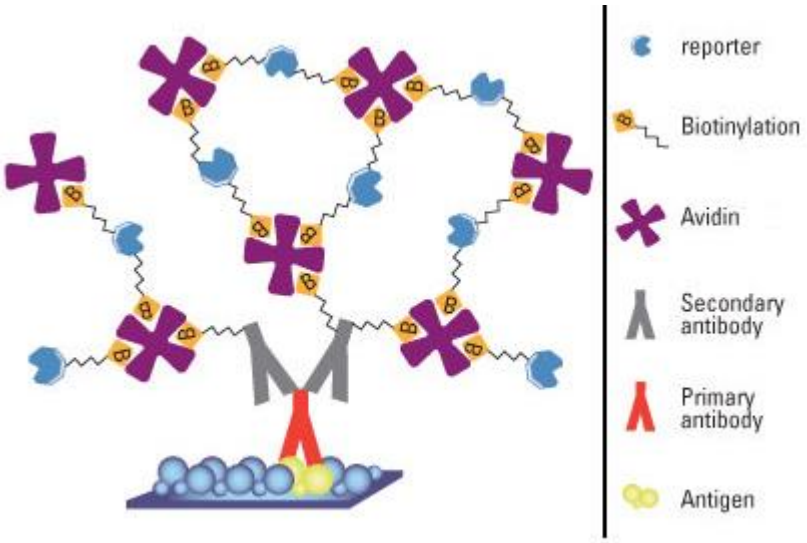

Figure 12: The concept of signal amplification-Using a secondary antibody and then an avidin-biotin complex to bind to the primary antibody results in a large reporter complex bound to a single epitope, thereby providing a stronger signal when the substrate is applied. Diagram adapted from ThermoFisher

After this was washed off with PBS-T for 5 mins, the slides were incubated with Avidin-Biotin complex (Vectastain Elite RTU ABC kit, Vector labs, cat# PK-7100) for 30 mins for further signal amplification. Another 5 min wash in PBS-T was done and the signal was developed via a 5 min incubation with diaminobenzidine (DAB) (ImmPACT DAB kit, Vector labs, cat# SK-4105) made up in the diluent provided according to the kit instructions. A further 5 min PBS-T wash took place before counterstaining with a 5 min incubation in 50% haematoxylin in dH_2O (DAKO cat# S3301). 300µL of appropriate solution was put onto each slide at every stage.

The slides were briefly rinsed with dH_2O before being transferred to a warm water bath (tap water) at ~45°C. They were then put through the solvent gradient in Table 3 in reverse order. Once the slides had completed their 5 min incubation in the third change of xylene, they were cover slipped as above, left to air dry for 20 mins and placed in warm ovens (approx. 45°C) to dry further overnight.

The slides were observed and scanned using an Aperio scanner (Leica) and images captured digitally using an Aperio ImageScope software.

Staining intensity was measured in FiJi software using the 'staining intensity' tool. Intensity was measured relative to that of the hippocampus, which was deemed 100% as this is a region known to have particularly high expression of mGluR5. For each slide analysed, the darkest area of the hippocampus on each image (determined automatically by the software, avoiding user bias) was selected and deemed 100% for the purpose of calibration. The outlines of the regions of interest on each slide were selected manually using the freehand shape tool, which introduced some potential for both manual error and user bias which were unavoidable given the resources available. The cut-off for detection intensity was determined using a section of white matter which does not contain any mGluR5 and was deemed zero. The software was calibrated individually for each slide since there was some variation in general staining intensity between slides stained on different days.

Validation of Antibody Used:

The antibody I used to label mGluR5 (Merck Millipore cat# AB5675) has been used in numerous studies that have resulted in publication of peer-reviewed papers. (Zhong *et al.*, 2012; Grolla *et al.*, 2013; Andreeva *et al.*, 2014; Loweth *et al.*, 2014; Haas *et al.*, 2014; Xu *et al.*, 2014).

In addition, I validated the antibody myself, using the protocol described previously but with brain tissue from a genetically-modified animal that did not express any mGluR5 (Figure 13). This tissue was provided by Eli Lilly.

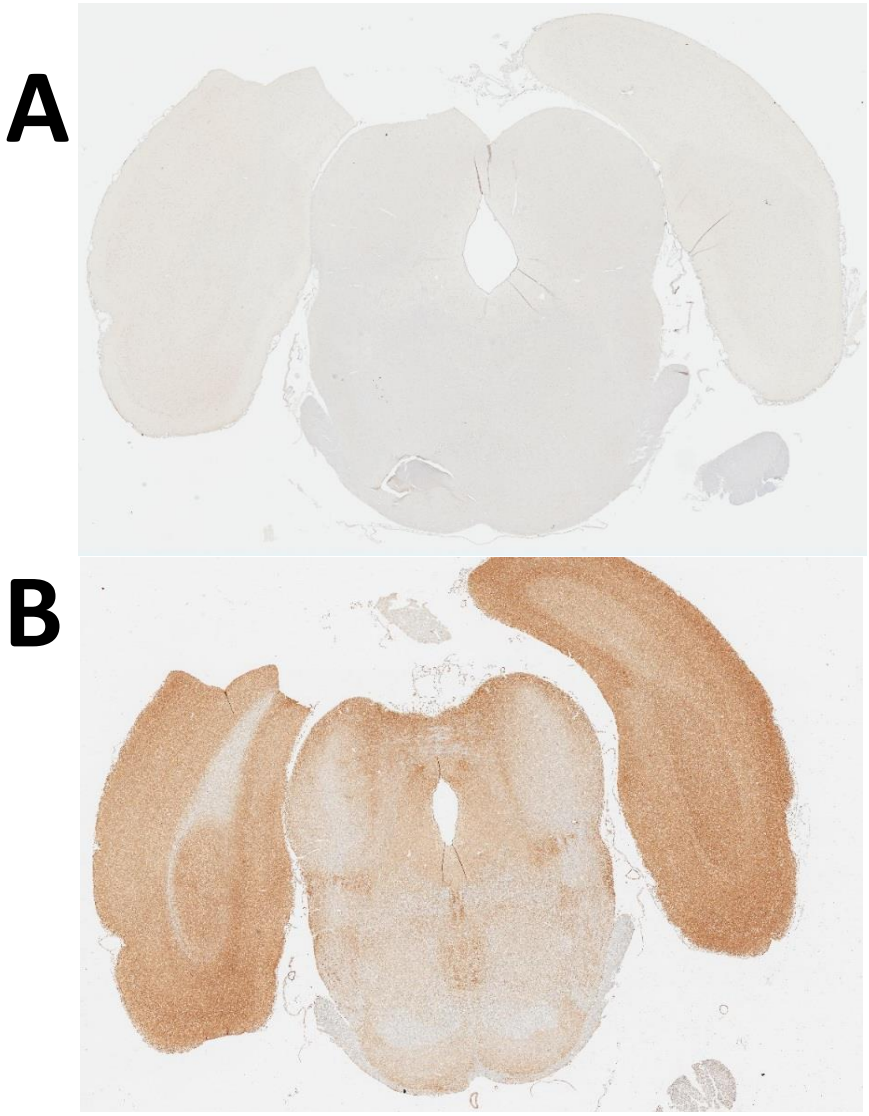

Figure 13: Section of brain tissue at the level of the PAG treated with anti-mGluR5 antibody (Merck Millipore cat# AB5675) according to the protocol outlined previously. **A:** Tissue from an mGluR5 knockout animal (no mGluR5 receptor present). **B:** Comparable section from a wild-type animal. This validation process was undertaken in order to show that the antibody used in the experiments was specific to mGluR5 and does not bind indiscriminately.

Results:

No significant difference in expression of mGluR5 between SHR and Wistar was observed (Figure 14). Substantial expression of mGluR5 was detected in the PVN and rNTS, where staining intensity was more than 60% relative to that of the hippocampus. Moderate expression was observed in the cNTS and dlPAG, where staining intensity was between 30 and 40% and mild expression was detected in the vlPAG and the A5 area of the ventrolateral pons, where relative staining intensity was roughly between 15 and 20% (Figure 14).

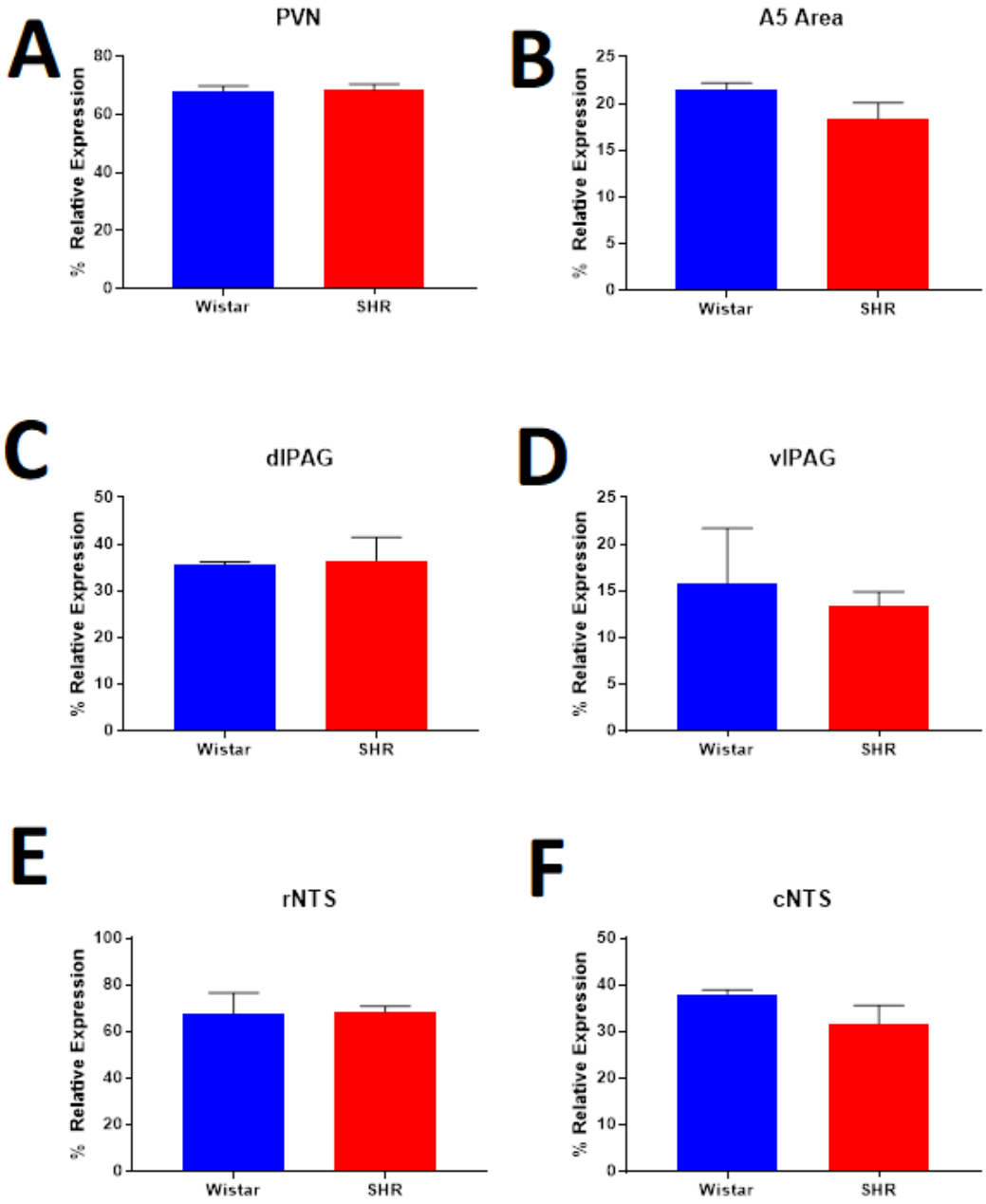

Figure 14: % staining intensity relative to the hippocampus, which was deemed to have 100% intensity. Measurements made using 'staining intensity' tool in Fiji. Wistars n = 6 SHR n = 7 No significant differences were observed between the two strains. No staining was detected in either the rostral or caudal portions of the RVLM or the CVLM in Wistars or SHRs. Error bars represent SEM. **A:** Paraventricular nucleus of the hypothalamus, **B:** A5 Area of the ventrolateral pons, **C:** Dorsolateral periaqueductal grey area, **D:** Ventrolateral periaqueductal grey area, **E:** Rostral Nucleus of the solitary tract, **F:** Caudal nucleus of the solitary tract

Representative Images:

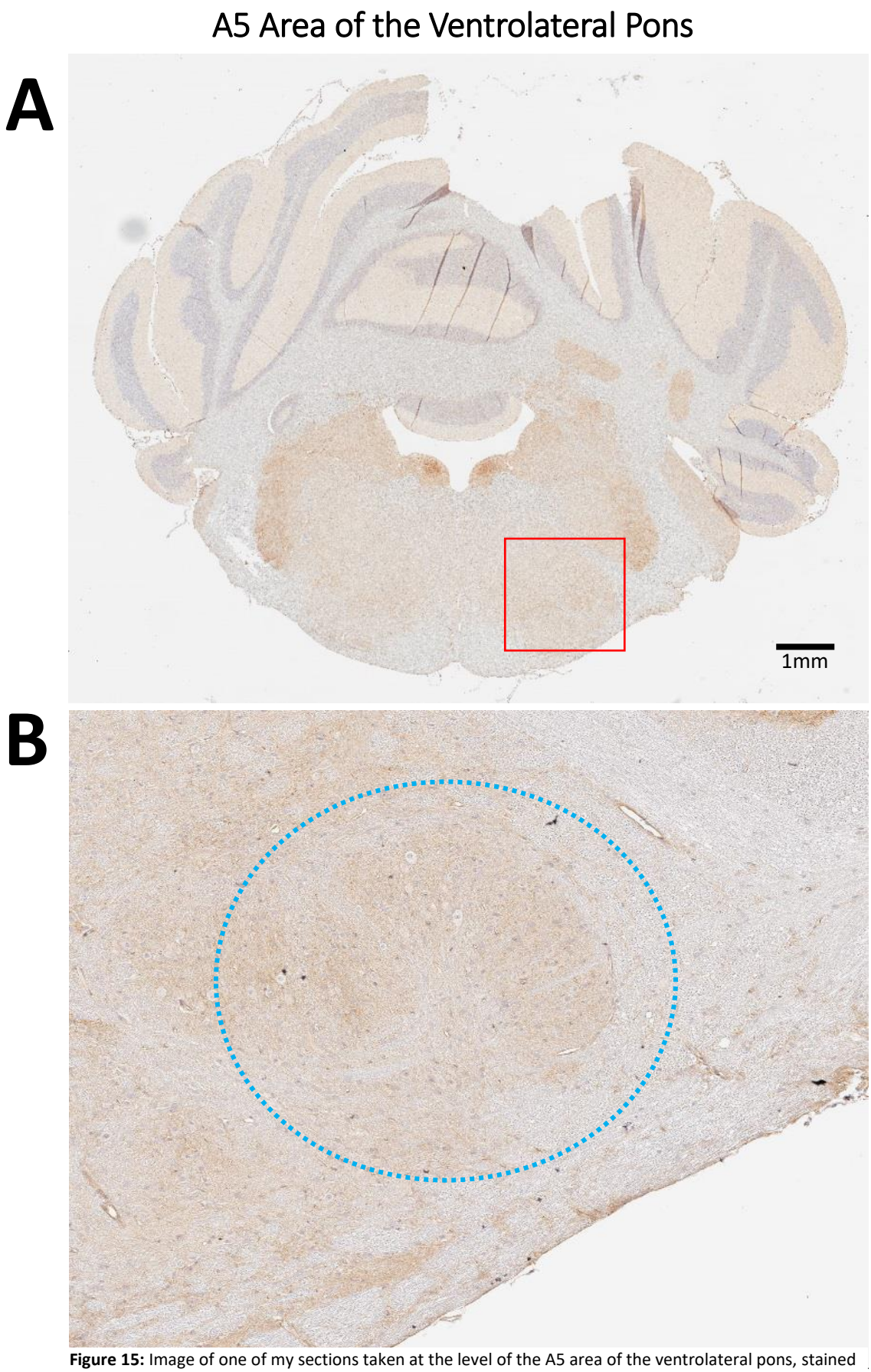

Figure 15: Image of one of my sections taken at the level of the A5 area of the ventrolateral pons, stained for mGluR5. Brown areas indicate presence of the receptor. **A:** View of the whole section **B:** Zoomed-in view of the area of interest, indicated by the red square in panel A.

RVLM (green circle) + Rostral NTS (red square)

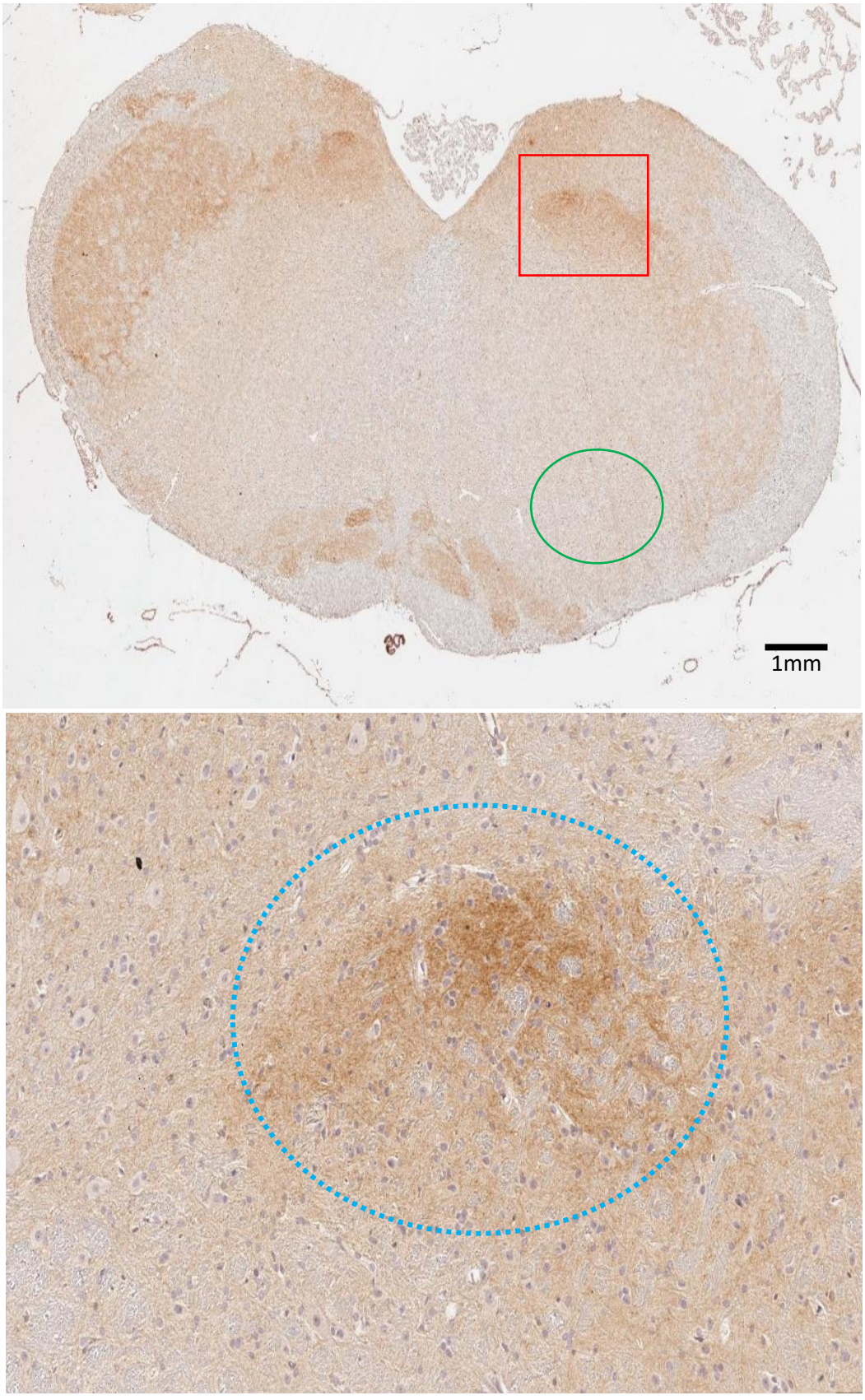

Figure 16: Image of one of my sections at the level of the rostral NTS, stained for mGluR5. Brown areas indicate presence of the receptor. **A:** View of the whole section **B:** Zoomed-in view of the area of interest, rostral NTS circled in blue. Green circle in panel A indicates RVLM. No staining was detected in the RVLM.

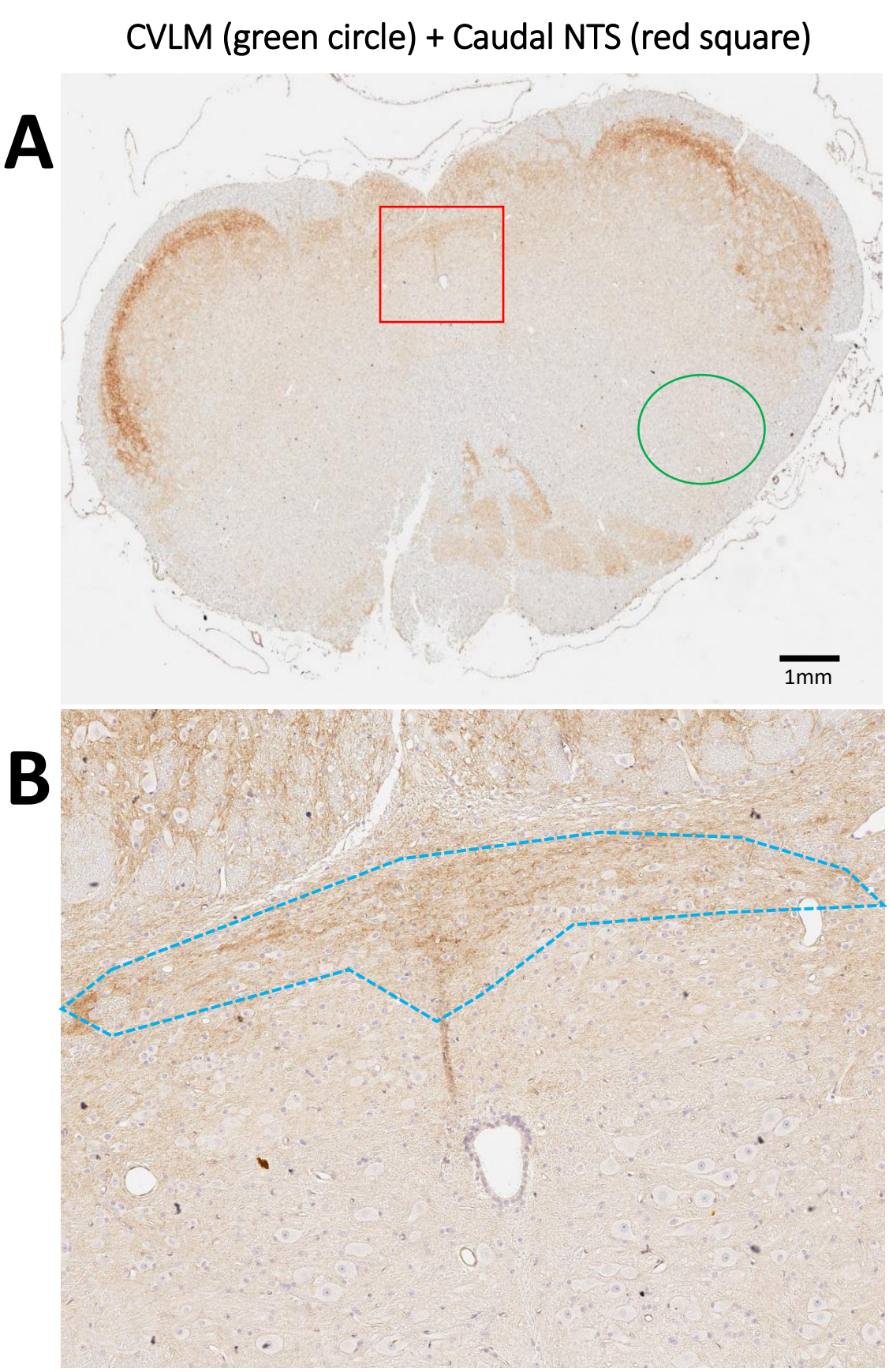

Figure 17: Image of one of my sections at the level of the caudal NTS, stained for mGluR5. Brown areas indicate presence of the receptor. **A:** View of the whole section **B:** Zoomed-in view of the area of interest, caudal NTS outlined in blue. Green circle in panel A indicates CVLM. No staining was detected in the CVLM.

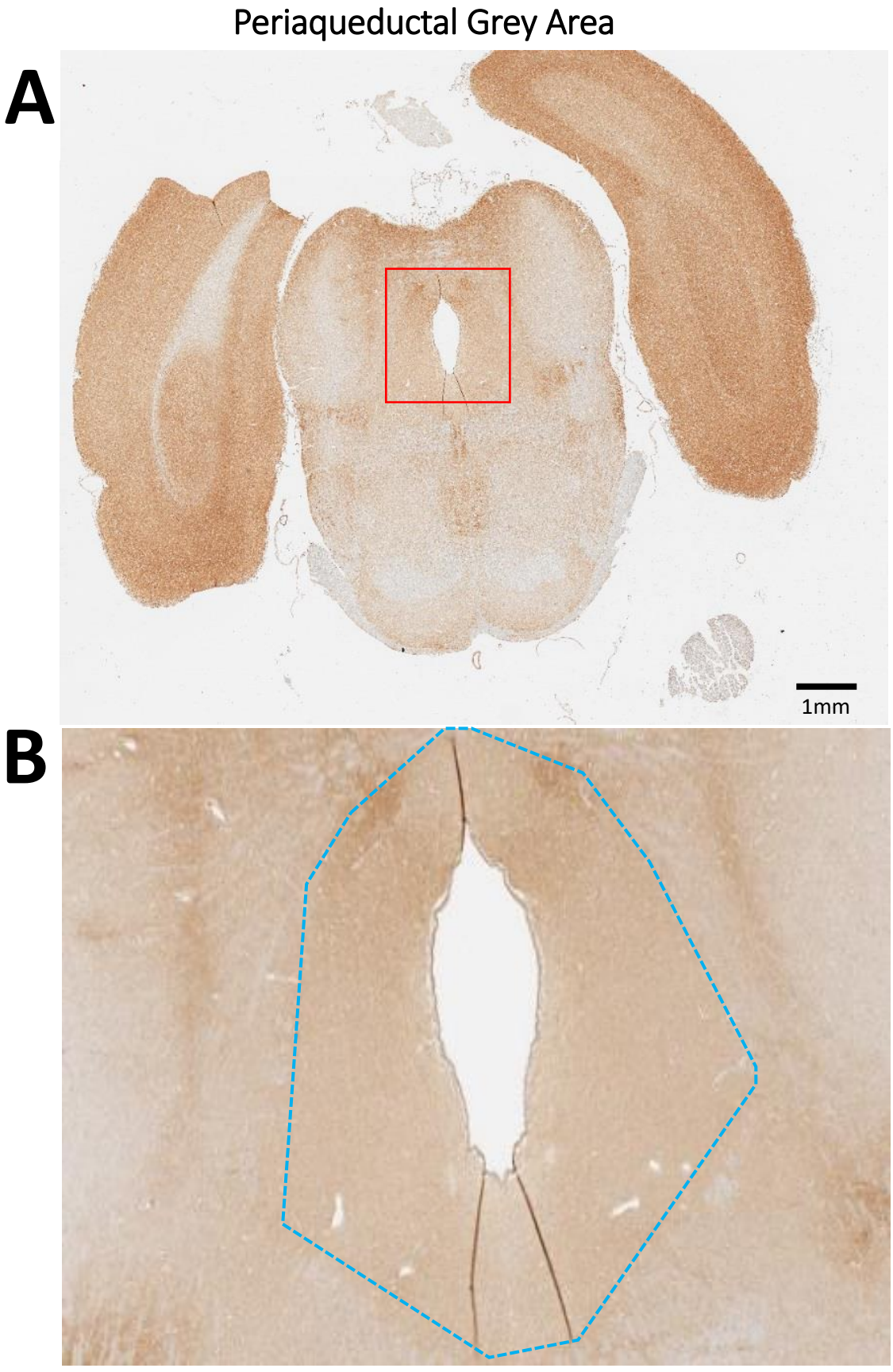

Figure 18: Image of one of my sections at the level of the periaqueductal grey area, stained for mGluR5. Brown areas indicate presence of the receptor. **A:** View of the whole section **B:** Zoomed-in view of the area of interest, periaqueductal grey area outlined in blue.

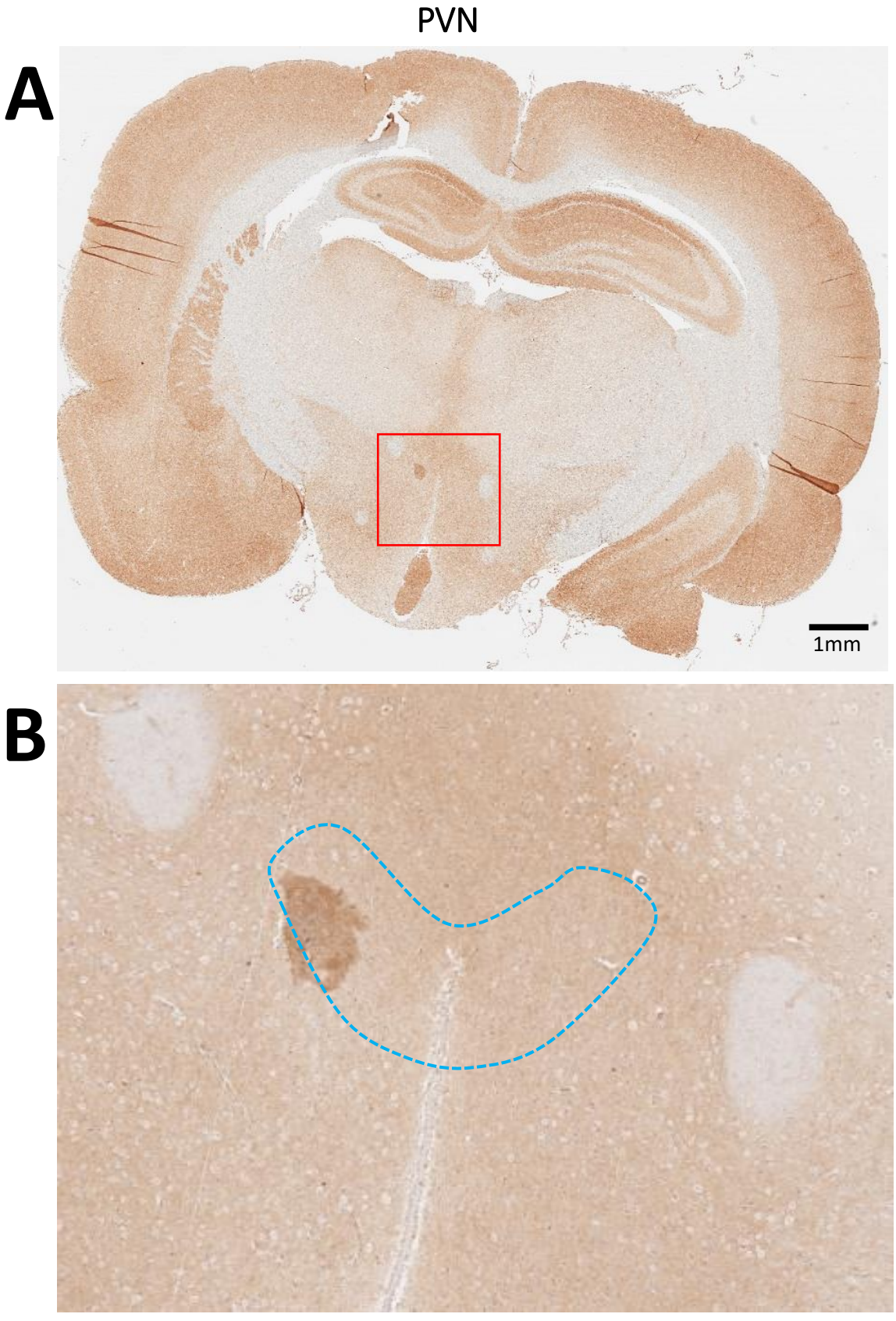

Figure 19: Image of one of my sections at the level of the PVN, stained for mGluR5. Brown areas indicate presence of the receptor. **A:** View of the whole section **B:** Zoomed-in view of the area of interest, PVN outlined in blue.

Discussion:

mGluR5 is Expressed in Several Key Nuclei Involved in Autonomic Regulation of Blood Pressure:

NTS:

Substantial expression of mGluR5 was detected in the NTS (Figure 14 panels E and F). The NTS is a major integrator of cardiovascular afferent information (see Chapter 1).

Expression in the NTS was higher in the rostral portion of the nucleus. The NTS does not have a laminar structure separating second order interneurons receiving afferent sensory information from neurones that project to other areas in the brainstem. However, there is some viscerotopic organization of the nucleus; the rostral portion primarily receives sensory afferents conveying gustatory and other orosensory information (Subramanian, 1995; Norgren, 2011) via cranial nerves V, VII, IX and the Vagus (Beckstead & Norgren, 1979; Nomura & Mizuno, 1981; Contreras *et al.*, 1982; Bradley *et al.*, 1985; Hanamori & Smith, 1989). The cardiorespiratory afferents synapse with NTS interneurons in the caudal portion of the nucleus (Altschuler *et al.*, 1989; Ciriello *et al.*, 1994). Detection of mGluR5 here is particularly pertinent to this thesis as this caudal subregion of the NTS is heavily involved in blood pressure control. There does not appear to be any viscerotopic organization of efferent neurons responsible for cardiorespiratory control. However, neurons in the NTS have many long dendrites (Standish *et al.*, 1995) and it may be the case that afferents synapse onto these dendrites rather than the somas. Because of this, all of the NTS potentially contains neurones or dendrites that could project to, and modulate, neural circuits controlling sympathetic outflow; therefore, detection of mGluR5

in any part of the NTS is important – a systemically administered compound modulating mGluR5 has the potential to modulate sympathetic outflow at the level of the NTS and thereby affect blood pressure.

PVN:

Strong expression of mGluR5 was detected in the PVN (Figure 14, panel A).

This is highly significant since this nucleus contains parvocellular neurones that innervate the RVLM (home of the pre-motor sympathetic neurones) and to the intermediolateral cell column where the pre-ganglionic sympathetic motor neurons are located. The PVN magnocellular neurons control vasopressin secretion into the blood stream and the nucleus also has projections to other regions involved in blood pressure control (see Chapter 1).

As is the case in the NTS, the presence of mGluR5 in this nucleus provides the potential for altering blood pressure since the PVN constitutes a critical component of the neuronal circuitry controlling sympathetic outflow. Expression of the receptor in this particular nucleus is especially pertinent to my research since the PVN is a cardiorespiratory control region that is vulnerable to dysfunction caused by immune cell infiltration due to its proximity to the CVOs, which have an incomplete BBB that is compromised in hypertension (see Chapter 1). It is possible that immune cell infiltration causes abnormal neuronal activity within the PVN, which leads to abnormal activity downstream and ultimately increased sympathetic outflow. If this is the case, modulation of mGluR5 could potentially correct the overstimulation of neurons in the PVN and thereby normalize sympathetic outflow to the cardiovascular effector organs, reducing blood pressure.

PAG:

Some expression of mGluR5 was detected in the vlPAG and dlPAG (Figure 14, panels C and D), although the staining intensity was considerably lower than it was in the NTS and PVN. Regardless, the presence of the receptor in these regions provides the potential for blood pressure modulation via mGluR5 since they are known to contain neurones which project to the RVLM and the hypothalamic PVN as discussed in Chapter 1.

A5:

mGluR5 was detected in the A5 area but this finding is not especially helpful since the A5 noradrenergic neurones of interest within this region are disperse (see Chapter 1). Because of this, it is possible that the staining observed was due to expression on neurones that are not involved in cardiovascular homeostasis and that the neurones of interest do not express the receptor.

CVLM and RVLM:

No expression of mGluR5 was detected in the CVLM or the RVLM. This is surprising since the majority of the signaling to the caudal ventral lateral medulla is known to be glutamatergic but mediated by non-NMDA receptors (see Chapter 1). There is some pharmacological evidence that mGluR5 is expressed in the RVLM (Urban *et al.*, 2003). Perhaps the concentration of receptor at this region was below what would be picked up by my analysis.

No Significant Difference in mGluR5 Expression between SHRs and Normotensive Wistar Controls:

According to my data, mGluR5 density as measured compared to the density in the hippocampus does not appear to be upregulated in the SHR. However, Li

and Pan found that expression of the receptor was increased in SHR (Li *et al.*, 2014). Li and Pan used Western blotting and qPCR to measure the quantity of protein extracted from the nuclei, which is a much more accurate method than IHC for quantification and therefore their data is likely more reliable. Li and Pan used WKY rats as controls which could possibly explains the discrepancy although this is unlikely since WKY rats and Wistars are closely related. Even if there is no difference in the levels of expression of mGluR5 between Wistar and SHR, this does not necessarily mean that signaling via these receptors is not altered in the hypertensive SHR. It is possible that more glutamate is released at the synapses of SHR or that reuptake of glutamate from the synaptic cleft is reduce and thereby there is more excitatory signaling along autonomic pathways despite there being no appreciable increase in receptors. It is also possible that the signaling pathway in SHR is more responsive or that an additional pathway is recruited downstream of mGluR5.

Limitations and Further Study:

As alluded to above, IHC is not the best method for accurate quantification of protein expression within a tissue. If I needed to quantify the expression of mGluR5 I could have used Western blotting or measured mRNA using qPCR. However, the primary purpose of this study was not to accurately quantify mGluR5 expression but to screen various key cardiovascular control nuclei for the presence of the receptor in order to determine whether this receptor could constitute a potential target for modulation of blood pressure. The study achieved this aim. Indeed, it has unearthed a number of potential nuclei including the NTS, PAG and PVN.

Ideally I would like to have expanded the study by performing immunofluorescence staining and co-staining for tyrosine hydroxylase in order to determine whether the catecholamine containing neurones (A1, A2, A5, C1 – see Chapter 1) co-express mGluR5 in particular since my blanket IHC stain of the A5 area of the ventrolateral pons does not provide information regarding expression of mGluR5 in neurons that are known to be involved in the control of blood pressure. Unfortunately, my placement at Lilly was not long enough to allow for this. Overall this study did provide evidence of the presence of mGluR5 in several key nuclei responsible for blood pressure control and justifies moving on to in vivo modulation of the receptor.

Chapter 3: In Vivo Pharmacological Modulation of mGluR5

Introduction:

Systemic administration of a positive allosteric modulator of mGluR5 has caused increases in blood pressure in ferrets, as discussed in Chapter 1.

Li and Pan administered compounds that modulate mGluR5 into the PVN specifically in 2010 (see Chapter 1). They bilaterally injected LY367385 or MPEP, specific mGluR1 and mGluR5 antagonists respectively, into the PVN of SHR and WKY rats. They observed reductions in both sympathetic nerve activity and blood pressure in SHR but not in WKY rats, suggesting that group 1 mGluRs are present in the PVN and that they are involved in producing or contributing to the hypertension, probably via increasing sympathetic outflow. The effects elicited by MPEP were significantly greater than those by LY367385, suggesting a particularly significant role for mGluR5 (Li and Pan, 2010). They also observed increases in sympathetic nerve activity and blood pressure of SHR and WKY rats when they injected DHPG into the PVN. DHPG is a non-specific agonist of both group 1 mGluRs. These effects were significantly attenuated when DHPG was co-administered with MPEP and were abolished when it was co-administered with both MPEP and LY367385, reinforcing the findings from the antagonist experiments. Given the fact that Eli Lilly and company used ferrets for their systemic study and there is no ferret model of congenital hypertension as well as the fact that partly due to their greater similarity to humans, rats are the standard animal used for research into hypertension, I intended to investigate the effects of modulation of mGluR5 in the SHR (see Chapter 1) and normotensive Wistar rats. Also, the ferret study

from Lilly and the microinjection study from Li and Pan were both acute studies. I intended to observe the effects of chronic modulation of the receptor using twice daily intraperitoneal injections. I used the same positive allosteric modulator used by Lilly (LSN2814617) in normotensive rats, since it is known to produce a hypertensive response in normotensive ferrets. The response observed at 3mg/Kg was only a little less pronounced than at much larger doses, so I used 3mg/Kg as the top end of my dosing range. The main focus of these experiments was testing mGluR5 antagonists on SHR since it is possible that such compounds could be of some therapeutic use if they prove to be anti-hypertensive. The most widely used mGluR5 antagonist is 2-Methyl-6-(phenylethynyl) pyridine (MPEP) and for this reason I used the compound in my study. However, because MPEP is known to have some activity as a positive allosteric modulator of mGluR4 (Mathiesen *et al.*, 2003) and is less potent than the more recently developed 3-((2-Methyl-4-thiazolyl)ethynyl)pyridine (MTEP), which has no known activity at any receptor other than mGluR5, I tested MTEP as well.

In order to help determine the appropriate dosing schedule I did a small pharmacokinetic study. I injected 8 male Wistar rats with MPEP (8mg/Kg) and another 8 with MTEP (4mg/Kg). I then withdrew blood via tail vein bleed into Eppendorf tubes (see Methods section of this chapter) and span the cells down in a mini centrifuge (Eppendorf) in order to isolate the plasma, which I collected, froze at -80°C and sent to Eil Lilly and Company (Windlesham, Surrey, UK) for HPLC analysis (Figure 20 and Figure 21).

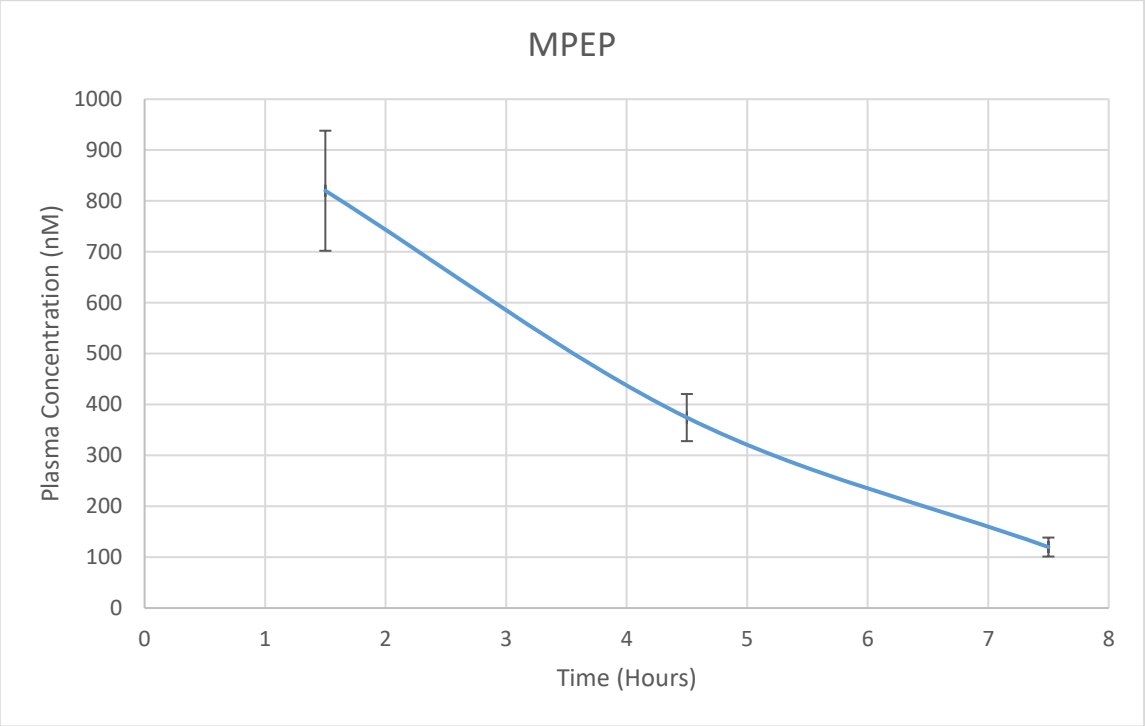

Figure 20: Pharmacokinetic study on MPEP. 8 male Wistar rats were given an I.P. injection of 8mg/Kg MPEP at T=0. Blood was withdrawn via tail vein bleed at the three time points (1.5, 4.5 and 7.5 hours) and the plasma concentration was measured via HPLC by staff at Eli Lily and Company. Error bars show SEM.

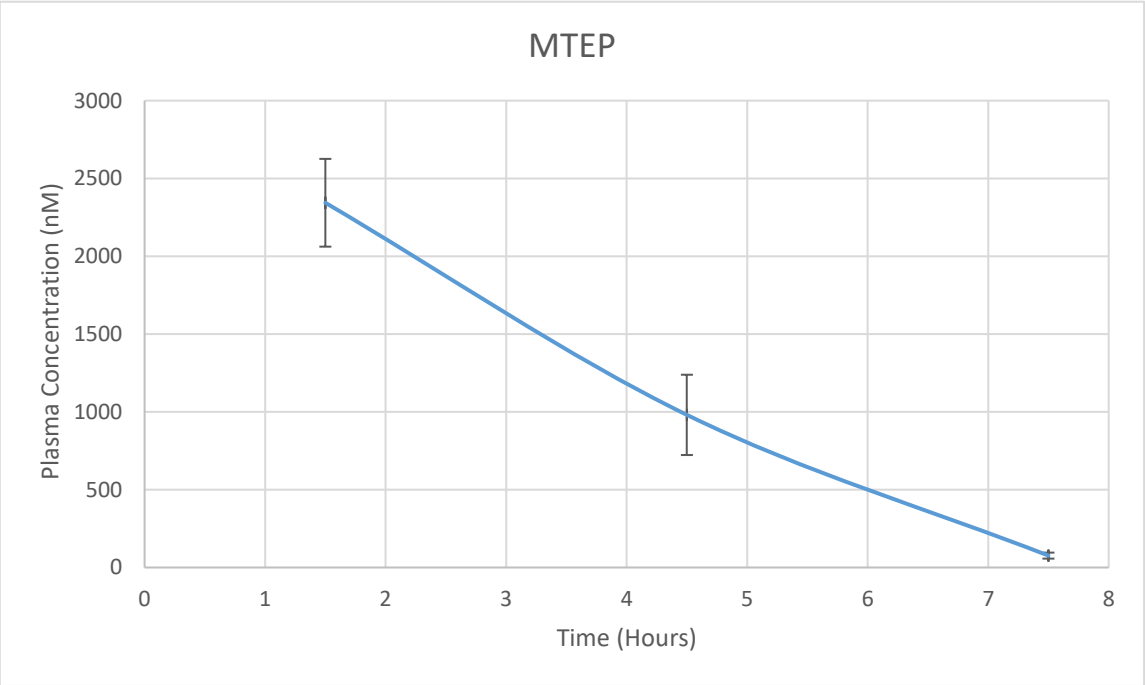

Figure 21: Pharmacokinetic study on MTEP. 8 male Wistar rats were given an I.P. injection of 4mg/Kg MTEP at T=0. Blood was withdrawn via tail vein bleed at the three time points (1.5, 4.5 and 7.5 hours) and the plasma concentration was measured via HPLC by staff at Eli Lily and Company. Error bars show SEM.

Based on this data I decided that it would be necessary to inject the animals twice per day, once in the morning and once in the evening. Ideally, the animals would have been given three injections equally spaced throughout each day, but this was not practical.

Many groups use the tail cuff method to measure blood pressure in animals (Kubota *et al.*, 2006). This is not ideal because it gives artificially high readings due to the animals experiencing handling stress and also because data has to be collected manually and the number of data points is thereby limited to what is practically possible. I used radio-telemetry. This is a technique in which blood pressure and heart rate are measured by a small device that is implanted inside the abdominal cavity of the animal and the data is relayed to acquisition software on a connected computer (see methods section of this chapter). This system is superior to the tail cuff method since data is acquired continuously whilst the animal is undisturbed in its home cage, leading to more accurate measurement and substantially reducing the incidence of anomalous results.

Methods:

Experiment Design:

All animal experiments were performed in accordance with institutional guidelines and the UK Home Office (Scientific Procedures) Act (1986) with project approval from the University of Bristol, University ethics of research committee, under Home Office personal license number ICCF4B573 and project license number 70/7868.

Blood pressure and heart rate data were collected via radio-telemetry: A setup in which a device implanted in the abdomen of each animal receives BP and HR information via a catheter inserted into the descending aorta and transmits it to a

receiver platform beneath the animal's home cage. This allows chronic measurement of HR and BP without disturbing the animal, which avoids the artificially high/variable readings obtained by the tail-cuff method.

Animals were given unlimited access to water and standard chow throughout the study.

Each experiment was divided into four phases: Baseline, Vehicle, Treatment and Washout. During the baseline phase, the animals were left undisturbed for one week. In the vehicle phase, the animals were given intraperitoneal injections of 1ml vehicle twice daily for one week. In the treatment phase, the animals were given intraperitoneal injections of 1ml appropriate drug solution twice daily for one week. The immediate 30 mins of recorded data succeeding injections was excluded in order to account for handling stress. In the washout phase the animals were once again left undisturbed for 1 week.

Data was collected and analysed using Spike2 (CED).

Implantation of Radio-Telemetry Device:

Male Wistar rats or male SHRs at ~300g were sourced from Harlan, UK. The animals were anaesthetised via intra-muscular injection of ketamine (60 mg kg^{-1}) and medetomidine (250 mg kg^{-1}). The depth of anaesthesia was assessed by the presence or absence of the pedal withdrawal reflex when the animal was subjected to noxious pinching of the foot. Once anaesthetised, the animal was placed on its back and its abdomen was shaved using electric clippers (Wahl).

The animal was placed on a heated pad and a surgical drape was placed over it with the shaved abdomen area exposed. This area was cleaned with Hydrex Pink Surgical Scrub and a midline incision of the abdominal wall was made using a scalpel. The intestines were moved aside to reveal the abdominal aorta and a

sterile gauze horseshoe, moistened with sterile saline, was inserted into the abdominal cavity in such a way as to hold the intestines out of sight and maintain good vision of the aorta. Stainless steel retractors were used to assist with this.

Under a dissecting microscope (Leica), a ligation aid (FST cat #18062-12) was used to separate the aorta and the vena cava below the renal bifurcation and above the femoral bifurcation. Ligation sutures (FST) were placed at both locations. These were pulled tight, using haemostats to weight them down and a small vascular clip (FST cat# 18055-04) was applied above the top ligation suture in order to occlude blood flow. A 21G needle (BD microlance 3) was used to make an incision in the lower portion of the aorta into which the catheter of the transmitter (DSI TA11PA-C40) was inserted, caudal to the root of the left renal artery. A small amount of tissue adhesive (Vetbond) was applied to the catheter-insertion site and a small cellulose patch (Fisher cat# NC9590679) was glued over it.

The small vascular clip was then removed and the ligation sutures loosened. In the event that bleeding occurred, these were briefly tightened again and more tissue adhesive was applied as necessary. Finally, the sutures, gauze horseshoe and retractor were removed, the intestines put back in place and the surgical wound was closed using single interrupted sutures and fixing the transmitter to the inside of the abdominal wall in the process.

The anaesthesia was reversed with a subcutaneous injection of atipamezole (1 mg kg^{-1}) and ~2ml of Hartman's solution was injected subcutaneously for the purpose of rehydration. The animal was then returned to its home cage for recovery. Subcutaneous injections of meloxicam (1 mg kg^{-1}) were used for pain management. Usually only one injection was given (on the day of the surgery)

but in some cases additional injections were given after seeking advice from the named veterinary surgeon when an animal appeared to be in pain one or two days post-surgery.

Drug Solutions and Injection Procedure:

LSN2814617:

This drug did not dissolve in saline. The following vehicle was advised by the manufacturer (Eli Lilly):

1% Hydroxyethylcellulose (sigma); 0.25% Polysorbate 80 (sigma); 0.05% Antifoam (DowCorning RD emulsion) v/v in sterile saline. This vehicle did not completely dissolve the drug. Sonication was required. The drug suspension was put into a 50ml Falcon tube on ice and was sonicated at 45% amplitude with a Sonics Vibracell probe sonicator for 30 mins. This produced a very fine suspension suitable for intraperitoneal injections. A clear solution could not be achieved.

MPEP and MTEP:

Both of the antagonists dissolved easily in sterile saline at room temperature with mild mixing.

Injections:

On injection days animals were taken one by one in their home cages to a procedure room, placed into a thin, transparent restraint tube (Decapicones, Braintree Scientific) and given intraperitoneal injections of vehicle or appropriate drug treatment (prepared as described above) before being returned to their home cages. No other drugs (sedatives etc.) were given. The two injections were given 8-12 hours apart on each injection day.

Results:

Twice-daily IP injections of 0.3mg/Kg LSN2814617 into normotensive male Wistar rats produced a significant increase in BP ($p=0.032$) and heart rate ($p=0.041$) on the first day only. Increasing the dose of LSN2814617 to 1mg/Kg produced a significant ($p=0.039$) increase in BP of a greater magnitude than at the lower dose. The HR at this dose also trended upwards, although the increase was not statistically significant. The maximum dose of 3mg/Kg LSN2814617 produced a significant ($P=0.029$) increase in BP that was greater still than that obtained with 1mg/Kg and a similar upwards but non-significant trend was observed in the HR. Increasing the dose did not produce significant effects on days beyond day 1, in every case the BP and HR trended back towards baseline after day 1.

No significant effects were produced by twice daily IP injection with MPEP into male SHRs at 1,3 or 9mg/Kg. However, MTEP produced a significant ($p=0.044$) decrease in BP on day 1 at 1mg/Kg and a slightly larger significant ($p=0.038$) decrease on day 1 at 6mg/Kg. No significant effects on HR were observed and as with LSN2814617, the BP trended back towards baseline after the first day.

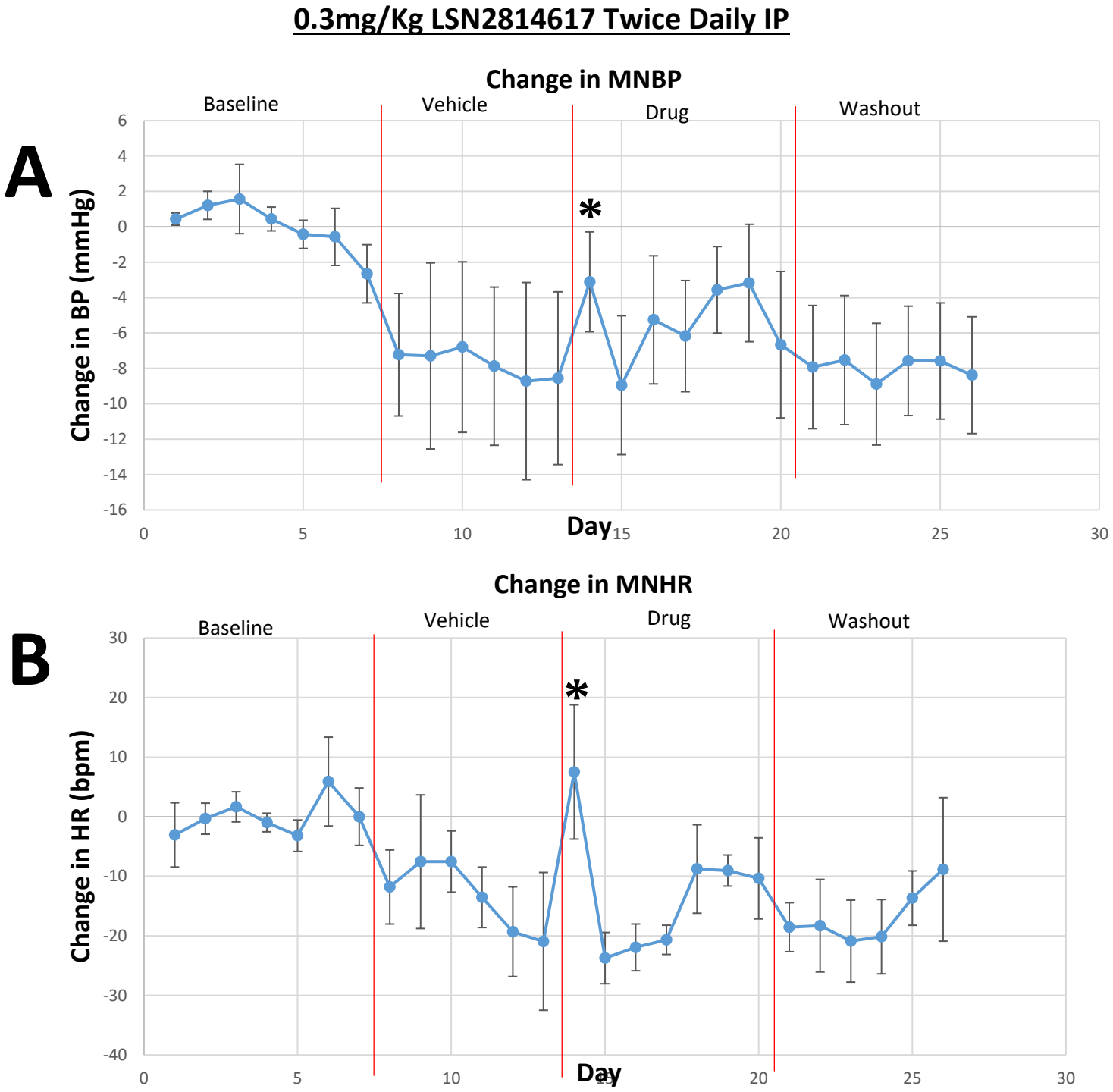

Figure 22: Effect of twice daily intraperitoneal injections of 0.3mg/Kg LSN2814617 on blood pressure (Panel A) and heart rate (Panel B) on 300g normotensive male Wistar rats. Animals were left untreated for an initial 7 days (baseline period), given vehicle only for the next 6 days, given LSN2814617 for the next 7 days and then left untreated for the final 6 days (washout period). Each datapoint shows mean of readings taken every 10 mins throughout each day. 30 minutes of data excluded after each injection in order to minimise impact of handling stress. Error bars show SEM. n=8

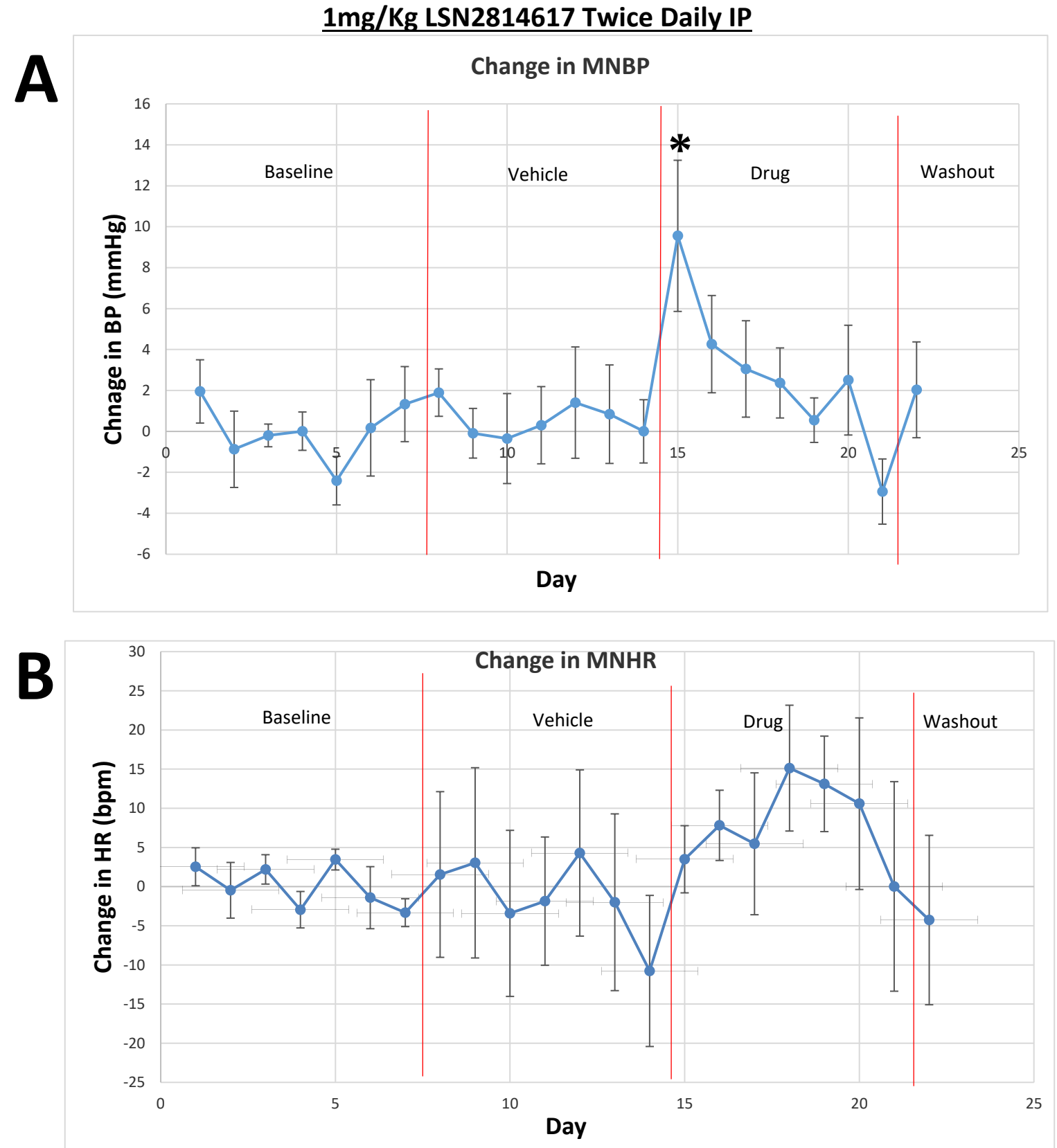

Figure 23: Effect of twice daily intraperitoneal injections of 1mg/Kg LSN2814617 on blood pressure (Panel A) and heart rate (Panel B) on 300g normotensive male Wistar rats. Animals were left untreated for an initial 7 days (baseline period), given vehicle only for the next 7 days, given LSN2814617 for the next 7 days and then left untreated for the final 1 day (washout period was cut short by a power cut, which stopped recording of data). Each datapoint shows mean of readings taken every 10 mins throughout each day. 30 minutes of data excluded after each injection in order to minimise impact of handling stress. Error bars show SEM. n=6

3mg/Kg LSN2814617 Twice Daily IP

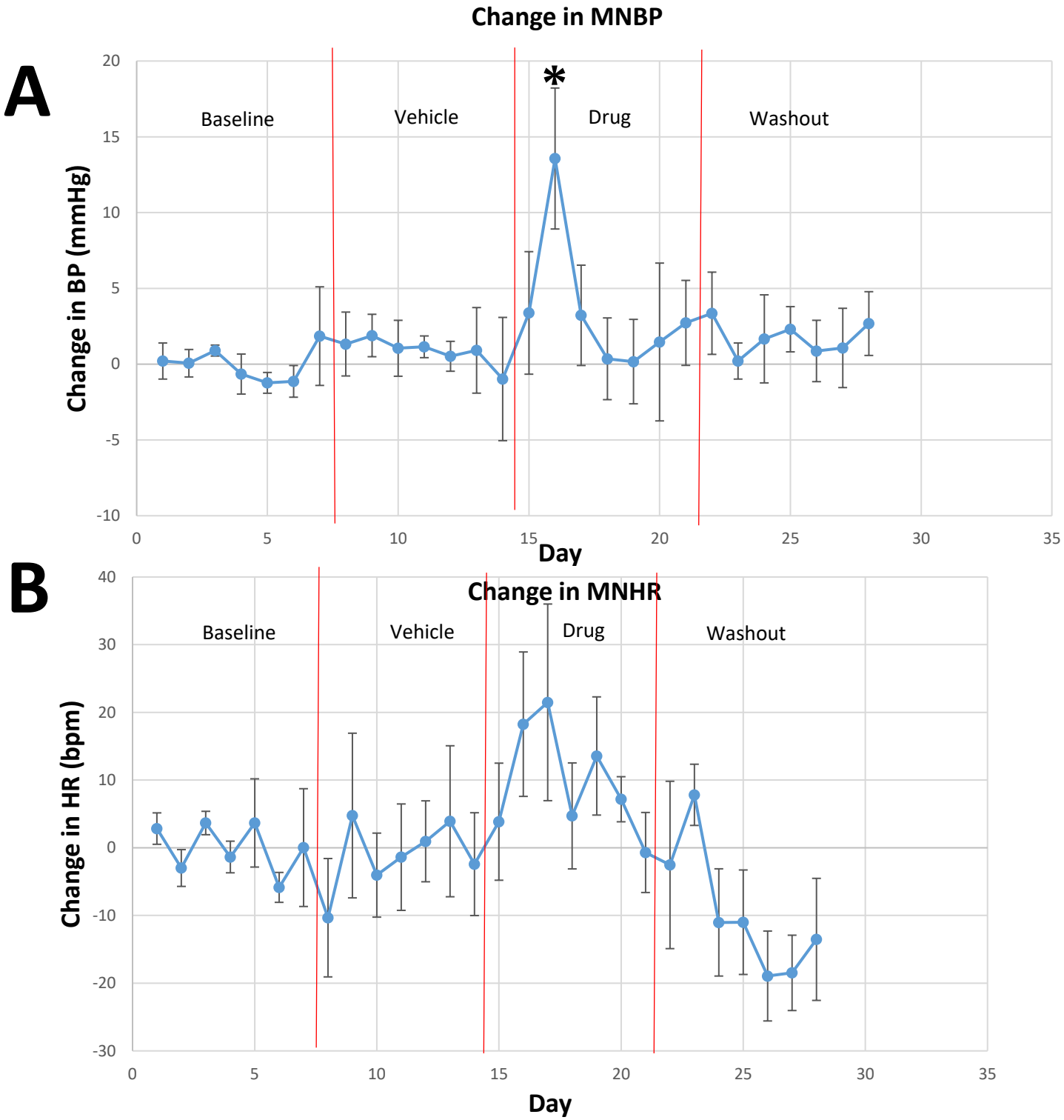

Figure 24: Effect of twice daily intraperitoneal injections of 3mg/Kg LSN2814617 on blood pressure (Panel A) and heart rate (Panel B) on 300g normotensive male Wistar rats. Animals were left untreated for an initial 7 days (baseline period), given vehicle only for the next 7 days, given LSN2814617 for the next 7 days and then left untreated for the final 7 days (washout period). Each datapoint shows mean of readings taken every 10 mins throughout each day. 30 minutes of data excluded after each injection in order to minimise impact of handling stress. Error bars show SEM. n=8

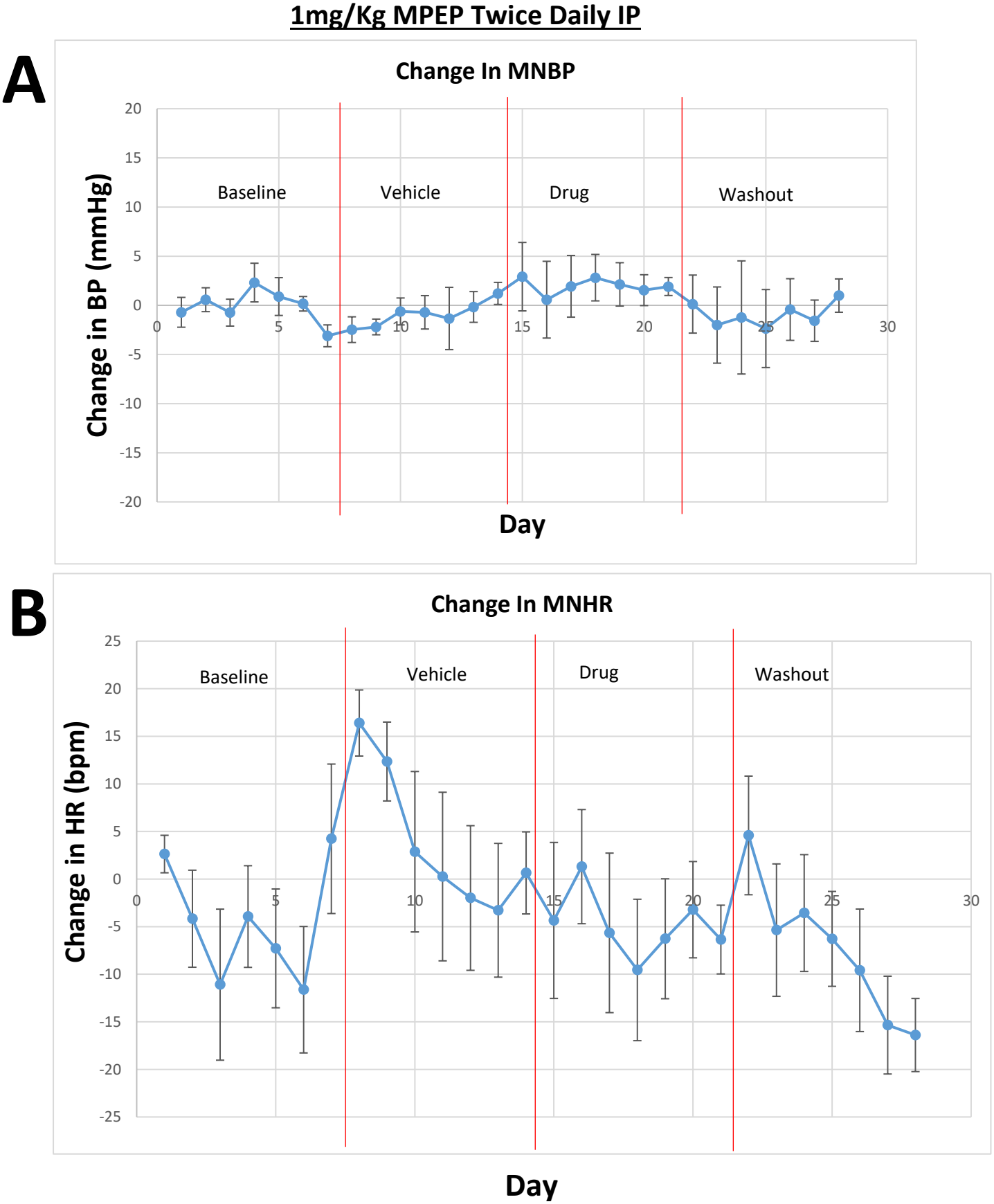

Figure 25: Effect of twice daily intraperitoneal injections of 1mg/Kg MPEP on blood pressure (Panel A) and heart rate (Panel B) on 300g hypertensive male SHR rats. Animals were left untreated for an initial 7 days (baseline period), given vehicle only for the next 7 days, given MPEP for the next 7 days and then left untreated for the final 7 days (washout period). Each datapoint shows mean of readings taken every 10 mins throughout each day. 30 minutes of data excluded after each injection in order to minimise impact of handling stress. Error bars show SEM. n=8

3mg/Kg MPEP Twice Daily IP

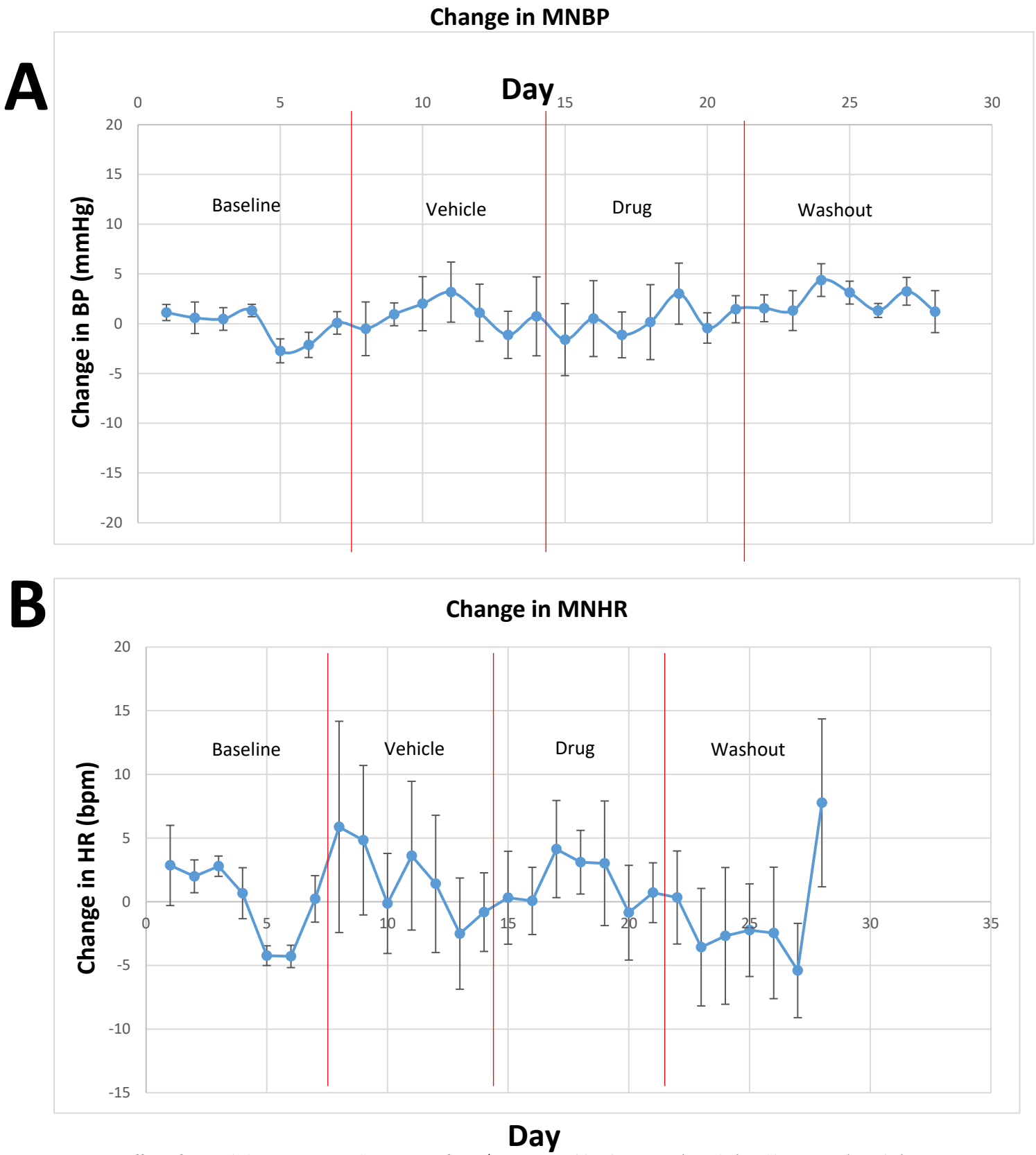

Figure 26: Effect of twice daily intraperitoneal injections of 3mg/Kg MPEP on blood pressure (Panel A) and heart rate (Panel B) on 300g hypertensive male SHR rats. Animals were left untreated for an initial 7 days (baseline period), given vehicle only for the next 7 days, given MPEP for the next 7 days and then left untreated for the final 7 days (washout period). Each datapoint shows mean of readings taken every 10 mins throughout each day. 30 minutes of data excluded after each injection in order to minimise impact of handling stress. Error bars show SEM. n=8

6mg/Kg MPEP Twice Daily IP

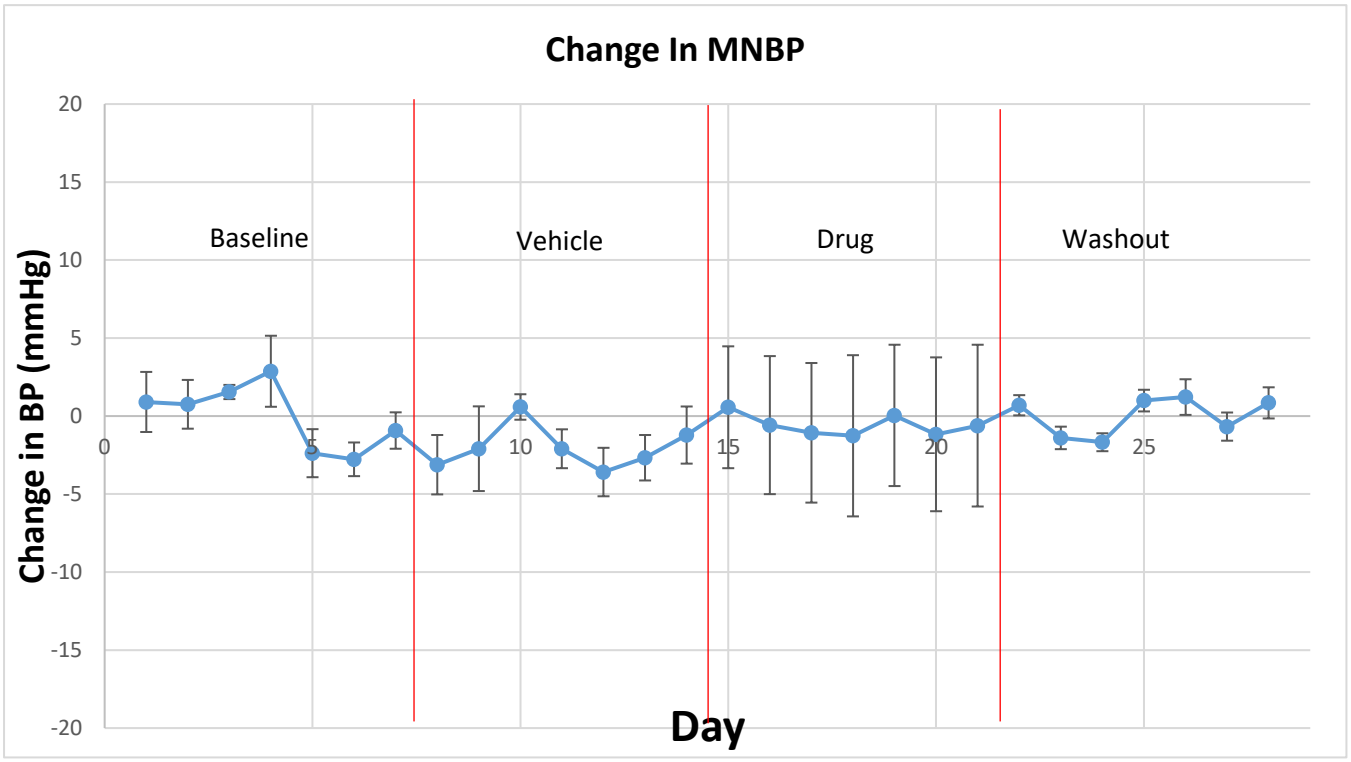

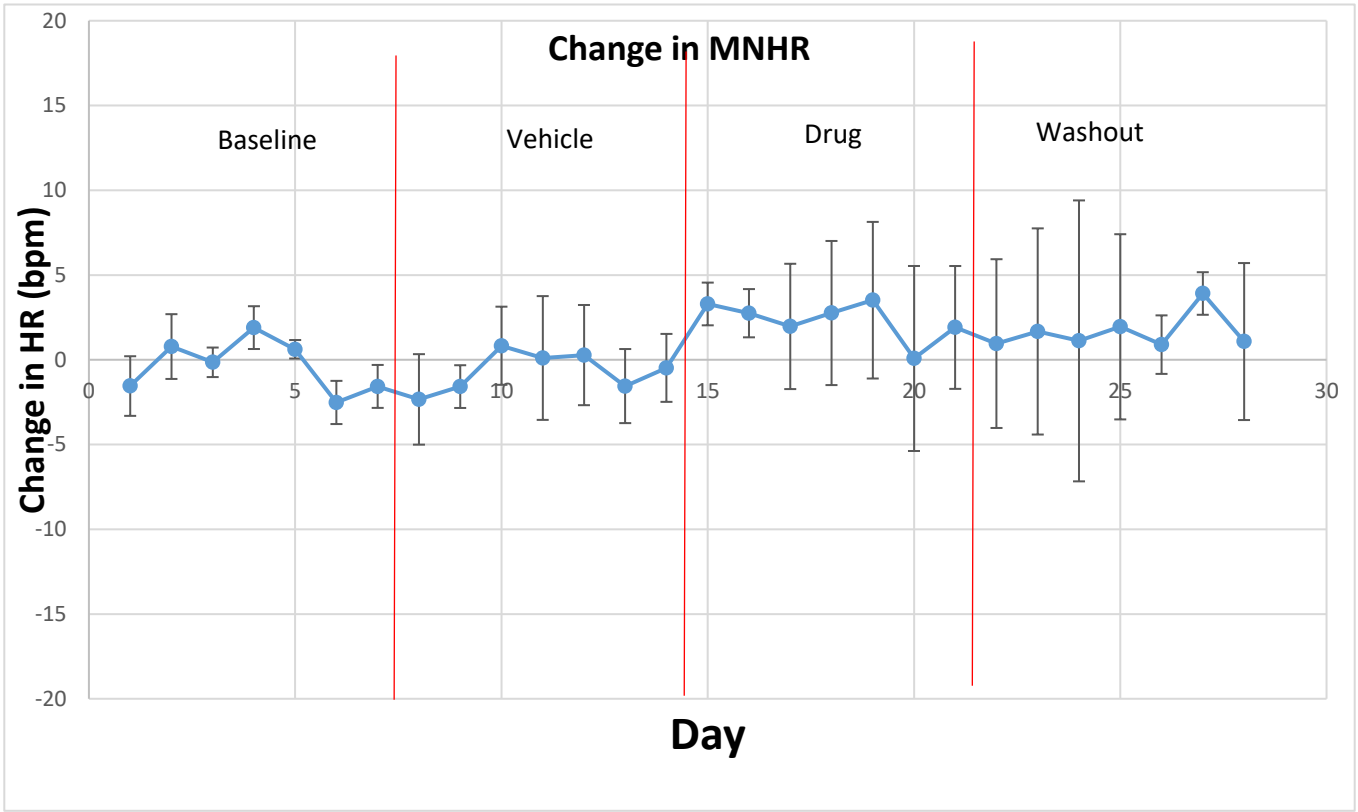

Figure 27: Effect of twice daily intraperitoneal injections of 3mg/Kg MPEP on blood pressure (Panel A) and heart rate (Panel B) on 300g hypertensive male SHR rats. Animals were left untreated for an initial 7 days (baseline period), given vehicle only for the next 7 days, given MPEP for the next 7 days and then left untreated for the final 7 days (washout period). Each datapoint shows mean of readings taken every 10 mins throughout each day. 30 minutes of data excluded after each injection in order to minimise impact of handling stress. Error bars show SEM. n=6

1mg/Kg MTEP Twice Daily IP

A

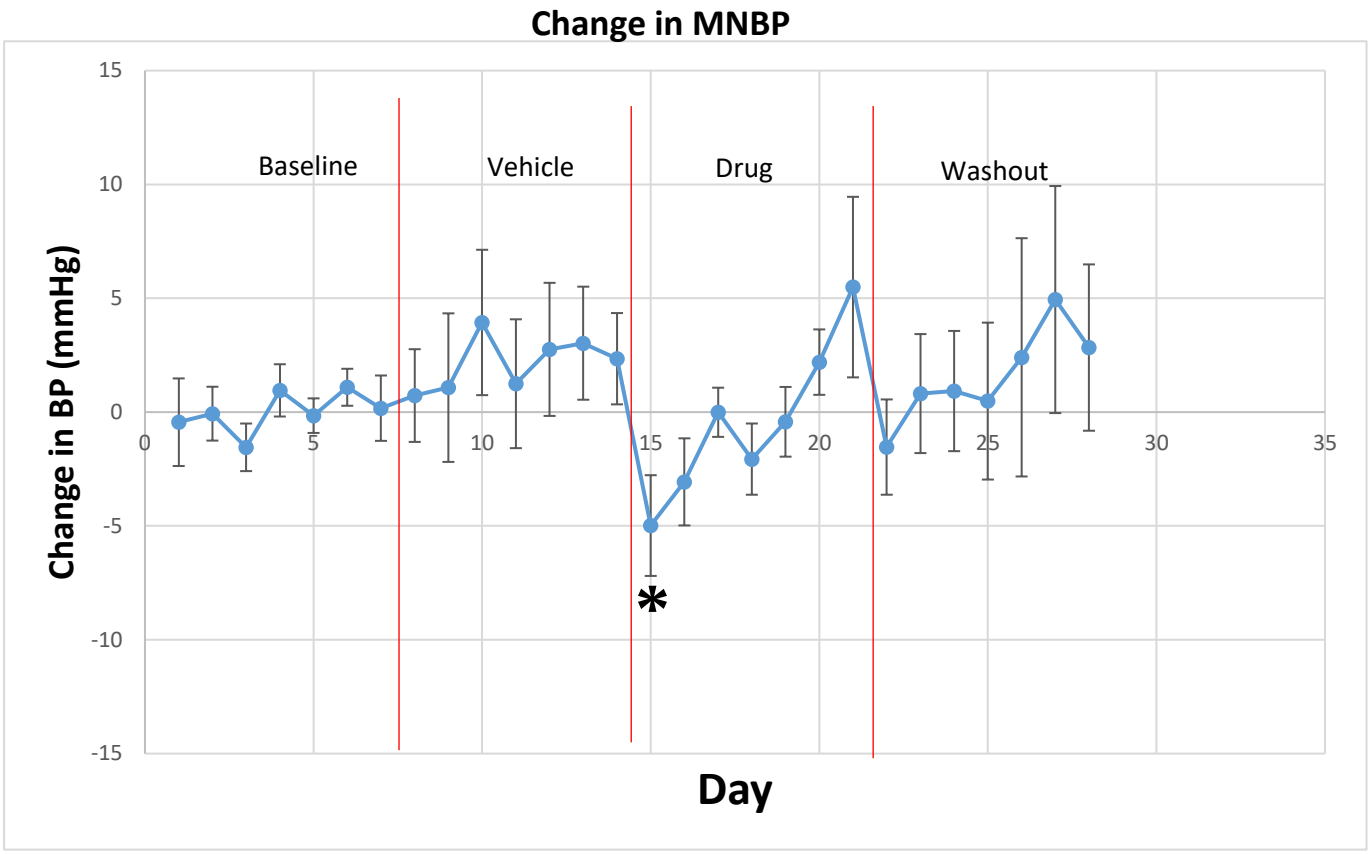

B

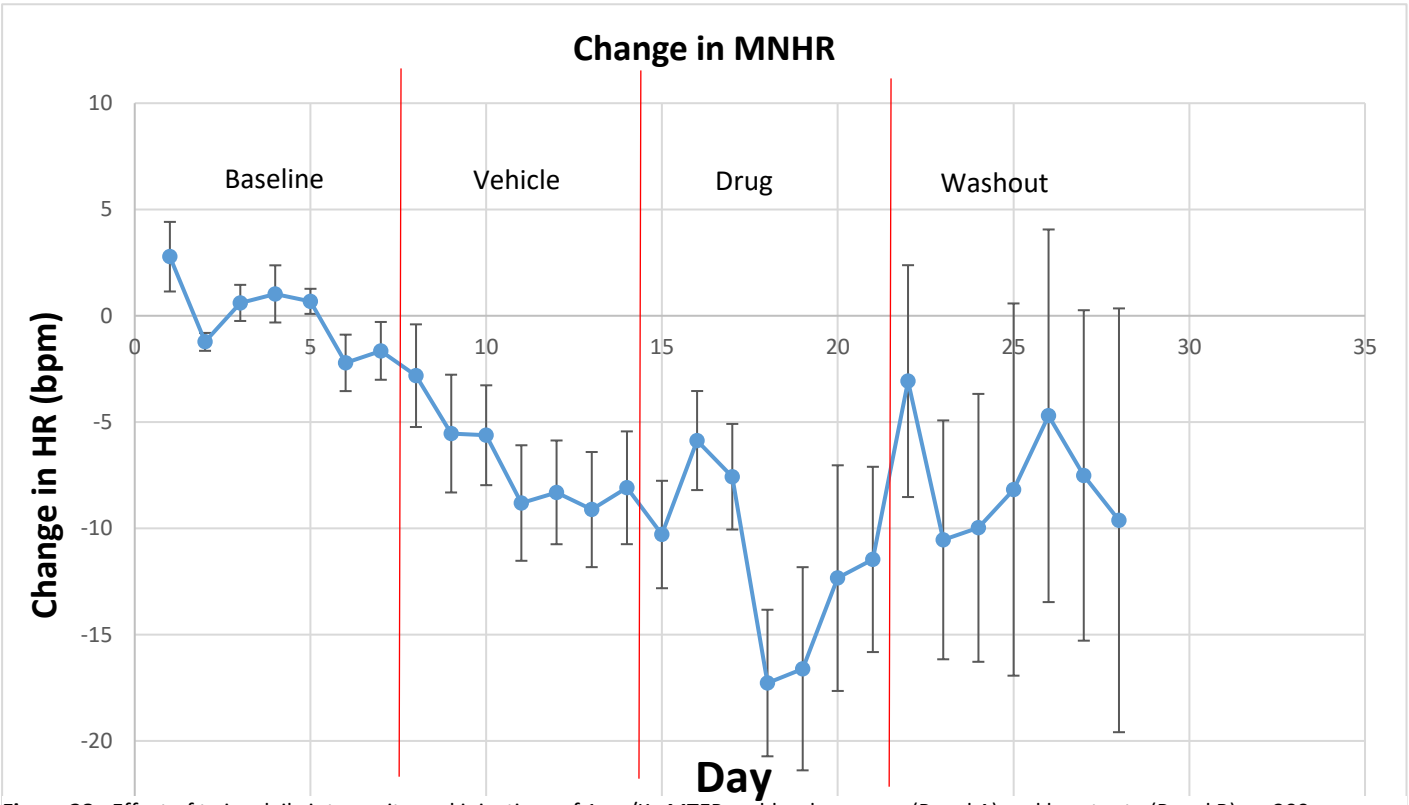

Figure 28: Effect of twice daily intraperitoneal injections of 1mg/Kg MTEP on blood pressure (Panel A) and heart rate (Panel B) on 300g hypertensive male SHR rats. Animals were left untreated for an initial 7 days (baseline period), given vehicle only for the next 7 days, given MPEP for the next 7 days and then left untreated for the final 7 days (washout period). Each datapoint shows mean of readings taken every 10 mins throughout each day. 30 minutes of data excluded after each injection in order to minimise impact of handling stress. Error bars show SEM. n=6

6mg/Kg MTEP Twice Daily IP

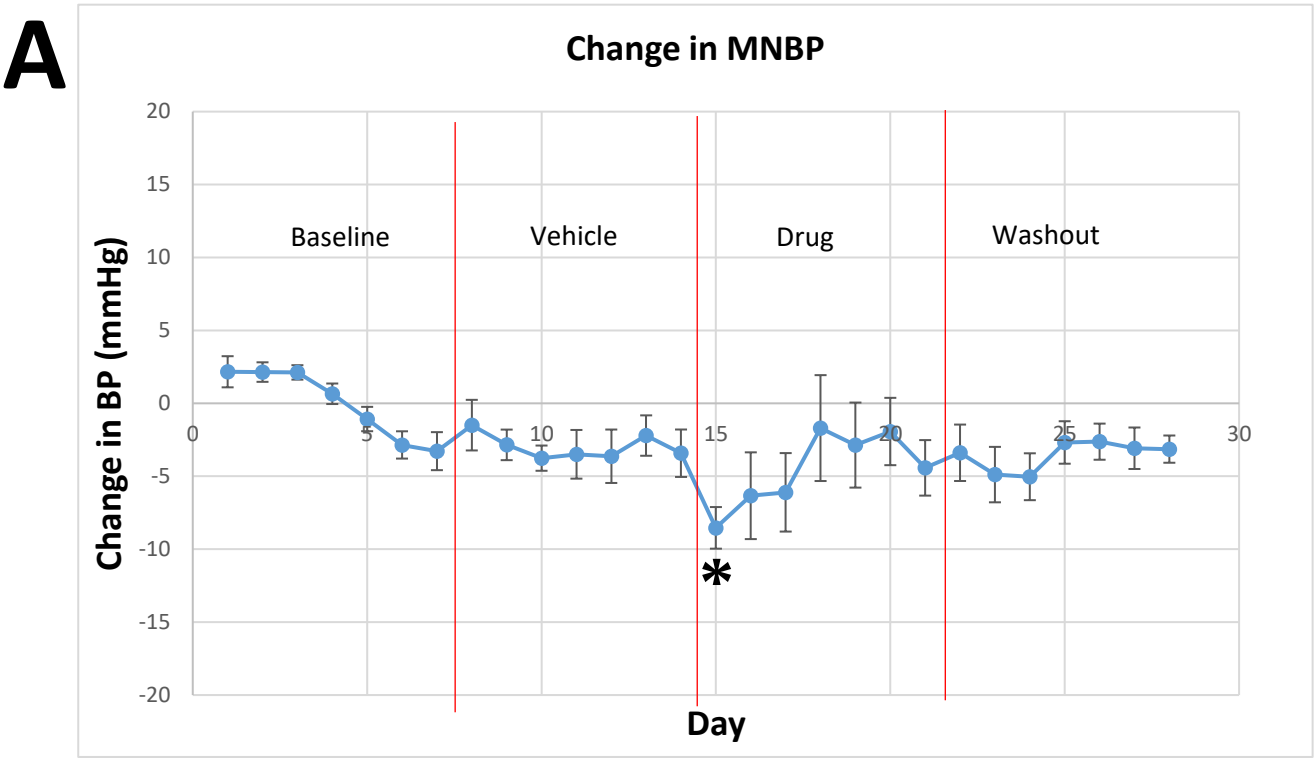

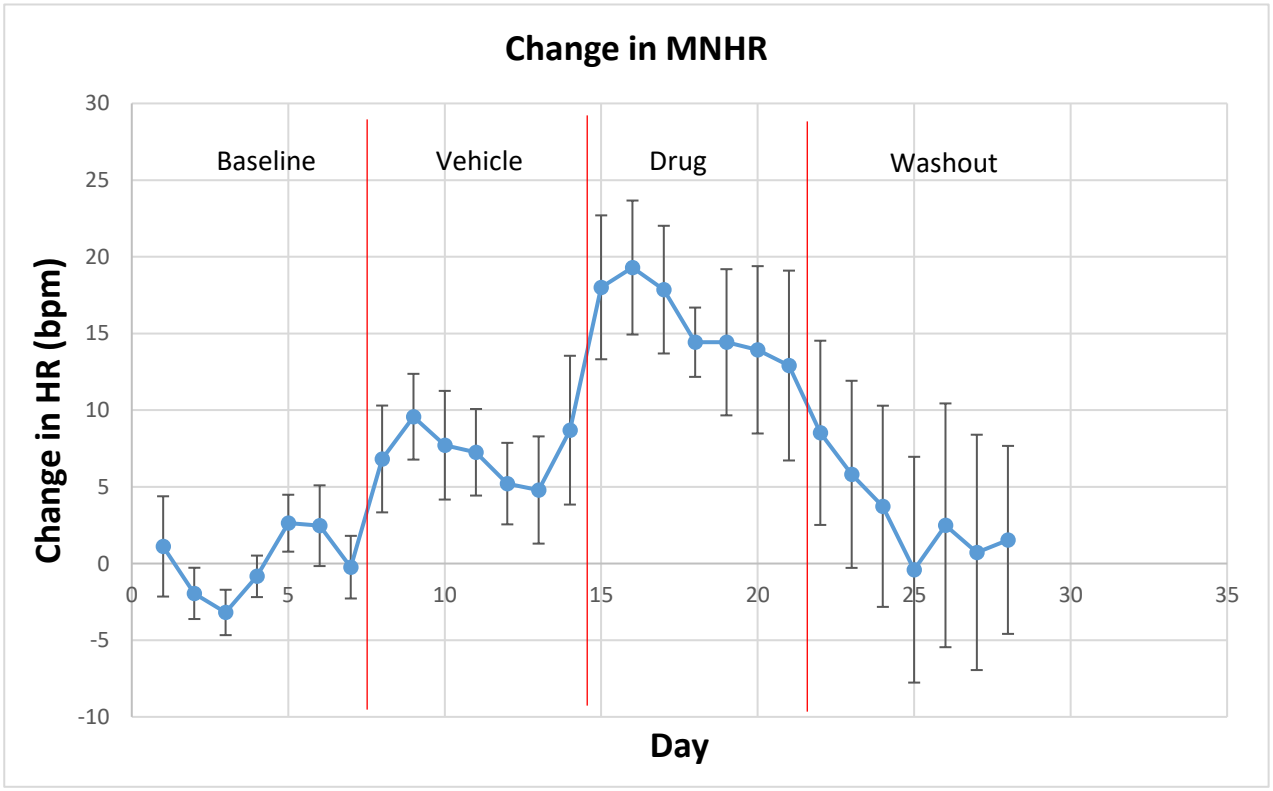

Figure 29: Effect of twice daily intraperitoneal injections of 3mg/Kg MTEP on blood pressure (Panel A) and heart rate (Panel B) on 300g hypertensive male SHR rats. Animals were left untreated for an initial 7 days (baseline period), given vehicle only for the next 7 days, given MPEP for the next 7 days and then left untreated for the final 7 days (washout period). Each datapoint shows mean of readings taken every 10 mins throughout each day. 30 minutes of data excluded after each injection in order to minimise impact of handling stress. Error bars show SEM. n=6

Discussion:

Positive Allosteric Modulation of mGluR5 Via Twice Daily Injections of LSN2814617 Increases Blood Pressure and Heart Rate on a Temporary Basis:

Twice daily intraperitoneal administration of LSN2814617 significantly raised blood pressure in normotensive Wistar rats (Figures 22, 23 and 24). However, the effect appears to be transient such that within 2-3 days pressures return to normal after that period. This increase did not occur after injections of vehicle controls so non-pharmacological factors such as stress can be ruled out. The fact that the compound raised blood pressure initially was not surprising, given the preliminary data provided by Eli Lilly and Company (Figure 10) although their data came from experiments in ferrets and the effect may not have occurred in rats. Their use of a different animal may also explain the fact that the pressure increase they observed was significantly larger than what I observed in rats, reflecting a possible species difference. Interestingly, the tolerance appears to have manifested more quickly at higher doses.

There are multiple mechanisms that could explain the tolerance to the compound. Firstly, it is possible that the blood pressure response returns to baseline after 2-3 days due to pharmacokinetic tolerance; time-dependent changes in the distribution or metabolism of the drug may be resulting in a lower concentration of pharmacologically active compound at the site of mGluR5 receptors in the nuclei of interest. Tolerance occurring via this mechanism is known to affect many compounds targeting receptors in the CNS, for example phenytoin, phenobarbital and carbamazepine (Nijhawan *et al.*, 1990; Hussein *et al.*, 2013). These anti-epileptic drugs cause an increase in hepatic enzymes

which result in a faster rate of metabolism (Nijhawan *et al.*, 1990; Hussein *et al.*, 2013). Because of the increase in the rate of metabolism of the drug, higher subsequent doses must be given in order to maintain desired serum concentrations.

The distribution of the PAM could be affected by induction of drug-efflux transporters such as p-glycoprotein or proteins belonging to the multi-drug resistance family (MRPs), which are expressed on a variety of cell membranes including endothelial cells comprising the BBB (Schinkel & Jonker, 2003). An increase in expression of these proteins in response to the PAM could result in less drug reaching the CNS (Löscher & Potschka, 2005). Additionally, induction of MRPs in the proximal tubule of the kidney or the canalicular membranes of hepatocytes could promote increased excretion of the PAM via the urine and bile.

Another possibility is that the animals are exhibiting pharmacodynamic tolerance; the PAM is eliciting a response within the target neuronal network which reduces the effect of the drug when it is administered again. Synaptic activity is known to induce Homer1a (Brakeman *et al.*, 1997; Vazdarjanova *et al.*, 2002), which uncouples mGluR5 from its postsynaptic effectors (Xiao *et al.*, 2000; Kammermeier & Worley, 2007). It is possible that increased activity of mGluR5 as a result of the PAM initially results in increased neuronal excitability and thereby activity, which induces Homer1a, resulting in uncoupling of the receptor from its downstream effectors, restoring neuronal activity to baseline.

In addition, the responsiveness of GPCRs is modulated at the level of the G-protein by proteins known as regulators of G-protein signalling (RGS), which promote guanosine triphosphate hydrolysis by the alpha subunit of G-proteins,

which feeds back and terminates GPCR signalling pathways (De Vries *et al.*, 2000).

Alternatively, or perhaps additionally, interaction between the PAM and the receptor or the increase in neuronal signalling resulting from said interaction may induce endocytosis of the receptor or down-regulation of receptor expression.

Over-stimulation of GPCRs (both acute and chronic) is known to be protected against by a process of receptor internalisation in response to agonists. In the case of persistent stimulation, when agonist binds to a receptor, G-protein coupled receptor kinases (GRKs) bind the receptor-agonist complex, resulting in phosphorylation of the receptor (Krupnick & Benovic, 1998; Ferguson, 2001). Arrestins then also bind to the cytoplasmic face of the receptor, preventing G-protein interaction. The binding of Arrestins facilitates receptor endocytosis via the clathrin-coated pit pathway (Moore *et al.*, 2007). This process is outlined in Figure 30.

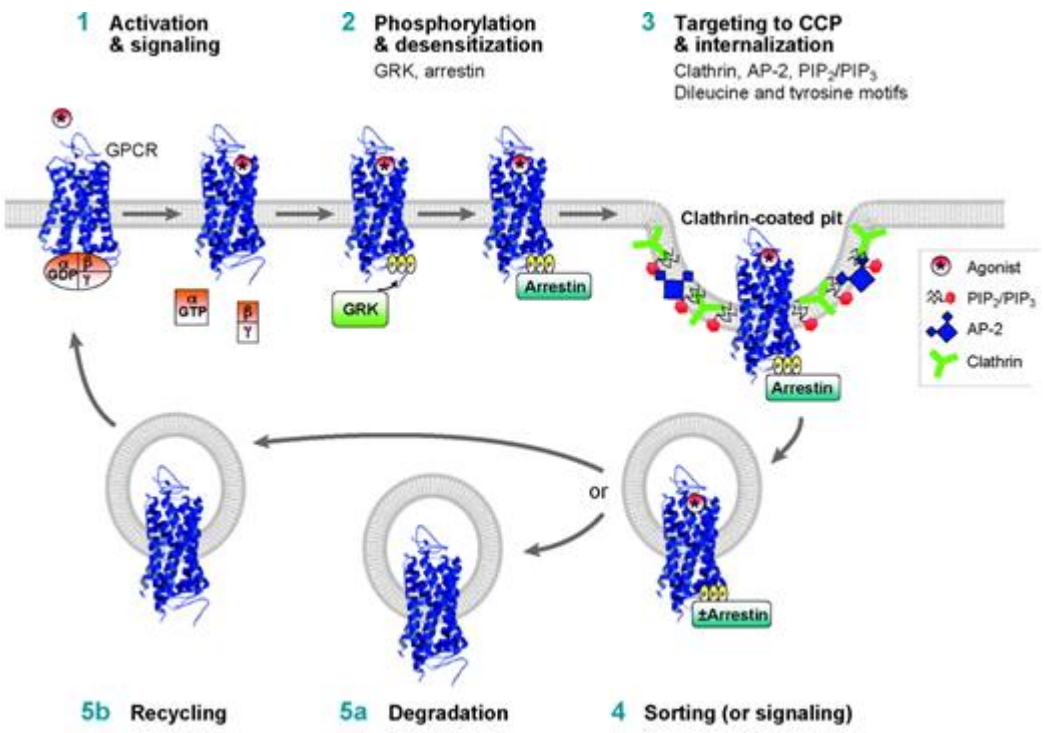

Figure 30: Schematic adapted from Moore *et al.*, 2007 outlining endocytosis of GPCRs via the clathrin-coated pit pathway. GTP = GTP binding protein, GRK GRK = G-protein coupled receptor kinase, PIP2 = Phosphatidylinositol 4,5-bisphosphate, PIP3 = Phosphatidylinositol (3,4,5)-trisphosphate, AP2 = AP2 adaptor complex.

Fourgeaud *et al.* showed that mGluR5 can be endocytosed by a clathrin-independent pathway (Fourgeaud *et al.*, 2003). It was later discovered that this occurs via the Caveolar/Lipid Raft Pathway (Francesconi *et al.*, 2009). Caveolae are cone-shaped invaginations of the plasma memberane (Anderson, 1993; Razani *et al.*, 2002). Caveolins, structural proteins, are essential for the integrity of caveolae (Cameron *et al.*, 1997). In this regard, caveolins serve a similar function to clathrin in clathrin-coated pits. Neurones do not possess caveolae but caveolin proteins are expressed in these cells and other cells lacking caveolae, such as leukocytes (Head & Insel, 2007). Caveolins serve a purpose as scaffolding proteins in these cells and may be involved in signal transduction (Head and Insel, 2007). More research on the involvement of caveolins in mGluR5 internalisation specifically is required.

The degree to which an agonist induces receptor endocytosis varies depending on the ligand; a single dose of cocaine causes a significant reduction in surface expression of mGluR5 (Fourgeaud *et al.*, 2004).

Finally, it is possible that mGluR5 does not have a significant influence on neural circuitry that is involved in long-term blood pressure control. If modulation of the receptor does not change the blood pressure 'set-point' then homeostatic mechanisms (outside of the circuity that mGluR5 does influence) will return the pressure to the set-point and the altered mGluR5 signalling will be dealt with in the same manner as any other hyper/hypotensive stimulus by, for example, blood volume modification.

In addition to increasing blood pressure, the PAM caused a significant increase in heart rate that persisted for the same period as the pressor response. An increase in blood pressure coupled with an increase in heart rate was not expected since a blood pressure increase should induce a baroreceptor reflex reduction in heart rate mediated via activation of the vagus and inhibition of sympathetic activity. The fact that both blood pressure and heart rate increased simultaneously could suggest that the PAM is depressing the baroreflex, thereby allowing both blood pressure and heart rate to rise. This effect would most likely occur due to modulation of signalling in the PVN, since stimulation of neurones in this region is sympathoexcitatory due to the inhibitory effects this has on the baroreflex signalling in the NTS (Figure 2). This fits with data from Li and Pan (2010), who found that agonism of mGluR5 in the PVN raised blood pressure, heart rate and SNA. Alternatively, or additionally, my observations may be due in part to mGluR5 activity in the periphery. The receptor is present in the heart itself and perhaps LSN2814617 elicits effects by acting directly on the organ to

increase the rate of contraction and blood pressure (Gill *et al.*, 1999; Xie *et al.*, 2015).

Twice-Daily Intraperitoneal Injections of MPEP has no significant effect on Blood Pressure in SHRs:

Twice-Daily Injections of MPEP in SHRs did not produce the reduction in blood pressure that was expected (Figures 25, 26 and 27). This could be explained by the fact that MPEP has off-target effects at NMDA receptors (O'Leary *et al.*, 2000; Movsesyan *et al.*, 2001) and mGluR4 (Mathiesen *et al.*, 2003). It is also possible that the dose used was too low. Although a wide-range of literature was consulted for dose-selection purposes, most studies using MPEP are conducted in order to study psychological conditions such as addiction and observable effects in this field may manifest at low doses, sub-threshold to a blood pressure response. Financial considerations also had to be made - doses as high as 50mg/Kg as used in some studies, would not have been possible here.

mGluR5 Antagonism via Twice-Daily Intraperitoneal Injections of MTEP Reduces Blood Pressure in SHRs on a Temporary Basis:

Twice-daily injections of MTEP did produce a reduction in blood pressure. The magnitude of the effect was similar to what was observed with the PAM. This was expected based on the preliminary data from Lilly and my own data showing the blood pressure rising in response to the PAM. It also fits with data from Li and Pan (2010), who found that antagonism of mGluR5 in the PVN reduced blood pressure. However, Li and Pan also found that the heart rate was reduced along with blood pressure, which I did not find – I found no significant differences in heart rate after treatment with MTEP but the heart rate data was erratic and was trending in opposite directions for each of the doses before the

drug was even administered (Figures 28 and 29). I am not confident that my heart rate data is reliable in this study due to the instability observed in the vehicle phase.

Precious little research into the involvement of mGluR5 in blood pressure control has been conducted. Taking the findings of Li and Pan into account with my own and the fact that Holbein *et al.*, found that activation of mGluRs in the PVN is sympathoexcitatory (Holbein *et al.*, 2012), I would conclude that modulation of mGluR5 affects blood pressure control at the level of the sympathoexcitatory neurones of the PVN but add in the caveat that we do not have evidence to rule out direct involvement of other key nuclei or indeed activity of mGluR5 in the periphery. It is unlikely that systemic mGluR5 antagonism will ever be used as a treatment for hypertension due to the likelihood of off-target affects manifesting as a result of modulation of a receptor that is widely expressed, especially in the cortex.

Limitations and Future Studies:

As discussed, the fact that the drug was administered systemically in this study makes it impossible to determine with any certainty the specific mechanism for mGluR5 modulation. Initially I planned to administer the compounds via ICV infusion but the solubility of LSN2814617 in any physiological vehicle was extremely poor, so this was not possible; even using a vehicle specifically recommended by the manufacturer and with extensive sonication the end result was a very fine suspension rather than a solution. This was appropriate for intraperitoneal injection but was not appropriate for use in osmotic minipumps, which would have been the preferred delivery method.

The fact that the animals were injected twice daily may have caused them to be stressed – adding in a confounding variable that would have been eliminated if it was possible to use a continuous, automatic drug delivery system such as the osmotic minipumps. This stress due to repeated handling and injection may explain the large standard errors observed with heart rate data even during the vehicle phase.

Even with continuous, hands-off drug delivery, the fact that the PAM and both antagonists cross the BBB would not resolve the issue of being unable to locate the exact nucleus mediating the observed effects on blood pressure. Instead, additional studies need to follow the lead of Li and Pan, microinjecting compounds modulating mGluR5 into the various nuclei responsible for blood pressure control. In this way the involvement of each nucleus could be tested on an individual basis. It would also be useful to administer the drugs intracerebroventricularly whilst also systemically administering compounds with the 'opposite' effect that are restricted to the periphery. E.g. Give MTEP centrally and an mGluR5 agonist that cannot cross the BBB via an IV or IP injection. Assuming the agonist and antagonist effects of the compounds would effectively cancel each other out in the periphery, the antagonist (MPEP) acting alone in the CNS would allow for confirmation of the hypothesis that the effects on blood pressure I have observed were indeed due to activity on central blood pressure control neuronal circuitry rather than on peripheral targets. Unfortunately drugs suitable for such a study do not currently exist.

In order to gain a mechanistic understanding of the effects I observed, I would have liked to do spectral analysis of heart rate variability (Karemaker, 1997). This would allow me an insight into balance between the sympathetic and

parasympathetic components of autonomic outflow. Unfortunately, I did not have time to do this. Ideally, I would have been able to actually measure SNA but this was not possible.

It would have been interesting to conduct an experiment in which I followed the compounds modulating mGluR5 with administration of hexamethonium. Hexamethonium blocks the nicotinic acetylcholine receptors utilised by the sympathetic system and the parasympathetic ganglia. Because of this, hexamethonium causes a large decrease in blood pressure by eliminating autonomic outflow. Although hexamethonium blocks both sympathetic and parasympathetic activity, this experiment would allow an indirect measurement of any changes caused by mGluR5 modulation in sympathetic drive controlling vasomotor tone specifically, since in the case that LSN2814617 increases vasomotor tone and MTEP reduces it, a larger drop in blood pressure would be observed with the PAM compared to MTEP upon administration of hexamethonium and the resultant loss of vasomotor tone, which is maintained exclusively by the sympathetic system.

Chapter 4: Assessment of T-Cell Phenotype in Normotensive Vs. Hypertensive Humans

Introduction:

Cluster of Differentiation:

Leukocytes express a multitude of cell surface proteins that can be used for immunophenotyping since the combination of proteins expressed by a cell depends on the type of cell, the function of the cell and the condition the cell is in (e.g. antigen experienced vs. naïve cells). These proteins are functional and include receptors, ligands for receptors on other cells or adhesion molecules involved in activities such as leukocyte recruitment to sites of inflammation. A protocol known as Cluster of Differentiation (CD) has been developed in order to identify these proteins. The proteins are given a numerical CD designation at Human Leukocyte Differentiation Antigens (HLDA) workshop conferences (http://www.hcdm.org/) which are held around the world periodically. These CD numbers are then used as standard nomenclature by the scientific community.

Fluorescence-Activated Cell Sorting (FACS) – A Method to Phenotype Cells:

A common technique for identifying CD markers is Fluorescence-Activated Cell Sorting (FACS), which is a specialised form of flow cytometry. Basic flow cytometry uses lasers to identify cells based on their light-scattering properties. A cell suspension is fed into the machine

and through a nozzle, the cells are arranged into a single file. The cells are passed in front of a laser and light scattered from the cells is detected by an electronic sensor array. One detector directly in front of the laser detects forward scatter (FSC) and others to the side detect side scatter (SSC). FSC is correlated with the size of the cell and SSC with the granularity. With information on both size and granularity of cells in the sample it is possible to identify them. For example, in a whole blood sample, the small cells with low granularity are lymphocytes and large cells with high granularity are granulocytes (Figure 31). FACS data is displayed on dot plots where the axes represent a measure of the scaled intensity of light pulses received by the detectors of the flow cytometer. Tests are run before an experiment to ensure that cells at both the upper and lower limit of what is being measured are on scale. The machine is calibrated differently depending on the cell types being studied and the units on the axes are essentially arbitrary – cells are considered larger or more granular in relation to each other and objective measurements of these parameters are not made.

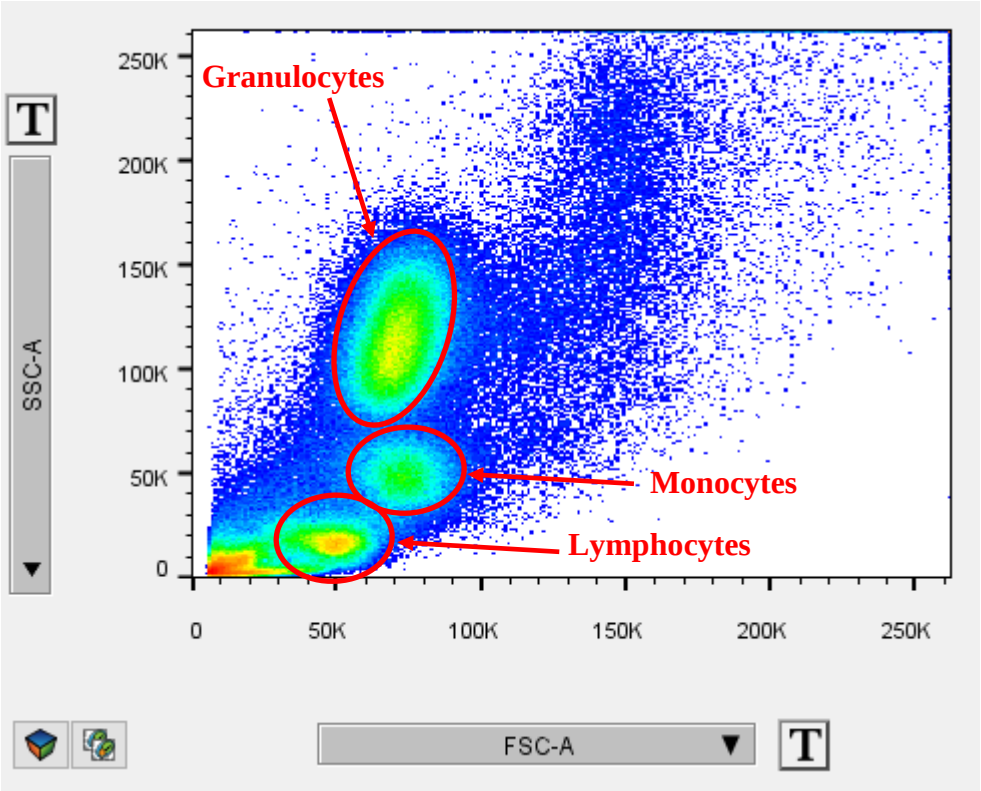

Figure 31: Example from my data showing graphical representation of FSC Vs. SSC and identification of cell population based on this information. Lymphocytes are small and less granular than other cells and so constitute the lower left cell population (the cluster in the far bottom left is debris – always present in FACS samples). Granulocytes, macrophages etc. are larger and much more granular. **FSC:** Forward scatter (correlates to the size of a cell), **SSC:** Side scatter (correlates to cell granularity).

The use of FACS allows for investigation of specific CD markers on a cell as it passes through the laser beam. Prior to running the samples on the flow cytometer, the cells are labelled with antibodies for CD markers of interest. These antibodies are conjugated to a fluorescent chemical (fluorophore) which emits light of a specific wavelength when it is excited by a laser (Figure 32). The emitted light acts as a reporting signal.

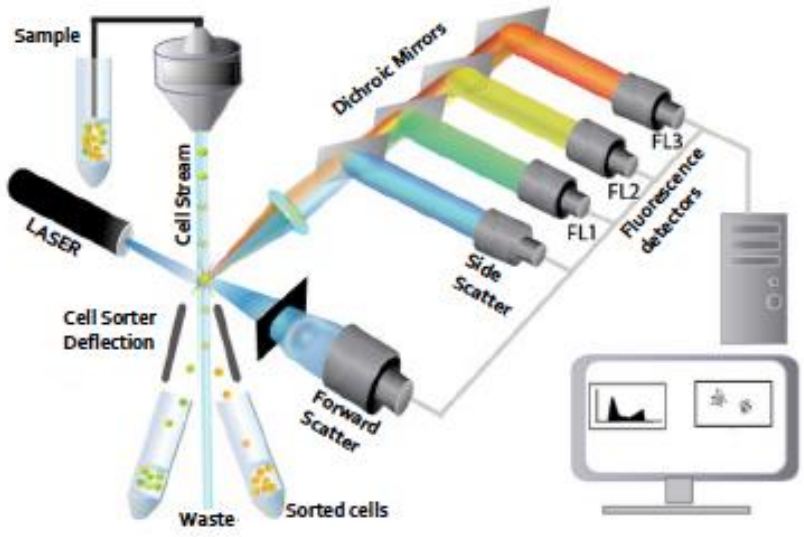

Figure 32: *Schematic outlining FACS data acquisition. (Roy J Carver Biotechnology Centre, University of Illinois)* Cells are run in single file in front of a laser. The light hitting a cell scatters due to refraction and light scattered by the cell is passed through a series of dichroic mirrors, each reflecting a specific proportion of the beam to a corresponding detector depending on wave length. This separation allows individual colours emitted by a labelled cell to be detected and quantified, thereby identifying CD markers on the cell. For example, if a cells in a tube are incubated with antibodies for markers A, B and C and the three antibodies are conjugated to fluorophores that emit red, blue and green light respectively, high readings at the detectors for red and green light and nothing at the blue light detector would indicate that the individual cell passing in front of the laser at that given moment expresses markers A and C but not B. Other cells in the tube may express different combinations of markers and could be similarly identified on an individual basis as they pass through the laser in single file.

Before experimental cells are run through the flow cytometer, microbeads are used to calibrate the machine. Unlabelled beads are used to denote a negative signal and individual tubes of beads labelled with each of the fluorophores to be used in the experiment are used to denote a positive signal for each emission wavelength. The emission wavelengths of the fluorophores will overlap to some extent and this is mitigated by compensation, which is outlined later in this chapter.

The FSC, SSC and fluorescence of each cell is integrated in the data acquisition software and displayed graphically. Figure 33 shows a plot of FSC vs. APC used to identify cells positive for CD3 (T cells). The cells were labelled with an antibody for CD3 that was conjugated to allophycocyanin (APC). The cells emitting bright signals at the emission wavelength of APC can be identified as CD3+. On these fluorescence plots, the FSC is not important and SSC or fluorescence at another wavelength could have been plotted instead. Here we are only interested whether or not the cells are positive for APC.

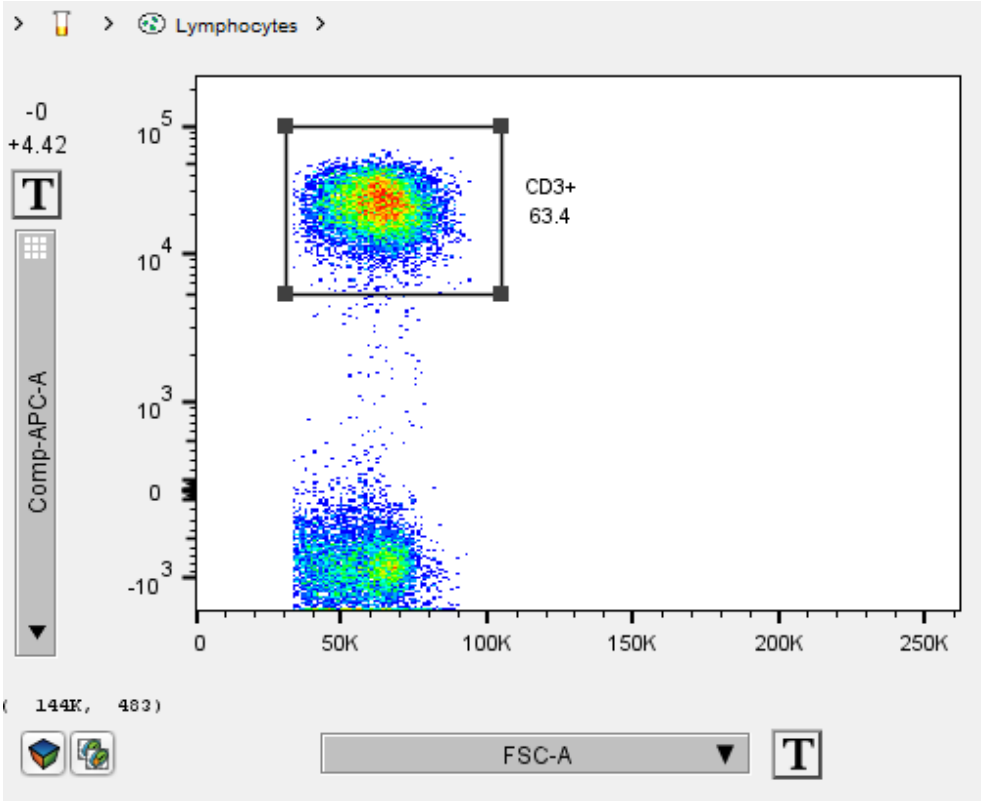

Figure 33: Example from my data showing identification of CD3+ cells in a situation where the cells were labelled with an anti-CD3 antibody conjugated to APC. The Y axis is a measure of fluorescence at 660nm, which is the emission wavelength of this fluorophore. Clear positive and negative cell populations are visible. The 63.4 number is the % of cells of the parent cell group (in this case lymphocytes) that express the antigen of interest.

CD Molecules of Interest:

CD4 and CD8:

Given the evidence discussed in Chapter 1 implicating T lymphocytes in hypertension, the focus of this chapter is to investigate the immunophenotype of T cells in hypertensive versus normotensive humans. All T cells express CD3 and because of this it is a standard marker used to pick the T cells out of the lymphocyte population (Figure 33). In addition to this, I include antibody panels designed to compare the ratio of helper T cells to cytotoxic T cells.

Helper T cells can be identified by expression of CD4 in addition to CD3 (they are CD3+CD4+ cells). CD4 is an immunoglobulin co-receptor that works alongside the T cell receptor in binding to antigen-presenting cells such as dendritic cells. The T cell receptor is the polymorphic binding unit that binds to a specific antigen whereas CD4 binds the non-variant regions of MHC class II (König *et al.*, 1992, 1995). Lck (lymphocyte-specific protein tyrosine kinase) is associated with the cytoplasmic tails of CD4 (Rudd *et al.*, 1988; Barber *et al.*, 1989) and binding of CD4 to the MHC II/antigen complex brings Lck into range to phosphorylate the intracellular chains of CD3 and the T cell Receptor (Alberts *et al.*, 2002). This begins a signalling cascade resulting in intracellular calcium mobilisation and thereby activation of transcription factors including NFκB, which regulate production of proteins required for proliferation and differentiation of the helper T lymphocyte (Figure 34). This is known as activation. CD8 plays the same role as CD4 but on cytotoxic T cells and it interacts with MHC Class I rather than MHC Class II. Only dedicated antigen-presenting cells such as dendritic cells present antigen within the context of

MHC Class II. MHC Class I is found on the surface of all nucleated cells and is the vehicle for presentation of antigen derived from intracellular pathogens or dysfunctional cells.

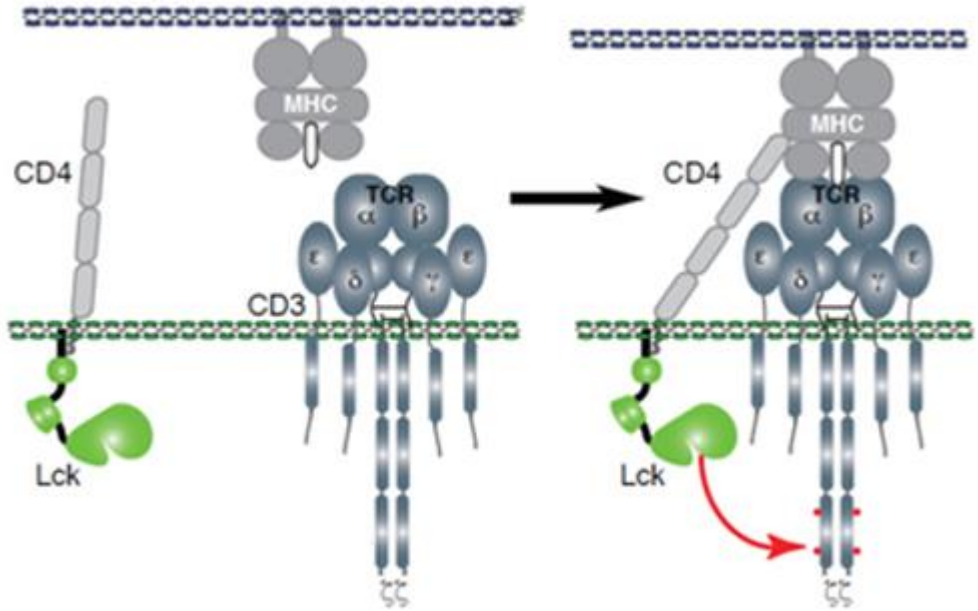

Figure 34: Overview of initial stage of T cell activation (figure adapted from Art Weiss Lab, University of California, San Francisco). Lck = Lymphocyte-specific protein tyrosine kinase, MHC= major histocompatibility complex, TCR = T cell receptor.

CD45 Isotypes - CD45RO and CD45RA:

One subset of both CD4+ and CD8+ T cells derived from activation/differentiation is the memory cell. Most of the cells derived from proliferation of activated T cells undergo apoptosis once they lack stimulation from their corresponding antigen (after the pathogenic source has been eliminated). The memory cell, however, along with some long-lived effector cells survives long-term and remains in circulation or in secondary lymph nodes ready to rapidly expand to large numbers of effector cells if required (Farber *et al.*, 2014).

Memory and naïve cells express different isoforms of CD45. CD45 is expressed on all T cells and plays a role in cell signalling in a similar manor to CD3. Antigen-experienced cells express the RO isoform (CD45RO) and naïve cells

express the RA isoform (CD45RA) (Machura *et al.*, 2008). Because of this, CD45RO Vs. CD45RA expression can and be used to test the hypothesis that modification of endogenous proteins, possibly as a result of oxidative stress due to increased ROS in hypertension, causes them to be recognised as non-self (neo-antigen formation) and cause inflammation, which exacerbates existing hypertension.

CD62L and CD197:

Memory cells can be divided into central memory cells and effector memory cells. Central memory cells express CD62L and CD197. CD62L, also known as L-Selectin, is an adhesion molecule involved in the homing of lymphocytes to secondary lymph nodes via high endothelial venules (Warnock *et al.*, 1998).

High-endothelial venules are post-capillary venules located in secondary lymph organs (except the spleen, which lymphocytes enter via arterioles). The endothelial cells of the high endothelial venules express glycosylation-dependent cell adhesion molecule-1 (GlyCAM-1), to which CD62L binds weakly, which causes the cell to roll along the wall of the venule. This rolling is aided by interaction between lymphocyte function-associated antigen 1 (LFA-1), an integrin expressed on all lymphocytes, and intercellular adhesion molecule 1 (ICAM-1), an immunoglobulin found on endothelial cells. This LFA-1 to ICAM-1 interaction is strengthened by a conformational change in LFA-1 caused by CD197 on the lymphocyte binding to CCL21 (DeFranco *et al.*, 2007), which diffuses out from the lymphoid organ and the distinct cuboidal endothelial cells of the high endothelial venule. The bond between the lymphocyte and the endothelium is now sufficiently strong as to allow diapedesis to occur; the cell leaves the venule and moves through the endothelium into the lymph node.

Cells that are CD45RO+CD62L+CD197+ can be identified as central memory cells because they express the marker for memory cells and the proteins that are used to access the lymph node. Cells that are CD45RO+CD62L-CD197- are deemed effector memory cells because they express the memory cell marker but lack the proteins required to access the lymph node and therefore remain in circulation ready to enter peripheral tissues via adhesion molecules such as P-selectin, which is externalised by endothelial cells in response to chemicals such as histamine, which are released in response to perceived pathogens (Hamann & Syrbe, 2000).

CD196:

CD196 is expressed on memory T cells and is a G-protein coupled receptor for macrophage inflammatory Protein-3 alpha, which is a chemotactic cytokine that attracts lymphocytes and also neutrophils to an extent (Hieshima *et al.*, 1997). This is another marker that can be used to investigate the possibility of more antigen-experienced cells in hypertensives as it is involved in pro-inflammatory signalling. Increased expression of CD196 would be indicative of a pro-inflammatory immunophenotype.

CD11b:

CD11b is found on monocytes, macrophages, neutrophils, natural killer cells and granulocytes such as eosinophils and basophils. Staining these markers allows for quantification of cells of the innate immune system, which may be altered in hypertensives versus normotensives.

Summary of Aims:

The aim of this study was to investigate possible differences in immunophenotype in hypertensive humans compared to normotensive controls. Special focus was given to investigating differences in the proportion of cells that are antigen-experienced vs. those that are naïve with a view to testing the hypothesis that chronic antigen exposure is involved in the pathology of hypertension.

Methods:

Blood Collection:

Blood was collected by a phlebotomist from normotensive healthy human volunteers and hypertensive human patients at the Clinical Research and Imaging Centre at Bristol University (CRIC Bristol). The hypertensives were involved in a variety of studies, but all blood used for this study was taken before any intervention. All participants gave informed consent for participation in the study and all procedures were conducted under institutionally approved protocols for human subjects research. Blood was collected into vacutainers containing EDTA to prevent clotting and stored in a fridge at 4°C until collection later the same day. 8 mL was taken per patient.

Isolation of Peripheral Blood Mononuclear Lymphocytes:

In the case of each sample, blood was transferred into 50ml Falcon tubes and diluted 1:1 with HBSS+HEPES (stock solution made up by putting 10ml HEPES into 500mL HBSS). This mixture was the layered carefully onto 15ml of histopaque 1077 (Sigma cat # 10771-100ml) in another 50ml Falcon tube. These tubes were then spun at 1600rpm for 30 minutes with the centrifuge break off, at room temperature. The buffy coat layer at the interface between the plasma and

the red cells was collected with a disposable glass pasteur pipette (Corning cat #7095D-9) and the cells were diluted with HBSS+HEPES to 50 ml in a 50ml Falcon tube. These were spun at 300g (1500rpm) for 10 minutes at room temperature, the supernatant was discarded and the cells resuspended in 50ml HBSS+HEPES. They were then spun again for 20 mins at 200g (1000rpm) in order to remove platelets, resuspended in 50ml HBSS+HEPES and washed again with a 10 minute spin at 300g. Then cells were then resuspended in 3ml FACS buffer, which consisted of 0.5% bovine serum albumin (Sigma) in PBS (Dulbecco tablets). The cells were then counted using trypan blue (Sigma cat # T8154-100ML) staining. Trypan blue is a dye that does not enter live cells as it cannot cross the cell membrane. This allows live cells to be quantified more easily against a blue background.

Trypan Blue Staining:

For each tube, a 20μL of sample of the cell suspension was added to 20μL of trypan blue in small Eppendorf tubes and mixed via pipette. The cell suspension was then placed on a haemocytometer and the cells were counted using an inverted Leica microscope. One million cells were put into three 5ml, round bottomed FACS tubes (FisherScientific cat # 14-959-2A) – one million cells for each of the three antibody panels that were to be used per animal - and topped up to 2ml with FACS buffer. The tubes were spun at 1200rpm for 10 mins, the supernatant was vacuum-aspirated and the cells were resuspended in 1ml FACS buffer ready for antibody staining.

Antibody Staining:

The four antibody panels that were used are displayed in Table 4.

	CD marker	Fluorescent conjugate	Reason for interest in CD marker
Panel A	CD3	APC	Denotes T cell
	CD45RO	FITC	Expressed by antigen-experienced cells
	CD4	PacBlue	Denotes helper T cell
	CD8a	APC/Cy7 (tandem)	Denotes cytotoxic T cell
	CD62L	PE	Involved in homing to lymph nodes
Panel B	CD3	APC	Denotes T cell
	CD62L	PE	Involved in homing to lymph nodes
	CD197	AF488	Involved in homing to lymph nodes
	CD4	PacBlue	Denotes helper T cell
	CD8a	APC/Cy7 (tandem)	Denotes cytotoxic T cell
Panel C	CD3	APC	Denotes T cell
	CD45RO	FITC	Expressed by antigen-experienced cells
	CD45RA	AF700	Expressed by naive cells
	CD196	PE	Is pro-inflammatory
Panel D	CD4	PacBlue	Denotes helper T cell
	CD8a	PE/Cy7 (tandem)	Denotes cytotoxic T cell
	CD11b	PerCP/Cy5.5 (tandem)	Expressed by cells of innate immune system
	CD69	BV650	Activation marker

Table 4: Display of antibody panel composition. Consult glossary of terms for full names of fluorophores.

The mastermix for each panel was made up with 1.5 µL of each appropriate antibody per subject in 100µL of FACS buffer per sample plus 10µL extra for every 6 samples in order to account for loss due to multiple pipette-tip changes.

E.g. Blood collected from 2 people:

4 panels for 2 subjects= 8 samples. Mastermix for each panel is made up by putting 3µL of each appropriate antibody into 220µL of FACS buffer.

The antibody mastermix tubes were mixed using a vortex machine and then 100µL of appropriate mastermix was added to the corresponding sample tubes

E.g. Blood collected from 2 subjects:

2x Panel A, 2x Panel B, 2x Panel C, 2x Panel D tubes, each with one million cells from corresponding subject suspended in 1ml FACS buffer and 100µL of appropriate mastermix added for staining.

Tubes were wrapped in aluminium foil and placed in a fridge at 4°C for 20 minutes. They were then topped up to 2ml with FACS buffer and spun at 1200RPM for 10 minutes. The supernatant was vacuum-aspirated and the stained cells were resuspended in 250µL FACS buffer and 62.5µL paraformaldehyde (PFA). The PFA was included in order to fix the cells so that they can be analysed at a later date. The cells were wrapped in foil and refrigerated until they were run on a flow cytometer (BD LSRII) not more than one week later.

Flow Cytometry:

Compensation:

When designing an antibody panel for FACS it is important to choose fluorescent conjugates that have as little spectral overlap as possible. The detection range in flow cytometry is limited to ~370nm-~800nm and although conjugates used are known to exhibit bright emissions at a specific wavelengths they also emit some light across a range of wavelengths on either side of the spectrum - they have broad emission spectra.

An example of spectral overlap is shown in Figure 35:

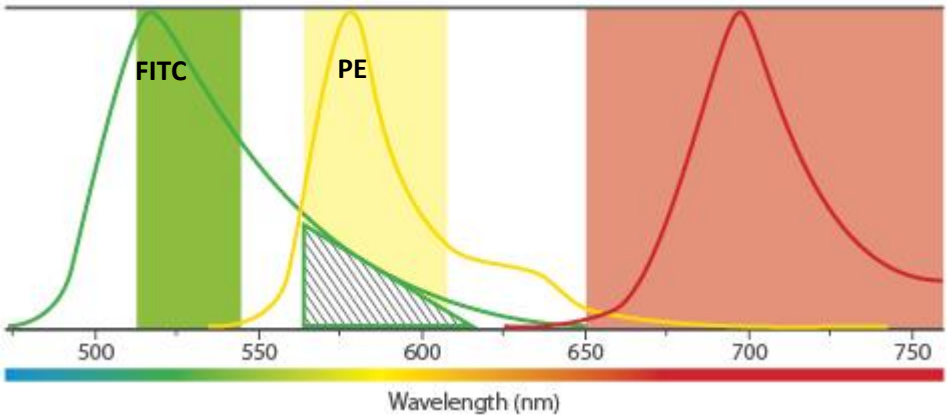

Figure 35: Example of spectral overlap of emission spectra of commonly used fluorophores. Diagram adapted from ebioscience.

In Figure 35 we see that FITC emissions spill into the range in which the flow cytometer will be detecting PE. Left unchecked, running samples stained with FITC would also give false positive readings for PE.

When performing multicolour cytometry it is inevitable that some spectral overlap will occur between the various colours that are used, even if care has been taken to minimize overlap during panel design. Because of this, before running samples on a flow cytometer it is essential to run compensation controls to account for overlap of emission spectra from the various fluorescent conjugates that are used in an experiment.

Compensation controls use beads stained with each of the fluorescent conjugates used in the experiment (positive controls), as well as beads that are unstained (negative controls). These beads are run one colour at a time and the software (BD FACSDiva) uses an algorithm to subtract overlapping emissions from the positive readings for each of the individual conjugates so that an individual conjugate can be detected accurately.

Preparation of the beads for compensation controls was done on the day the samples were to be run on the flow cytometer. Antibody solutions were made up by adding 1.5µL of each antibody for each fluorescent conjugate used in the experiment to 100µL FACS buffer (10 tubes total- FITC, APC, PE, PacBlue, APC-Cy7, AF488, AF700, PE-Cy7, PerCP-Cy5.5 and BV650). Separate FACS tubes were prepared for each fluorescent conjugate and one drop each of positive and negative compensation beads (BD cat# 552845) were added to each. The appropriate antibody solution was added to each of the tubes and they were mixed via vortex. The tubes were left at room temperature until they were used for compensation controls ~20 minutes later.

All sample tubes were vortexed thoroughly before use on the flow cytometer, as cells collect at the bottom of the tubes after being left undisturbed in the fridge for several days and require resuspension. Data was collected in BD FACSDiva. CD3 (APC) was used as a stopping gate which ensured that 10,000 CD3+ cells were collected for each sample except in the case of panel D (which did not contain antibodies for CD3) in which case approximately double the number of total cells was collected in relation to the other panels. A cell population was deemed positive for an antigen if it had a higher fluorescence than the unstained control. Once data collection was complete it was exported into FlowJo (Tree Star Inc.) for analysis.

Gating/Analysis:

Gating:

Gating refers to the selection of a cell population within a flow cytometry data set as presented in a dot plot (see for example Figures 31 and 33 shown previously). Cells can be identified base on size and granularity (Figure 31) or

by their expression of a particular antigen or antigens inferred by the measurement of fluorescent labels attached to said antigens (Figure 33). Gating onto identified cell populations allows quantification of the proportion of cells in a sample expressing antigens of interest, thereby allowing the cell type to be determined based on knowledge of cell biology.

FMO:

A fluorescence minus one (FMO) control was performed to assist with gating. In an FMO, cells are stained with versions of each panel with one of the antibodies missing and the tubes are run on the flow cytometer as normal. This produces plots that are useful for gating, especially if positive and negative cell populations are close together due to low levels of expression of a target antigen or if a fluorescent conjugate is not very bright.

An example from one of my FMOs is shown in Figure 36. In this example, Panel C was run without FITC, the fluorochrome that provided the most difficult positive populations to gate onto (Panel A) and then with FITC (panel B).

A

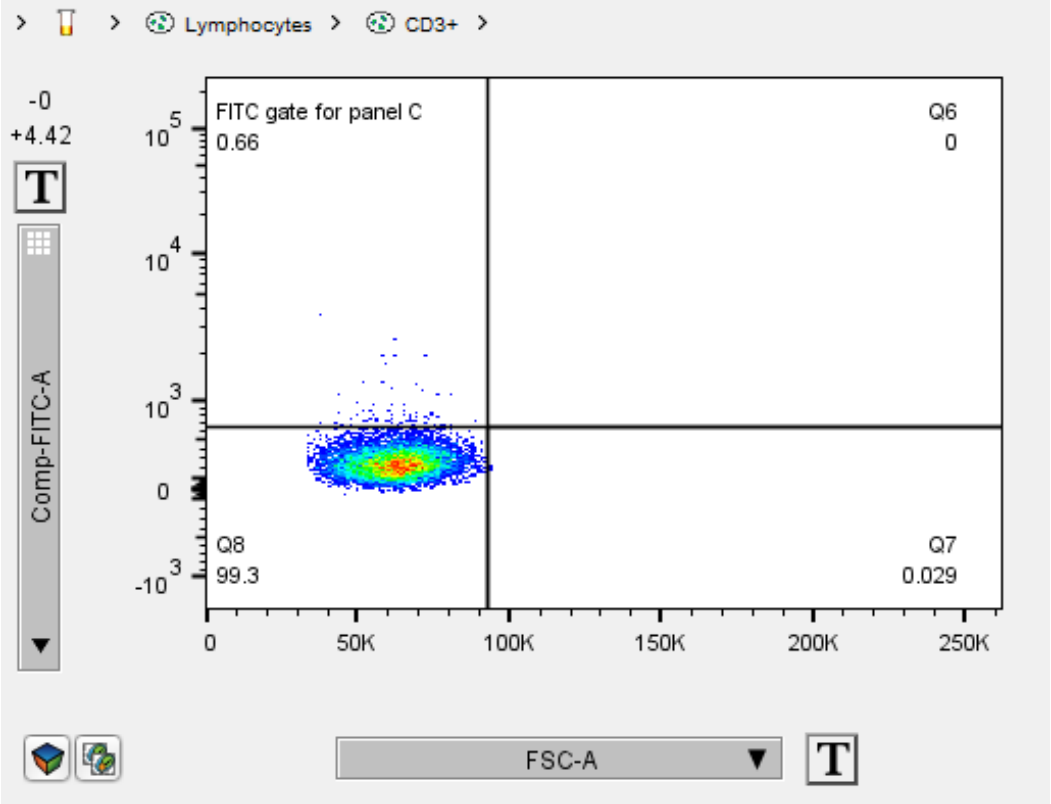

B

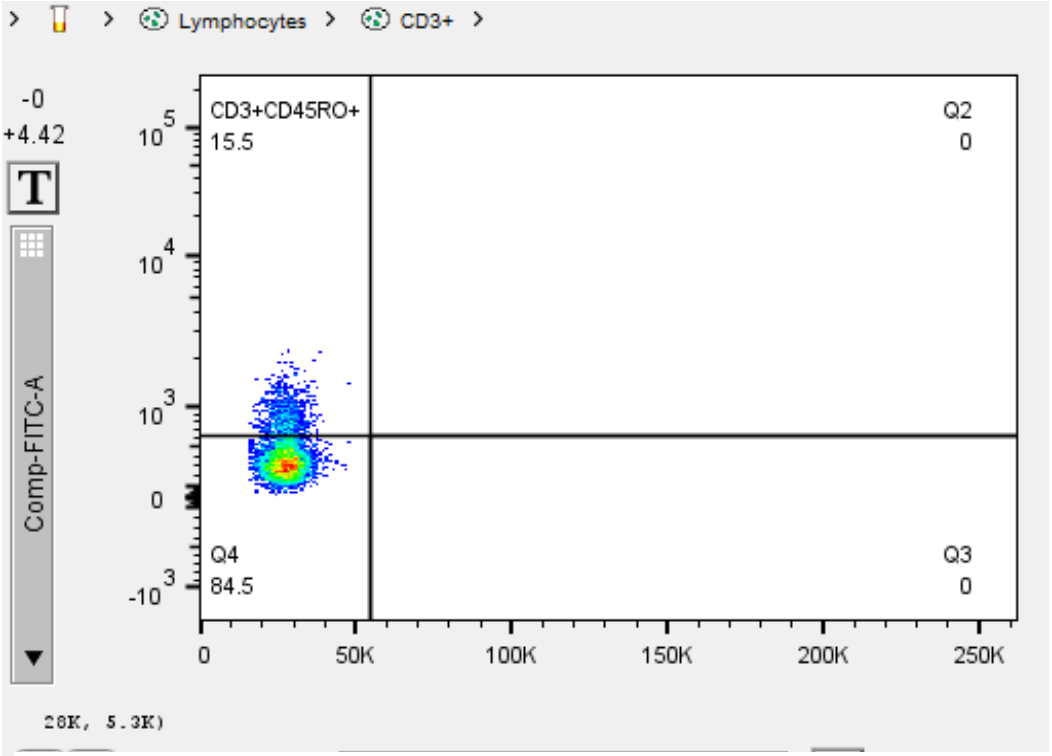

Figure 36: Flow cytometry dot plots showing **A:** Antibody panel C run without FITC and **B**: With FITC included. Comparing the two plots allows the identification of cell groups that are labelled with FITC since cells brighter than those in the negative cell population can be considered positive (note the logarithmic scale on the Y axis). The Y axis shows the intensity of the light emitted by FITC, known because the wavelength of the light emitted by the fluorophore is known and the fluorophores used in multicolour panels are chosen in order to minimize spectral overlap-any overlap that does exist is mitigated using compensation controls as outlined earlier. The X axis shows forward scatter, which correlates to the size of the cells. The 'gate' denoting the boundary between positive and negative populations was placed manually, which is why FMO controls are helpful – user bias is reduced.

In the FMO, we know that no FITC is present so when we compare it to complete experimental samples, everything brighter than the cell population shown on the FMO can be considered positive (there are a few clearly anomalous results that are excluded in the FMO). Having a plot demonstrating what panel C looks like without FITC included allows for more confident gating on to the positive cell group in the experimental samples. This is especially valuable when the positive and negative cell groups are touching as in this example.

Gating Strategy:

For Panels A-C an initial gate sought to pick out the lymphocytes based on their size and granularity (FSC Vs. SSC). Then T cells were isolated by gating cells positive for APC (CD3+ cells). These cells are T lymphocytes. Further gating was used to identify various T-cell subtypes depending on the antibody panel.

Figure 37 shows the initial lymphocyte gate.

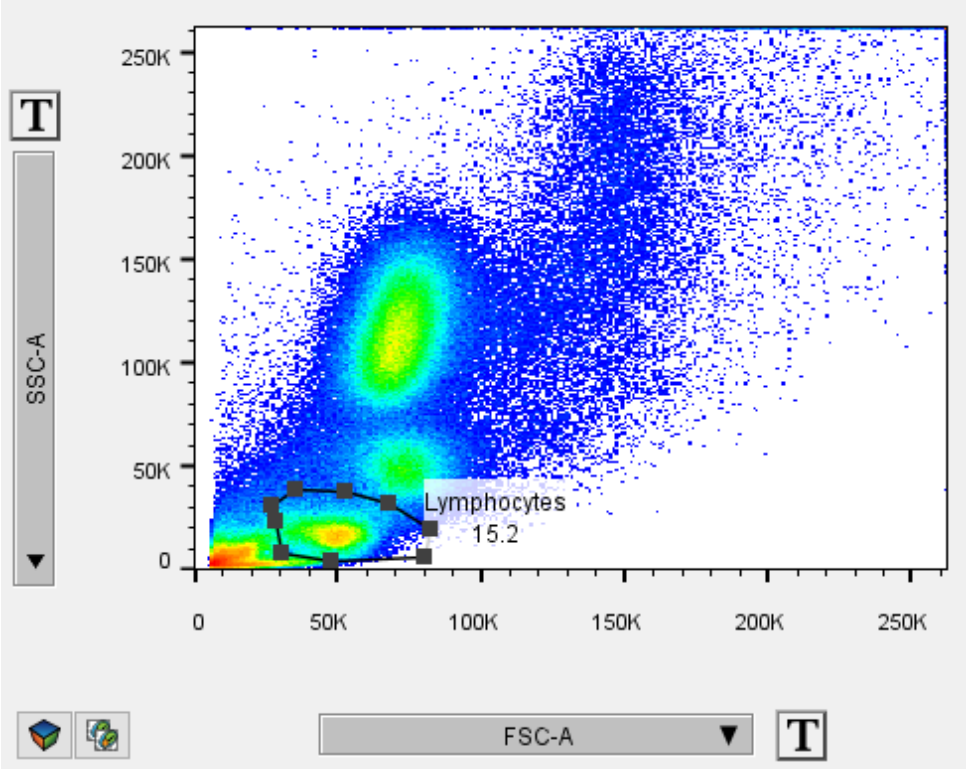

Figure 37: Lymphocyte population identified base on the forward scatter (size) and side scatter (granularity).

Drilling down further allows identification of specific cell populations:

Panel A Specific:

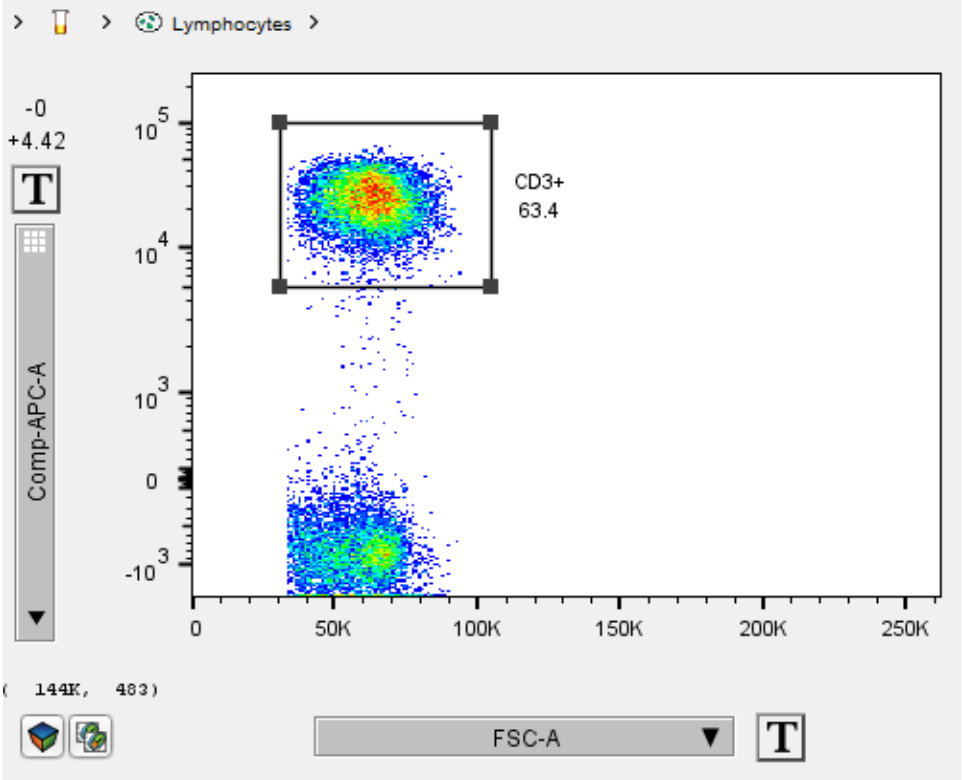

Figure 38: T cells within the lymphocyte population identified based on their expression of CD3, determined by fluorescent emission from APC-conjugated antibodies for CD3.

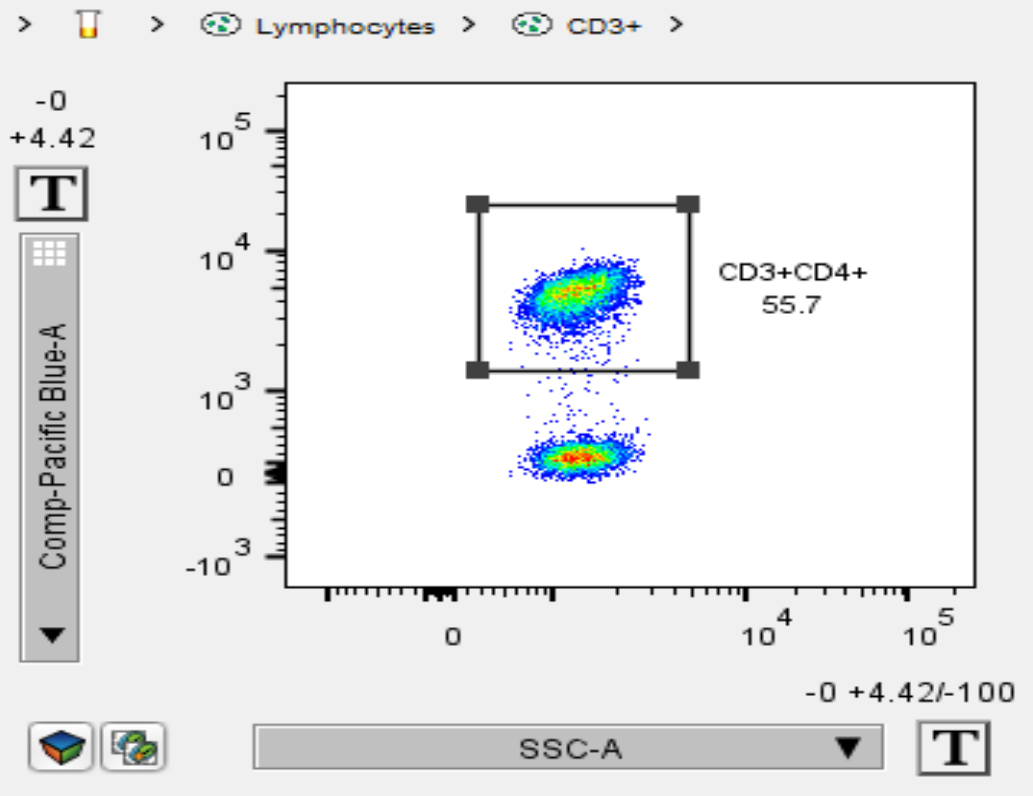

Figure 39: Identification of Helper T cells within the T cell population based on their expression of CD4, determined by fluorescent emission from Pacific Blu-conjugated antibodies for CD4.

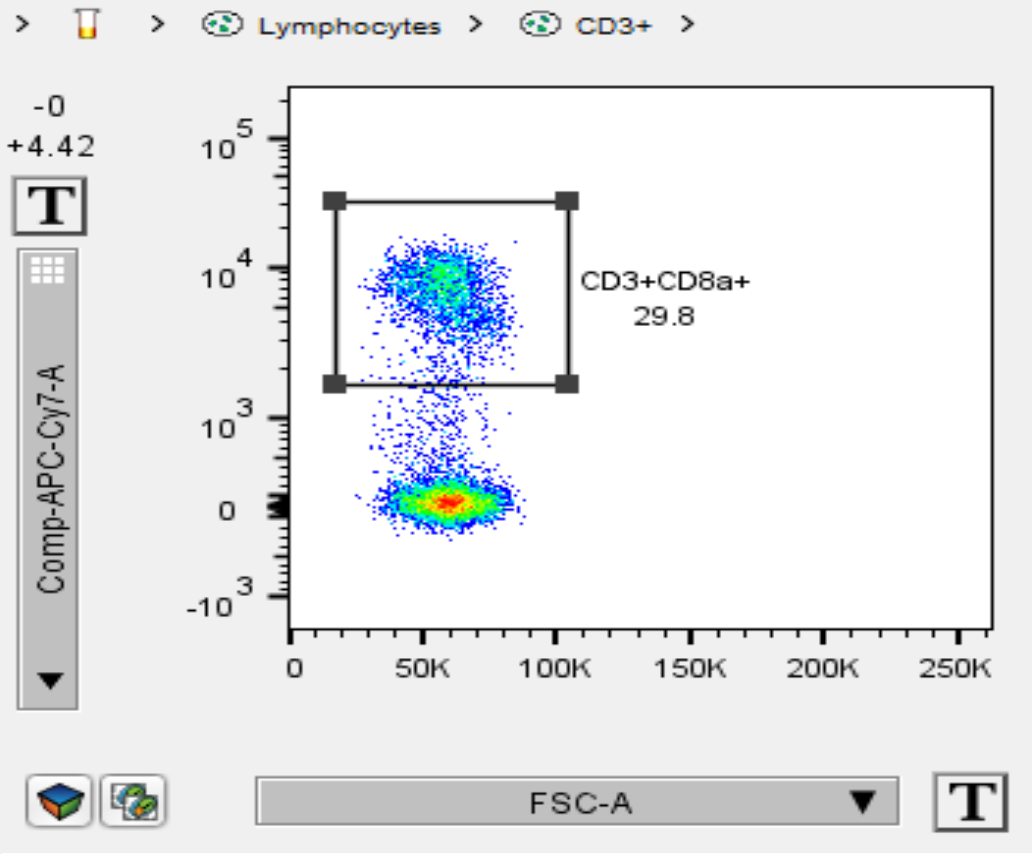

Figure 40: Identification of cytotoxic T cells within the T cell population based on their expression of CD8a, determined by fluorescent emission from APC/Cy7-conjugated antibodies for CD8a.

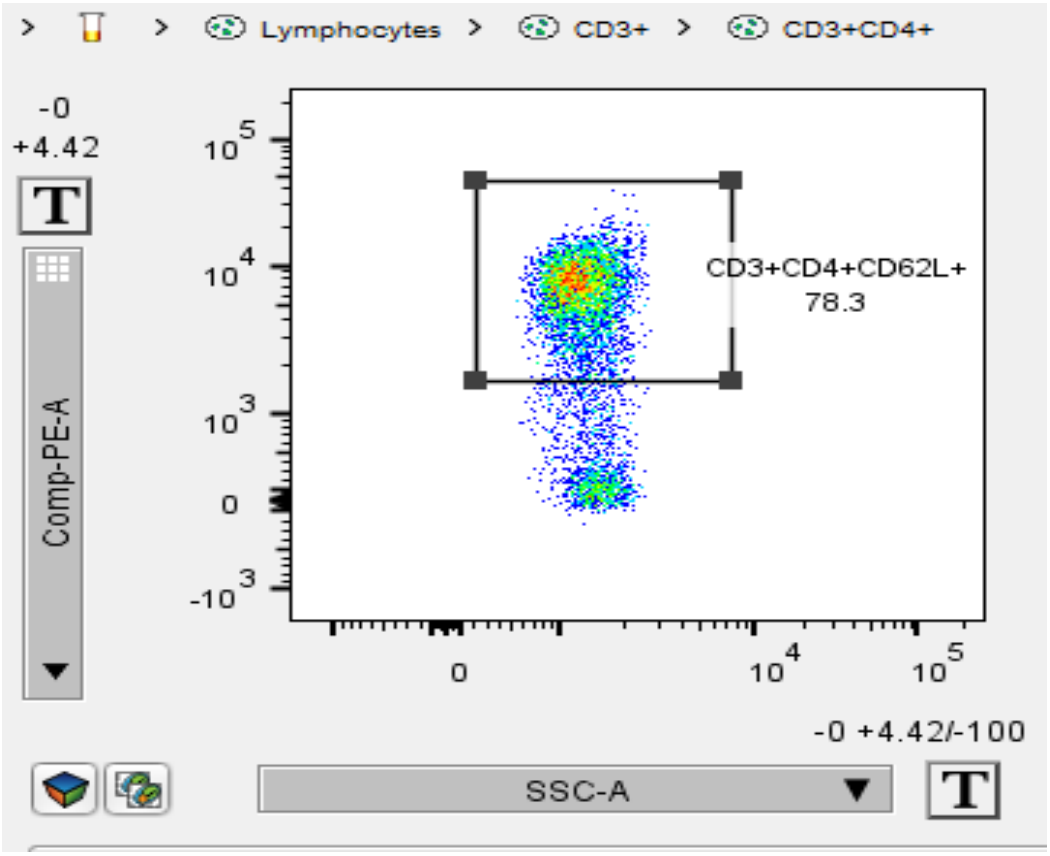

Figure 41: Identification of T cells expressing CD62L within the Helper T cell population, determined by fluorescent emission from PE-conjugated antibodies for CD62L.

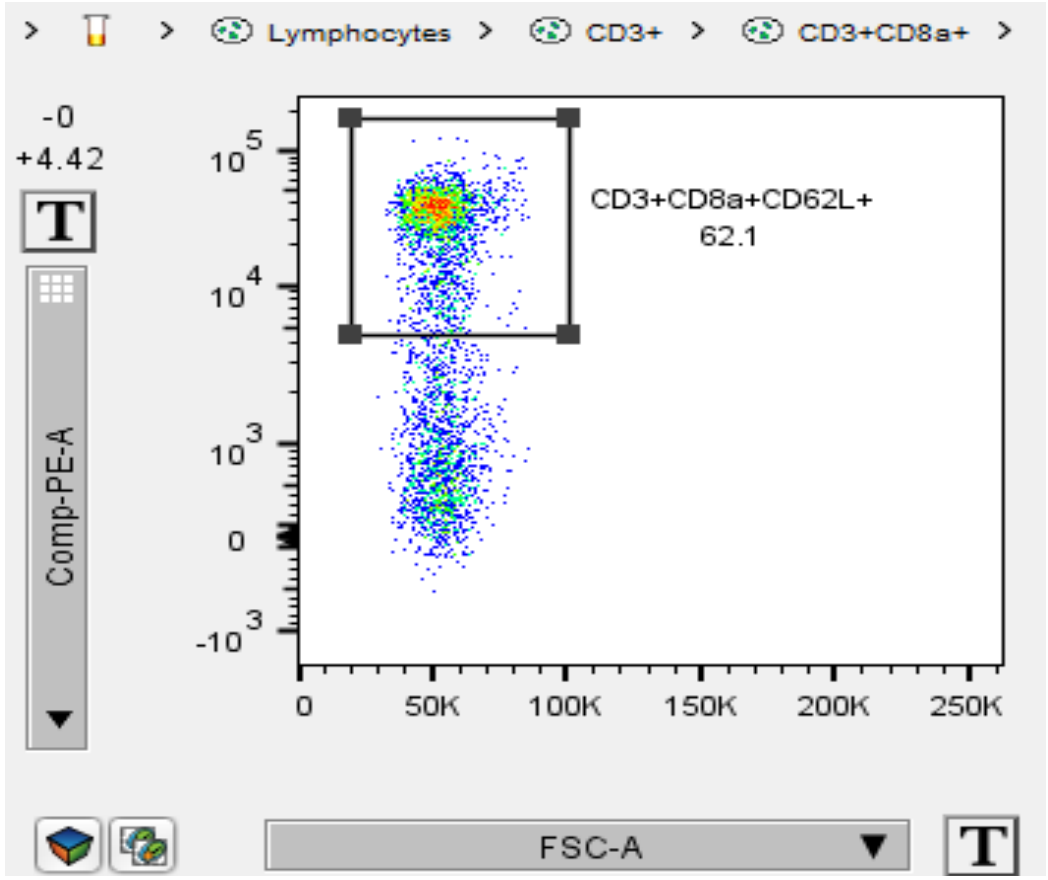

Figure 42: Identification of cells expressing CD62L within the cytotoxic T cell population determined by fluorescent emission from PE-conjugated antibodies for CD62L.

Panel B specific:

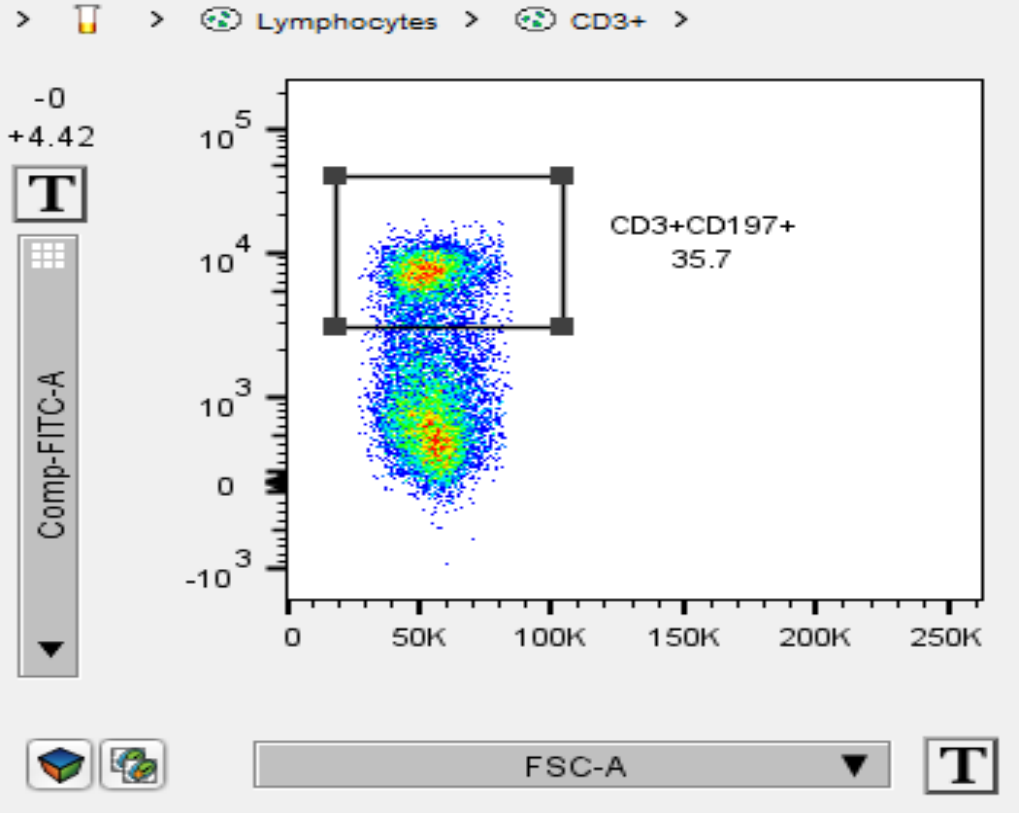

Figure 43: Identification of cells expressing CD197 within the T cell population determined by fluorescent emission from FITC-conjugated antibodies for CD197.

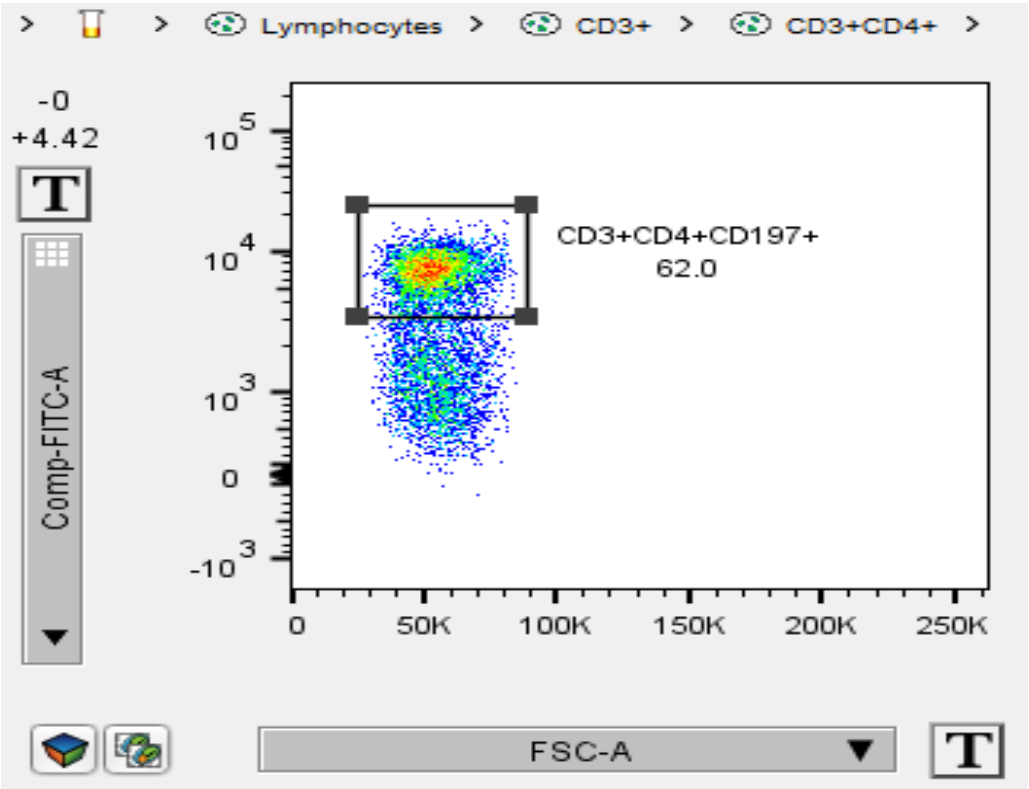

Figure 44: Identification of cells expressing CD197 within the Helper T cell population determined by fluorescent emission from FITC-conjugated antibodies for CD197.

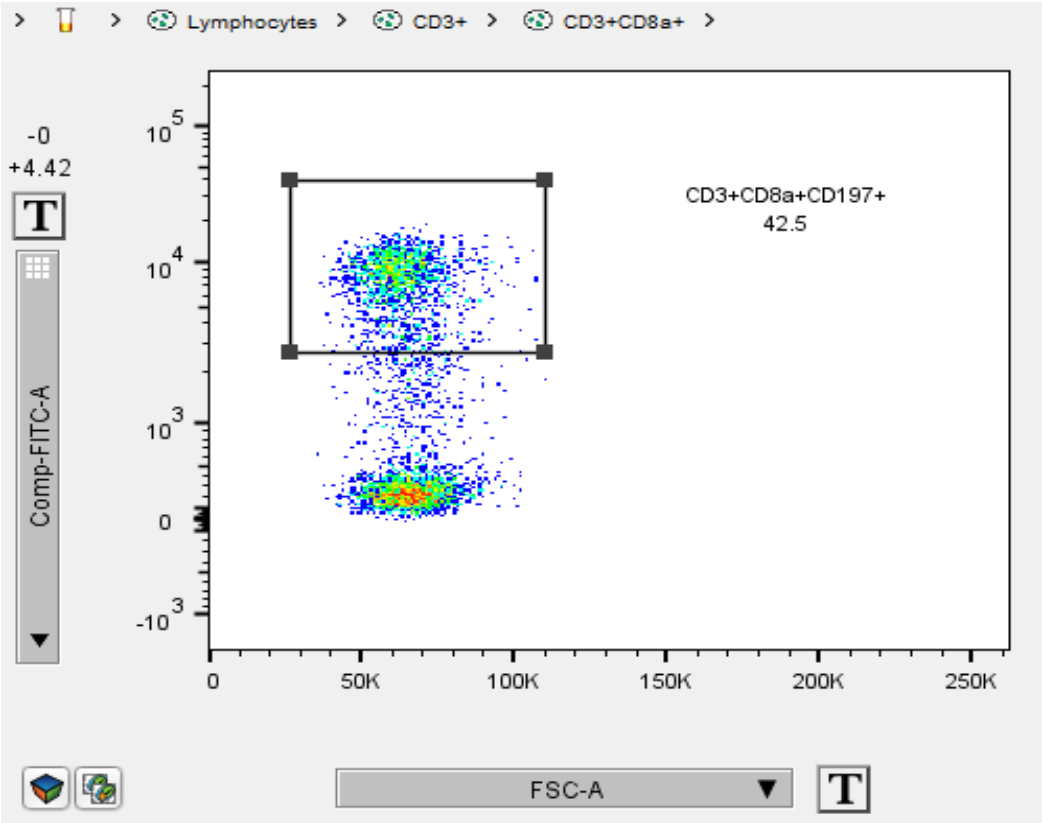

Figure 45: Identification of cells expressing CD197 within the Cytotoxic T cell population determined by fluorescent emission from FITC-conjugated antibodies for CD197.

Panel C specific:

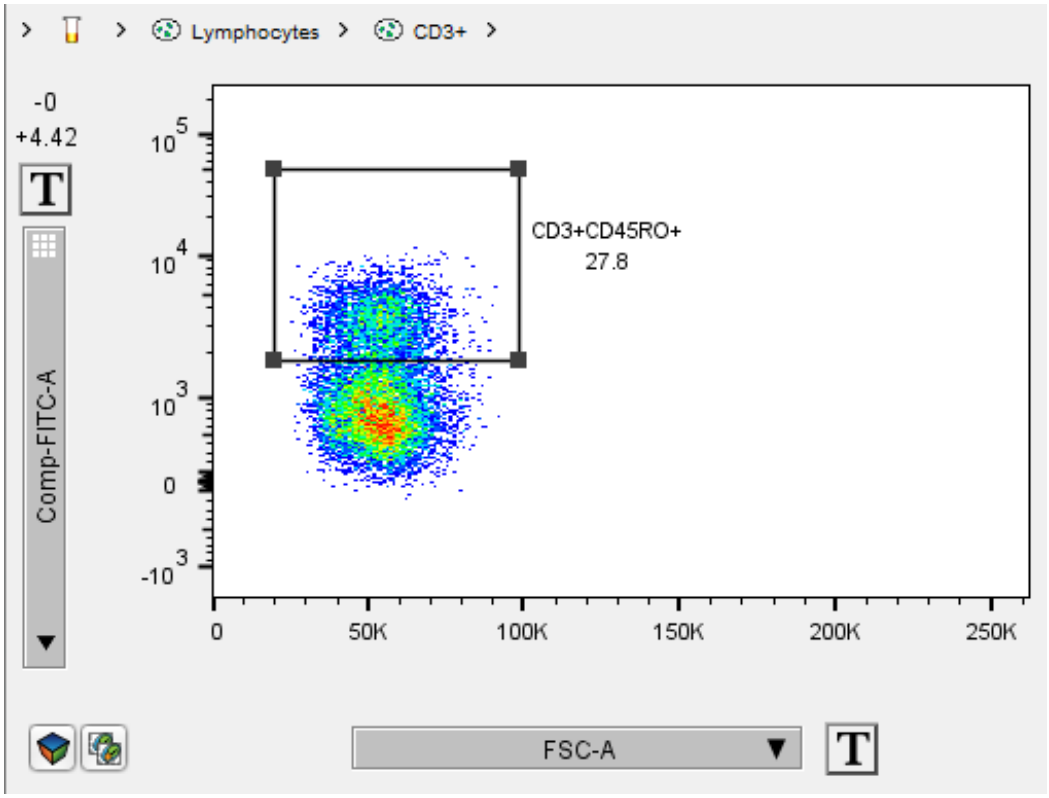

Figure 46: Identification of memory T cells within the T cell population determined by fluorescent emission from FITC-conjugated antibodies for CD45RO.

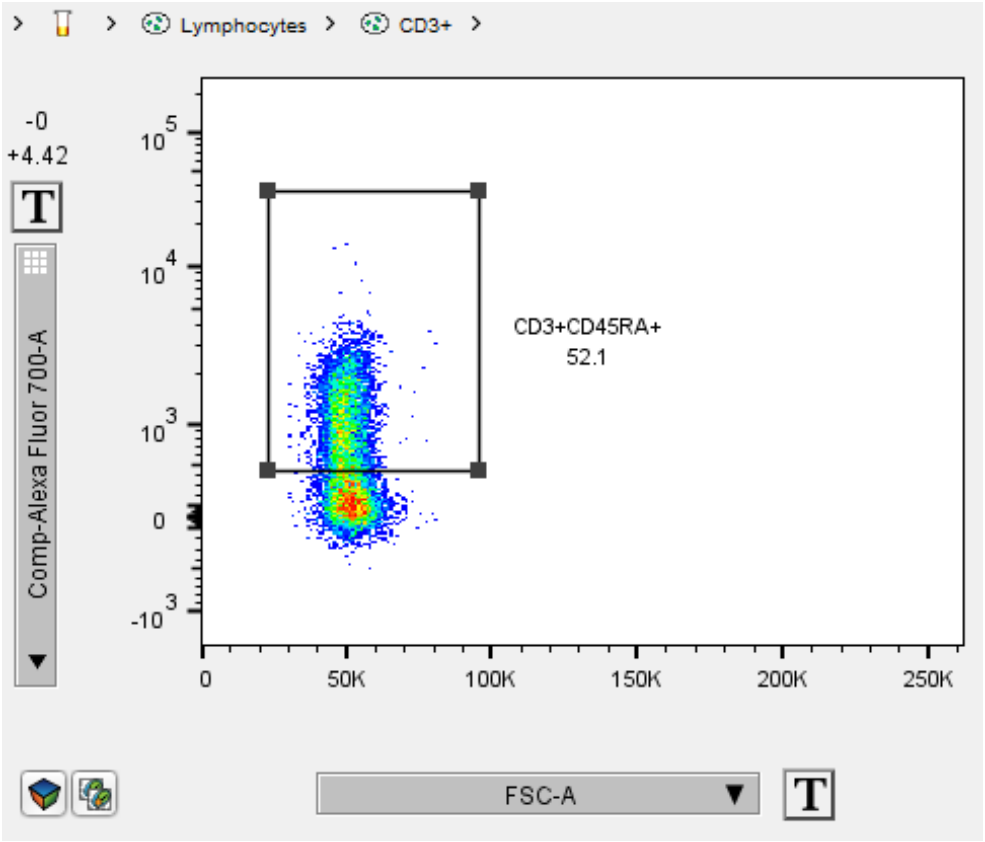

Figure 47: Identification of naive T cells within the T cell population determined by fluorescent emission from AF700-conjugated antibodies for CD45RA.

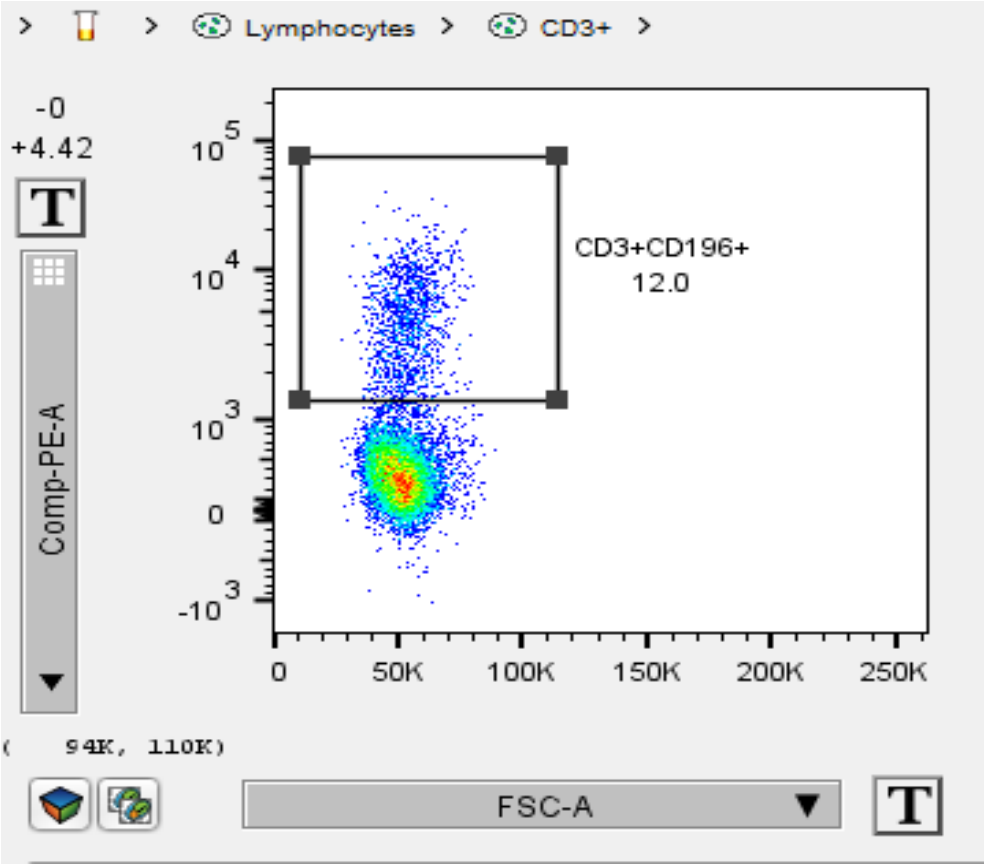

Figure 48: Identification of cells expressing CD196 within the T cell population determined by fluorescent emission from PE-conjugated antibodies for CD196

Panel D specific:

All cells were included in the initial gate when quantifying CD11b+ cells as these cells are not T Lymphocytes but cells of the innate immune system such as monocytes, granulocytes, macrophages, and natural killer cells. The cluster of debris in the bottom left of the initial FSC Vs. SSC plot is excluded but all cells included in the initial gate.

An example of the initial gate for Panel D is shown in Figure 49:

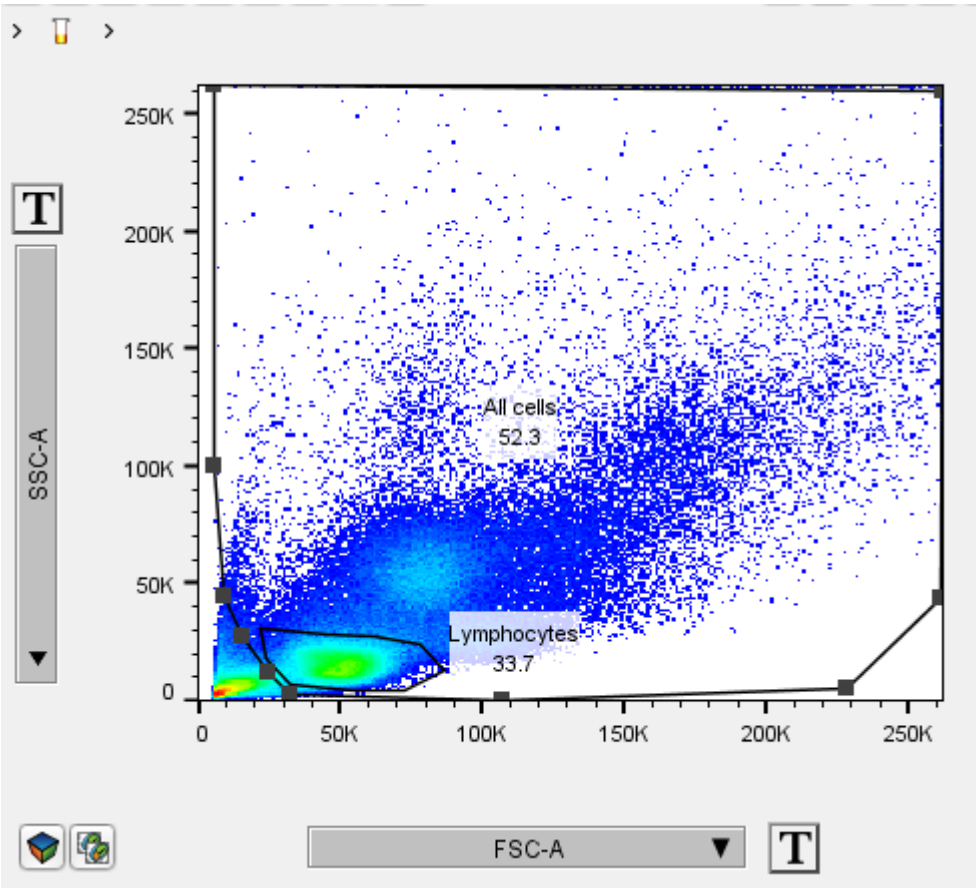

Figure 49: Initial gate for Panel D. All cells are included in the gate, the cluster of debris in the bottom left is excluded.

The 'All cells' gate was the initial gate, rather than the lymphocyte gate and no subsequent gate was required before gating on CD11b+ cells (Figure 50).

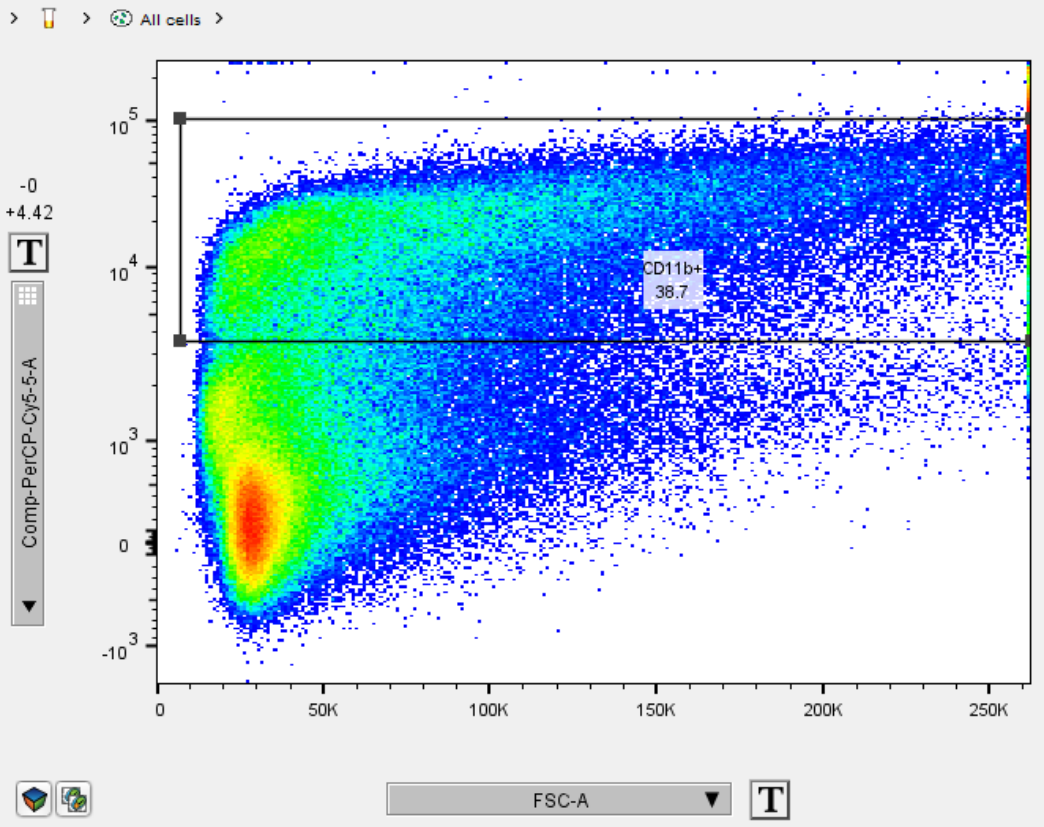

Figure 50: identification of cells of all sizes (hence the x-axis forward scatter spread) expressing CD11b, determined by fluorescent emission from PerCP/Cy5.5-conjugated antibodies for CD11b.

Measurement of CD69 expression on both CD4+ and CD8a+ cells was attempted with panel D but failed.

The % of T cells expressing each of the antigens measured or % of all cells expressing CD11b from each subject were averaged and subjects were grouped into normotensive (NTN) and hypertensive (HTN) based on blood pressure data collected at the Clinical Research and Imaging Centre at Bristol University (CRIC Bristol). They were further subdivided based on sex. Subjects that had recently taken medication known or suspected to effect immunophenotype (such as ibuprofen) were excluded from the study.

Results:

Significant Differences in T-cell Phenotype of Human Hypertensives Compared to Normotensive Controls in Males but Not in Females:

CD62L expression on CD8a+ cytotoxic T cells was significantly reduced in hypertensive males, P=0.017 (Figure 51C) but not in females (Figure 52C). Similarly, CD197 expression was significantly reduced on CD8a+ cytotoxic T cells in hypertensive males compared to normotensive controls, P=0.013 (Figure 51E). This finding was not observed in females. (Figure 52E).

Expression of the RO isotype of CD45 on T cells was increased in hypertensive human males compared to normotensive controls, P=0.006 (Figure 51F). The inverse was seen in the case of the RA isotype; CD45RA expression on T cells was decreased in hypertensives compared to normotensive controls, P=0.009 (Figure 51F). The same trends were observed in females but the results were not statistically significant (Figure 52F).

An increase in the percentage of T cells expressing CD196 was observed in hypertensive human males compared to normotensive controls, P=0.020 (Figure 51F). This difference was not observed in females (Figure 52F).

No Significant Differences in Expression of Several Proteins in T-cells and Cells of the Innate Immune System Between Hypertensive and Normotensive Humans:

No differences in the percentage of T cells expressing CD4 or CD8a were observed between hypertensive patients and normotensive controls in either the male (Figure 51A) or female (Figure 52A) groups.

In addition, no significant difference in the percentage of CD4+ helper T cells expressing CD62L was observed between hypertensive patients and normotensive controls in either the male (Figure 51B) or female (Figure 52B) groups. No significant difference in expression of CD197 was observed on CD4+ helper T cells between the hypertensive or normotensive groups (Figures 51D and 52D).

Finally, no difference in the percentage of all leukocytes expressing CD11b were observed between hypertensive patients and normotensive controls in either the male (Figure 51G) or female (Figure 52G) groups.

Males:

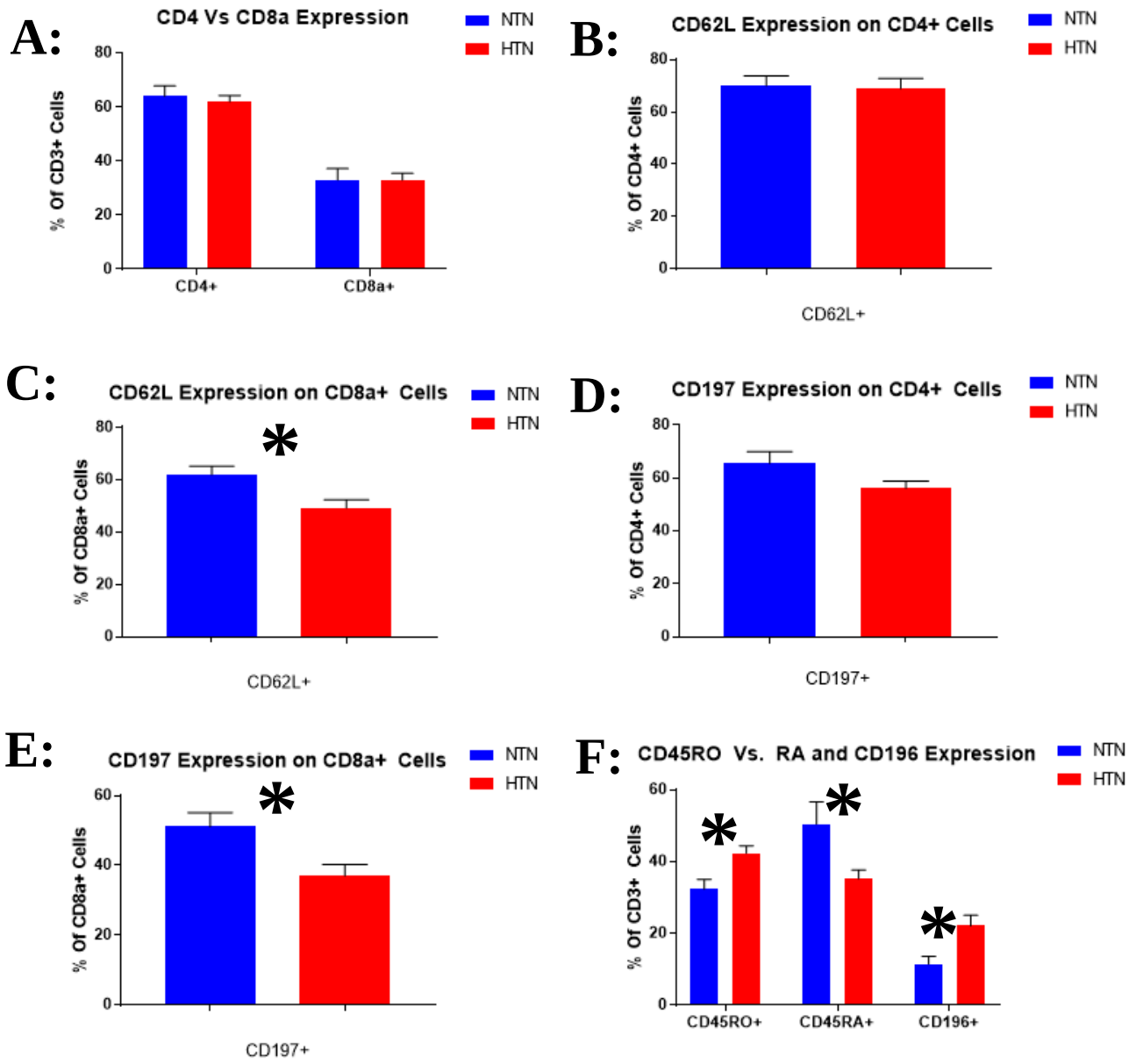

Figure 51: T cell phenotype in Hypertensive human males Vs. aged-matched normotensive controls. **A:** CD4+ Vs. CD8a+ cells. **B & C:** CD62L expression on CD4+ and CD8a+ cells respectively. **D & E:** Expression of CD197 on CD4+ and CD8a+ cells respectively. **F:** CD45RO Vs CD45RA and CD196 expression on T cells. **G:** % of all leukocytes expressing CD11b. Hypertensives exhibit a significant reduction of CD62L and CD197 on CD8a+ cells, a significant increase in CD45RO+ T cells, a significant reduction in CD45RA+ T cells and a significant increase in T cells expressing CD196. HTN n=32 NTN n=18 Error bars represent SEM. P-values determined by T-test were as follows **C:** 0.017, **E:** 0.013, **F:** CD45RO: 0.006 CD45RA: 0.009, CD196: 0.020

Females:

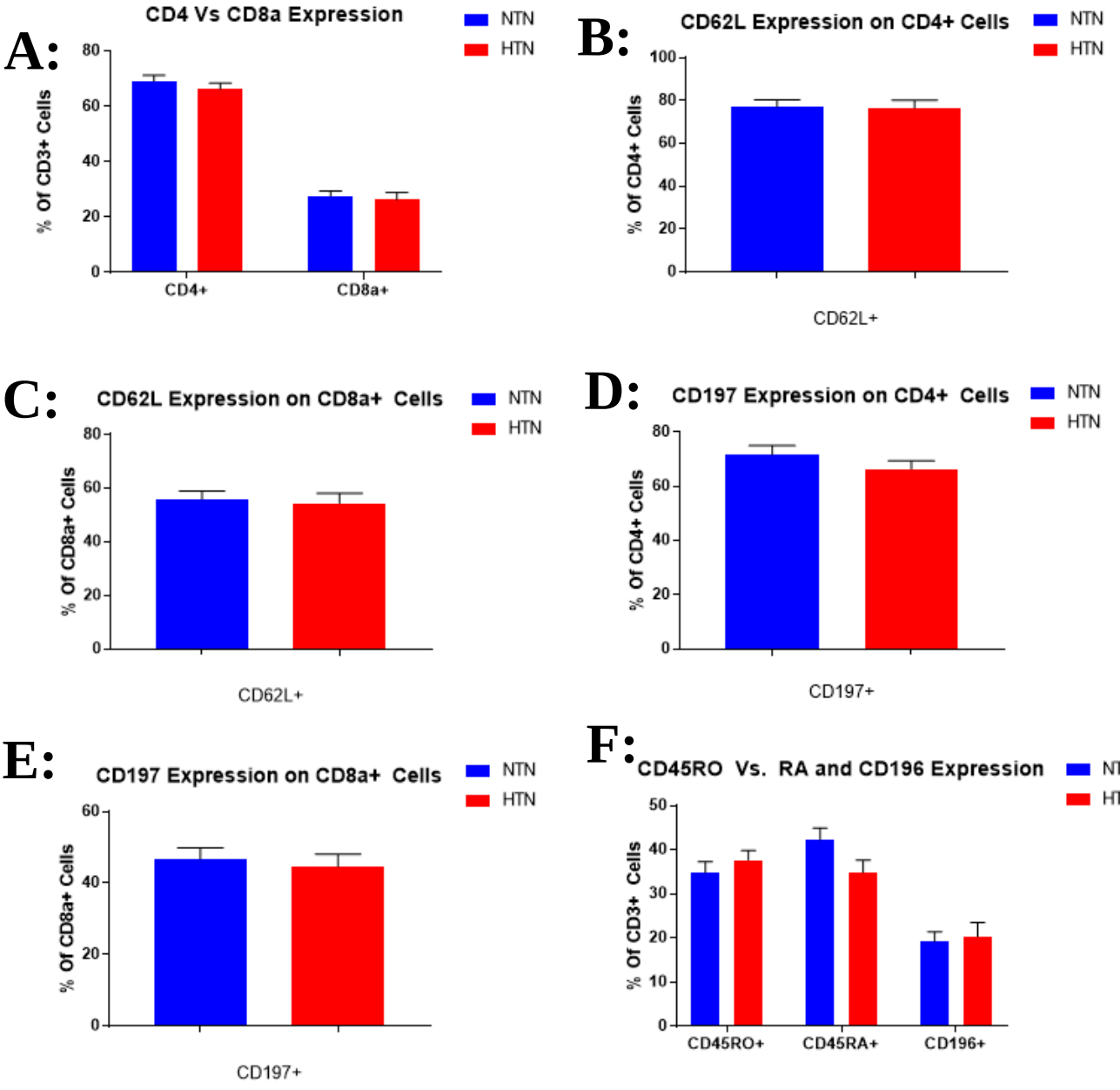

Figure 52: T cell phenotype in Hypertensive human females Vs. aged-matched normotensive controls. **A:** CD4+ Vs. CD8a+ cells. **B & C:** CD62L expression on CD4+ and CD8a+ cells respectively. **D & E:** Expression of CD197 on CD4+ and CD8a+ cells respectively. **F:** CD45RO Vs CD45RA and CD196 expression on T cells. **G:** % of all leukocytes expressing CD11b. No significant differences were observed. HTN n= 31, NTN n = 23 Error bars represent SEM. P-values determined by T-test.

Discussion:

Increased CD45RO+ T-Cells and Reduced CD45RA+ T-Cells in Hypertensive Human Males:

The fact that hypertensive human males exhibited a significant increase in the percentage of T cells expressing the RO isotype of CD45 and a significant decrease in expression of the RA isotype (Figure 51) supports the hypothesis that chronic antigen exposure is implicated in either the generation and/or maintenance of hypertension (Figure 7) since the RO isotype is expressed on antigen experienced cells and the RA isotype is expressed on naïve cells, as discussed in Chapter 1.

My study was descriptive and does not provide any mechanistic insight into why these changes occur in hypertension. However, as referenced in Chapter 1, there is evidence that due to oxidative stress (which is increased in hypertension), isoketals accumulate in dendritic cells, which cause CD8a+ T cells to adopt a pro-inflammatory phenotype characterised by production of INF-γ and IL-17 (Kirabo *et al.*, 2014).

IFNγ is an important pro-inflammatory cytokine with a variety of functions (Schroder *et al.*, 2004). It stimulates macrophages, resulting in an increase of antigen-presenting activity as well as increasing lysosome activity, it activates natural killer cells, it activates inducible nitric oxide synthase, increases the expression of MHCI on all cells and MHCII on antigen-presenting cells (thereby promoting antigen collection, processing and presentation, which leads to amplification of the inflammatory signal) and it promotes leukocyte adhesion and binding required for recruitment of leukocytes to sites of inflammation.

Another pro-inflammatory cytokine of note is IL-17. It is mostly produced by specialised TH_{17} helper T cells but is also produced by activated CD8+ cytotoxic T cells. IL-17 promotes the synthesis of other cytokines such as IL-6 and TNFα by a variety of other cells including endothelial cells and macrophages. Although IL-17 is important mediator of helpful and necessary inflammation, it is also implicated in auto-immune disease (Kuwabara *et al.*, 2017) and the fact that hypertension promotes a shift of CD8+ cytotoxic T cells to a pro-inflammatory phenotype, resulting in production of INF-γ and IL-17, exacerbates hypertension as discussed in Chapter 1 (pages 36 and 37).

The increased ratio of antigen-experienced to naïve T cells I observed supports the hypothesis that hypertension causes the production of reactive oxygen species which modify endogenous proteins such that they are no longer recognised as self and, hence, an auto-immune inflammatory response occurs. This is pro-hypertensive as discussed in Chapter1.

Reduced Expression of CD62L and CD197 in Hypertensive Human Males:

The observed reduction of CD62L and CD197 expression in hypertensive human males (Figure 51) is further evidence that the proportion of T cells that are antigen-experienced is increased in hypertension. Specifically, these findings point to a greater percentage of effector memory T cells in the circulation in conditions of hypertension as these proteins are shed by antigen-experienced cells which remain in the peripheral circulation ready to encounter their corresponding antigen and rapidly differentiate into effector cells in order to combat an invading pathogen, or possibly contribute to auto-immune disease. Statistically significant differences in the expression of these two proteins were observed in CD8a+ cytotoxic T-cells specifically (Figure 51 panels C and E).

An increase in the proportion of cytotoxic T cells that are in the circulation of hypertensive males increases the possibility that these cells could enter the brain parenchyma via a compromised BBB (Biancardi & Stern, 2016) and disrupting neuronal signalling in brain nuclei such as the PVN and the RVLM, thereby driving hypertension, as described in Chapter 1 (pages 51-54). Pro-inflammatory cytokines (such as TNFα, IL-1β, IL-6, IFNγ and IL-17) released by infiltrating T cells could activate microglia in the CNS, exacerbating inflammation and production of ROS within the CNS. This promotes neurohumoral excitation, which increases sympathetic outflow and is pro-hypertensive (Kang *et al.*, 2009; Cardinale *et al.*, 2012; Sriramula *et al.*, 2013).

Increased incidence of immune cells infiltrating the CNS is one way in which reduced expression of CD62L and CD197 on T cells may be contributing to hypertension.

Due to the increase in pro-inflammatory cytokines in hypertension, in particular IL-17 and IFNγ, vascular infiltration of T cells is increased (Madhur *et al.*, 2010). An increase in activated cells in the circulation makes this more likely to happen. This promotes pathological vascular remodelling (vessel hardening) which prevents vessels dilating properly, increasing blood pressure through greater vascular resistance. The simple fact that hypertensive males have a greater number of cytotoxic T cells circulating within the vessels means that the damage they do as outlined in Chapter 1 is more severe. This includes inhibition of NO-mediated vasodilation and promotion of T-cell-derived-ANG-II-mediated vasoconstriction.

Increased Expression of CD196 in Hypertensive Human Males:

Expression of CD196 was increased in hypertensive human males (Figure 51). CD196 is a receptor for Macrophage Inflammatory Protein-3 (MIP-3), which is a chemokine that is a powerfully chemotactic for lymphocytes (Baba *et al.*, 1997) and is therefore involved in pro-inflammatory signalling so this finding provides further evidence that a pro-inflammatory T-cell phenotype is associated with human hypertension.

No Significant Differences in T-Cell Phenotype between Normotensive and Hypertensive Human Females:

It is important to note that there was no significant differences in T-cell phenotype between hypertensive and normotensive women (Figure 52). This may be due to protective female hormones. Post-menopausal women have higher blood pressure than age-matched women who are pre-menopausal (Weiss, 1972; Staessen *et al.*, 1989) and women suffering with premature ovarian failure also suffer with hypertension at a higher rate than age-matched women with healthy ovaries (Sandberg & Ji, 2012). There are many known differences in the control of blood pressure and the pathology of hypertension between men and women, such as females having greater levels of NO in the vasculature or males having enhanced vasoconstriction (Zimmerman & Sullivan, 2013).

As discussed earlier, adoptive transfer of T cells from WT mice into $RAG^{-/-}$ mice restores their propensity to develop hypertension in response to ANGII infusion (Guzik *et al.*, 2007). Both the $RAG^{-/-}$ mice and the donor WT mice in this study were male. Interestingly, the same procedure does not restore vulnerability to ANGII mediated hypertension in female mice (Pollow *et al.*, 2014). Further, if female CD3+ T cells are transferred into male $RAG^{-/-}$ mice, the subsequent

ANGII-induced hypertensive response is significantly less severe than it is when male donor cells are utilised (Ji *et al.*, 2014).

T_{regs} play a pivotal role in regulating healthy immune responses to pathogens as well as preventing auto-immune disease. They produce IL-10, an anti-inflammatory cytokine which inhibits synthesis of pro-inflammatory cytokines (Chen & Liu, 2009). Adoptive transfer of T_{regs} into age-matched male mice limits ANGII-induced increases in blood pressure (Barhoumi *et al.*, 2011). This combined with the fact that castration of healthy men reduces circulating T_{regs} (Page *et al.*, 2006) suggests a deleterious role for testosterone in hypertension and may begin to explain why men are more prone to hypertension than women. It may also offer a partial explanation as to why I observed a pro-inflammatory immunophenotype in hypertensive men but not in women. Fitting with this, estrogen stimulates the production of T_{regs} in mice and estrogen-stimulated differentiation of helper T cells into T_{regs} is blocked by estrogen antagonists (Tai *et al.*, 2008). Taken together these studies suggest that testosterone is pro-hypertensive and oestrogen protects against hypertension. However, the reality is not that simple; gonadectomy increases inflammatory markers in both males and females (Tipton *et al.*, 2014) suggesting that both sex hormones are anti-inflammatory. More research is needed to understand this.

The prevailing cytokine milieu affects the differentiation of naïve T cells. High concentrations of TGF-β and low concentrations of IL-6 promote differentiation into TH_{17} cells (which secrete pro-inflammatory IL-17) and low concentrations of TGF-β combined with high concentrations of IL-6 promote differentiation

into T_{regs} (Zheng, 2013). The ratio favouring T_{regs} prevails in females and as such females produce more T_{regs} (Tipton *et al.*, 2014).

Building upon the sex differences noted above, when I compared the immunophenotypes of pre and post-menopausal hypertensive women (see Apendix A) I found that the post-menopausal women exhibited trends such that their immunophenotype was closer to that of men than pre-menopausal women. Young men disproportionately control blood pressure by controlling peripheral vascular resistance, whereas young women preferentially maintain blood pressure by controlling cardiac output (Hart *et al.*, 2012). Young (premenopausal) women have a weak relationship between muscle sympathetic nerve activity and blood pressure compared to men (Charkoudian *et al.*, 2017). This is partly due to estradiol augmenting the vasodilator response mediated by β-adrenoreceptors (Charkoudian *et al*., 2017). SNA increases with age and as women age, menopause results in the loss of female hormones, SNA, peripheral resistance and blood pressure become more closely related, in a manner comparable to men (Charkoudian *et al*., 2017).

No Difference in Expression of CD11b in Leukocytes of Hypertensive Vs. Normotensive Humans:

No changes were observed in expression of CD11b between hypertensive and normotensive groups in either males or females (Figures 51 and 52). This protein is expressed by a wide variety of cells of the innate immune system as discussed earlier. Therefore, this observation suggests that it is the adaptive immune response specifically that is contributing to hypertension.

Limitations and Further Study:

Overall my data support the neoantigen hypothesis (Harrison *et al*., 2011) and the notion that a pro-inflammatory immunophenotype maintains and/or exacerbates hypertension in human males. Although I gained some insight into

Pre vs. post-menopausal women, the n was low when the women were split up to assess this. In the future it would be interesting to take a large cohort of women and look at this in more detail. Also, it would be useful to expand the antibody panels to include additional markers of interest such as CD44, an activation marker involved in leukocyte recruitment and secretion of cytokines (Sneath & Mangham, 1998) and CD69, an early activation marker (Lindsey *et al.*, 2007) that controls T-cell differentiation into TH-17 cells (Fuente *et al.*, 2014). Inclusion of antibodies for these markers would allow for better characterisation of the immunophenotype of T cells in hypertension.

It should be noted that many of the hypertensive patients used in this study were taking anti-hypertensive medications and these medications had the potential to act as confounding factors in the study. It is not possible to recruit large numbers of untreated hypertensive due to moral and ethical concerns, but 13 of the males initially entering the study as normotensive volunteers were in fact found to be hypertensive during screenings and therefore constituted a small group of untreated hypertensives to study since blood was taken from them before they moved on to treatment. Analysing these patients alone yielded the same findings as when all patients were taken together (See Appendix B), indicating that the medications the patients were taking did not influence immunophenotype. Any patient that was taking anti-inflammatory drugs such as ibuprofen or diclofenac was excluded from this study.

Chapter 5: Effect of mGluR5 Modulation on T-Cell Phenotype in Rats

Introduction:

Given the evidence that T cells are involved in hypertension (see Chapter 1) and that hypertensive human males exhibit an altered immunophenotype that is indicative of an increase in antigen-experienced cells and increased proportion of activated cells (see Chapter 4), I intended to investigate whether there is also an altered immunophenotype in SHR compared to normotensive Wistar controls. I used FACS as discussed in Chapter 4 to examine leukocytes isolated from whole blood collected from the tail veins of the animals.

In addition to comparing the immunophenotypes of the two strains of rat without any other intervention, I intended to investigate how mGluR5 modulation effects it. In chapter 1 I provided examples of situations in which immunosuppressive therapies caused reductions in blood pressure and in chapter 3 I presented data showing that modulation of mGluR5 causes changes in blood pressure, at least in the short term. In this chapter I observed the immunophenotype of the animals at baseline, after vehicle treatment, after drug treatment and one week after drug treatment (washout). It is possible that the effects of mGluR5 modulation on blood pressure manifest, at least in part, due to changes in the immune system resulting from altered sympathetic outflow. Does the blood pressure increase caused by positive allosteric modulation of mGluR5 coincide with increased activation of T cells and is the reverse true in the case of mGluR5 antagonism? I investigated these questions in this chapter.

Markers of Interest:

CD4 and CD8a:

As was the case in Chapter 4, I intended to determine the proportions of helper and cytotoxic T cells circulating in the subjects and I used CD4 and CD8 respectively as markers to identify these leukocyte subtypes.

CD44:

CD44 is a transmembrane glycoprotein involved in a variety of functions including lymphocyte migration and activation. It is used as a marker for antigen experienced cells in rodents (Sneath & Mangham, 1998). The protein is expressed on both central and effector memory cells and is more commonly used as a marker of these cells in rodents than CD45RO.

CD62L:

As discussed in Chapter 4, CD62L, is an adhesion molecule involved in the homing of lymphocytes to secondary lymph nodes via high endothelial venules. It is present on naïve memory cells as they need to enter secondary lymph organs in order to encounter antigen and it is also present on central memory cells as they need to return to locate to secondary lymph organs where they will reside until re-encountering their antigen in which case they rapidly expand to many effector cells in order to neutralise the source of the antigen. The absence of CD62L is used to differentiate between CD44+ effector and CD44+ central memory cells; the latter lack CD62L and remain in circulation and tissues.

CD3+CD4+CD44+CD62L+ = Central memory helper T cell

CD3+CD8+CD44+CD62L- = Effector memory cytotoxic T cell

CD11b/c:

CD11c is a marker found on monocytes, macrophages and neutrophils and CD11b is found on these cells as well as other cells of the innate immune system, as mentioned in Chapter 4. Staining for both markers allows for quantification of cells of the immune system, numbers of which may vary between the hypertensives and normotensives as a result of activity by helper T cells (cytokine production etc.).

Summary of Aims:

The aim of this study was to investigate the effect of modulation of mGluR5 on immunophenotype and to expose any possible differences in immunophenotype in SHR compared to normotensive controls. As in Chapter 4, focus was given to investigating differences in the proportion of cells that are antigen-experienced vs. those that are naïve with a view to testing the hypothesis that chronic antigen exposure is involved in the pathology of hypertension. In this instance, CD44 was used as the key indicator for activation / antigen experience and CD62L was used to differentiate between central and effector memory cells. Upregulation of CD44 and downregulation of CD62L would be indicative of an inflammatory phenotype in which there are more antigen-experienced cells.

Methods:

Blood Collection:

All animal experiments were performed in accordance with institutional guidelines and the UK Home Office (Scientific Procedures) Act (1986) with project approval from the University of Bristol, University ethics of research

committee, under Home Office personal license number ICCF4B573 and project license number 70/7868.

Blood was collected at four time-points during the in vivo mGluR5 studies in Chapter 3: The animals used in this study were those same animals and no additional drugs were given for the purpose of this study. The four blood-collection time points were: At the end of the week of baseline recordings (no drugs administered), after one week of vehicle treatment, after one week of drug treatment and after one week of washout.

Blood for the first three time-points was collected via tail vein bleed. The animals were placed into a perspex box (custom-made with air holes, approximately 70% the volume of a standard home cage) warmed via an electric heat pad to approximately 27°C for approximately 10 minutes before being moved to a restraint tube with the tail protruding. The tail was quickly cleaned with warm water (approx. 40°C) and (Hydrex Pink Surgical Scrub) before venous insertion of a 24G Terumo Sureflo IV catheter. 1ml of blood was then allowed to drip into an Eppendorf tube containing 150µL of EDTA to prevent clotting. In the event that a bleed was unsuccessful a fresh cannula was used to make up to two additional attempts. After bleeding was completed, sterile gauze was held over the wound until bleeding stopped and the tail was carefully cleaned before the animal was returned to its home cage. Collected blood was immediately stored in a fridge at 4°C.

For the fourth time-point (post-washout) blood was collected via cardiac puncture. The animals were given an overdose of sodium pentobarbital administered via intraperitoneal injection. In each case the animal's chest was opened upon loss of the foot pinch reflex but before death and blood collected

from the heart via an EDTA-rinsed needled inserted intraventricularly. The blood was transferred to an Eppendorf tube containing 150µL of EDTA to prevent clotting and immediately placed in a fridge at 4°C.

FACS:

Red Blood Cell Lysis:

The blood for each animal was transferred into a 50ml Falcon tube and 10 ml of red blood cell lysis buffer was added (eBiosciences cat#00-4300-54). The tubes were agitated and then left to sit at room temperature for 10 mins before they were topped up to 50ml with PBS (Dulbecco tabs) and spun at 1200RPM for 10 mins. The supernatant was discarded and the above process repeated.

After the 2nd wash the cells were resuspended in 3ml of FACS buffer and cells were counted using trypan blue staining as in Chapter 4.

Antibody Staining:

The three antibody panels that were used are displayed in Table 5:

	CD marker	Fluorescent conjugate	Reason for interest in CD marker
Panel A	CD3	PE	Denotes T cell
	CD45	V450	Denotes T cell
	αβTCR	FITC	Denotes T cell
	CD62L	AF647	Involved in homing to lymph nodes
Panel B	CD3	PE	Denotes T cell
	CD45	V450	Denotes T cell
	CD44	FITC	Expressed by antigen-experienced cells
	CD11	EF660	Expressed by cells of innate immune system
Panel C	CD3	PE	Denotes T cell
	CD45	V450	Denotes T cell
	CD4	APC	Denotes helper T cell
	CD8	PerCP	Denotes cytotoxic T cell

Table 5: Display of antibody panel composition. Consult glossary of terms for full names of fluorophores.

The mastermix for each panel was made up with 1.5 µL of each appropriate antibody per sample in 100µL of FACS buffer per sample plus 10µL extra for every 6 tubes in order to account for loss due to multiple pipette-tip changes.

E.g. Blood collected from 6 animals:

3 panels for 6 animals=18 samples. Mastermix for each panel is made up by putting 9µL of appropriate antibody into 1830µL of FACS buffer.

The antibody mastermix tubes were mixed using a vortex machine and then 100µL of appropriate mastermix was added to the corresponding sample tubes

E.g. Blood collected from 6 animals:

6x Panel A, 6x Panel B, 6x Panel C tubes, each with one million cells from corresponding animal suspended in 1ml FACS buffer and 100µL of appropriate mastermix added for staining.

Tubes were wrapped in aluminium foil and placed in a fridge at 4°C for 20 minutes. They were then topped up to 2ml with FACS buffer and spun at 1200RPM for 10 minutes. The supernatant was vacuum-aspirated and the stained cells were resuspended in 250µL FACS buffer and 62.5µL paraformaldehyde (PFA). The PFA was included in order to fix the cells so that they can be analysed at a later date. The cells were wrapped in foil and refrigerated until they were run on a flow cytometer (BD LSRII) not more than one week later.

Flow Cytometry:

Preparation of the beads for compensation controls was done on the day the samples were to be run on the flow cytometer. Antibody solutions were made up by adding 1.5µL of each antibody for each fluorescent conjugate used in the

experiment to 100µL FACS buffer (7 tubes total- V450, PE, FITC, AF647, APC, EF660 and PerCP). Separate FACS tubes were prepared for each fluorescent conjugate and one drop each of positive and negative beads (BD cat# 552845) were added to each. The appropriate antibody solution was added to each of the tubes and they were mixed via vortex. The tubes were left at room temperature until used for compensation controls ~20 minutes later.

All sample tubes were vortexed thoroughly before use on the flow cytometer, as cells collect at the bottom of the tubes after being left undisturbed in the fridge for several days and require resuspension. Data was collected in BD FACSDiva. CD3 (V450) was used as a stopping gate and 10,000 CD3+ cells were collected for each sample. A cell population was deemed positive for an antigen if it had a higher fluorescence than the unstained control. Once data collection was completed it was exported into FlowJo (Tree Star Inc.) for analysis.

Gating/Analysis:

After samples were run on the flow cytometer, analysis was performed using FlowJo software (V10). For all antibody panels an initial gate sought to pick out the lymphocytes based on their size and granularity (FSC Vs. SSC). Then T cells were isolated using a plot of V450 Vs. PE and gating the cells that were positive for both. These cells express both CD45 and CD3, confirming them as T lymphocytes. Further gating was used to identify various T-cell subtypes depending on the antibody panel. An FMO control experiment was performed to assist with gating as in Chapter 4.

Lymphocyte gate was drawn as shown in Figure 53:

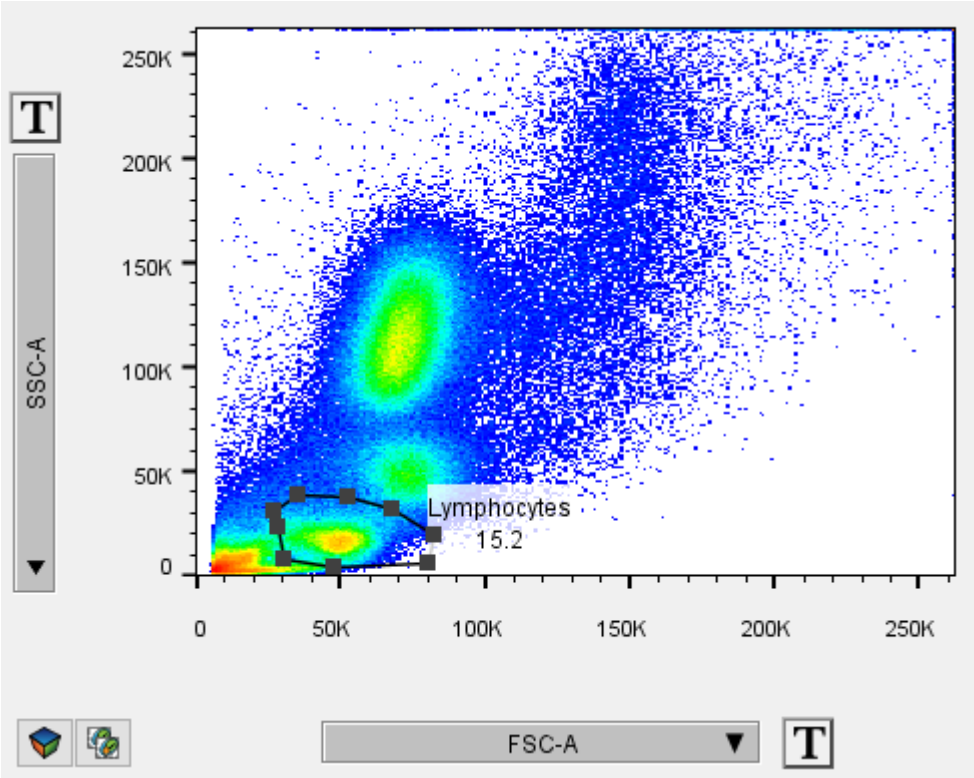

Figure 53: Lymphocyte population identified base on the forward scatter (size) and side scatter (granularity).

T cells were identified as shown in Figure 54:

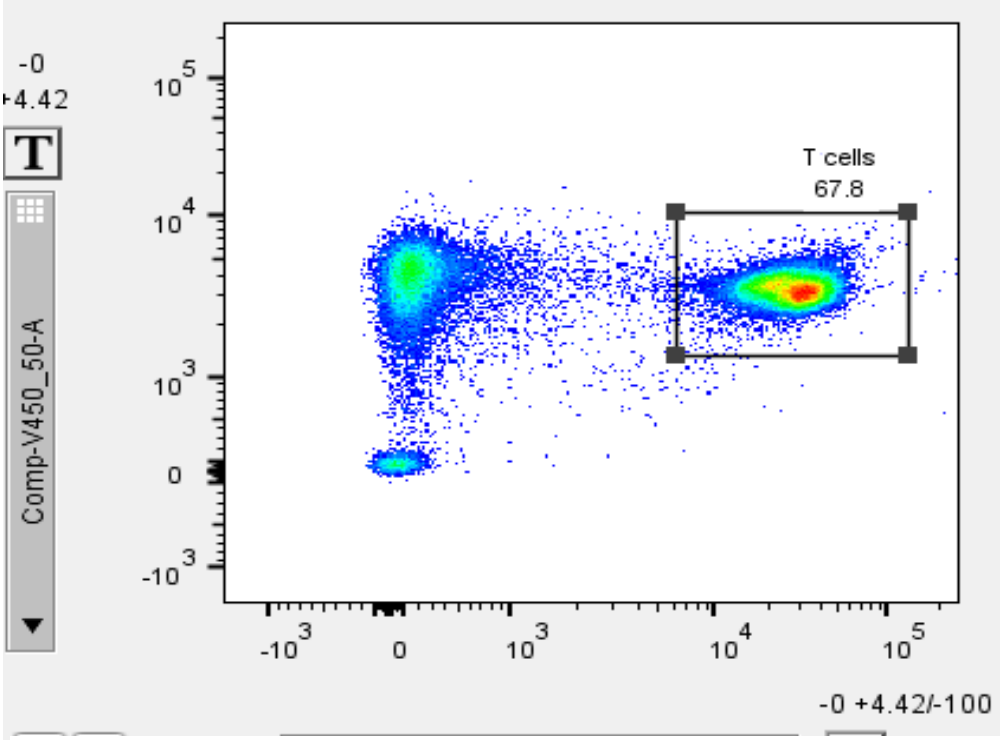

Figure 54: T cells within the lymphocyte population identified based on their expression of both CD3 and CD45, determined by fluorescent emission from both PE-conjugated antibodies for CD3 and V450-conjugated antibodies for CD45.

Panel A specific:

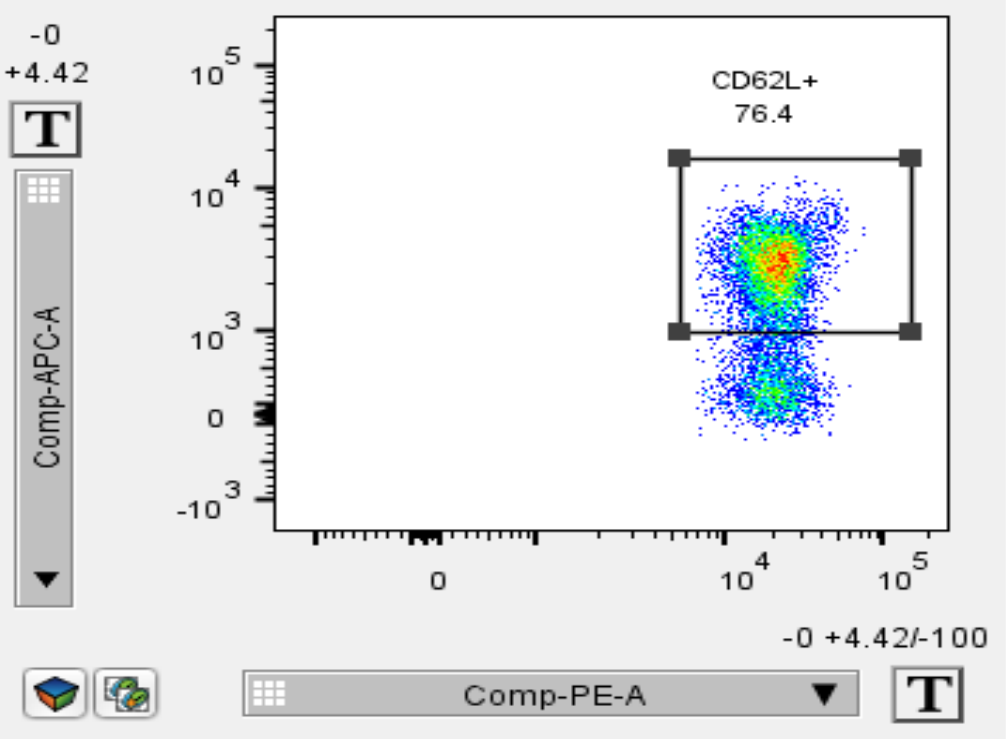

Figure 55: CD62L+ cells within the T cell population identified by fluorescent emission from APC-conjugated antibodies for CD62L.

Panel B Specific:

Initial gate example:

The ‘All cells’ gate is the initial gate, rather than the lymphocyte gate and no subsequent gate is required before gating on CD11b+ cells.

Note: All cells are included in the initial gate when quantifying CD11b+ cells as these cells are not T Lymphocytes but cells of the innate immune system such as monocytes, granulocytes, macrophages, and natural killer cells. The cluster of debris in the bottom left of the initial FSC Vs. SSC plot is excluded but all cells included in the initial gate.

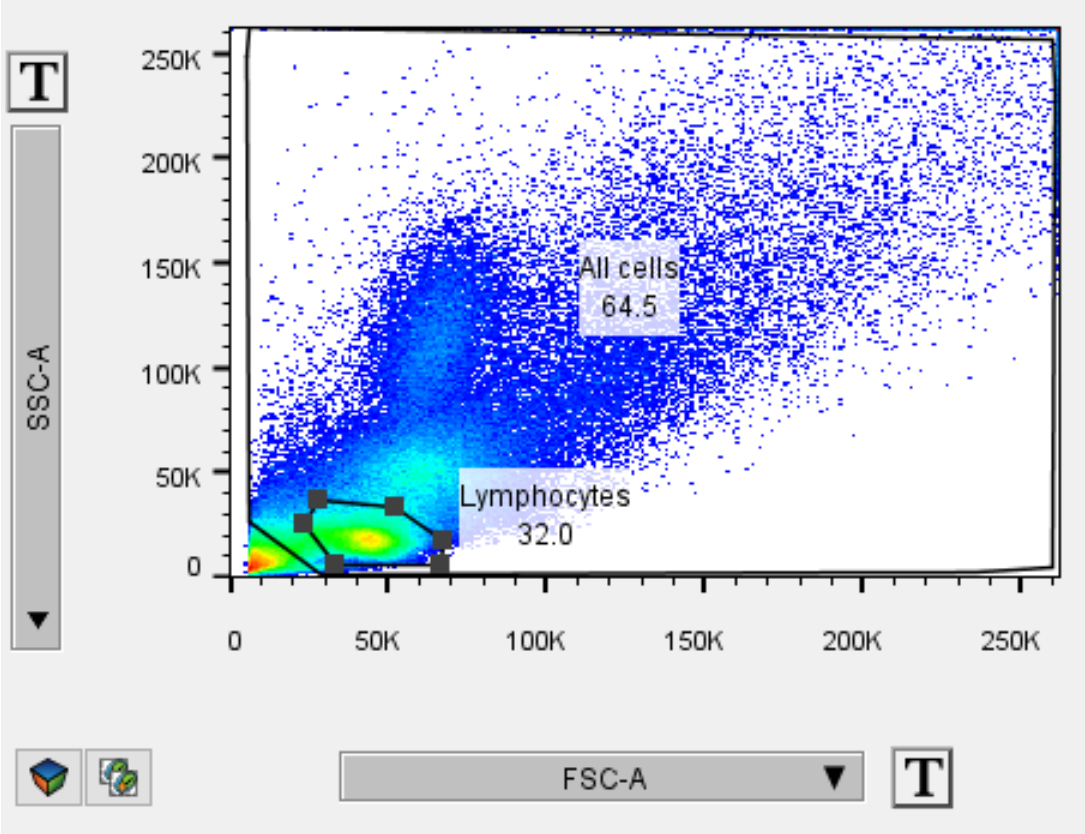

Figure 56: Initial gate for Panel B. All cells are included in the gate, the cluster of debris in the bottom left is excluded.

CD11b+ cells within the ‘all cells’ gate were selected as shown in Figure 57:

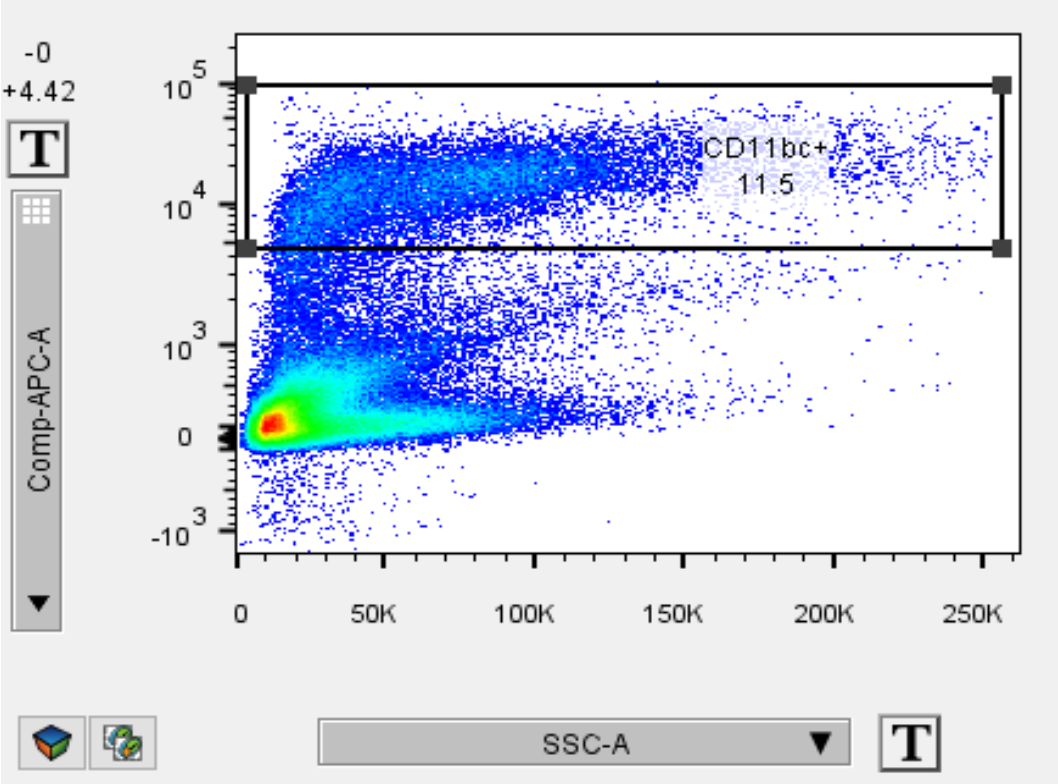

Figure 57: CD11b+ cells identified by fluorescent emission from EF660-conjugated antibodies for CD11b. The Y-axis shows APC because the fluorescent emission from EF660 is at the same wavelength as APC and the same detector is used.

CD3+CD44+ Cells within the lymphocyte population were selected as shown in Figure 58.

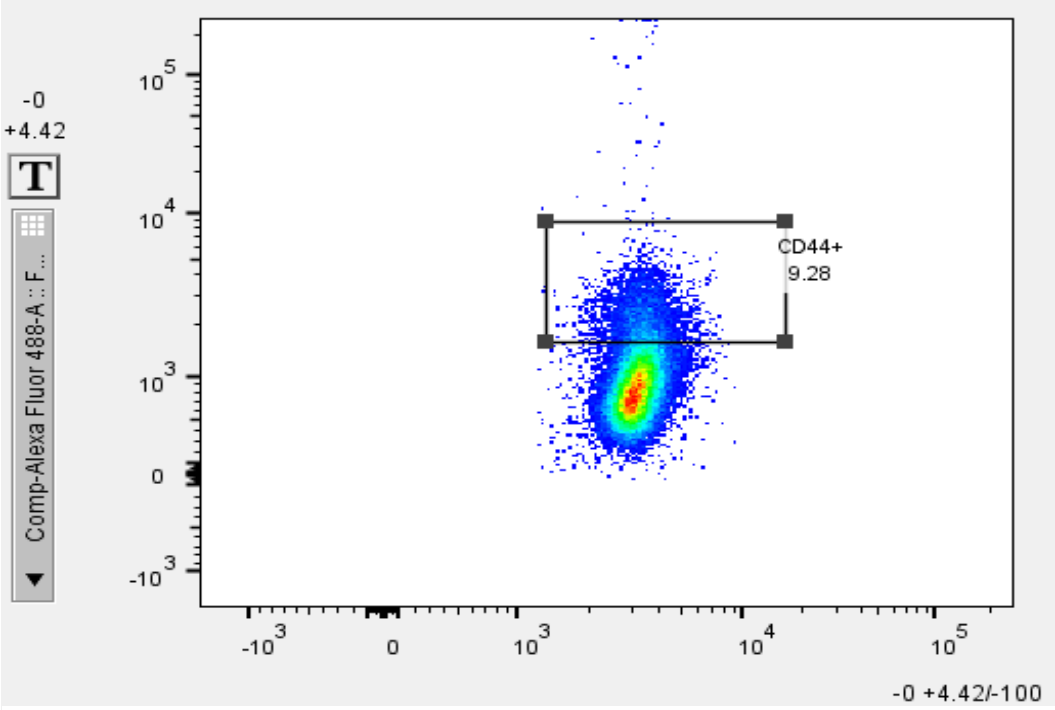

Figure 58: Antigen-experienced cells within the lymphocyte population identified by the fluorescent emission from anti-CD44 antibodies conjugated to AF488.

Panel C Specific:

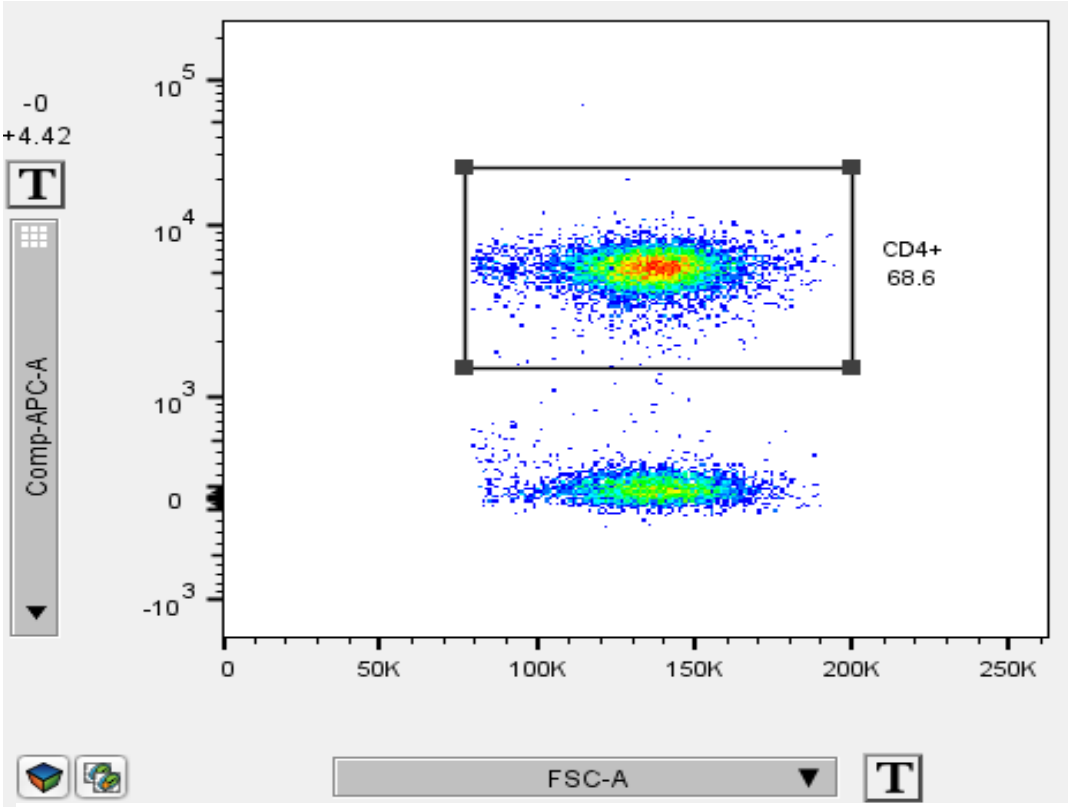

Figure 59: Helper T cells within the lymphocyte population identified by the fluorescent emission from anti-CD4 antibodies conjugated to AF488.

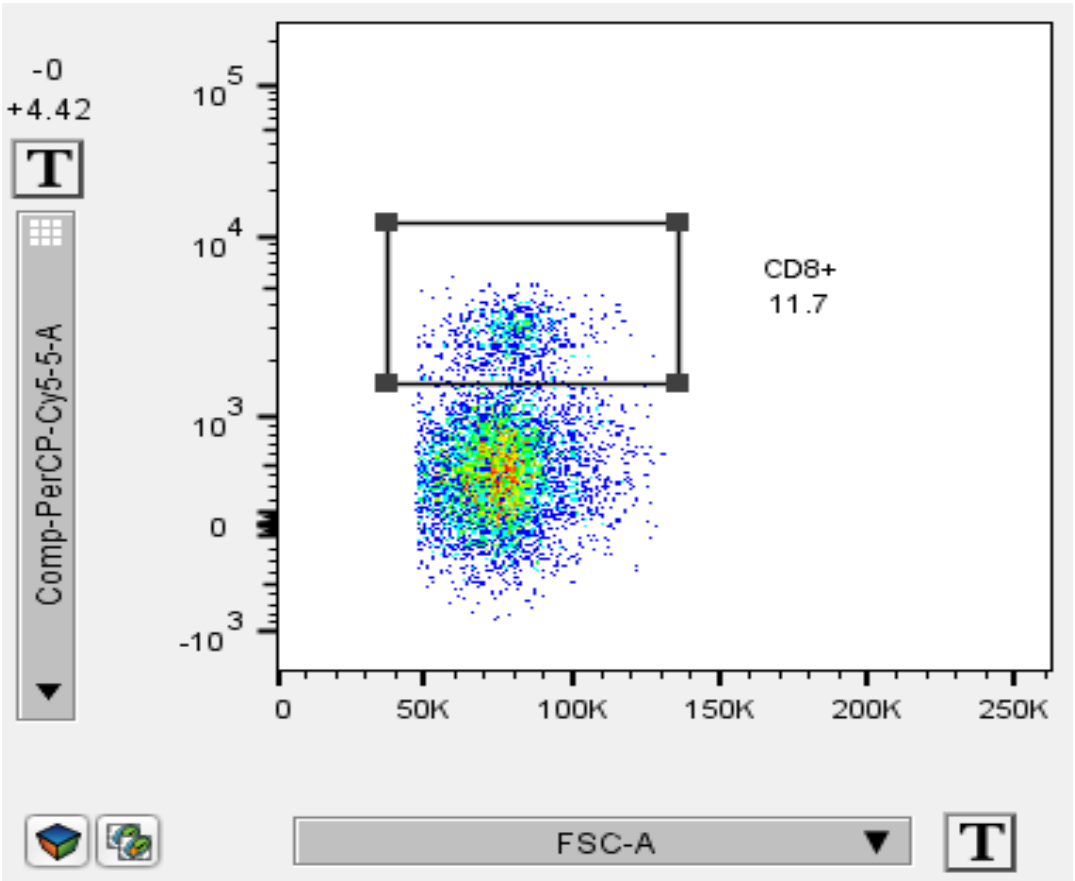

Figure 60: Cytotoxic T cells within the lymphocyte population identified by the fluorescent emission from anti-CD8 antibodies conjugated to PerCP/Cy5.5.

The % of T cells expressing each of the antigens measured from each animal were averaged for each stage of the study (baseline, vehicle, drug treatment, washout). The same was done for the total % all of cells expressing CD11b.

Results:

No significant difference in the expression of CD4, CD8, CD62L, CD44 or CD11b was observed as a result of either positive allosteric modulation of mGluR5 using LSN2814617 or of antagonism of the receptor using MPEP or MTEP (Figure 61).

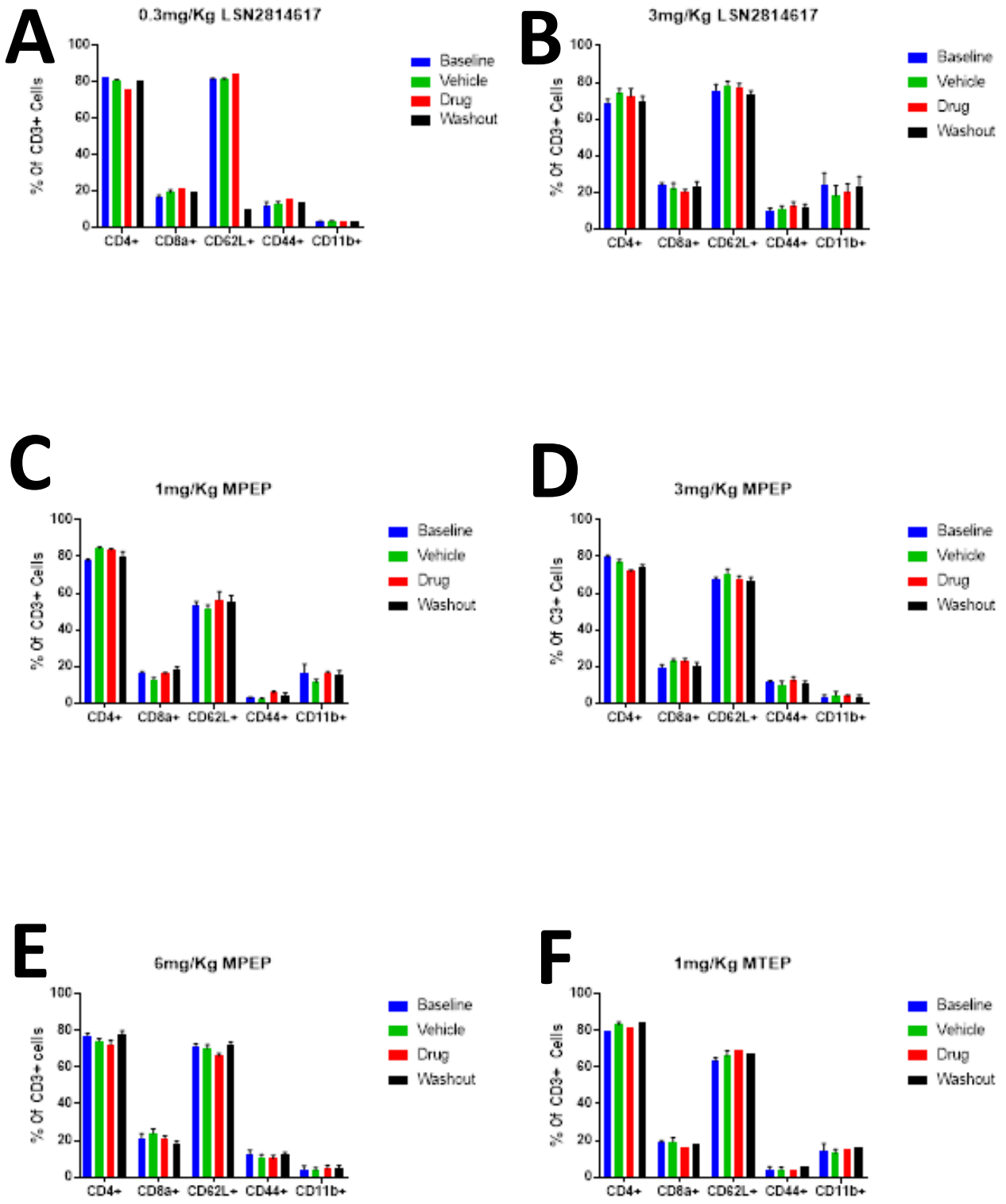

Figure 61: Expression of CD markers of interest on CD3+ T cells isolated from rats as determined by FACS. Blood was taken from Wistars for the LSN2814617 study (**A and B)** and SHRs for MPEP (**C-E**) and MTEP (**F**). Blood was drawn after a one week period of baseline, vehicle, drug and washout. No significant differences were observed. P-Values determined by T-test. Error bars show SEM.

Discussion:

No Significant Differences in Immunophenotype Were Observed in Response to Modulation of mGluR5:

No significant difference in the expression of CD4, CD8, CD62L, CD44 or CD11b was observed as a result of either positive allosteric modulation of mGluR5 using LSN2814617 (Figure 61 A and B) or of antagonism of the receptor using MPEP (Figure 61 C-E) or MTEP (Figure 61 F). This may be due to the fact that blood was drawn via tail vein bleed at the end of each one-week phase (baseline, vehicle, drug and washout). The results from Chapter 3 show that changes in blood pressure resulting from modulation of mGluR5 disappeared after 2-3 days so it is possible that any changes in immunophenotype that did occur were missed by the time blood was collected. It is of course possible that no changes occurred – the results from my study do not allow any decisive conclusion to be made.

The rationale for this study was that the sympathetic nervous system is pro-inflammatory as discussed in Chapter 1. We published a paper recently (Marvar *et al.*, 2016) demonstrating that inhibition of leukotriene B4 receptor reduces blood pressure and improves autonomic function (baroreflex) in SHR – The immune system is most certainly involved in hypertension in rats as well as humans.

No Significant Differences in Immunophenotype Were Observed between SHR and Normotensive Wistar Controls.

The rats receiving LSN2814617 (Figure 61 A and B) were normotensive Wistars and those receiving the antagonists were hypertensive SHRs (Figure 61 C-F). No significant difference in the expression of CD4, CD8, CD62L, CD44 or

CD11b was observed between Wistars and SHRs. This was not expected since the results from Chapter 4, as well as those from a paper we published recently (Marvar *et al.*, 2014) show that hypertensive human males exhibit a pro-inflammatory phenotype constituting an increase in the percentage of T-cells that are antigen-experienced. There are a wide array of differences between the immune systems of humans and rodents (Mestas & Hughes, 2004). Potentially of significance to this particular study is the fact that human T cells express MHCII whereas those of rodents do not. MHCII allows human T cells to take up, process and present antigen and the fact that they also express B7 co-stimulatory protein means they are able to amplify inflammatory responses by activating other cells of the adaptive immune system (Barnaba *et al.*, 1994; Denton *et al.*, 1999), a role reserved for specialist antigen presenting cells in rodents. It is possible that this attenuates the hypertensive effect of 'neoantigens' formed by oxidative modification of endogenous proteins because the antigenic signal is not amplified in the same way as it is in humans.

Hypertension has a variety of causes and these may be different depending on the individual. Perhaps in the case of humans, inflammation is a major driving factor in many and in others it is not, leaving an inflammatory component in the average human. SHRs are inbred so they are more likely to share particularities of mechanistic causes of hypertension.

Lifestyle factors such as diet and behaviour (exercise etc.) are known to be contributing factors to hypertension as discussed in chapter 1. It is possible that pro-inflammatory factors such as poor diet and sedentary lifestyle in humans begin the inflammatory cycle we see in hypertension. These factors do not come

into play with experimental rats, which eat a healthy diet and maintain healthy levels of physical activity under laboratory conditions.

Limitations and Further work:

When this study began, I did not know what effect the PAM or the antagonists would have on blood pressure over the course of the week-long treatment phase and I did not anticipate the tolerance that I observed. If I was to study this further, I would take blood samples from the animals at the peak of the observed effects on blood pressure in order to determine whether T cells exhibit a more pro-inflammatory phenotype when blood pressure is increased or vice versa.

Chapter 6: Conclusions

In Chapter 2, I demonstrated that mGluR5 is expressed in a variety of key nuclei of the medulla, midbrain and hypothalamus that are known to be involved in autonomic regulation of blood pressure. My findings build upon the work of Li and Pan, who previously inferred the presence of mGluR5 in the PVN by microinjecting compounds that modulate mGluR5 and eliciting measurable pressor and depressor responses. Li and Pan also quantified mGluR5 isolated from tissue homogenates of the PVN using Western Blotting and qPCR, providing further evidence of mGluR5 expression in this nucleus (Li and Pan, 2010).

Prior to my study there was limited evidence of mGluR5 expression in the PAG. Palazzo *et al.* inferred the presence of mGluR5 in the PAG when they found that MPEP abrogated responses they had elicited via cannabinoid receptor stimulation (Palazzo *et al.*, 2012). One group had previously localised mGluR5 in the NTS (Hay *et al.*, 1999) and another provided evidence for the expression of Group 1 mGluRs in the NTS and CVLM, although their methods were not selective for either mGluR1 or mGluR5 and so this study does not provide evidence of mGluR5 expression in these nuclei specifically (Austgen *et al.*, 2009). To my knowledge, no group has published convincing evidence of mGluR5 expression in the A5 area or the CVLM.

My immunohistochemistry study provides corroborating evidence of mGluR5 expression in the PVN, NTS and PAG, using a different methodology to those used by previous groups. The staining observed in the A5 area of the ventrolateral pons potentially points to a novel finding of mGluR5 expression in

this area but due to the limitations discussed in Chapter 2 it is not possible for me to conclude that the A5 adrenergic neurons in particular express mGluR5.

In Chapter 3, I demonstrated that positive allosteric modulation of mGluR5 via LSN2814617 causes an increase in blood pressure and that blood pressure can be reduced with MTEP, a selective antagonist for the receptor. These findings were not surprising given the fact that mGluR5 activation is known to increase neuronal excitability and that the receptor is expressed in nuclei involved in blood pressure control and where excitatory signalling is glutamatergic as discussed in Chapter 1.

The observation that the effects of mGluR5 modulation were tolerated relatively quickly (in that both BP and HR trended back to baseline despite continued drug administration) was surprising. The mechanism by which this tolerance occurred cannot be determined from my study but I discussed some of the possibilities in Chapter 3. This tolerance of the pharmacological effects of the compounds, combined with the fact that systemic modulation of glutamatergic signalling would likely cause a variety of off-target effects, reduces the possibility that MTEP will ever be used as a novel therapeutic agent to control hypertension in humans. Regardless, the effects I observed provide a practical demonstration that mGluR5 plays a role in signalling that is integral to the control of blood pressure. As I discussed in Chapter 3, my study does not determine the degree to which mGluR5 modulation affects sympathetic outflow specifically and additional studies would be required to determine this.

In Chapter 4, I clearly demonstrated a relationship between the adaptive immune system and hypertension. My investigation of the balance between the CD45RO and CD45RA isotypes of CD45 expressed by T cells, along with expression of

CD62L, CD196 and CD197 builds upon the novel findings we published previously (Marvar *et al.*, 2014). The expansion of this work provides further valuable insight into how the adaptive immune system promotes hypertension. My finding that the percentage of T-cells that are antigen experienced is significantly increased in hypertensive human males is in agreement with the hypothesis that hypertension causes the production of reactive oxygen species which modify endogenous proteins such that they are no longer recognised as self, promoting an auto-immune inflammatory response which itself is pro-hypertensive (Figure 7). My findings do not, however, directly support this hypothesis since I do not have any evidence for the existence of 'neoantigens', I show only that T cells are activated in hypertension. My findings fit with data from other groups implicating T cells in hypertension as discussed in Chapter 1, thereby contributing to the growing body of evidence linking the adaptive immune system with hypertension.

Chapter 5 did not provide such valuable insight. All that can be determined from this study is that male SHRs do not exhibit a pro-inflammatory immunophenotype as hypertensive human males do and that pharmacological modulation of mGluR5 does not cause long-term changes in T-cell immunophenotype. Whether or not mGluR5 modulation causes short-term changes in immunophenotype that coincide with the pressor and depressor effects I observed is a question that I failed to answer due to the possibility that my blood-sampling time point may have missed this effect.

Overall my project has demonstrated that mGluR5 plays a role in modulating the control of blood pressure and that the adaptive immune system is involved in either the generation or maintenance of hypertension.

Appendices:

Appendix A:

A

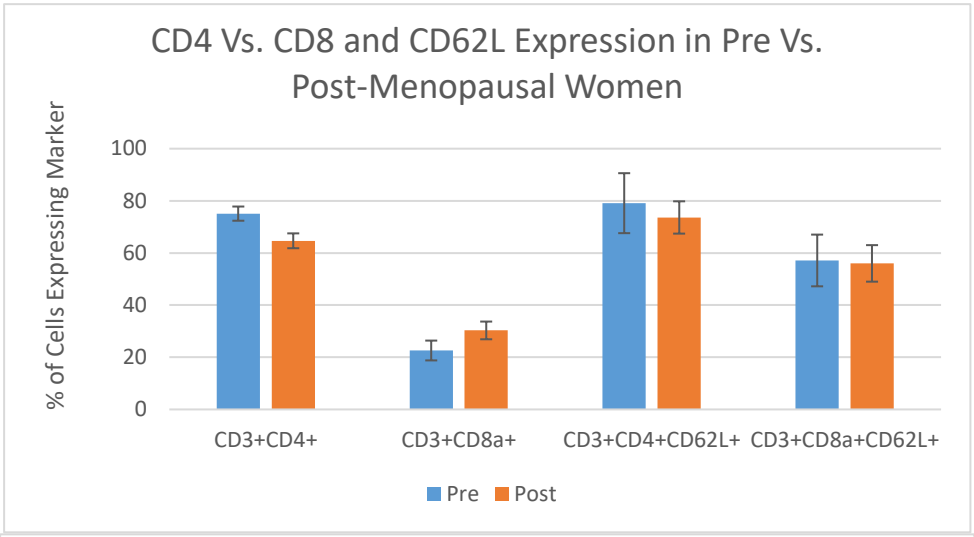

B

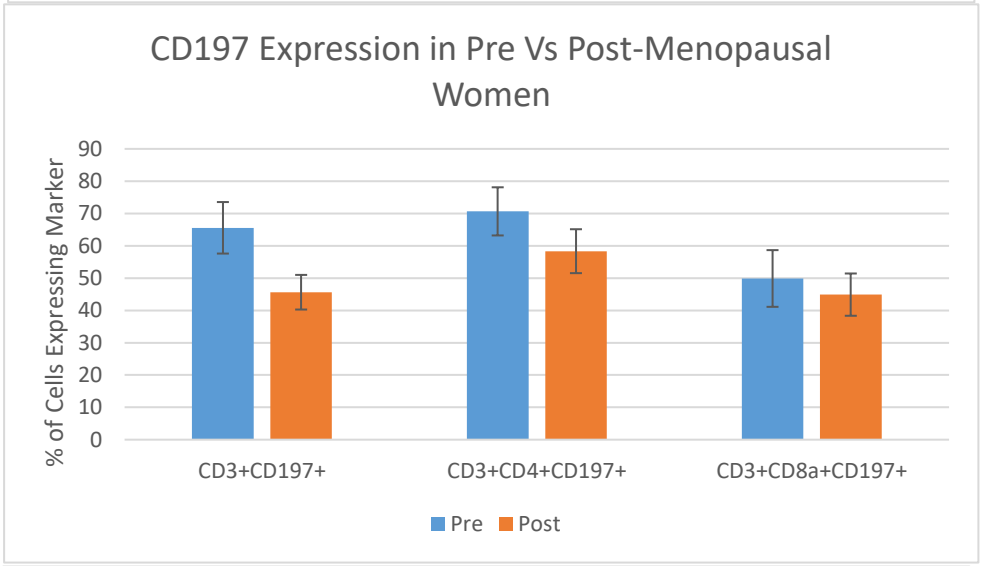

C

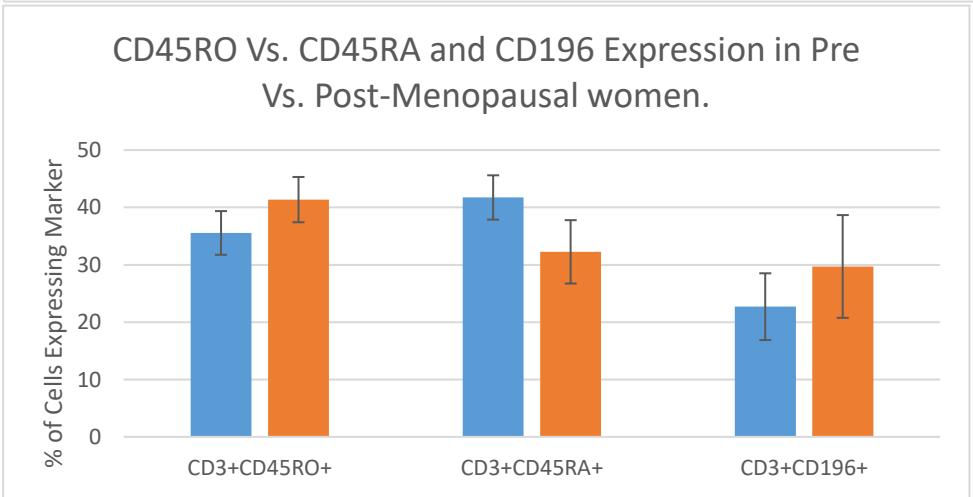

Figure 62: T cell phenotype in post-menopausal hypertensive human females vs. aged-matched normotensive controls. **A:** CD4+ vs. CD8a+ T cells and CD62L expression on each of the two subpopulations. **B:** CD197 expression on all T cells, helper T cells and cytotoxic T cells respectively. **C:** CD45RO vs. CD45RA expression and CD196 expression. Error bars show SEM.

Appendix B:

A

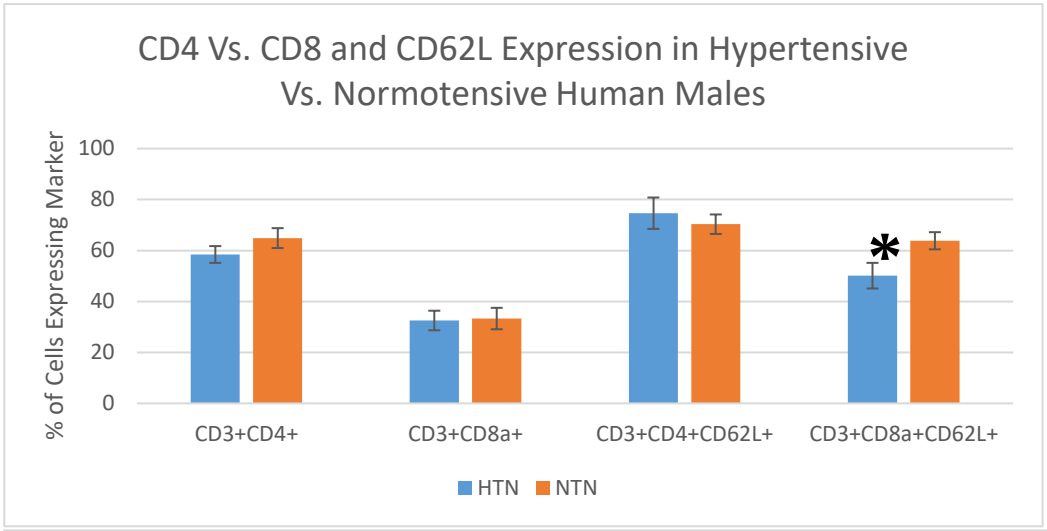

B

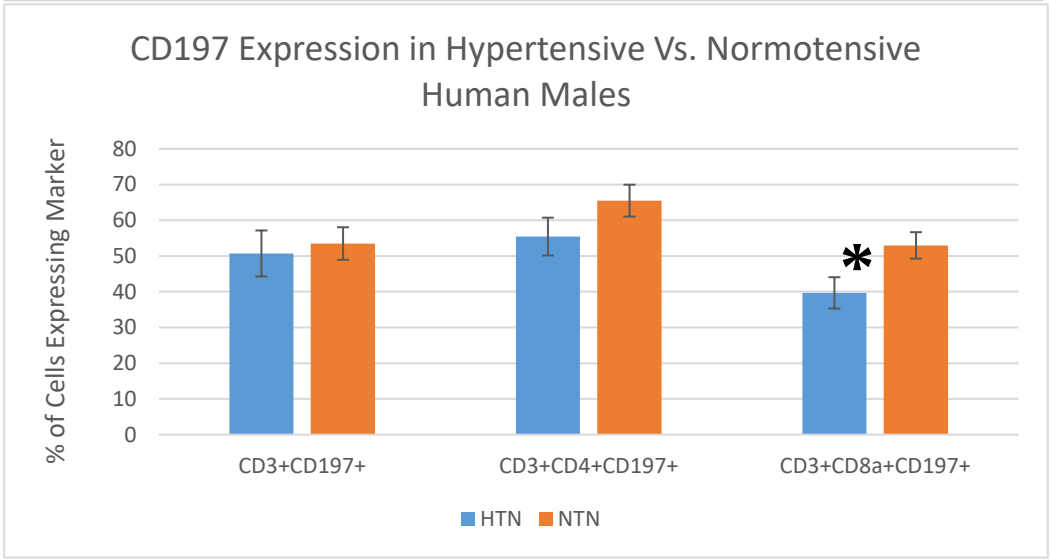

C

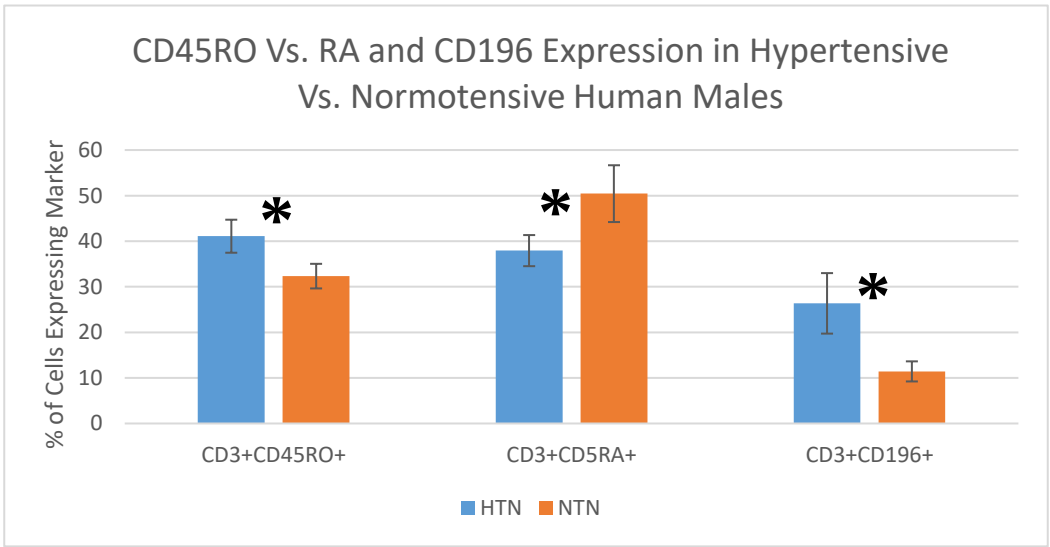

Figure 63: T cell phenotype in **untreated** hypertensive human males vs. aged-matched normotensive controls. **A:** CD4+ vs. CD8a+ T cells and CD62L expression on each of the two subpopulations. **B:** CD197 expression on all T cells, helper T cells and cytotoxic T cells respectively. **C:** CD45RO vs. CD45RA expression and CD196 expression. Error bars show SEM.

Appendix C:

Formulations for Solutions Used in Chapter 2:

Iron Alum: Dissolve 140g of ferric-ammonium sulfate crystals in 400ml of hot water. Leave to cool then filter and make up to a volume of 500ml with dilute (6 N) nitric acid.

Solochrome Solution: Add 0.5ml conc. sulphuric acid to 0.2g solochrome cyanine RS (Eriochrome cyanine R). Stir until dissolved. Add 96ml of distilled water and 4ml of 10% aqueous iron alum. Mix and filter.

References:

Abbott SB, Kanbar R, Bochorishvili G, Coates MB, Stornetta RL & Guyenet PG (2012). C1 neurons excite locus coeruleus and A5 noradrenergic neurons along with sympathetic outflow in rats. *J Physiol* **590,** 2897–2915.

Abbott SBG, Stornetta RL, Socolovsky CS, West GH & Guyenet PG (2009). Photostimulation of channelrhodopsin-2 expressing ventrolateral medullary neurons increases sympathetic nerve activity and blood pressure in rats. *J Physiol* **587,** 5613–5631.

Aicher SA, Kurucz OS, Reis DJ & Milner TA (1995). Nucleus tractus solitarius efferent terminals synapse on neurons in the caudal ventrolateral medulla that project to the rostral ventrolateral medulla. *Brain Res* **693,** 51–63.

Akine A, Montanaro M & Allen AM (2003). Hypothalamic paraventricular nucleus inhibition decreases renal sympathetic nerve activity in hypertensive and normotensive rats. *Auton Neurosci Basic Clin* **108,** 17–21.

Alaniz RC, Thomas SA, Perez-Melgosa M, Mueller K, Farr AG, Palmiter RD & Wilson CB (1999). Dopamine beta-hydroxylase deficiency impairs cellular immunity. *Proc Natl Acad Sci U S A* **96,** 2274–2278.

Alberts B, Johnson A, Lewis J, Raff M, Roberts K & Walter P (2002). *Molecular Biology of the Cell*, 4th edn. Garland Science.

Altschuler SM, Bao X, Bieger D, Hopkins DA & Miselis RR (1989). Viscerotopic representation of the upper alimentary tract in the rat: Sensory ganglia and nuclei of the solitary and spinal trigeminal tracts. *J Comp Neurol* **283,** 248–268.

Anderson EA, Sinkey CA, Lawton WJ & Mark AL (1989). Elevated sympathetic nerve activity in borderline hypertensive humans. Evidence from direct intraneural recordings. *Hypertens Dallas Tex 1979* **14,** 177–183.

Anderson RG (1993). Caveolae: where incoming and outgoing messengers meet. *Proc Natl Acad Sci U S A* **90,** 10909–10913.

Ando H, Zhou J, Macova M, Imboden H & Saavedra JM (2004). Angiotensin II AT1 receptor blockade reverses pathological hypertrophy and inflammation in brain microvessels of spontaneously hypertensive rats. *Stroke* **35,** 1726–1731.

Andrade R & Aghajanian GK (1982). Single cell activity in the noradrenergic A-5 region: responses to drugs and peripheral manipulations of blood pressure. *Brain Res* **242,** 125–135.

Andreeva K, Zhang M, Fan W, Li X, Chen Y, Rebolledo-Mendez JD & Cooper NG (2014). Time-dependent Gene Profiling Indicates the Presence of Different Phases for Ischemia/Reperfusion Injury in Retina. *Ophthalmol Eye Dis* **6,** 43–54.

Andresen MC & Kunze DL (1994). Nucleus Tractus Solitarius—Gateway to Neural Circulatory Control. *Annu Rev Physiol* **56,** 93–116.

Anon (n.d.). WHO | Raised blood pressure. *WHO*. Available at: http://www.who.int/gho/ncd/risk_factors/blood_pressure_prevalence_text/en/ [Accessed September 13, 2017].

Austgen JR, Fong AY, Foley CM, Mueller PJ, Kline DD, Heesch CM & Hasser EM (2009). Expression of group i metabotropic glutamate receptors on phenotypically different cells within the nucleus of the solitary tract in the rat. *Neuroscience* **159,** 701–716.

Baba M, Imai T, Nishimura M, Kakizaki M, Takagi S, Hieshima K, Nomiyama H & Yoshie O (1997). Identification of CCR6, the specific receptor for a novel lymphocyte-directed CC chemokine LARC. *J Biol Chem* **272,** 14893–14898.

Balsari A, Marolda R, Gambacorti-Passerini C, Sciorelli G, Tona G, Cosulich E, Taramelli D, Fossati G, Parmiani G & Cascinelli N (1986). Systemic administration of autologous, alloactivated helper-enriched lymphocytes to patients with metastatic melanoma of the lung. A phase I study. *Cancer Immunol Immunother CII* **21,** 148–155.

Bandler R, Keay KA, Floyd N & Price J (2000). Central circuits mediating patterned autonomic activity during active vs. passive emotional coping. *Brain Res Bull* **53,** 95–104.

Banks WA (2005). Blood-brain barrier transport of cytokines: a mechanism for neuropathology. *Curr Pharm Des* **11,** 973–984.

Barber EK, Dasgupta JD, Schlossman SF, Trevillyan JM & Rudd CE (1989). The CD4 and CD8 antigens are coupled to a protein-tyrosine kinase (p56lck) that phosphorylates the CD3 complex. *Proc Natl Acad Sci U S A* **86,** 3277–3281.

Barhoumi T, Kasal DA, Li MW, Shbat L, Laurant P, Neves MF, Paradis P & Schiffrin EL (2011). T regulatory lymphocytes prevent angiotensin II-induced hypertension and vascular injury. *Hypertens Dallas Tex 1979* **57,** 469–476.

Barnaba V, Watts C, de Boer M, Lane P & Lanzavecchia A (1994). Professional presentation of antigen by activated human T cells. *Eur J Immunol* **24,** 71–75.

Beckstead RM & Norgren R (1979). An autoradiographic examination of the central distribution of the trigeminal, facial, glossopharyngeal, and vagal nerves in the monkey. *J Comp Neurol* **184,** 455–472.

Bellinger DL, Millar BA, Perez S, Carter J, Wood C, ThyagaRajan S, Molinaro C, Lubahn C & Lorton D (2008). Sympathetic modulation of immunity: relevance to disease. *Cell Immunol* **252,** 27–56.

Berridge MJ (2009). Inositol trisphosphate and calcium signalling mechanisms. *Biochim Biophys Acta BBA - Mol Cell Res* **1793,** 933–940.

Besedovsky H, del Rey A, Sorkin E & Dinarello CA (1986). Immunoregulatory feedback between interleukin-1 and glucocorticoid hormones. *Science* **233,** 652–654.

Biancardi VC & Stern JE (2016). Compromised blood-brain barrier permeability: novel mechanism by which circulating angiotensin II signals to sympathoexcitatory centres during hypertension. *J Physiol* **594,** 1591–1600.

Blessing W (1997). *The Lower Brainstem and Bodily Homeostasis*. Oxford University Press.

Blessing WW (1988). Depressor neurons in rabbit caudal medulla act via GABA receptors in rostral medulla. *Am J Physiol* **254,** H686-692.

Blood Pressure UK (2017). Blood Pressure : Blood pressure chart. Available at: http://www.bloodpressureuk.org/BloodPressureandyou/Thebasics/Bloodpressurechart [Accessed September 3, 2017].

Borovikova LV, Ivanova S, Nardi D, Zhang M, Yang H, Ombrellino M & Tracey KJ (2000*a*). Role of vagus nerve signaling in CNI-1493-mediated suppression of acute inflammation. *Auton Neurosci Basic Clin* **85,** 141–147.

Borovikova LV, Ivanova S, Zhang M, Yang H, Botchkina GI, Watkins LR, Wang H, Abumrad N, Eaton JW & Tracey KJ (2000*b*). Vagus nerve stimulation attenuates the systemic inflammatory response to endotoxin. *Nature* **405,** 458–462.

Boscan P & Paton JFR (2005). Excitatory convergence of periaqueductal gray and somatic afferents in the solitary tract nucleus: role for neurokinin 1 receptors. *Am J Physiol Regul Integr Comp Physiol* **288,** R262-269.

Bradley RM, Mistretta CM, Bates CA & Killackey HP (1985). Transganglionic transport of HRP from the circumvallate papilla of the rat. *Brain Res* **361,** 154–161.

Braga VA, Paton JFR & Machado BH (2007). Ischaemia-induced sympathoexcitation in spinalyzed rats. *Neurosci Lett* **415,** 73–76.

Brakeman PR, Lanahan AA, O'Brien R, Roche K, Barnes CA, Huganir RL & Worley PF (1997). Homer: a protein that selectively binds metabotropic glutamate receptors. *Nature* **386,** 284–288.

Brandon KW & Rand MJ (1961). Acetylcholine and the sympathetic innervation of the spleen. *J Physiol* **157,** 18–32.

Bräuner-Osborne H, Wellendorph P & Jensen AA (2007). Structure, pharmacology and therapeutic prospects of family C G-protein coupled receptors. *Curr Drug Targets* **8,** 169–184.

Brown DL & Guyenet PG (1985). Electrophysiological study of cardiovascular neurons in the rostral ventrolateral medulla in rats. *Circ Res* **56,** 359–369.

Buettner GR (2011). Superoxide Dismutase in Redox Biology: The roles of superoxide and hydrogen peroxide. *Anticancer Agents Med Chem* **11,** 341–346.

Burke PGR, Abbott SBG, Coates MB, Viar KE, Stornetta RL & Guyenet PG (2014). Optogenetic stimulation of adrenergic C1 neurons causes sleep state-dependent cardiorespiratory stimulation and arousal with sighs in rats. *Am J Respir Crit Care Med* **190,** 1301–1310.

Burtenshaw D, Hakimjavadi R, Redmond EM & Cahill PA (2017). Nox, Reactive Oxygen Species and Regulation of Vascular Cell Fate. *Antioxidants*; DOI: 10.3390/antiox6040090.

Byrum CE & Guyenet PG (1987). Afferent and efferent connections of the A5 noradrenergic cell group in the rat. *J Comp Neurol* **261,** 529–542.

Cai H, Griendling KK & Harrison DG (2003). The vascular NAD(P)H oxidases as therapeutic targets in cardiovascular diseases. *Trends Pharmacol Sci* **24,** 471–478.

Cameron PL, Ruffin JW, Bollag R, Rasmussen H & Cameron RS (1997). Identification of caveolin and caveolin-related proteins in the brain. *J Neurosci Off J Soc Neurosci* **17,** 9520–9535.

Cardinale JP, Sriramula S, Mariappan N, Agarwal D & Francis J (2012). Angiotensin II-induced hypertension is modulated by nuclear factor-κBin the paraventricular nucleus. *Hypertens Dallas Tex 1979* **59,** 113–121.

Carretero OA & Oparil S (2000). Essential hypertension. Part I: definition and etiology. *Circulation* **101,** 329–335.

Carrive P (1993). The periaqueductal gray and defensive behavior: functional representation and neuronal organization. *Behav Brain Res* **58,** 27–47.

Carrive P, Bandler R & Dampney RA (1988). Anatomical evidence that hypertension associated with the defence reaction in the cat is mediated by a direct projection from a restricted portion of the midbrain periaqueductal grey to the subretrofacial nucleus of the medulla. *Brain Res* **460,** 339–345.

Chan RK & Sawchenko PE (1998). Organization and transmitter specificity of medullary neurons activated by sustained hypertension: implications for understanding baroreceptor reflex circuitry. *J Neurosci Off J Soc Neurosci* **18,** 371–387.

Charkoudian N, Hart ECJ, Barnes JN & Joyner MJ (2017). Autonomic control of body temperature and blood pressure: influences of female sex hormones. *Clin Auton Res Off J Clin Auton Res Soc* **27,** 149–155.

Chen J & Liu XS (2009). Development and function of IL-10 IFN-gamma-secreting CD4(+) T cells. *J Leukoc Biol* **86,** 1305–1310.

Chen QH, Haywood JR & Toney GM (2003). Sympathoexcitation by PVN-injected bicuculline requires activation of excitatory amino acid receptors. *Hypertens Dallas Tex 1979* **42,** 725–731.

Ciriello J, Kline RL, Zhang TX & Caverson MM (1984). Lesions of the paraventricular nucleus alter the development of spontaneous hypertension in the rat. *Brain Res* **310,** 355–359.

Ciriello J, Schultz CG & Roder S (1994). Collateral axonal projections from ventrolateral medullary non-catecholaminergic neurons to central nucleus of the amygdala. *Brain Res* **663,** 346–351.

Contreras RJ, Beckstead RM & Norgren R (1982). The central projections of the trigeminal, facial, glossopharyngeal and vagus nerves: an autoradiographic study in the rat. *J Auton Nerv Syst* **6,** 303–322.

Coote JH & Macleod VH (1974). Proceedings: Baroreceptor reflex inhibition of a spinal sympathetic reflex. *J Physiol* **239,** 110P-111P.

Coote JH, Yang Z, Pyner S & Deering J (1998). Control of sympathetic outflows by the hypothalamic paraventricular nucleus. *Clin Exp Pharmacol Physiol* **25,** 461–463.

Cravo SL & Morrison SF (1993). The caudal ventrolateral medulla is a source of tonic sympathoinhibition. *Brain Res* **621,** 133–136.

Cushing H (1901). *Concerning a Definite Regulatory Mechanism of the Vaso-motor Centre which Controls Blood Pressure During Cerebral Compression*.

Dampney R a. L, Horiuchi J, Killinger S, Sheriff MJ, Tan PSP & McDowall LM (2005). Long-term regulation of arterial blood pressure by hypothalamic nuclei: some critical questions. *Clin Exp Pharmacol Physiol* **32,** 419–425.

Dampney RA (1994). Functional organization of central pathways regulating the cardiovascular system. *Physiol Rev* **74,** 323–364.

Dampney RA, Blessing WW & Tan E (1988). Origin of tonic GABAergic inputs to vasopressor neurons in the subretrofacial nucleus of the rabbit. *J Auton Nerv Syst* **24,** 227–239.

Dampney RAL, Polson JW, Potts PD, Hirooka Y & Horiuchi J (2003). Functional organization of brain pathways subserving the baroreceptor reflex: studies in conscious animals using immediate early gene expression. *Cell Mol Neurobiol* **23,** 597–616.

Davies SS, Amarnath V & Roberts LJ (2004). Isoketals: highly reactive gamma-ketoaldehydes formed from the H2-isoprostane pathway. *Chem Phys Lipids* **128,** 85–99.

Davies SS, Bodine C, Matafonova E, Pantazides BG, Bernoud-Hubac N, Harrison FE, Olson SJ, Montine TJ, Amarnath V & Roberts LJ (2011). Treatment with a γ-ketoaldehyde scavenger prevents working memory deficits in hApoE4 mice. *J Alzheimers Dis JAD* **27,** 49–59.

De Vries L, Zheng B, Fischer T, Elenko E & Farquhar MG (2000). The regulator of G protein signaling family. *Annu Rev Pharmacol Toxicol* **40,** 235–271.

Dean C & Seagard JL (1997). Mapping of carotid baroreceptor subtype projections to the nucleus tractus solitarius using c-fos immunohistochemistry. *Brain Res* **758,** 201–208.

DeFranco A, Locksley R & Robertson M (2007). *Immunity: The Immune Response in Infectious and Inflammatory Disease*, New Ed edition. OUP Oxford, London : Sunderland, Me.

Del Maschio A, De Luigi A, Martin-Padura I, Brockhaus M, Bartfai T, Fruscella P, Adorini L, Martino G, Furlan R, De Simoni MG & Dejana E (1999). Leukocyte recruitment in the cerebrospinal fluid of mice with experimental meningitis is inhibited by an antibody to junctional adhesion molecule (JAM). *J Exp Med* **190,** 1351–1356.

Denton MD, Geehan CS, Alexander SI, Sayegh MH & Briscoe DM (1999). Endothelial Cells Modify the Costimulatory Capacity of Transmigrating Leukocytes and Promote Cd28-Mediated Cd4+ T Cell Alloactivation. *J Exp Med* **190,** 555–566.

Dickinson CJ & Thomson AD (1960). A post mortem study of the main cerebral arteries with special reference to their possible role in blood pressure regulation. *Clin Sci* **19,** 513–538.

Dikalova A, Clempus R, Lassègue B, Cheng G, McCoy J, Dikalov S, San Martin A, Lyle A, Weber DS, Weiss D, Taylor WR, Schmidt HHHW, Owens GK, Lambeth JD & Griendling KK (2005). Nox1 overexpression potentiates angiotensin II-induced hypertension and vascular smooth muscle hypertrophy in transgenic mice. *Circulation* **112,** 2668–2676.

Doba N & Reis DJ (1973). Acute fulminating neurogenic hypertension produced by brainstem lesions in the rat. *Circ Res* **32,** 584–593.

Esler M, Lambert E & Schlaich M (2010). Rebuttal from Esler, Lambert, and Schlaich. *J Appl Physiol Bethesda Md 1985* **109,** 2000–2001.

Essen L-O, Perisic O, Katan M, Wu Y, Roberts MF & Williams RL (1997). Structural Mapping of the Catalytic Mechanism for a Mammalian Phosphoinositide-Specific Phospholipase C †,‡. *Biochemistry* **36,** 1704–1718.

Farber DL, Yudanin NA & Restifo NP (2014). Human memory T cells: generation, compartmentalization and homeostasis. *Nat Rev Immunol* **14,** 24–35.

Farkas E, Jansen AS & Loewy AD (1998). Periaqueductal gray matter input to cardiac-related sympathetic premotor neurons. *Brain Res* **792,** 179–192.

Felder RB (2010). Mineralocorticoid Receptors, Inflammation and Sympathetic Drive in Heart Failure. *Exp Physiol* **95,** 19–25.

Ferguson SS (2001). Evolving concepts in G protein-coupled receptor endocytosis: the role in receptor desensitization and signaling. *Pharmacol Rev* **53,** 1–24.

Fletcher JM, Lalor SJ, Sweeney CM, Tubridy N & Mills KHG (2010). T cells in multiple sclerosis and experimental autoimmune encephalomyelitis. *Clin Exp Immunol* **162,** 1–11.

Fliser D, Buchholz K, Haller H & EUropean Trial on Olmesartan and Pravastatin in Inflammation and Atherosclerosis (EUTOPIA) Investigators (2004). Antiinflammatory effects of angiotensin II subtype 1 receptor blockade in hypertensive patients with microinflammation. *Circulation* **110,** 1103–1107.

Forette F, Seux ML, Staessen JA, Thijs L, Birkenhäger WH, Babarskiene MR, Babeanu S, Bossini A, Gil-Extremera B, Girerd X, Laks T, Lilov E, Moisseyev V, Tuomilehto J, Vanhanen H, Webster J, Yodfat Y & Fagard R (1998). Prevention of dementia in randomised double-blind placebo-controlled Systolic Hypertension in Europe (Syst-Eur) trial. *Lancet Lond Engl* **352,** 1347–1351.

Fourgeaud L, Bessis A-S, Rossignol F, Pin J-P, Olivo-Marin J-C & Hémar A (2003). The metabotropic glutamate receptor mGluR5 is endocytosed by a clathrin-independent pathway. *J Biol Chem* **278,** 12222–12230.

Fourgeaud L, Mato S, Bouchet D, Hémar A, Worley PF & Manzoni OJ (2004). A single in vivo exposure to cocaine abolishes endocannabinoid-mediated long-term depression in the nucleus accumbens. *J Neurosci Off J Soc Neurosci* **24,** 6939–6945.

Francesconi A, Kumari R & Zukin RS (2009). Regulation of Group I Metabotropic Glutamate Receptor Trafficking and Signaling by the Caveolar/Lipid Raft Pathway. *J Neurosci* **29,** 3590–3602.

Fuente H de la, Cruz-Adalia A, Hoyo GM del, Cibrián-Vera D, Bonay P, Pérez-Hernández D, Vázquez J, Navarro P, Gutierrez-Gallego R, Ramirez-Huesca M, Martín P & Sánchez-Madrid F (2014). The Leukocyte Activation Receptor CD69 Controls T Cell Differentiation through Its Interaction with Galectin-1. *Mol Cell Biol* **34,** 2479–2487.

Fujita M, Ando K, Kawarazaki H, Kawarasaki C, Muraoka K, Ohtsu H, Shimizu H & Fujita T (2012). Sympathoexcitation by brain oxidative stress mediates arterial pressure elevation in salt-induced chronic kidney disease. *Hypertens Dallas Tex 1979* **59,** 105–112.

Fukuda S & Schmid-Schönbein GW (2002). Centrifugation attenuates the fluid shear response of circulating leukocytes. *J Leukoc Biol* **72,** 133–139.

Fukuda S, Yasu T, Kobayashi N, Ikeda N & Schmid-Schönbein GW (2004). Contribution of fluid shear response in leukocytes to hemodynamic resistance in the spontaneously hypertensive rat. *Circ Res* **95,** 100–108.

Gage JR, Fonarow G, Hamilton M, Widawski M, Martínez-Maza O & Vredevoe DL (2004). Beta blocker and angiotensin-converting enzyme inhibitor therapy is associated with decreased Th1/Th2 cytokine ratios and inflammatory cytokine production in patients with chronic heart failure. *Neuroimmunomodulation* **11,** 173–180.

Ganta CK, Lu N, Helwig BG, Blecha F, Ganta RR, Zheng L, Ross CR, Musch TI, Fels RJ & Kenney MJ (2005). Central angiotensin II-enhanced splenic cytokine gene expression is mediated by the sympathetic nervous system. *Am J Physiol Heart Circ Physiol* **289,** H1683-1691.

Gelin C, Sloma I, Charron D & Mooney N (2009). Regulation of MHC II and CD1 antigen presentation: from ubiquity to security. *J Leukoc Biol* **85,** 215–224.

Gill SS, Pulido OM, Mueller RW & McGuire PF (1999). Immunochemical localization of the metabotropic glutamate receptors in the rat heart. *Brain Res Bull* **48,** 143–146.

Gisterå A & Hansson GK (2017). The immunology of atherosclerosis. *Nat Rev Nephrol* **13,** 368–380.

Goodchild AK & Moon EA (2009). Maps of cardiovascular and respiratory regions of rat ventral medulla: focus on the caudal medulla. *J Chem Neuroanat* **38,** 209–221.

Gorbet MB & Sefton MV (2004). Biomaterial-associated thrombosis: roles of coagulation factors, complement, platelets and leukocytes. *Biomaterials* **25,** 5681–5703.

Granger DN & Kvietys PR (2015). Reperfusion injury and reactive oxygen species: The evolution of a concept. *Redox Biol* **6,** 524–551.

Granstam SO, Granstam E, Fellström B & Lind L (1998). Effects of endothelin receptor type A antagonism and nitric oxide synthase inhibition on cerebral blood flow in hypertensive rats. *Acta Physiol Scand* **164,** 213–218.

Grassi G (1998). Role of the sympathetic nervous system in human hypertension. *J Hypertens* **16,** 1979–1987.

Grolla AA, Sim JA, Lim D, Rodriguez JJ, Genazzani AA & Verkhratsky A (2013). Amyloid-β and Alzheimer's disease type pathology differentially affects the calcium signalling toolkit in astrocytes from different brain regions. *Cell Death Dis* **4,** e623.

Gryglewski RJ, Palmer RM & Moncada S (1986). Superoxide anion is involved in the breakdown of endothelium-derived vascular relaxing factor. *Nature* **320,** 454–456.

Guyenet PG (2006). The sympathetic control of blood pressure. *Nat Rev Neurosci* **7,** 335–346.

Guyenet PG & Brown DL (1986). Nucleus paragigantocellularis lateralis and lumbar sympathetic discharge in the rat. *Am J Physiol* **250,** R1081-1094.

Guyenet PG, Koshiya N, Huangfu D, Verberne AJ & Riley TA (1993). Central respiratory control of A5 and A6 pontine noradrenergic neurons. *Am J Physiol* **264,** R1035-1044.

Guzik TJ, Hoch NE, Brown KA, McCann LA, Rahman A, Dikalov S, Goronzy J, Weyand C & Harrison DG (2007). Role of the T cell in the genesis of angiotensin II induced hypertension and vascular dysfunction. *J Exp Med* **204,** 2449–2460.

Haas LT, Kostylev MA & Strittmatter SM (2014). Therapeutic molecules and endogenous ligands regulate the interaction between brain cellular prion protein (PrPC) and metabotropic glutamate receptor 5 (mGluR5). *J Biol Chem* **289,** 28460–28477.

Hamann A & Syrbe U (2000). T-cell trafficking into sites of inflammation. *Rheumatol Oxf Engl* **39,** 696–699.

Hanamori T & Smith DV (1989). Gustatory innervation in the rabbit: central distribution of sensory and motor components of the chorda tympani, glossopharyngeal, and superior laryngeal nerves. *J Comp Neurol* **282,** 1–14.

Harden TK, Waldo GL, Hicks SN & Sondek J (2011). Mechanism of Activation and Inactivation of Gq/Phospholipase C-β Signaling Nodes. *Chem Rev* **111,** 6120–6129.

Harris TJ, Waltman TJ, Carter SM & Maisel AS (1995). Effect of prolonged catecholamine infusion on immunoregulatory function: implications in congestive heart failure. *J Am Coll Cardiol* **26,** 102–109.

Harrison DG, Guzik TJ, Lob HE, Madhur MS, Marvar PJ, Thabet SR, Vinh A & Weyand CM (2011). Inflammation, immunity, and hypertension. *Hypertens Dallas Tex 1979* **57,** 132–140.

Hart EC, Joyner MJ, Wallin BG & Charkoudian N (2012). Sex, ageing and resting blood pressure: gaining insights from the integrated balance of neural and haemodynamic factors. *J Physiol* **590,** 2069–2079.

Hay M, McKenzie H, Lindsley K, Dietz N, Bradley SR, Conn PJ & Hasser EM (1999). Heterogeneity of metabotropic glutamate receptors in autonomic cell groups of the medulla oblongata of the rat. *J Comp Neurol* **403,** 486–501.

Hayward LF (2007). Midbrain modulation of the cardiac baroreflex involves excitation of lateral parabrachial neurons in the rat. *Brain Res* **1145,** 117–127.

Head BP & Insel PA (2007). Do caveolins regulate cells by actions outside of caveolae? *Trends Cell Biol* **17,** 51–57.

Helmke BP, Bremner SN, Zweifach BW, Skalak R & Schmid-Schönbein GW (1997). Mechanisms for increased blood flow resistance due to leukocytes. *Am J Physiol* **273,** H2884-2890.

Helmke BP, Sugihara-Seki M, Skalak R & Schmid-Schönbein GW (1998). A mechanism for erythrocyte-mediated elevation of apparent viscosity by leukocytes in vivo without adhesion to the endothelium. *Biorheology* **35,** 437–448.

Helwig BG, Craig RA, Fels RJ, Blecha F & Kenney MJ (2008). Central nervous system administration of interleukin-6 produces splenic sympathoexcitation. *Auton Neurosci Basic Clin* **141,** 104–111.

Hermans E & Challiss RA (2001). Structural, signalling and regulatory properties of the group I metabotropic glutamate receptors: prototypic family C G-protein-coupled receptors. *Biochem J* **359,** 465–484.

Herrera J, Ferrebuz A, MacGregor EG & Rodriguez-Iturbe B (2006). Mycophenolate mofetil treatment improves hypertension in patients with psoriasis and rheumatoid arthritis. *J Am Soc Nephrol JASN* **17,** S218-225.

Hieshima K, Imai T, Baba M, Shoudai K, Ishizuka K, Nakagawa T, Tsuruta J, Takeya M, Sakaki Y, Takatsuki K, Miura R, Opdenakker G, Damme JV, Yoshie O & Nomiyama H (1997). A novel human CC chemokine PARC that is most homologous to macrophage-inflammatory protein-1 alpha/LD78 alpha and chemotactic for T lymphocytes, but not for monocytes. *J Immunol* **159,** 1140–1149.

Hilaire G, Viemari J-C, Coulon P, Simonneau M & Bévengut M (2004). Modulation of the respiratory rhythm generator by the pontine noradrenergic A5 and A6 groups in rodents. *Respir Physiol Neurobiol* **143,** 187–197.

Hoch NE, Guzik TJ, Chen W, Deans T, Maalouf SA, Gratze P, Weyand C & Harrison DG (2009). Regulation of T-cell function by endogenously produced angiotensin II. *Am J Physiol Regul Integr Comp Physiol* **296,** R208-216.

Holbein W, Bardgett M, Andrade MA, Herrera-Rosales M, Calderon AS & Toney GM (2012). Role of group 1 metabotropic glutamate receptors (mGluR) in the hypothalamic paraventricular nucleus (PVN) in sympathetic and blood pressure control during water deprivation. *FASEB J* **26,** 893.3-893.3.

ter Horst GJ, Luiten PG & Kuipers F (1984). Descending pathways from hypothalamus to dorsal motor vagus and ambiguus nuclei in the rat. *J Auton Nerv Syst* **11,** 59–75.

Huber JD, Egleton RD & Davis TP (2001). Molecular physiology and pathophysiology of tight junctions in the blood-brain barrier. *Trends Neurosci* **24,** 719–725.

Hussein RRS, Soliman RH, Abdelhaleem Ali AM, Tawfeik MH & Abdelrahim MEA (2013). Effect of antiepileptic drugs on liver enzymes. *Beni-Suef Univ J Basic Appl Sci* **2,** 14–19.

Huston JM, Ochani M, Rosas-Ballina M, Liao H, Ochani K, Pavlov VA, Gallowitsch-Puerta M, Ashok M, Czura CJ, Foxwell B, Tracey KJ & Ulloa L (2006). Splenectomy inactivates the cholinergic antiinflammatory pathway during lethal endotoxemia and polymicrobial sepsis. *J Exp Med* **203,** 1623–1628.

Inui K, Murase S & Nosaka S (1994). Facilitation of the arterial baroreflex by the ventrolateral part of the midbrain periaqueductal grey matter in rats. *J Physiol* **477,** 89–101.

Jackson SH, Devadas S, Kwon J, Pinto LA & Williams MS (2004). T cells express a phagocyte-type NADPH oxidase that is activated after T cell receptor stimulation. *Nat Immunol* **5,** 818–827.

Jankowski V, Vanholder R, van der Giet M, Henning L, Tölle M, Schönfelder G, Krakow A, Karadogan S, Gustavsson N, Gobom J, Webb J, Lehrach H, Giebing G, Schlüter H, Hilgers KF, Zidek W & Jankowski J (2005). Detection of angiotensin II in supernatants of stimulated mononuclear leukocytes by matrix-assisted laser desorption ionization time-of-flight/time-of-flight mass analysis. *Hypertens Dallas Tex 1979* **46,** 591–597.

Ji H, Zheng W, Li X, Liu J, Wu X, Zhang MA, Umans JG, Hay M, Speth RC, Dunn SE & Sandberg K (2014). Sex-specific T-cell regulation of angiotensin II-dependent hypertension. *Hypertens Dallas Tex 1979* **64,** 573–582.

Jones JF (2001). Vagal control of the rat heart. *Exp Physiol* **86,** 797–801.

Jones JF, Wang Y & Jordan D (1998). Activity of C fibre cardiac vagal efferents in anaesthetized cats and rats. *J Physiol* **507 (Pt 3),** 869–880.

Jr CAJ, Travers P, Walport M, Shlomchik MJ, Jr CAJ, Travers P, Walport M & Shlomchik MJ (2001). *Immunobiology*, 5th edn. Garland Science.

Judy WV, Watanabe AM, Henry DP, Besch HR, Murphy WR & Hockel GM (1976). Sympathetic nerve activity: role in regulation of blood pressure in the spontaenously hypertensive rat. *Circ Res* **38,** 21–29.

Kammermeier PJ & Worley PF (2007). Homer 1a uncouples metabotropic glutamate receptor 5 from postsynaptic effectors. *Proc Natl Acad Sci* **104,** 6055–6060.

Kanbar R, Depuy SD, West GH, Stornetta RL & Guyenet PG (2011). Regulation of visceral sympathetic tone by A5 noradrenergic neurons in rodents. *J Physiol* **589,** 903–917.

Kang S, Lee S-P, Kim KE, Kim H-Z, Mémet S & Koh GY (2009). Toll-like receptor 4 in lymphatic endothelial cells contributes to LPS-induced lymphangiogenesis by chemotactic recruitment of macrophages. *Blood* **113,** 2605–2613.

Karemaker JM (1997). Heart rate variability: why do spectral analysis? *Heart* **77,** 99–101.

Kato A, Ozawa F, Saitoh Y, Fukazawa Y, Sugiyama H & Inokuchi K (1998). Novel members of the Vesl/Homer family of PDZ proteins that bind metabotropic glutamate receptors. *J Biol Chem* **273,** 23969–23975.

Kirabo A et al. (2014). DC isoketal-modified proteins activate T cells and promote hypertension. *J Clin Invest* **124,** 4642–4656.

Koeners MP, Lewis KE, Ford AP & Paton JF (2016). Hypertension: a problem of organ blood flow supply–demand mismatch. *Future Cardiol* **12,** 339–349.

Koh KK, Ahn JY, Han SH, Kim DS, Jin DK, Kim HS, Shin M-S, Ahn TH, Choi IS & Shin EK (2003). Pleiotropic effects of angiotensin II receptor blocker in hypertensive patients. *J Am Coll Cardiol* **42,** 905–910.

König R, Huang L-Y & Germain RN (1992). MHC class II interaction with CD4 mediated by a region analogous to the MHC class I binding site for CD8. *Nature* **356,** 796–798.

König R, Shen X & Germain RN (1995). Involvement of both major histocompatibility complex class II alpha and beta chains in CD4 function indicates a role for ordered oligomerization in T cell activation. *J Exp Med* **182,** 779–787.

Konior A, Schramm A, Czesnikiewicz-Guzik M & Guzik TJ (2014). NADPH oxidases in vascular pathology. *Antioxid Redox Signal* **20,** 2794–2814.

Koshiya N & Guyenet PG (1994). A5 noradrenergic neurons and the carotid sympathetic chemoreflex. *Am J Physiol* **267,** R519-526.

Krupnick JG & Benovic JL (1998). The role of receptor kinases and arrestins in G protein-coupled receptor regulation. *Annu Rev Pharmacol Toxicol* **38,** 289–319.

Kubo T & Kihara M (1987). Studies on GABAergic mechanisms responsible for cardiovascular regulation in the rostral ventrolateral medulla of the rat. *Arch Int Pharmacodyn Ther* **285,** 277–287.

Kuwabara T, Ishikawa F, Kondo M & Kakiuchi T (2017). The Role of IL-17 and Related Cytokines in Inflammatory Autoimmune Diseases. *Mediators Inflamm* **2017,** 3908061.

Landmesser U, Cai H, Dikalov S, McCann L, Hwang J, Jo H, Holland SM & Harrison DG (2002). Role of p47(phox) in vascular oxidative stress and hypertension caused by angiotensin II. *Hypertens Dallas Tex 1979* **40,** 511–515.

Leaders FE & Dayrit C (1965). THE CHOLINERGIC COMPONENT IN THE SYMPATHETIC INNERVATION TO THE SPLEEN. *J Pharmacol Exp Ther* **147,** 145–152.

Lewis DI & Coote JH (1995). Chemical mediators of spinal inhibition of rat sympathetic neurones on stimulation in the nucleus tractus solitarii. *J Physiol* **486 (Pt 2),** 483–494.

Li D-P & Pan H-L (2007). Glutamatergic inputs in the hypothalamic paraventricular nucleus maintain sympathetic vasomotor tone in hypertension. *Hypertens Dallas Tex 1979* **49,** 916–925.

Li D-P & Pan H-L (2010). Increased group I metabotropic glutamate receptor activity in paraventricular nucleus supports elevated sympathetic vasomotor tone in hypertension. *Am J Physiol Regul Integr Comp Physiol* **299,** R552-561.

Li D-P, Zhu L-H, Pachuau J, Lee H-A & Pan H-L (2014). mGluR5 Upregulation Increases Excitability of Hypothalamic Presympathetic Neurons through NMDA Receptor Trafficking in Spontaneously Hypertensive Rats. *J Neurosci* **34,** 4309–4317.

Lindsey WB, Lowdell MW, Marti GE, Abbasi F, Zenger V, King KM & Lamb LS (2007). CD69 expression as an index of T-cell function: assay standardization, validation and use in monitoring immune recovery. *Cytotherapy* **9,** 123–132.

Lipski J, Kanjhan R, Kruszewska B & Rong WF (1995). Criteria for intracellular identification of pre-sympathetic neurons in the rostral ventrolateral medulla in the rat. *Clin Exp Hypertens N Y N 1993* **17,** 51–65.

Llewellyn-Smith IJ & Anthony Verberne (2011). *Central Regulation of Autonomic Functions, Second Edition*. Oxford University Press.

Lloyd CM & Hessel EM (2010). Functions of T cells in asthma: more than just TH2 cells. *Nat Rev Immunol* **10,** 838–848.

Lob HE, Marvar PJ, Guzik TJ, Sharma S, McCann LA, Weyand C, Gordon FJ & Harrison DG (2010). Induction of hypertension and peripheral inflammation by reduction of extracellular superoxide dismutase in the central nervous system. *Hypertens Dallas Tex 1979* **55,** 277–283, 6p following 283.

Lob HE, Schultz D, Marvar PJ, Davisson RL & Harrison DG (2013). Role of the NADPH oxidases in the subfornical organ in angiotensin II-induced hypertension. *Hypertens Dallas Tex 1979* **61,** 382–387.

Loewy AD, Gregorie EM, McKellar S & Baker RP (1979*a*). Electrophysiological evidence that the A5 catecholamine cell group is a vasomotor center. *Brain Res* **178,** 196–200.

Loewy AD, McKellar S & Saper CB (1979*b*). Direct projections from the A5 catecholamine cell group to the intermediolateral cell column. *Brain Res* **174,** 309–314.

Löscher W & Potschka H (2005). Blood-Brain Barrier Active Efflux Transporters: ATP-Binding Cassette Gene Family. *NeuroRx* **2,** 86–98.

Lovick TA (1992). Midbrain influences on ventrolateral medullo-spinal neurones in the rat. *Exp Brain Res* **90,** 147–152.

Loweth JA, Scheyer AF, Milovanovic M, LaCrosse AL, Flores-Barrera E, Werner CT, Li X, Ford KA, Le T, Olive MF, Szumlinski KK, Tseng KY & Wolf ME (2014). Synaptic depression via mGluR1 positive allosteric modulation suppresses cue-induced cocaine craving. *Nat Neurosci* **17,** 73–80.

van Maanen MA, Stoof SP, Larosa GJ, Vervoordeldonk MJ & Tak PP (2010). Role of the cholinergic nervous system in rheumatoid arthritis: aggravation of arthritis in nicotinic acetylcholine receptor α7 subunit gene knockout mice. *Ann Rheum Dis* **69,** 1717–1723.

Machura E, Mazur B, Pieniazek W & Karczewska K (2008). Expression of naive/memory (CD45RA/CD45RO) markers by peripheral blood CD4+ and CD8 + T cells in children with asthma. *Arch Immunol Ther Exp (Warsz)* **56,** 55–62.

MacNeil BJ, Jansen AH, Janz LJ, Greenberg AH & Nance DM (1997). Peripheral endotoxin increases splenic sympathetic nerve activity via central prostaglandin synthesis. *Am J Physiol* **273,** R609-614.

Madhur MS, Lob HE, McCann LA, Iwakura Y, Blinder Y, Guzik TJ & Harrison DG (2010). Interleukin 17 promotes angiotensin II-induced hypertension and vascular dysfunction. *Hypertens Dallas Tex 1979* **55,** 500–507.

Maiorov DN, Malpas SC & Head GA (2000). Influence of pontine A5 region on renal sympathetic nerve activity in conscious rabbits. *Am J Physiol Regul Integr Comp Physiol* **278,** R311-319.

Maiorov DN, Wilton ER, Badoer E, Petrie D, Head GA & Malpas SC (1999). Sympathetic response to stimulation of the pontine A5 region in conscious rabbits. *Brain Res* **815,** 227–236.

Mancia G, Grassi G, Giannattasio C & Seravalle G (1999). Sympathetic activation in the pathogenesis of hypertension and progression of organ damage. *Hypertens Dallas Tex 1979* **34,** 724–728.

Martin DS & Haywood JR (1992). Sympathetic nervous system activation by glutamate injections into the paraventricular nucleus. *Brain Res* **577,** 261–267.

Marvar P, Cruise T, Hart E, Burchell A, Ratcliffe L, Nightingale A & Paton J (2014). Increased memory and decreased naïve T cells in human hypertension (1074.9). *FASEB J* **28,** 1074.9.

Marvar PJ, Hendy EB, Cruise TD, Walas D, DeCicco D, Vadigepalli R, Schwaber JS, Waki H, Murphy D & Paton JFR (2016). Systemic leukotriene B4 receptor antagonism lowers arterial blood pressure and improves autonomic function in the spontaneously hypertensive rat. *J Physiol* **594,** 5975–5989.

Marvar PJ, Thabet SR, Guzik TJ, Lob HE, McCann LA, Weyand C, Gordon FJ & Harrison DG (2010). Central and peripheral mechanisms of T-lymphocyte activation and vascular inflammation produced by angiotensin II-induced hypertension. *Circ Res* **107,** 263–270.

Marvar PJ, Vinh A, Thabet S, Lob HE, Geem D, Ressler KJ & Harrison DG (2012). T lymphocytes and vascular inflammation contribute to stress-dependent hypertension. *Biol Psychiatry* **71,** 774–782.

Masuda N, Ootsuka Y & Terui N (1992). Neurons in the caudal ventrolateral medulla mediate the somato-sympathetic inhibitory reflex response via GABA receptors in the rostral ventrolateral medulla. *J Auton Nerv Syst* **40,** 91–98.

Mathiesen JM, Svendsen N, Bräuner-Osborne H, Thomsen C & Ramirez MT (2003). Positive allosteric modulation of the human metabotropic glutamate receptor 4 (hmGluR4) by SIB-1893 and MPEP. *Br J Pharmacol* **138,** 1026–1030.

Matsuno K, Yamada H, Iwata K, Jin D, Katsuyama M, Matsuki M, Takai S, Yamanishi K, Miyazaki M, Matsubara H & Yabe-Nishimura C (2005). Nox1 is involved in angiotensin II-mediated hypertension: a study in Nox1-deficient mice. *Circulation* **112,** 2677–2685.

McAllen RM & Spyer KM (1978). The baroreceptor input to cardiac vagal motoneurones. *J Physiol* **282,** 365–374.

Merai R, Siegel C, Rakotz M, Basch P, Wright J, Wong B, DHSc & Thorpe P (2016). CDC Grand Rounds: A Public Health Approach to Detect and Control Hypertension. *MMWR Morb Mortal Wkly Rep* **65,** 1261–1264.

Mestas J & Hughes CCW (2004). Of Mice and Not Men: Differences between Mouse and Human Immunology. *J Immunol* **172,** 2731–2738.

Milner TA, Morrison SF, Abate C & Reis DJ (1988). Phenylethanolamine N-methyltransferase-containing terminals synapse directly on sympathetic preganglionic neurons in the rat. *Brain Res* **448,** 205–222.

Minagawa M, Narita J, Tada T, Maruyama S, Shimizu T, Bannai M, Oya H, Hatakeyama K & Abo T (1999). Mechanisms underlying immunologic states during pregnancy: possible association of the sympathetic nervous system. *Cell Immunol* **196,** 1–13.

Minakami R, Katsuki F & Sugiyama H (1993). A variant of metabotropic glutamate receptor subtype 5: an evolutionally conserved insertion with no termination codon. *Biochem Biophys Res Commun* **194,** 622–627.

Minson JB, Llewellyn-Smith IJ, Chalmers JP, Pilowsky PM & Arnolda LF (1997). c-fos identifies GABA-synthesizing barosensitive neurons in caudal ventrolateral medulla. *Neuroreport* **8,** 3015–3021.

Moore CAC, Milano SK & Benovic JL (2007). Regulation of receptor trafficking by GRKs and arrestins. *Annu Rev Physiol* **69,** 451–482.

Morishita R, Gibbons GH, Ellison KE, Lee W, Zhang L, Yu H, Kaneda Y, Ogihara T & Dzau VJ (1994). Evidence for direct local effect of angiotensin in vascular hypertrophy. In vivo gene transfer of angiotensin converting enzyme. *J Clin Invest* **94,** 978–984.

Morrison SF, Milner TA & Reis DJ (1988). Reticulospinal vasomotor neurons of the rat rostral ventrolateral medulla: relationship to sympathetic nerve activity and the C1 adrenergic cell group. *J Neurosci Off J Soc Neurosci* **8,** 1286–1301.

Movsesyan VA, O'Leary DM, Fan L, Bao W, Mullins PG, Knoblach SM & Faden AI (2001). mGluR5 antagonists 2-methyl-6-(phenylethynyl)-pyridine and (E)-2-methyl-6-(2-phenylethenyl)-pyridine reduce traumatic neuronal injury in vitro and in vivo by antagonizing N-methyl-D-aspartate receptors. *J Pharmacol Exp Ther* **296,** 41–47.

Muller DN, Shagdarsuren E, Park J-K, Dechend R, Mervaala E, Hampich F, Fiebeler A, Ju X, Finckenberg P, Theuer J, Viedt C, Kreuzer J, Heidecke H, Haller H, Zenke M & Luft FC (2002). Immunosuppressive treatment protects against angiotensin II-induced renal damage. *Am J Pathol* **161,** 1679–1693.

Nance DM & Sanders VM (2007). Autonomic innervation and regulation of the immune system (1987-2007). *Brain Behav Immun* **21,** 736–745.

Naraghi R, Gaab MR, Walter GF & Kleineberg B (1992). Arterial hypertension and neurovascular compression at the ventrolateral medulla. *J Neurosurg* **77,** 103–112.

Nataraj C, Oliverio MI, Mannon RB, Mannon PJ, Audoly LP, Amuchastegui CS, Ruiz P, Smithies O & Coffman TM (1999). Angiotensin II regulates cellular immune responses through a calcineurin-dependent pathway. *J Clin Invest* **104,** 1693–1701.

Natarajan M & Morrison SF (1999). Adrenal epinephrine secretion is not regulated by sympathoinhibitory neurons in the caudal ventrolateral medulla. *Brain Res* **827,** 169–175.

Neil JJ & Loewy AD (1982). Decreases in blood pressure in response to L-glutamate microinjections into the A5 catecholamine cell group. *Brain Res* **241,** 271–278.

Netzer F, Bernard J-F, Verberne AJM, Hamon M, Camus F, Benoliel J-J & Sévoz-Couche C (2011). Brain circuits mediating baroreflex bradycardia inhibition in rats: an anatomical and functional link between the cuneiform nucleus and the periaqueductal grey. *J Physiol* **589,** 2079–2091.

Nguyen H, Chiasson VL, Chatterjee P, Kopriva SE, Young KJ & Mitchell BM (2013). Interleukin-17 causes Rho-kinase-mediated endothelial dysfunction and hypertension. *Cardiovasc Res* **97,** 696–704.

Niijima A (1995). An electrophysiological study on the vagal innervation of the thymus in the rat. *Brain Res Bull* **38,** 319–323.

Niijima A (1996). The afferent discharges from sensors for interleukin 1 beta in the hepatoportal system in the anesthetized rat. *J Auton Nerv Syst* **61,** 287–291.

Niijima A, Hori T, Aou S & Oomura Y (1991). The effects of interleukin-1 beta on the activity of adrenal, splenic and renal sympathetic nerves in the rat. *J Auton Nerv Syst* **36,** 183–192.

Nijhawan R, Wierzbicki AS, Tozer R, Lascelles PT & Patsalos PN (1990). Antiepileptic drugs, hepatic enzyme induction and raised serum alkaline phosphatase isoenzymes. *Int J Clin Pharmacol Res* **10,** 319–323.

Niswender CM & Conn PJ (2010). Metabotropic glutamate receptors: physiology, pharmacology, and disease. *Annu Rev Pharmacol Toxicol* **50,** 295–322.

Nomura S & Mizuno N (1981). Central distribution of afferent and efferent components of the chorda tympani in the cat as revealed by the horseradish peroxidase method. *Brain Res* **214,** 229–237.

Norgren R (2011). Central Neural Mechanisms of Taste. In *Comprehensive Physiology*. John Wiley & Sons, Inc. Available at: http://onlinelibrary.wiley.com/doi/10.1002/cphy.cp010324/abstract [Accessed December 15, 2017].

Notley CA, Inglis JJ, Alzabin S, McCann FE, McNamee KE & Williams RO (2008). Blockade of tumor necrosis factor in collagen-induced arthritis reveals a novel immunoregulatory pathway for Th1 and Th17 cells. *J Exp Med* **205,** 2491–2497.

O'Leary DM, Movsesyan V, Vicini S & Faden AI (2000). Selective mGluR5 antagonists MPEP and SIB-1893 decrease NMDA or glutamate-mediated neuronal toxicity through actions that reflect NMDA receptor antagonism. *Br J Pharmacol* **131,** 1429–1437.

Oseka M & Koźniewska E (1997). Dependence of basal cerebral blood flow and cerebral vascular resistance in spontaneously hypertensive rats upon vasoconstrictor prostanoids. *Acta Neurochir Suppl* **70,** 228–230.

Page ST, Plymate SR, Bremner WJ, Matsumoto AM, Hess DL, Lin DW, Amory JK, Nelson PS & Wu JD (2006). Effect of medical castration on CD4+ CD25+ T cells, CD8+ T cell IFN-gamma expression, and NK cells: a physiological role for testosterone and/or its metabolites. *Am J Physiol Endocrinol Metab* **290,** E856-863.

Palazzo E, Luongo L, Bellini G, Guida F, Marabese I, Boccella S, Rossi F, Maione S & de Novellis V (2012). Changes in cannabinoid receptor subtype 1 activity and interaction with metabotropic glutamate subtype 5 receptors in the periaqueductal gray-rostral ventromedial medulla pathway in a rodent neuropathic pain model. *CNS Neurol Disord Drug Targets* **11,** 148–161.

Paxinos G & Watson C (2007). *The Rat Brain in Stereotaxic Coordinates*, 6th edn. Academic Press.

Pelosi GG, Resstel LBM & Corrêa FMA (2007). Dorsal periaqueductal gray area synapses modulate baroreflex in unanesthetized rats. *Auton Neurosci Basic Clin* **131,** 70–76.

Persell SD (2011). Prevalence of resistant hypertension in the United States, 2003-2008. *Hypertens Dallas Tex 1979* **57,** 1076–1080.

Pijacka W, Katayama PL, Salgado HC, Lincevicius GS, Campos RR, McBryde FD & Paton JFR (2018). Variable role of carotid bodies in cardiovascular responses to exercise, hypoxia and hypercapnia in spontaneously hypertensive rats. *J Physiol* **596,** 3201–3216.

Pober JS, Kluger MS & Schechner JS (2001). Human endothelial cell presentation of antigen and the homing of memory/effector T cells to skin. *Ann N Y Acad Sci* **941,** 12–25.

Pollow DP, Uhrlaub J, Romero-Aleshire MJ, Sandberg K, Nikolich-Zugich J, Brooks HL & Hay M (2014). Sex Differences in T-Lymphocyte Tissue Infiltration and Development of Angiotensin II HypertensionNovelty and Significance. *Hypertension* **64,** 384–390.

Purves D, Augustine GJ, Fitzpatrick D, Katz LC, LaMantia A-S, McNamara JO & Williams SM (2001). Autonomic Regulation of Sexual Function. *Neurosci 2nd Ed*. Available at: https://www.ncbi.nlm.nih.gov/books/NBK11157/ [Accessed October 16, 2018].

Raaz U, Toh R, Maegdefessel L, Adam M, Nakagami F, Emrich FC, Spin JM & Tsao PS (2014). Hemodynamic regulation of reactive oxygen species: implications for vascular diseases. *Antioxid Redox Signal* **20,** 914–928.

Rashida Gnanaprakasam JN, Wu R & Wang R (2018). Metabolic Reprogramming in Modulating T Cell Reactive Oxygen Species Generation and Antioxidant Capacity. *Front Immunol*; DOI: 10.3389/fimmu.2018.01075.

Razani B, Woodman SE & Lisanti MP (2002). Caveolae: from cell biology to animal physiology. *Pharmacol Rev* **54,** 431–467.

Rodríguez-Iturbe B, Quiroz Y, Herrera-Acosta J, Johnson RJ & Pons HA (2002). The role of immune cells infiltrating the kidney in the pathogenesis of salt-sensitive hypertension. *J Hypertens Suppl Off J Int Soc Hypertens* **20,** S9-14.

Roloff EVL, Walas D, Moraes DJA, Kasparov S & Paton JFR (2018). Differences in autonomic innervation to the vertebrobasilar arteries in spontaneously hypertensive and Wistar rats. *J Physiol* **596,** 3505–3529.

Romano C, van den Pol AN & O'Malley KL (1996). Enhanced early developmental expression of the metabotropic glutamate receptor mGluR5 in rat brain: protein, mRNA splice variants, and regional distribution. *J Comp Neurol* **367,** 403–412.

Rosas-Ballina M, Olofsson PS, Ochani M, Valdés-Ferrer SI, Levine YA, Reardon C, Tusche MW, Pavlov VA, Andersson U, Chavan S, Mak TW & Tracey KJ (2011). Acetylcholine-synthesizing T cells relay neural signals in a vagus nerve circuit. *Science* **334,** 98–101.

Rosin DL, Chang DA & Guyenet PG (2006). Afferent and efferent connections of the rat retrotrapezoid nucleus. *J Comp Neurol* **499,** 64–89.

Ross CA, Ruggiero DA, Joh TH, Park DH & Reis DJ (1984). Rostral ventrolateral medulla: selective projections to the thoracic autonomic cell column from the region containing C1 adrenaline neurons. *J Comp Neurol* **228,** 168–185.

Roychowdhury S, McMullen MR, Pritchard MT, Li W, Salomon RG & Nagy LE (2009). Formation of gamma-ketoaldehyde-protein adducts during ethanol-induced liver injury in mice. *Free Radic Biol Med* **47,** 1526–1538.

Rudd CE, Trevillyan JM, Dasgupta JD, Wong LL & Schlossman SF (1988). The CD4 receptor is complexed in detergent lysates to a protein-tyrosine kinase (pp58) from human T lymphocytes. *Proc Natl Acad Sci* **85,** 5190–5194.

Salomon RG, Kaur K & Batyreva E (2000). Isolevuglandin-protein adducts in oxidized low density lipoprotein and human plasma: a strong connection with cardiovascular disease. *Trends Cardiovasc Med* **10,** 53–59.

Sandberg K & Ji H (2012). Sex differences in primary hypertension. *Biol Sex Differ* **3,** 7.

Sanders VM & Straub RH (2002). Norepinephrine, the beta-adrenergic receptor, and immunity. *Brain Behav Immun* **16,** 290–332.

Sanz-Rosa D, Oubiña MP, Cediel E, de Las Heras N, Vegazo O, Jiménez J, Lahera V & Cachofeiro V (2005). Effect of AT1 receptor antagonism on vascular and circulating inflammatory mediators in SHR: role of NF-kappaB/IkappaB system. *Am J Physiol Heart Circ Physiol* **288,** H111-115.

Saper CB, Romanovsky AA & Scammell TE (2012). Neural circuitry engaged by prostaglandins during the sickness syndrome. *Nat Neurosci* **15,** 1088–1095.

Sato T & Ishii H (2017). Regulation of hemodynamics in major salivary glands by parasympathetic vasodilation. *J Oral Biosci* **59,** 80–86.

Schenberg LC, Brandão CA & Vasquez EC (1995). Role of periaqueductal gray matter in hypertension in spontaneously hypertensive rats. *Hypertens Dallas Tex 1979* **26,** 1125–1128.

Schinkel AH & Jonker JW (2003). Mammalian drug efflux transporters of the ATP binding cassette (ABC) family: an overview. *Adv Drug Deliv Rev* **55,** 3–29.

Schreihofer AM & Guyenet PG (1997). Identification of C1 presympathetic neurons in rat rostral ventrolateral medulla by juxtacellular labeling in vivo. *J Comp Neurol* **387,** 524–536.

Schreihofer AM, Stornetta RL & Guyenet PG (2000). Regulation of sympathetic tone and arterial pressure by rostral ventrolateral medulla after depletion of C1 cells in rat. *J Physiol* **529 Pt 1,** 221–236.

Schroder K, Hertzog PJ, Ravasi T & Hume DA (2004). Interferon-γ: an overview of signals, mechanisms and functions. *J Leukoc Biol* **75,** 163–189.

Seaberg EC, Muñoz A, Lu M, Detels R, Margolick JB, Riddler SA, Williams CM, Phair JP & Multicenter AIDS Cohort Study (2005). Association between highly active antiretroviral therapy and hypertension in a large cohort of men followed from 1984 to 2003. *AIDS Lond Engl* **19,** 953–960.

Seagard JL, van Brederode JF, Dean C, Hopp FA, Gallenberg LA & Kampine JP (1990). Firing characteristics of single-fiber carotid sinus baroreceptors. *Circ Res* **66,** 1499–1509.

Shi L, Palacio-Mancheno P, Badami J, Shin DW, Zeng M, Cardoso L, Tu R & Fu BM (2014). Quantification of transient increase of the blood–brain barrier

permeability to macromolecules by optimized focused ultrasound combined with microbubbles. *Int J Nanomedicine* **9,** 4437–4448.

Sneath RJ & Mangham DC (1998). The normal structure and function of CD44 and its role in neoplasia. *Mol Pathol* **51,** 191–200.

Soloviev MM, Ciruela F, Chan WY & McIlhinney RA (2000). Molecular characterisation of two structurally distinct groups of human homers, generated by extensive alternative splicing. *J Mol Biol* **295,** 1185–1200.

Spyer KM (1994). Annual review prize lecture. Central nervous mechanisms contributing to cardiovascular control. *J Physiol* **474,** 1–19.

Sriramula S, Cardinale JP & Francis J (2013). Inhibition of TNF in the Brain Reverses Alterations in RAS Components and Attenuates Angiotensin II-Induced Hypertension. *PLOS ONE* **8,** e63847.

Staessen J, Bulpitt CJ, Fagard R, Lijnen P & Amery A (1989). The influence of menopause on blood pressure. *J Hum Hypertens* **3,** 427–433.

Standish A, Enquist LW, Miselis RR & Schwaber JS (1995). Dendritic morphology of cardiac related medullary neurons defined by circuit-specific infection by a recombinant pseudorabies virus expressing beta-galactosidase. *J Neurovirol* **1,** 359–368.

Stanek KA, Neil JJ, Sawyer WB & Loewy AD (1984). Changes in regional blood flow and cardiac output after L-glutamate stimulation of A5 cell group. *Am J Physiol* **246,** H44-51.

Steinman L (2004). Elaborate interactions between the immune and nervous systems. *Nat Immunol* **5,** 575–581.

Stumpf C, Auer C, Yilmaz A, Lewczuk P, Klinghammer L, Schneider M, Daniel WG, Schmieder RE & Garlichs CD (2011). Serum levels of the Th1 chemoattractant interferon-gamma-inducible protein (IP) 10 are elevated in patients with essential hypertension. *Hypertens Res Off J Jpn Soc Hypertens* **34,** 484–488.

Subramanian V (1995). The Rat Nervous System, 2nd ed., edited by George Paxinos. Academic Press, San Diego, 1994, ISBN 0-12-54763-3 (case), 1,136 pp., $169.00. *J Neurochem* **65,** 471–471.

Sun MK & Guyenet PG (1985). GABA-mediated baroreceptor inhibition of reticulospinal neurons. *Am J Physiol* **249,** R672-680.

Sun W & Panneton WM (2005). Defining projections from the caudal pressor area of the caudal ventrolateral medulla. *J Comp Neurol* **482,** 273–293.

Suzuki H, Zweifach BW & Schmid-Schönbein GW (1995). Dependence of elevated mesenteric arteriolar tone on glucocorticoids in spontaneously hypertensive rats. *Int J Microcirc Clin Exp* **15,** 309–315.

Suzuki H, Zweifach BW & Schmid-Schönbein GW (1996). Glucocorticoid modulates vasodilator response of mesenteric arterioles in spontaneously hypertensive rats. *Hypertens Dallas Tex 1979* **27,** 114–118.

Swanson MA, Lee WT & Sanders VM (2001). IFN-gamma production by Th1 cells generated from naive CD4+ T cells exposed to norepinephrine. *J Immunol Baltim Md 1950* **166,** 232–240.

Syrovatkina V, Alegre KO, Dey R & Huang X-Y (2016). Regulation, Signaling, and Physiological Functions of G-Proteins. *J Mol Biol* **428,** 3850–3868.

Tai P, Wang J, Jin H, Song X, Yan J, Kang Y, Zhao L, An X, Du X, Chen X, Wang S, Xia G & Wang B (2008). Induction of regulatory T cells by physiological level estrogen. *J Cell Physiol* **214,** 456–464.

Takagishi M, Waki H, Bhuiyan MER, Gouraud SS, Kohsaka A, Cui H, Yamazaki T, Paton JFR & Maeda M (2010). IL-6 microinjected in the nucleus tractus solitarii attenuates cardiac baroreceptor reflex function in rats. *Am J Physiol Regul Integr Comp Physiol* **298,** R183-190.

Takeda K, Nakata T, Takesako T, Itoh H, Hirata M, Kawasaki S, Hayashi J, Oguro M, Sasaki S & Nakagawa M (1991). Sympathetic inhibition and attenuation of spontaneous hypertension by PVN lesions in rats. *Brain Res* **543,** 296–300.

Tavares L, Lima D & Coimbra A (1997). The Pontine A5 Noradrenergic Cells which Project to the Spinal Cord Dorsal Horn are Reciprocally Connected with the Caudal Ventrolateral Medulla in the Rat. *Eur J Neurosci* **9,** 2452–2461.

Taxini CL, Takakura AC, Gargaglioni LH & Moreira TS (2011). Control of the central chemoreflex by A5 noradrenergic neurons in rats. *Neuroscience* **199,** 177–186.

Tian N, Gu J-W, Jordan S, Rose RA, Hughson MD & Manning RD (2007). Immune suppression prevents renal damage and dysfunction and reduces arterial pressure in salt-sensitive hypertension. *Am J Physiol Heart Circ Physiol* **292,** H1018-1025.

Tipton AJ, Baban B & Sullivan JC (2014). Female SHR Have a Compensatory Increase in Renal Regulatory T Cells in Response to Elevations in Blood Pressure. *Hypertension* **64,** 557–564.

Touyz RM, Alves-Lopes R, Rios FJ, Camargo LL, Anagnostopoulou A, Arner A & Montezano AC (2018). Vascular smooth muscle contraction in hypertension. *Cardiovasc Res* **114,** 529–539.

Tracey KJ (2002). The inflammatory reflex. *Nature* **420,** 853–859.

Trott DW & Harrison DG (2014). The immune system in hypertension. *Adv Physiol Educ* **38,** 20–24.

Tu JC, Xiao B, Yuan JP, Lanahan AA, Leoffert K, Li M, Linden DJ & Worley PF (1998). Homer binds a novel proline-rich motif and links group 1 metabotropic glutamate receptors with IP3 receptors. *Neuron* **21,** 717–726.

Turrin NP & Rivest S (2004). Unraveling the molecular details involved in the intimate link between the immune and neuroendocrine systems. *Exp Biol Med Maywood NJ* **229,** 996–1006.

Urban MO, Hama AT, Bradbury M, Anderson J, Varney MA & Bristow L (2003). Role of metabotropic glutamate receptor subtype 5 (mGluR5) in the maintenance of cold hypersensitivity following a peripheral mononeuropathy in the rat. *Neuropharmacology* **44,** 983–993.

Uschakov A, McGinty D, Szymusiak R & McKinley MJ (2009). Functional correlates of activity in neurons projecting from the lamina terminalis to the ventrolateral periaqueductal gray. *Eur J Neurosci* **30,** 2347–2355.

Utsuyama M & Hirokawa K (2002). Differential expression of various cytokine receptors in the brain after stimulation with LPS in young and old mice. *Exp Gerontol* **37,** 411–420.

Vara D & Pula G (2014). Reactive oxygen species: physiological roles in the regulation of vascular cells. *Curr Mol Med* **14,** 1103–1125.

Vazdarjanova A, McNaughton BL, Barnes CA, Worley PF & Guzowski JF (2002). Experience-dependent coincident expression of the effector immediate-early genes arc and Homer 1a in hippocampal and neocortical neuronal networks. *J Neurosci Off J Soc Neurosci* **22,** 10067–10071.

Viel EC, Lemarié CA, Benkirane K, Paradis P & Schiffrin EL (2010). Immune regulation and vascular inflammation in genetic hypertension. *Am J Physiol Heart Circ Physiol* **298,** H938-944.

Waki H, Gouraud SS, Maeda M & Paton JFR (2008). Specific inflammatory condition in nucleus tractus solitarii of the SHR: novel insight for neurogenic hypertension? *Auton Neurosci Basic Clin* **142,** 25–31.

Waki H, Liu B, Miyake M, Katahira K, Murphy D, Kasparov S & Paton JFR (2007). Junctional adhesion molecule-1 is upregulated in spontaneously hypertensive rats: evidence for a prohypertensive role within the brain stem. *Hypertens Dallas Tex 1979* **49,** 1321–1327.

Waldburger J-M & Firestein GS (2010). Regulation of Peripheral Inflammation by the Central Nervous System. *Curr Rheumatol Rep* **12,** 370–378.

Wang G, Zhou P, Repucci MA, Golanov EV & Reis DJ (2001). Specific actions of cyanide on membrane potential and voltage-gated ion currents in rostral ventrolateral medulla neurons in rat brainstem slices. *Neurosci Lett* **309,** 125–129.

Wang N, Orr-Urtreger A, Chapman J, Rabinowitz R & Korczyn AD (2003). Deficiency of nicotinic acetylcholine receptor beta 4 subunit causes autonomic cardiac and intestinal dysfunction. *Mol Pharmacol* **63,** 574–580.

Warnock RA, Askari S, Butcher EC & von Andrian UH (1998). Molecular mechanisms of lymphocyte homing to peripheral lymph nodes. *J Exp Med* **187,** 205–216.

Watkins LR, Goehler LE, Relton JK, Tartaglia N, Silbert L, Martin D & Maier SF (1995). Blockade of interleukin-1 induced hyperthermia by subdiaphragmatic vagotomy: evidence for vagal mediation of immune-brain communication. *Neurosci Lett* **183,** 27–31.

Weiss NS (1972). Premature menopause and aortoiliac occlusive disease. *J Chronic Dis* **25,** 133–138.

Wilcox CS (2005). Oxidative stress and nitric oxide deficiency in the kidney: a critical link to hypertension? *Am J Physiol Regul Integr Comp Physiol* **289,** R913-935.

Willette RN, Barcas PP, Krieger AJ & Sapru HN (1983). Vasopressor and depressor areas in the rat medulla. Identification by microinjection of L-glutamate. *Neuropharmacology* **22,** 1071–1079.

Willette RN, Barcas PP, Krieger AJ & Sapru HN (1984). Endogenous GABAergic mechanisms in the medulla and the regulation of blood pressure. *J Pharmacol Exp Ther* **230,** 34–39.

Witowski J, Książek K & Jörres A (2004). Interleukin-17: a mediator of inflammatory responses. *Cell Mol Life Sci CMLS* **61,** 567–579.

Xiao B, Tu JC, Petralia RS, Yuan JP, Doan A, Breder CD, Ruggiero A, Lanahan AA, Wenthold RJ & Worley PF (1998). Homer regulates the association of group 1 metabotropic glutamate receptors with multivalent complexes of homer-related, synaptic proteins. *Neuron* **21,** 707–716.

Xiao B, Tu JC & Worley PF (2000). Homer: a link between neural activity and glutamate receptor function. *Curr Opin Neurobiol* **10,** 370–374.

Xie F, Yi S, Hao L, Zhang Y & Zhong J (2015). Role of group I metabotropic glutamate receptors, mGluR1/mGluR5, in connexin43 phosphorylation and inhibition of gap junctional intercellular communication in H9c2 cardiomyoblast cells. *Mol Cell Biochem* **400,** 213–222.

Xu J, Antion MD, Nomura T, Kraniotis S, Zhu Y & Contractor A (2014). Hippocampal metaplasticity is required for the formation of temporal associative memories. *J Neurosci Off J Soc Neurosci* **34,** 16762–16773.

Yin S & Niswender CM (2014). Progress toward advanced understanding of metabotropic glutamate receptors: structure, signaling and therapeutic indications. *Cell Signal* **26,** 2284–2297.

Zahner MR & Pan H-L (2005). Role of paraventricular nucleus in the cardiogenic sympathetic reflex in rats. *Am J Physiol Regul Integr Comp Physiol* **288,** R420-426.

Zanella S, Roux JC, Viemari JC & Hilaire G (2006). Possible modulation of the mouse respiratory rhythm generator by A1/C1 neurones. *Respir Physiol Neurobiol* **153,** 126–138.

Zhang M, Mao Y, Ramirez SH, Tuma RF & Chabrashvili T (2010). Angiotensin II induced cerebral microvascular inflammation and increased blood-brain barrier permeability via oxidative stress. *Neuroscience* **171,** 852–858.

Zhang Z-H, Wei S-G, Francis J & Felder RB (2003). Cardiovascular and renal sympathetic activation by blood-borne TNF-alpha in rat: the role of central prostaglandins. *Am J Physiol Regul Integr Comp Physiol* **284,** R916-927.

Zheng SG (2013). Regulatory T cells vs Th17: differentiation of Th17 versus Treg, are the mutually exclusive? *Am J Clin Exp Immunol* **2,** 94–106.

Zhong X, Li H & Chang Q (2012). MeCP2 phosphorylation is required for modulating synaptic scaling through mGluR5. *J Neurosci Off J Soc Neurosci* **32,** 12841–12847.

Zimmerman MA & Sullivan JC (2013). Hypertension: what's sex got to do with it? *Physiol Bethesda Md* **28,** 234–244.

Zimmerman MC, Lazartigues E, Sharma RV & Davisson RL (2004). Hypertension caused by angiotensin II infusion involves increased superoxide production in the central nervous system. *Circ Res* **95,** 210–216.